



**Titre:** Modeling the viscosity of liquid solutions used in aluminum alloys production  
Title:

**Auteur:** Shima Mizani  
Author:

**Date:** 2008

**Type:** Mémoire ou thèse / Dissertation or Thesis

**Référence:** Mizani, S. (2008). Modeling the viscosity of liquid solutions used in aluminum alloys production [Master's thesis, École Polytechnique de Montréal]. PolyPublie.  
Citation: <https://publications.polymtl.ca/8350/>

 **Document en libre accès dans PolyPublie**  
Open Access document in PolyPublie

**URL de PolyPublie:** <https://publications.polymtl.ca/8350/>  
PolyPublie URL:

**Directeurs de recherche:** Patrice Chartrand  
Advisors:

**Programme:** Unspecified  
Program:

UNIVERSITÉ DE MONTRÉAL

MODELING THE VISCOSITY OF LIQUID SOLUTIONS USED IN ALUMINUM

ALLOYS PRODUCTION

SHIMA MIZANI

DÉPARTEMENT DE GÉNIE CHIMIQUE

ÉCOLE POLYTECHNIQUE DE MONTRÉAL

MÉMOIRE PRÉSENTÉ EN VUE DE L'OBTENTION  
DU DIPLÔME DE MAÎTRISE ÈS SCIENCES APPLIQUÉES  
(GÉNIE CHIMIQUE)

JUIN 2008



Library and  
Archives Canada

Bibliothèque et  
Archives Canada

Published Heritage  
Branch

Direction du  
Patrimoine de l'édition

395 Wellington Street  
Ottawa ON K1A 0N4  
Canada

395, rue Wellington  
Ottawa ON K1A 0N4  
Canada

*Your file    Votre référence*  
*ISBN: 978-0-494-46066-5*  
*Our file    Notre référence*  
*ISBN: 978-0-494-46066-5*

**NOTICE:**

The author has granted a non-exclusive license allowing Library and Archives Canada to reproduce, publish, archive, preserve, conserve, communicate to the public by telecommunication or on the Internet, loan, distribute and sell theses worldwide, for commercial or non-commercial purposes, in microform, paper, electronic and/or any other formats.

The author retains copyright ownership and moral rights in this thesis. Neither the thesis nor substantial extracts from it may be printed or otherwise reproduced without the author's permission.

**AVIS:**

L'auteur a accordé une licence non exclusive permettant à la Bibliothèque et Archives Canada de reproduire, publier, archiver, sauvegarder, conserver, transmettre au public par télécommunication ou par l'Internet, prêter, distribuer et vendre des thèses partout dans le monde, à des fins commerciales ou autres, sur support microforme, papier, électronique et/ou autres formats.

L'auteur conserve la propriété du droit d'auteur et des droits moraux qui protègent cette thèse. Ni la thèse ni des extraits substantiels de celle-ci ne doivent être imprimés ou autrement reproduits sans son autorisation.

---

In compliance with the Canadian Privacy Act some supporting forms may have been removed from this thesis.

Conformément à la loi canadienne sur la protection de la vie privée, quelques formulaires secondaires ont été enlevés de cette thèse.

While these forms may be included in the document page count, their removal does not represent any loss of content from the thesis.

Bien que ces formulaires aient inclus dans la pagination, il n'y aura aucun contenu manquant.



**Canada**

UNIVERSITÉ DE MONTRÉAL

ÉCOLE POLYTECHNIQUE DE MONTRÉAL

Ce mémoire intitulé :

MODELING THE VISCOSITY OF LIQUID SOLUTIONS USED IN ALUMINUM  
ALLOYS PRODUCTION

présenté par : MIZANI Shima

en vue de l'obtention du diplôme de : Maîtrise ès sciences appliquées

a été dûment accepté par le jury d'examen constitué de:

M. PELTON Arthur, Ph.D., président

M. CHARTRAND Patrice, Ph.D., membre et directeur de recherche

Mme HEUZEY Marie-Claude, Ph.D., membre

À mes parents et mes sœurs

## Acknowledgments

I would like to express my deepest gratitude to my research director, Professor Patrice Chartrand for his support, guidance and continuous encouragement throughout my two years of Master's project.

A special thanks goes to Dr. Christian Robelin for many helpful suggestions and discussions during these two years and for his endless patience and kindness. I would like to thank the jury members Professor Arthur Pelton and Professor Marie-Claude Heuzey who have accepted to evaluate this thesis.

I would like to thank all the CRCT members specially my two colleagues Ms. Liling Jin and Mr. Adarsh Shukla for their support and for the very pleasant time during these two years. A special thanks goes to Ms. Eve Belisle and Mme. Katherine Boucher for their help and support. I would like to thank Mr. Guillaume Lambotte for many helpful discussions and suggestions.

I would like to express my deepest appreciation to Mr. Shant Shahbikian for his support and encouragement and the useful discussions and suggestions during the course of this work. A special thanks goes to Ms. Banafsheh Rafii and Mr. Robin Giguère for their support and help at the times of my shortcomings and for the very pleasant time I spent with them.

At the end I would like to thank my family for their unconditional support and encouragement to pursue my interests, even when the interests went beyond boundaries of language, field and geography. I would like to thank my parents for believing in me, for their endless love and support and for always being there for me even if so far away.

## Résumé

Ce travail de maîtrise fait partie d'un projet de recherche VLAB (un Laboratoire Virtuel pour l'industrie de l'aluminium) ayant l'intention de développer des bases de données pour des propriétés thermodynamiques et physico-chimique exigées par l'industrie de l'aluminium. Ces bases de données peuvent être accédées par le logiciel thermochimique FactSage pour exécuter des calculs de propriétés thermodynamiques et physico-chimique multicomposantes pour les procédés impliqués dans l'industrie de l'aluminium.

L'objectif de ce travail de maîtrise est de modéliser la viscosité des solutions liquides multicomposantes formées pendant le traitement et la coulée de l'aluminium liquides et de ses alliages, en particulier, les mélanges de sels  $\text{NaCl-KCl-MgCl}_2\text{-CaCl}_2$  et l'alliage  $\text{Al-Zn-Si}$ . L'objectif principal est de développer une base de données de viscosité qui peut être utilisée pour des calculs de viscosité pour les solutions multicomposantes en fonction de la composition et de la température.

Les modèles de viscosité disponibles dans la littérature sont examinés et un modèle structural de la viscosité a été développé qui peut prédire la viscosité des systèmes multicomposants à l'aide d'information structurale provenant des modèles thermodynamiques et de densité. Une modification est proposée au modèle afin de mieux reproduire la dépendance de la composition de la viscosité des systèmes montrant un fort ordonnancement.

La dépendance en température de la viscosité dans ce modèle est donnée par l'équation d'Eyring (exponentielle). L'énergie d'activation visqueuse d'un système multi-composant est donnée par la somme des énergies d'activation des paires cation-cation seconds-

voisins présentes dans la solution. La dépendance en composition de la viscosité pour un mélange liquide est ainsi exprimée dans l'énergie d'activation visqueuse par la variation des fractions molaires des paires cation-cation seconds-voisins telles que calculées par le modèle thermodynamique. Les énergies d'activation des paires cation-cation seconds-voisins sont les paramètres du modèle et sont les fonctions linéaires de la température. Toutefois, pour les systèmes avec un fort ordonnancement, le modèle est modifié par l'introduction de termes dépendants de la composition dans l'énergie d'activation en plus des termes dépendants de la température.

Les paramètres du modèle sont optimisés sur la base des données expérimentales fiables. Une revue de la littérature extensive est faite pour recueillir les données expérimentales disponibles. Les méthodes de mesure expérimentale de la viscosité sont présentées et comparées les unes aux autres. La plupart des ensembles de données fiables sont choisis sur la base de l'examen critique des méthodes de mesure employées. En raison de l'incohérence entre les données unaires et binaires des ensembles de données dans la littérature, des fonctions de correction sont appliquées aux données expérimentales et les données binaires qui sont corrigées systématiquement si nécessaire.

Les courbes de viscosité calculées par la modification proposée au modèle reproduisent les points expérimentaux pour les systèmes binaires simples: NaCl-KCl,  $\text{MgCl}_2$ -CaCl<sub>2</sub>, CaCl<sub>2</sub>-NaCl et KCl-CaCl<sub>2</sub> ainsi que pour les systèmes fortement ordonnés: NaCl-MgCl<sub>2</sub>, KCl-MgCl<sub>2</sub>, RbCl-MgCl<sub>2</sub> et CsCl-MgCl<sub>2</sub>. Il y a peu de données expérimentales dans la littérature pour les systèmes multicomposantes, mais les prédictions du modèle pour le système NaCl-KCl-MgCl<sub>2</sub>-CaCl<sub>2</sub> peuvent raisonnablement bien se comparer avec les



données expérimentales disponibles rapportées pour un nombre limité de compositions et de températures. Les courbes de viscosité calculées par le modèle reproduisent bien les données expérimentales rapportées pour les alliages Al-Zn et Al-Si binaires.

En résumé, la modélisation de la viscosité des solutions de chlorures fondus et des alliages d'aluminium liquides donnent des résultats très satisfaisants. Une modification du modèle pour les solutions très ordonnée est proposée et présenté. Les paramètres dépendants de la composition sont ajoutés au modèle pour reproduire le comportement de la viscosité de ces systèmes. La forme modifiée du modèle peut bien reproduire le comportement de viscosité pour les liquides très ordonnés. Les paramètres optimisés du modèle sont ajoutés à la base de données pour calculer la viscosité des systèmes des sels fondus NaCl-KCl-MgCl<sub>2</sub>-CaCl<sub>2</sub> et des alliages liquides AL-Zn-Si. Cette base de données de viscosité est incluse dans les bases de données de FactSage 5.6 où la viscosité des systèmes multi-composants peut être calculée par le modèle de viscosité présenté en employant simultanément les modèles thermodynamiques et de densité.

## Abstract

This work is a part of VLAB (A Virtual Laboratory for the aluminum industry) project aiming to develop thermodynamic and physical properties databases required by the aluminum industry. These databases can be accessed through the FactSage thermochemical software to perform multi-component thermodynamic and physical property calculations for the processes involved in the aluminum industry.

The objective of this master project is to model the viscosity of liquid solutions involved in the aluminum production process namely, NaCl-KCl-MgCl<sub>2</sub>-CaCl<sub>2</sub> liquid solution and Al-Si-Zn liquid alloy. The main aim is to develop a viscosity database that can be used for the viscosity calculations of these multi-component mixtures at various compositions and temperatures.

The available viscosity models in the literature are reviewed and a structural based viscosity model is presented that can predict the viscosity of multi-component systems by simultaneously employing the density and thermodynamic models. A modification is proposed to the model to better reproduce the composition dependency of the viscosity in highly short-range ordered systems.

The temperature dependency of the viscosity in this model is given by an Eyring type exponential equation. The activation energy for viscous flow of a multi-component system is given by the summation of the activation energies of the second nearest neighbor (SNN) pairs present in the melt. The composition dependency of the viscosity for a liquid mixture is thereby expressed in the viscous activation energy term through the variation of the SNN pair fractions upon mixing (the SNN pair fractions being calculated

by the thermodynamic model). The activation energies for the SNN pairs are the parameters of the model given by linear functions of temperature. However for highly short-range ordered systems, the model is modified by introducing composition dependent terms in the activation energy as well as the temperature dependent terms.

The model parameters are optimized based on the reliable experimental data. A thorough literature review is performed to collect the available experimental data. The experimental viscosity measurement methods are introduced and compared to each other. The most reliable data sets are selected based on the critical review of the employed measurement methods. Due to the inconsistencies between the reported unary and binary data sets in the literature, correction functions are applied to the data and the systematically corrected binary data sets are employed for the optimizations.

The calculated viscosity curves by the proposed modified form of the model could well reproduce the viscosity behavior predicted by the experiments for simple binary systems: NaCl-KCl, MgCl<sub>2</sub>-CaCl<sub>2</sub>, NaCl- CaCl<sub>2</sub> and KCl- CaCl<sub>2</sub> as well as the highly short-range ordered systems: NaCl- MgCl<sub>2</sub>, KCl- MgCl<sub>2</sub>, RbCl- MgCl<sub>2</sub> and CsCl- MgCl<sub>2</sub>. There were few experimental data in the literature for multi-component molten salt systems, however the predictions of the model for NaCl-KCl-MgCl<sub>2</sub>-CaCl<sub>2</sub> system compare reasonably well with the available experimental data reported for a limited range of composition and temperature. The viscosity curves calculated by the model well reproduce the experimental data reported for the Al-Zn and Al-Si binary alloys.

In summary, the model leads to very satisfactory results for the molten chloride mixtures and liquid aluminum alloys studied in the present work. The proposed modification to the

model could properly reproduce the viscosity behavior of highly short-range ordered systems as a function of composition of the melt. The optimized model parameters as well as the modified composition dependent parameters are added to the viscosity database of the molten salts and liquid alloys. Employing the mentioned database, viscosity calculations for multi-component molten salts and aluminum alloys can be performed. This viscosity database is included in the FactSage 5.6 data bases where the viscosity of multi-component molten salts and binary aluminum alloys can be calculated through the presented viscosity model by simultaneously employing the thermodynamic and density models.

## Condensé en français

Ce travail de maîtrise fait partie du projet de recherche VLAB (un Laboratoire Virtuel pour l'industrie de l'aluminium) ayant l'intention de développer des bases de données pour des propriétés thermodynamiques et physico-chimique exigées par l'industrie de l'aluminium. Ces bases de données peuvent être accédées par le logiciel thermochimique FactSage pour exécuter des calculs de propriété thermodynamiques et physico-chimiques multi-composants pour les procédés impliqués dans l'industrie de l'aluminium. Particulièrement le modèle de viscosité présenté et modifié dans ce travail est employé pour développer une base de données de viscosité pour les sels fondus ( $\text{NaCl-KCl-MgCl}_2\text{-CaCl}_2$ ) et les métaux liquides ( $\text{Al-Zn-Si}$ ) impliqués dans le procédé de production de l'aluminium.

L'aluminium est le métal non ferreux le plus largement utilisé. Il est remarquable pour sa résistance à la corrosion et sa faible densité. Les composantes structurelles faites en aluminium et ses alliages sont indispensables à l'industrie aéronautique et très importantes dans d'autres domaines tels les transports et la construction. L'aluminium est l'élément métallique le plus abondant dans la croûte terrestre (~8 % poids de la surface solide de la terre) et est le troisième élément le plus abondant après l'oxygène et le silicium. En outre, en raison de sa nature hautement réactive, l'aluminium se retrouve surtout sous la forme d'oxyde ( $\text{Al}_2\text{O}_3$ ) combiné dans les différents minéraux. L'aluminium est produit directement par réduction électrolytique de l'oxyde d'aluminium ( $\text{Al}_2\text{O}_3$ ) dans un bain cryolithique (la production d'aluminium primaire) ou est obtenu par le recyclage. L'aluminium liquide produit par l'une ou l'autre de ces méthodes est ensuite traité à l'état

liquide pour enlever les alcalins, les inclusions et l'hydrogène afin d'obtenir la qualité requise pour la coulée du métal. L'industrie de l'aluminium est sous pression pour améliorer la qualité du métal, cependant qu'en même temps elle doit réduire les coûts et les émissions nocives pour l'environnement. Les impuretés présentes dans le métal peuvent influencer sur la stratégie de traitement du métal qui est utilisée. Deux des impuretés les plus indésirables sont les métaux alcalins et alcalino-terreux. La présence de métaux alcalins, même dans les niveaux de parties par millions, est nocive pour les propriétés mécaniques. L'injection de gaz est la technique la plus fréquente pour enlever les métaux alcalins. Jusqu'à présent, l'industrie de l'aluminium s'est fondée exclusivement sur l'utilisation d'un gaz réactif tel que le chlore pour l'injection. Le chlore injecté réagit avec les métaux alcalins en solution pour former des chlorures sous formes de particules solides ou de gouttelettes de sels fondus qui s'élèveront vers la surface du métal liquide tout en continuant d'échanger des solutés avec l'alliage. Bien que l'utilisation du chlore est très efficace dans l'élimination des métaux alcalins, il peut générer des inclusions et des émissions de chlorure d'hydrogène (les chlorures d'aluminium non réagis qui se forment au cours de l'injection de chlore réagissent avec l'humidité atmosphérique pour former le gaz HCl et les particules  $\text{Al}_2\text{O}_3$ ). C'est pourquoi un accent particulier est mis sur la minimisation de l'utilisation de chlore. La quantité de chlore employé doit être correctement optimisée pour obtenir l'efficacité du processus tout en réduisant les émissions environnementales. Le métal liquide traité ensuite passe par différents procédés de coulée dépendants de la demande.

Il existe différents types de solutions liquides impliquées dans la production d'aluminium à savoir, le bain cryolithique dans les cellules d'électrolyse, les alliages fondus contenant des impuretés et les solutions des sels fondus formées pendant le procédé de traitement. Modéliser avec précision les propriétés de transport des phases multi-composantes formées durant le procédé est important pour un design efficace du procédé. La viscosité est une propriété importante de transport qui est nécessaire pour les calculs de simulations du procédé. En plus, du point de vue théorique, la viscosité étant une propriété basé sur le structure du liquide, peut donner un aperçu plus clair sur le comportement des mélanges liquides au cours des différentes étapes du procédé.

Les mesures expérimentales de la viscosité à des températures élevées ( $\sim 900^\circ\text{C}$  dans les cellules de réduction et  $\sim 700^\circ\text{C}$  pendant les étapes de traitement) sont extrêmement difficiles. Les difficultés rencontrées sont dues à la forte réactivité du liquide avec les creusets et l'atmosphère, la dégradation rapide des échantillons et la présence d'impuretés. En raison des viscosités relativement faibles des sels fondus et des métaux liquides impliqués dans le procédé (généralement inférieur à  $5 \sim \text{mPa.s}$ ), une attention particulière doit être prise pour éviter l'apparition de turbulence au cours de la mesure de viscosité. En conséquence prédire la viscosité de ces solutions par des approches de modélisation est d'un intérêt particulier pour l'industrie de l'aluminium. La dérivation des expressions rigoureuses de viscosité des liquides est difficile puisque les mouvements des atomes ne peut pas être décrit avec précision en fonction du temps. Jusqu'à présent, les approches théoriques n'ont pas mené à des résultats satisfaisants pour prédire la viscosité à haute température et pour les systèmes industriels complexes tels que ceux qui sont

impliqués dans le procédé de production d'aluminium. En l'absence d'un tel modèle de viscosité rigoureux et précis, une approche semi-théorique (semi-empirique) reliant la viscosité aux autres propriétés physiques mesurables pourrait être pratique pour les applications industrielles. Les fluides liés au traitement du métal (alliages, sels fondus, etc.) étant Newtonien, leur viscosité est principalement affectée par la température et par la composition. Par conséquent, un modèle de viscosité doit fournir les variations de viscosité en fonction de la température et de la composition. Un modèle de viscosité a été récemment proposé par Robelin et Chartrand (2007) pour prédire la viscosité des solutions de cryolithe dans les cellules d'électrolyse. Dans le présent travail ce modèle est utilisé et modifié pour prédire les viscosités des solutions liquides liées au traitement des métaux pendant le procédé de production de l'aluminium comme les mélanges des sels fondus et les alliages d'aluminium liquides.

L'objectif général de ce projet de maîtrise est de modéliser la viscosité des solutions liquides impliquées dans le procédé de production d'aluminium. Les objectifs spécifiques sont les suivants:

- Modélisation de la viscosité des mélanges de sels  $\text{NaCl-KCl-MgCl}_2\text{-CaCl}_2$  et l'alliage  $\text{Al-Zn-Si}$  pour l'ensemble de la température et de la composition.
- Développer une base de données pour la viscosité des solutions liquides impliquées dans le procédé de traitement des métaux pendant la production d'aluminium.



Pour obtenir un aperçu plus clair du comportement de la viscosité des solutions liquides impliquées dans le procédé de production de l'aluminium, une revue de la littérature sur la viscosité de ces systèmes a été effectuée. Les méthodes expérimentales employées pour mesurer la viscosité de ces systèmes de même que les modèles de viscosité disponibles dans la littérature sont étudiés. Les modèles des viscosités proposés dans la littérature peuvent être divisé en trois catégories à savoir, théoriques, semi-empiriques (semi-théoriques) et des modèles empiriques. Les modèles théoriques portent essentiellement sur la viscosité d'un liquide pur à un état donné. Ils ne sont pas encore en mesure d'expliquer la dépendance de la composition de la viscosité dans des mélanges liquides. En l'absence d'une expression mathématique pratique pour les liquides qui peut mener à une viscosité physiquement raisonnable, plusieurs auteurs ont proposé divers "mécanismes" pour les écoulements visqueux en assumant un certain modèle du liquide. Ces approches sont appelées des modèles semi-empiriques (semi-théoriques). Les exemples bien connus de ce type de modèles proposés pour les liquides comme la théorie quasi-cristalline d'Andrade, la théorie du volume libre de Cohen et Turnbull et la théorie d'Eyring sont brièvement examinés dans le présent travail. Plusieurs autres auteurs ont essayé de trouver une relation empirique entre la viscosité et d'autres propriétés définies du liquide ou tout simplement de trouver une équation qui correspond le mieux à leurs données. Les modèles semi-empiriques et empiriques ont essentiellement été préoccupés par la dépendance en température de la viscosité. Seuls un petit nombre d'essais ont été faits pour expliquer le comportement de la viscosité de mélanges binaires en fonction de la composition. Dans ces approches, les termes dépendants de la composition ont été

ajoutés aux modèles semi-empiriques ou empiriques existants pour élargir ces modèles aux systèmes binaires et multi-composants. Toutefois, les termes proposés sont applicables seulement à certains systèmes binaires et ne peuvent être simplement étendus aux systèmes multi-composants. Au mieux, ils ne pouvaient donner qu'une prévision qualitative du comportement de la viscosité des systèmes multi-composants. Récemment Robelin et Chartrand (2007) mis au point un modèle de viscosité pour les systèmes multi-composants qui peut prédire de manière satisfaisante la viscosité des solutions cryolithiques employant simultanément les modèles thermodynamiques et de densité développés pour ces systèmes. Ce modèle est utilisé et modifié dans le présent travail pour prédire la viscosité des systèmes multi-composants étudiés. La dépendance en température de la viscosité dans ce modèle est donnée par une équation d'Eyring simplifiée à la forme suivante:

$$\eta = \frac{hN_A}{V_M} \exp\left(\frac{G^*}{RT}\right)$$

où  $h$  est la constante de Planck,  $N_A$  le nombre d'Avogadro,  $V_M$  est le volume molaire calculée par le modèle de densité en fonction de la température et la composition et  $G^*$  est l'énergie d'activation molaire du mélange liquide.

L'énergie d'activation visqueuse ( $G^*$ ) d'un mélange liquide est donnée par la somme des énergies d'activation qui sont définies pour les unités structurales dans la solution. Sur la base de l'image structurale dépeinte par le modèle thermodynamique quasichimique modifié, ces unités structurales dans les solutions liquides des chlorures fondus peuvent

être des paires cation-cation seconds-voisins. L'énergie d'activation ( $G^*$ ), est donnée par l'équation suivante:

$$G^* = \sum X_{ij} G_{ij}^*$$

Les fractions molaires des paires cation-cation seconds-voisins ( $X_{ij}$ ) sont calculées par le modèle thermodynamique (issues de l'entropie de configuration). De cette manière, la dépendance en composition de l'énergie d'activation est donnée par la variation des fractions molaires des paires cation-cation seconds-voisins lors du mélange. Dans la forme initiale du modèle, les énergies d'activation ( $G_{ij}^*$ ) correspondants des paires cation-cation seconds-voisins n'étaient que des fonctions de la température. Cependant, dans le présent travail, il a été montré que, pour des systèmes fortement ordonnés, une dépendance de composition des paramètres est nécessaire pour reproduire la viscosité sur l'ensemble de la composition. Par conséquent, le modèle est modifié dans la formulation ci-dessous par l'introduction des termes dépendants en composition:

$$G_{ij}^* = (G_{ij}^*)^{00} + (G_{ij}^*)^{10} \frac{X_{ii}}{X_{ii} + X_{ij} + X_{jj}} + (G_{ij}^*)^{01} \frac{X_{jj}}{X_{ii} + X_{ij} + X_{jj}}$$

$$(G_{ij}^*)^{00} = (c_{ij})^{00} + (d_{ij})^{00}T$$

$$(G_{ij}^*)^{10} = (c_{ij})^{10} + (d_{ij})^{10}T$$

$$(G_{ij}^*)^{01} = (c_{ij})^{01} + (d_{ij})^{01}T$$

où  $(c_{ij})^{00}$ ,  $(d_{ij})^{00}$ ,  $(c_{ij})^{10}$ ,  $(d_{ij})^{10}$ ,  $(c_{ij})^{01}$  et  $(d_{ij})^{01}$  sont les paramètres modifié du modèle (les paramètres  $(c_{ij})^{10}$ ,  $(d_{ij})^{10}$ ,  $(c_{ij})^{01}$  et  $(d_{ij})^{01}$  seront égal à zéro pour les composants purs).

Ces paramètres du modèle sont optimisés sur la base des données expérimentales trouvées dans la littérature pour les systèmes étudiés.

Pour obtenir les paramètres du modèle pour le système  $\text{NaCl-KCl-MgCl}_2\text{-CaCl}_2$ , les données de viscosité de quatre composantes purs à savoir  $\text{NaCl}$ ,  $\text{KCl}$ ,  $\text{MgCl}_2$  et  $\text{CaCl}_2$  et six systèmes binaires à savoir,  $\text{NaCl-KCl}$ ,  $\text{NaCl-MgCl}_2$ ,  $\text{NaCl-CaCl}_2$ ,  $\text{KCl-MgCl}_2$ ,  $\text{KCl-CaCl}_2$  et  $\text{MgCl}_2\text{-CaCl}_2$  étaient nécessaires. En conséquence une revue de la littérature extensive est faite pour recueillir les données de la littérature disponibles pour ces systèmes. Comme il y avait, dans certains cas, de grandes divergences entre les données expérimentales, une évaluation critique des données a été effectuée pour sélectionner les données les plus fiables pour les optimisations. En raison de l'incohérence entre les données unaires et binaires rapportées dans la littérature, les corrections systématiques sont appliquées aux données. Les données binaires corrigées sont utilisées pour les optimisations. Les courbes de viscosité calculées par le modèle reproduisent bien le comportement donné par les expériences pour des systèmes binaires simples:  $\text{NaCl-KCl}$ ,  $\text{MgCl}_2\text{-CaCl}_2$ ,  $\text{CaCl}_2\text{-NaCl}$  et  $\text{KCl-CaCl}_2$  ainsi que les systèmes très ordonnés:  $\text{NaCl-MgCl}_2$ ,  $\text{KCl-MgCl}_2$ . Pour justifier la modification proposée, deux autres systèmes binaires avec un degré plus élevé d'ordonnement, à savoir  $\text{RbCl-MgCl}_2$  et  $\text{CsCl-MgCl}_2$ , ont été étudiés. Employant la forme modifiée de  $G_{ij}^*$ , ce modèle peut reproduire le maximum observé dans les isothermes de viscosité pour ces systèmes. Toutefois en employant les énergies d'activation de la forme originale proposée par Robelin et Chartrand (2007), le modèle ne donne pas des résultats satisfaisants pour ces

systèmes par rapport aux données expérimentales. Il y avait peu de données expérimentales dans la littérature pour les systèmes multi-composants de sels fondus, mais les prédictions du modèle pour le système  $\text{NaCl-KCl-MgCl}_2\text{-CaCl}_2$  peuvent raisonnablement bien se comparer avec les données expérimentales disponibles que pour un nombre limité de compositions et de températures.

Le même type de revue de la littérature et d'évaluation critique a été réalisé en vue d'obtenir les paramètres du modèle pour les deux alliages binaires Al-Si et Al-Zn. Les courbes de viscosité calculées par le modèle reproduisent bien les données expérimentales rapportées pour les alliages binaires Al-Zn et Al-Si.

En résumé, un modèle de viscosité des solutions de chlorures fondus et des alliages d'aluminium liquide a été obtenu dans ce travail. Une modification du modèle est présentée pour les systèmes très complexes. Les paramètres dépendants de la composition ont été ajoutés au modèle pour reproduire le comportement de la viscosité de ces systèmes. La forme modifiée du modèle peut bien reproduire le comportement de viscosité pour les systèmes très ordonnée. Les paramètres optimisés du modèle forment une base de données pour prédire la viscosité des systèmes des sels fondus et d'alliages liquides. Avec cette base de données, les calculs de viscosité des solutions multi-composantes de sels fondus et d'alliages d'aluminium peuvent être effectués. Cette base de données est incluse dans les bases de données de FactSage 5.6.

Le présent travail peut être étendu afin de rendre possible les calculs des viscosités pour des systèmes plus complexes, contenant différents sels et éléments métalliques.

Dans le présent travail, les paramètres du modèle sont obtenus en employant les données expérimentales disponibles. En raison des difficultés rencontrées dans la mesure de la viscosité à haute température, il serait pratique de corréler la viscosité à des propriétés thermodynamiques: la possibilité d'une corrélation entre la valeur des énergies d'activation visqueuses à des propriétés thermodynamique telles que l'enthalpie de mélange reste à trouver.

Il est important de souligner que le présent modèle de viscosité est applicable uniquement pour les liquides incompressibles et Newtonien où la viscosité n'est seulement qu'une fonction de la température et de la composition. Toutefois, le modèle peut être élargi aux régions non-newtoniennes (où la viscosité devient dépendante du taux de cisaillement) par le biais d'une corrélation raisonnable entre le taux de cisaillement et la viscosité. Le modèle peut également être utilisé pour obtenir la viscosité des liquides contenant des particules solides (suspensions) par de nouvelles recherches sur l'effet des inclusions solides sur la comportement viscosité de ces solutions liquides.

En conclusion, ce projet a contribué au développement d'une base de données pour la viscosité des solutions liquides liées aux procédés de production de l'aluminium, à savoir les chlorures fondus alcalins et alcalino-terreux et les alliages d'aluminium. En utilisant cette base de données simultanément avec les bases de données thermodynamique et de

densité dans FactSage 5.6, les calculs de viscosité des solutions multi-composantes peuvent être effectués d'une manière pleinement cohérente.

## Table of Contents

<b>Acknowledgments .....</b>	<b>V</b>
<b>Résumé .....</b>	<b>VI</b>
<b>Abstract.....</b>	<b>IX</b>
<b>Condensé en français .....</b>	<b>XII</b>
<b>Table of Contents .....</b>	<b>XXIII</b>
<b>List of Tables .....</b>	<b>XXVII</b>
<b>List of Figures.....</b>	<b>XXIX</b>
<b>List of Appendices.....</b>	<b>XXXVII</b>
<b>Nomenclature .....</b>	<b>XXXVIII</b>
<b>1 Introduction.....</b>	<b>1</b>
1.1 Objectives .....	8
1.2 Methodology .....	8
<b>2 Viscosity of Molten Salts and Liquid Aluminum Alloys .....</b>	<b>10</b>
2.1 Necessity of Viscosity Knowledge in the Aluminum Industry .....	10
2.1.1 Aluminum Treatment Process.....	10
2.1.2 Casting .....	13
2.2 Definition of Viscosity.....	14
<b>3 Viscosity Measurement Methods for High Temperature Inorganic Liquids.....</b>	<b>19</b>



3.1	Oscillating Body Methods .....	20
3.1.1	Oscillating Sphere Method .....	21
3.1.2	Oscillating Cylinder Method.....	24
3.1.3	Oscillating Vessel Method.....	27
3.1.3.1	Meniscus Effect in Oscillating Vessel Viscometers .....	30
3.2	Capillary Method .....	31
3.3	Rotational Methods.....	34
3.4	Other Methods .....	36
3.5	Choice of Experimental Technique for Molten Salts and Liquid Metals .....	36
<b>4</b>	<b>Viscosity Models for Molten Salts and Liquid Metals.....</b>	<b>39</b>
4.1	Viscosity Models for Pure Liquids .....	40
4.1.1	Theoretical Models .....	40
4.1.1.1	Viscosity Behaviour of Molten Salts at High Shear Rates .....	43
4.1.2	Semi-Empirical (Semi-Theoretical) Models.....	50
4.1.2.1	The Quasi-Crystalline Theory of Andrade .....	51
4.1.2.2	The Free Volume Theory of Cohen and Turnbull .....	52
4.1.2.3	The Theory of Eyring.....	54
4.1.3	Empirical Models.....	57
4.2	Viscosity Models for Binary Liquid Solutions .....	59
4.2.1	Models Based on Viscosity-Thermodynamic Properties Correlations..	64
4.3	A Viscosity Model for Multi-Component Liquid Solutions.....	68
<b>5</b>	<b>Description of the Model Employed in the Present Work .....</b>	<b>72</b>

5.1	Modifying the Employed Viscosity Model.....	73
5.2	Modified Quasichemical Thermodynamic Model .....	75
5.3	Density Model.....	81
<b>6</b>	<b>Results and Discussion: Molten Salts.....</b>	<b>84</b>
6.1	Pure Molten Salts .....	84
6.1.1	General Discussion on Literature Data .....	84
6.1.2	NaCl .....	86
6.1.3	KCl .....	94
6.1.4	MgCl <sub>2</sub> .....	98
6.1.5	CaCl <sub>2</sub> .....	101
6.2	Binary Molten Salts .....	105
6.2.1	General Discussion on Literature Data .....	105
6.2.2	Data Correction .....	107
6.2.3	NaCl-KCl .....	113
6.2.4	CaCl <sub>2</sub> -MgCl <sub>2</sub> .....	119
6.2.5	KCl-CaCl <sub>2</sub> .....	124
6.2.6	NaCl-CaCl <sub>2</sub> .....	129
6.2.7	KCl-MgCl <sub>2</sub> .....	131
6.2.8	NaCl-MgCl <sub>2</sub> .....	136
6.2.9	Further Discussion on the Results.....	143
6.2.9.1	The Structure of Alkali Chloride-MgCl <sub>2</sub> Melts .....	143
6.2.9.2	RbCl .....	145

6.2.9.3	CsCl.....	147
6.2.9.4	RbCl-MgCl <sub>2</sub> .....	150
6.2.9.5	CsCl-MgCl <sub>2</sub> .....	152
6.3	Multi-Component Molten Salts .....	154
<b>7</b>	<b>Results and Discussion: Liquid Metals .....</b>	<b>168</b>
7.1	Pure Liquid Metals.....	169
7.1.1	General Discussion on Literature Data .....	169
7.1.2	Al.....	170
7.1.3	Zn .....	176
7.1.4	Si .....	178
7.2	Binary Liquid Metals .....	181
7.2.1	General Discussion on Literature Data .....	181
7.2.2	Al-Zn.....	182
7.2.3	Al-Si.....	188
<b>8</b>	<b>Example of the Application of the Model in Aluminum Treatment Process ....</b>	<b>196</b>
<b>9</b>	<b>Conclusions and Future Work.....</b>	<b>202</b>
<b>10</b>	<b>References .....</b>	<b>206</b>
	<b>Appendices.....</b>	<b>224</b>

## List of Tables

Table 1.1: Typical Impurity Levels in the Aluminum from Electrolytic Cells and Recycling Sources (Waite, 2002). .....	4
Table 4.1: Newtonian Viscosities for the BMHTF and MWGKL Models of NaCl Calculated from GK-EMD and NEMD Simulations (Galamba et al., 2005). .....	45
Table 4.2: Newtonian Viscosities for the BMHTF and MWGKL Models of KCl Calculated from GK-EMD and NEMD Simulations (Galamba et al., 2005). .....	45
Table 4.3: Different Possible Types of Viscosity Interactions in a Binary Mixture (McAllister, 1960). .....	63
Table 6.1: A Summary of the Experimental Methods for the Viscosity Measurements of Pure NaCl Reported in the Literature.....	92
Table 6.2: A Summary of the Experimental Methods for the Viscosity Measurements of Pure KCl Reported in the Literature .....	95
Table 6.3: A Summary of the Experimental Methods for the Viscosity Measurements of Pure $\text{MgCl}_2$ Reported in the Literature .....	99
Table 6.4: A Summary of the Experimental Methods for the Viscosity Measurements of Pure $\text{CaCl}_2$ Reported in the Literature.....	101
Table 6.5: A Summary of the Experimental Methods for the Viscosity Measurements of NaCl-KCl Reported in the Literature. ....	113
Table 6.6: A Summary of the Experimental Methods for the Viscosity Measurements of KCl- $\text{CaCl}_2$ Reported in the Literature.....	125

Table 6.7: A Summary of the Experimental Methods for the Viscosity Measurements of KCl-MgCl <sub>2</sub> Reported in the Literature.....	132
Table 6.8: A Summary of the Experimental Methods for the Viscosity Measurements of Pure RbCl Reported in the Literature.....	145
Table 6.9: A Summary of the Experimental Methods for the Viscosity Measurements of Pure CsCl Reported in the Literature. ....	148
Table 6.10: A Comparison Between the Calculated Viscosity Values and the Experimental Data of Zuca et al. (1991) for NaCl-KCl-MgCl <sub>2</sub> -CaCl <sub>2</sub> System.....	165
Table 7.1: A Summary of the Experimental Methods for the Viscosity Measurements of Pure Liquid Al Reported in the Literature (Lambotte, 2007). ....	170
Table 7.2: A Summary of the Experimental Methods for the Viscosity Measurements of Pure Liquid Zn Reported in the Literature (Lambotte, 2007). ....	176
Table 7.3: A Summary of the Experimental Methods for the Viscosity Measurements of Pure Liquid Si Reported in the Literature (Lambotte, 2007). ....	179
Table 7.4: A Summary of the Experimental Methods for the Viscosity Measurements of Al-Si Binary System Reported in the Literature. ....	188
Table 8.1: Hypothetical Properties of the Liquid Al-Zn-Si Alloy and the Injected Cl <sub>2</sub> -Ar and KCl-MgCl <sub>2</sub> Flux Employed for the Example of the Treatment Process. ....	197

## List of Figures

Figure 1.1: An Overview of the Aluminum Production Process.....	2
Figure 1.2: Typical Impurity Levels in Some Aluminum Products (Waite, 2002). ....	3
Figure 1.3: An Overview of the Metal Processing Steps (Waite, 2002).....	4
Figure 2.1: Standard Gibbs Energy of Formation of Several Sulphides, Oxides, Chlorides and Fluorides at 723°C per Mole of S, O, Cl <sub>2</sub> and F <sub>2</sub> Respectively (Utigard, 1991).....	12
Figure 2.2: Laminar Velocity Profile Generated in a Liquid Between Two Parallel Plates. ....	14
Figure 2.3: “Flow curves” for Some Simple Viscous Fluids: (a) Newtonian fluid, (b) fluid exhibiting yield stress, (c) “shear thinning” or “pseudoplastic” fluid, (d) “shear thickening” or “dilatant” fluid. ....	16
Figure 3.1: Viscosity Measurement Methods: (a) flow through capillary tube, (b) falling body, (c) rotation with constant velocity, (d) oscillating body (Dumas et al., 1970). ....	19
Figure 3.2: The Schematic of an Oscillating Sphere Viscometer.....	22
Figure 3.3: The Oscillating Sphere Viscometer used by Dumas et al. (1970).....	22
Figure 3.4: The Schematic of an Oscillating Cylinder Viscometer. ....	25
Figure 3.5: The Schematic of an Oscillating Vessel Viscometer. ....	27
Figure 3.6: The Oscillating Vessel Viscometer (Brooks et al., 2005). ....	28
Figure 3.7: The Schematic of a Capillary Viscometer (Brooks et al., 2005).....	32

Figure 3.8: The Schematic of a Rotating Cylinder Viscometer (Iida and Guthrie, 1987). .....	34
Figure 4.1: Comparison Between the Simulated and Experimental Viscosity Values for (a) NaCl and (b) KCl. Solid Line: Janz (1992); ♣GK-EMD-BMHTF; △GK-EMD MWGKL; ♠NEMD-BMHTF-MC; ▲NEMD-MWGKL-MC; ◇NEMD-BMHTF-Carreau; (Galamba et al., 2005). .....	46
Figure 4.2: Logarithm of the NEMD Shear Viscosity Against the Logarithm of Strain Rate for NaCl at 1100K (Galamba et al., 2005). .....	47
Figure 4.3: Logarithm of The NEMD Shear Viscosity Against the Logarithm of Strain Rate for KCl at 1050K (Galamba et al., 2005). .....	48
Figure 4.4: Logarithm of the NEMD Shear Viscosity Against the Logarithm of the Strain Rate at Different Temperatures for NaCl (Galamba et al., 2005). .....	49
Figure 4.5: Logarithm of the NEMD Shear Viscosity Against the Logarithm of the Strain Rate at Different Temperatures for KCl (Galamba et al., 2005). .....	49
Figure 4.6: Schematic of an Escape Process in the Flow of Liquid (Bird et al., 2002). .....	55
Figure 4.7: Types of Interactions in a Binary Mixture (Assuming a Three-Body Model) (McAllister, 1960). .....	63
Figure 4.8: Some Quadruplets in an Ionic Solution of Cations ( $A, B, C, \dots$ ) and Anions ( $X, Y, Z, \dots$ ). .....	70
Figure 5.1: Enthalpies of Mixing for the Alkali Chloride-MgCl <sub>2</sub> Liquid Solutions Calculated by Chartrand and Pelton (2001b). .....	76

Figure 5.2: Entropy of Mixing for the Alkali Chloride-MgCl <sub>2</sub> Liquid Solutions Calculated by Chartrand and Pelton (2001b).....	77
Figure 6.1: Comparison of NaCl Viscosity Data from the Different Participants of Molten Salts Standards Program, with the NSRDS-1968 Recommendation (Janz, 1980). ....	87
Figure 6.2: NaCl Viscosity Data for the Period 1908-1979, Shown as a Percent Departure Analysis with Torklep and Øye (1978) Data Set as Comparison Standard (Janz, 1980).....	90
Figure 6.3: Calculated and Experimental Viscosity of Pure Liquid NaCl.....	91
Figure 6.4: Calculated and Experimental Viscosity of Pure Liquid KCl .....	97
Figure 6.5: Calculated and Experimental Viscosity of Pure MgCl <sub>2</sub> .....	100
Figure 6.6: Calculated and Experimental Viscosity of Pure CaCl <sub>2</sub> . ....	103
Figure 6.7: The Extrapolation of the Viscosity Curves Calculated by the Model Parameters for NaCl, KCl, MgCl <sub>2</sub> and CaCl <sub>2</sub> Pure Salts Bellow Their Melting Points.....	104
Figure 6.8: The Correction Applied to the Binary Data of Murgulescu and Zuca (1965) for NaCl-KCl System at a Given Temperature, Based on the Estimated Error of its Corresponding Pure Data Sets. ....	108
Figure 6.9: The Corrected Data Sets for Pure NaCl. ....	110
Figure 6.10: The Corrected Data Sets for Pure KCl. ....	111
Figure 6.11: The Corrected Data Sets for Pure MgCl <sub>2</sub> . ....	111
Figure 6.12: The Corrected Data Sets for Pure CaCl <sub>2</sub> . ....	112



Figure 6.13: Calculated and Experimental Viscosity of NaCl-KCl Melt at Various Temperatures.....	116
Figure 6.14: Calculated and Experimental Viscosity of NaCl-KCl Melt at Various Mole Fractions of KCl. ....	117
Figure 6.15: A Comparison Between the Calculated Viscosity Isotherms and the Experimental Data of NaCl-KCl Melt. ....	118
Figure 6.16: A Comparison Between the Binary Data of Dumas et al. (1973) and Fan et al. (2004) for CaCl <sub>2</sub> -MgCl <sub>2</sub> Melt. ....	120
Figure 6.17: Calculated and Experimental Viscosity of CaCl <sub>2</sub> -MgCl <sub>2</sub> Melt at Various Temperatures.....	123
Figure 6.18: Calculated and Experimental Viscosity of CaCl <sub>2</sub> -MgCl <sub>2</sub> Melt at Various Mole Fractions of MgCl <sub>2</sub> .....	124
Figure 6.19: Calculated and Experimental Viscosity of KCl-CaCl <sub>2</sub> Melt at Various Temperatures.....	127
Figure 6.20: Calculated and Experimental Viscosity of KCl-CaCl <sub>2</sub> Melt at Various Mole Fractions of CaCl <sub>2</sub> . ....	128
Figure 6.21: Calculated and Experimental Viscosity of NaCl-CaCl <sub>2</sub> Melt at Various Temperatures.....	130
Figure 6.22: Calculated and Experimental Viscosity of NaCl-CaCl <sub>2</sub> Melt at Various Mole Fractions of CaCl <sub>2</sub> . ....	131
Figure 6.23: Calculated and Experimental Viscosity of KCl-MgCl <sub>2</sub> Melt at Various Temperatures.....	133

Figure 6.24: Calculated and Experimental Viscosity of KCl-MgCl <sub>2</sub> Melt at Various Mole Fractions of MgCl <sub>2</sub> . .....	134
Figure 6.25: A Comparison Between the Calculated Viscosity Isotherms and the Experimental Data of KCl-MgCl <sub>2</sub> Melt.....	135
Figure 6.26: A Comparison Between the Experimental and Calculated Viscosity of NaCl-MgCl <sub>2</sub> Melt at Various Temperatures (Employing the Initial Form of the Model).....	137
Figure 6.27: A Comparison Between the Experimental and Calculated Viscosity of NaCl-MgCl <sub>2</sub> Melt at Various Mole Fraction of MgCl <sub>2</sub> (Employing the Initial Form of the Model).....	138
Figure 6.28: A Comparison Between the Experimental Data and the Viscosity Isotherm Calculated by the Initial Form (the dashed line) and the Modified Form (the solid line) of the Model at 1073 K.....	140
Figure 6.29: Calculated and Experimental Viscosity of NaCl-MgCl <sub>2</sub> Melt at Various Temperatures (Employing the Modified Form of the Model). .....	141
Figure 6.30: A Comparison Between the Calculated Viscosity Isotherms of NaCl-MgCl <sub>2</sub> by the Modified Form of the Model and the Experimental Data. ....	142
Figure 6.31: Calculated and Experimental Viscosity of Pure RbCl .....	147
Figure 6.32: Calculated and Experimental Viscosity of Pure CsCl.....	149
Figure 6.33: Calculated and Experimental Viscosity of RbCl-MgCl <sub>2</sub> Melt at Various Temperatures (Employing the Modified Form of the Model). ....	151

Figure 6.34: Calculated and Experimental Viscosity of CsCl-MgCl <sub>2</sub> Melt at Various Temperatures (Employing the Modified Form of the Model). .....	153
Figure 6.35: A Comparison Between the Corresponding Pure NaCl, KCl and MgCl <sub>2</sub> Data Sets of Berenblit (1937) and Bondarenko (1966) and the 1988 NSRDS (Janz, 1988) Recommended Viscosity Values (the solid lines). .....	156
Figure 6.36: Calculated and Experimental Viscosity of NaCl-KCl-MgCl <sub>2</sub> Ternary System at Various Weight Percents of MgCl <sub>2</sub> with the Weight Ratio of NaCl/KCl Equal to 1. ....	158
Figure 6.37: Calculated and Experimental Viscosity of NaCl-KCl-MgCl <sub>2</sub> Ternary System at Various Temperatures with the Weight Ratio of NaCl/KCl Equal to 1. ....	159
Figure 6.38: Calculated and Experimental Viscosity of NaCl-KCl-MgCl <sub>2</sub> Ternary System at Various Temperatures with the Weight Ratio of NaCl/KCl Equal to 3. ....	160
Figure 6.39: Calculated and Experimental Viscosity of NaCl-KCl-MgCl <sub>2</sub> Ternary System at Various Temperatures with the Weight Ratio of NaCl/KCl Equal to 1/3. ....	161
Figure 6.40: A Comparison Between the Calculated Viscosity Isotherms ( $T = 1092K$ ) of NaCl-KCl-MgCl <sub>2</sub> Ternary System at various Weight Ratios of NaCl/KCl. ....	163
Figure 6.41: Calculated and Experimental Viscosity of NaCl-KCl-MgCl <sub>2</sub> -CaCl <sub>2</sub> System at Various Temperatures for Given Weight Percents of CaCl <sub>2</sub> and the Weight Ratio of NaCl/KCl Equal to 1. ....	165

Figure 6.42: Calculated and Experimental Viscosity of NaCl-KCl-MgCl <sub>2</sub> -CaCl <sub>2</sub> System at Various Weight Percents of CaCl <sub>2</sub> and the Weight Ratio of NaCl/KCl Equal to 1 for a Given Temperature. ....	167
Figure 7.1: Calculated and Experimental Viscosity of Pure Liquid Al (Up to 1966). ...	174
Figure 7.2: Calculated and Experimental Viscosity of Pure Liquid Al (After 1966). ....	175
Figure 7.3: Calculated and Experimental Viscosity of Pure Liquid Zn. ....	178
Figure 7.4: Calculated and Experimental Viscosity of Pure Liquid Si. ....	180
Figure 7.5: The Extrapolation of the Viscosity Curves Calculated by the Model Parameters for Al, Zn and Si Pure Metals Bellow Their Melting Points. ....	181
Figure 7.6: A Comparison Between the Data Set of Jones and Bartlett (1952) (Rotating Cylinder Method) and the Viscosity Data of Lihl et al. (1968) and Gebhardt and Detering (1959) (Oscillating Vessel Method) for Al-Zn Binary System. ....	183
Figure 7.7: Calculated and Experimental Viscosity of Al-Zn Melt at Various Temperatures. ....	186
Figure 7.8: Calculated and Experimental Viscosity of Al-Zn Melt at Various Mole Fractions of Zn. ....	187
Figure 7.9: A Comparison Between the Data Set of Jones and Bartlett (1952) (Rotating Cylinder Method) and the Viscosity Data of Lihl et al. (1968) and Gebhardt and Detering (1959) (Oscillating Vessel Method) for Al-Si Binary System. ....	190

Figure 7.10: A Comparison Between the Data Set of Geng et al. (2005) and the Viscosity Data of Lihl et al. (1968) and Gebhardt and Detering (1959) (Oscillating Vessel Method) for Al-Si Binary System. ....	192
Figure 7.11: Calculated and Experimental Viscosity of Al-Si Melt at Various Temperatures.....	194
Figure 7.12: Calculated and Experimental Viscosity of Al-Si Melt at Various Mole Fractions of Si. ....	195
Figure 8.1: The Amount of Alkali and Alkaline Earth Impurities per Metric Ton of Alloy During a Hypothetical Treatment Process as a Function of the Volume of the Injected Flux at Standard Temperature and Pressure. ....	198
Figure 8.2: The Reaction Products per Metric Ton of Alloy During a Hypothetical Treatment Process as a Function of the Volume of the Injected Flux at Standard Temperature and Pressure.....	199
Figure 8.3: The Liquid Salts Formed per Metric Ton of Alloy During a Hypothetical Treatment Process as a Function of the Volume of the Injected Flux at Standard Temperature and Pressure.....	200
Figure 8.4: The Viscosity of the Multi-Component Molten Salt Solution Formed During a Hypothetical Treatment Process as a Function of the Volume of the Injected Flux at Standard Temperature and Pressure. ....	201

**List of Appendices**

Appendix A: Numerical Values of the Model Parameters.....224

Appendix B: Numerical Values of the Modified Model Parameters.....226

Appendix C: Numerical Values of the Correction Functions.....227

## Nomenclature

Symbols	Description	Units
$a$	Distance traveled by an atom per jump	m
$A$	Deflection of photodiode position	rad
$d$	Atomic diameter	m
$D$	Diameter	m
$E_i$	Activation energy of component $i$	J/mol
$E_\eta$	Activation energy for viscous flow	J/mol
$g_i^0$	Molar standard Gibbs energy of component $i$	J/mol
$G_0^*$	Molar viscous activation energy at rest	J/mol
$G^*$	Molar viscous activation energy	J/mol
$G_i^*$	Molar viscous activation energy of component $i$	J/mol
$G_E^*$	Excess molar viscous activation energy	J/mol
$\Delta G_m$	Gibbs energy of mixing	J/mol
$G_{quad}^*$	Molar viscous activation energy for a quadruplet	J/mol
$G_{ij}^*$	Molar viscous activation energy of $(i,j)$ second nearest neighbour pair	J/mol
$\Delta g_{ij}$	Gibbs energy change for the formation of two moles of $(i,j)$ second nearest neighbor pairs	J/mol
$G$	Gibbs energy of solution	J
$h$	Planck's constant	J.s
$h_{1/2}$	The half of the cylinder height	m
$H$	Height	m

$\Delta H_m$	Enthalpy of mixing	J/mol
$I$	Moment of inertia	kg.m <sup>2</sup>
$L$	Length	m
$m$	Mass	kg
$M$	Molar mass	kg/mol
$M_A$	Atomic mass	1/ (1000 $N_A$ ) kg
$M_{Ai}$	Atomic mass of component $i$	1/ (1000 $N_A$ ) kg
$N_A$	Avogadro's number	1/mol
$n_{i/X}$	Number of moles of the pure liquid salt ( $i/X$ )	mol
$P$	Pressure	Pa
$Q$	Volumetric flow rate	m <sup>3</sup> /s
$R$	Gas constant	J/mol.K
$\Delta S^{config.}$	Configurational entropy of solution	J/K
$t$	Time	s
$T$	Absolute temperature	K
$T_m$	Melting temperature	K
$T_{avg.}$	Arbitrary mean temperature used for curve fitting	K
$T_u$	Additional arbitrary mean temperature used for curve fitting	K
$V$	Velocity	m/s
$v_x$	Velocity (x component)	m/s
$\nabla V$	Velocity gradient tensor	1/s
$(\nabla V)^T$	Transpose of velocity gradient tensor	1/s



$\frac{dv_x}{dy}$	Velocity gradient ( $xy$ component)	1/s
$V_M$	Molar volume	m <sup>3</sup> /mol
$v_f$	Free volume	m <sup>3</sup>
$V_A$	Atomic volume	m <sup>3</sup>
$X_i$	Mole fraction of component $i$	Dimensionless
$X_{ij}$	Mole fraction of ( $i,j$ ) second nearest neighbour pair	Dimensionless
$X_{quad.}$	Mole fraction of quadruplet	Dimensionless
$Y_i$	Coordination-equivalent site fraction of component $i$	Dimensionless
$Z_i$	Coordination number of component $i$	Dimensionless
$Z_{ij}^i$	The value of $Z_i$ when all the nearest neighbor of $i$ are $j$ s	Dimensionless
$\gamma_i$	Activity coefficients	Dimensionless
$\dot{\gamma}$	Shear rate	1/s
$\delta$	Distance between the adjacent layers of liquid	m
$\Delta$	The oscillation logarithmic decrement per units of $2\pi$	Dimensionless
$\Delta_0$	The oscillation logarithmic decrement per units of $2\pi$ in free atmosphere (gas)	Dimensionless
$\theta$	Period of oscillation	s
$\theta_0$	Period of oscillation in free atmosphere (gas)	s
$\kappa$	Boltzman constant	J/K
$\eta$	Viscosity	Pa.s
$\eta_0$	Zero shear viscosity at low shear rates	Pa.s
$\eta_i$	Viscosity of component $i$	Pa.s
$\eta^E$	Excess viscosity	Pa.s

$\Pi$	The oscillation logarithmic decrement	Dimensionless
$\rho$	Density	$\text{kg/m}^3$
$\tau$	Stress tenor,	Pa
$\tau_{yx}$	Stress tensor ( $xy$ component)	Pa
$\tau_0$	Yield stress	Pa
$\Gamma$	Torque	N.m
$\omega$	Angular velocity	1/s

## 1 Introduction

Aluminum is the most widely used non-ferrous metal for various applications. It is remarkable for its ability to resist corrosion and its light weight. Structural components made from aluminum and its alloys (alloys with many elements such as copper, zinc, magnesium, manganese and silicon) are vital to the aerospace industry and very important in other areas of transportation and construction. Aluminum is the most abundant metallic element in the Earth's crust (~8 wt% of the Earth's solid surface) and the third abundant element after oxygen and silicon. However due to its highly chemically reactive nature, aluminum is found mostly in the oxide form ( $\text{Al}_2\text{O}_3$ ) combined in different minerals. Aluminum can be either produced directly from electrolytic reduction of alumina ( $\text{Al}_2\text{O}_3$ ) in a cryolitic bath (primary aluminum production) or obtained by the recycling of the used aluminum products. In general, the aluminum production process consists of several steps which are illustrated in Fig. 1.1.

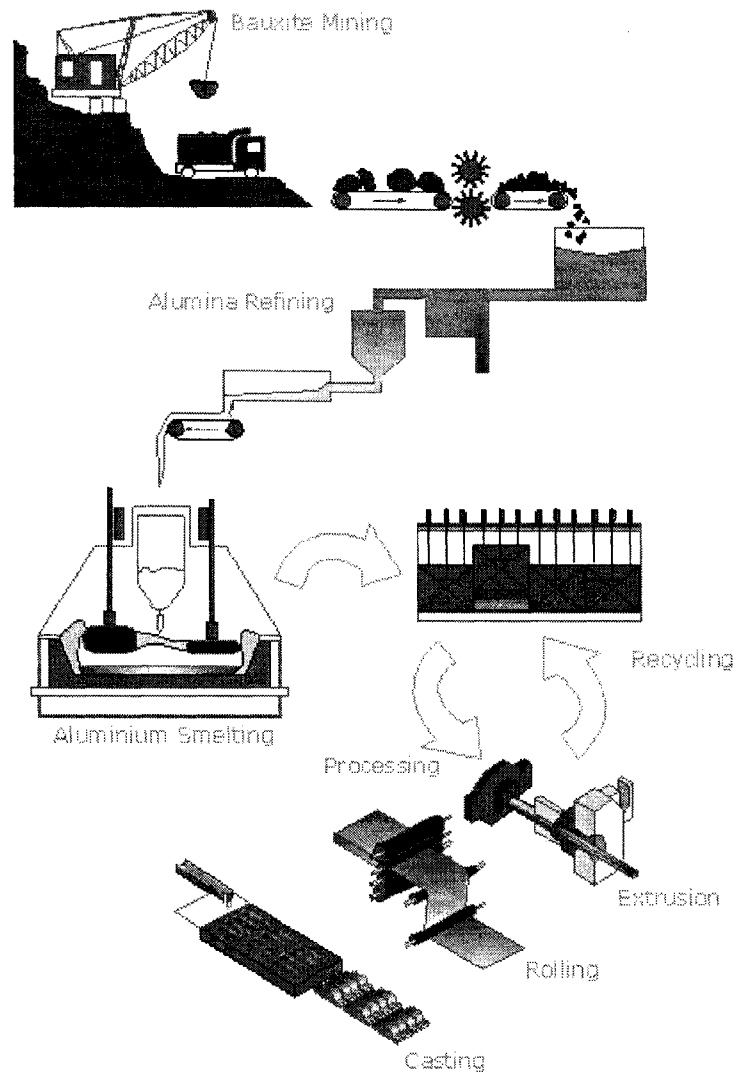


Figure 1.1: An Overview of the Aluminum Production Process\*.

As it is shown in Fig 1.1, the first step of the process is the bauxite mining. Bauxite, the main ore of aluminum, is a mixture of minerals containing mostly hydrated aluminum oxide ( $Al_2O_3 \cdot xH_2O$ ) and hydrated iron oxide ( $Fe_2O_3 \cdot xH_2O$ ). Alumina ( $Al_2O_3$ ) is extracted from bauxite by means of the Bayer process. The extracted alumina coming out

---

\* International Aluminium Institute (2000)

of the alumina refining step is used as the base material for the primary aluminum production through the Hall-Héroult process. In the Hall-Héroult process, the aluminum smelting is done by dissolving alumina in a bath of molten cryolite ( $Na_3AlF_6$ ) at temperatures around 950-980°C where the aluminum can be produced by the electrolysis. The produced liquid aluminum precipitated in the cathode, is denser than the molten cryolite and sinks to the bottom of the bath where it is periodically collected. The collected aluminum as well as the recycled aluminum scraps and used aluminum products go through the metal processing steps to retain the required metal quality. The metal quality refers to the degree to which an aluminum alloy is free of the following contaminants: alkali and alkaline-earth metals, non-metallic inclusions, and dissolved hydrogen. The aluminum industry has been under continual pressure to improve metal quality, while at the same time reduce costs and also reduce undesirable emissions to the environment. Fig. 2.1 shows the impurity levels permitted for various aluminum products.

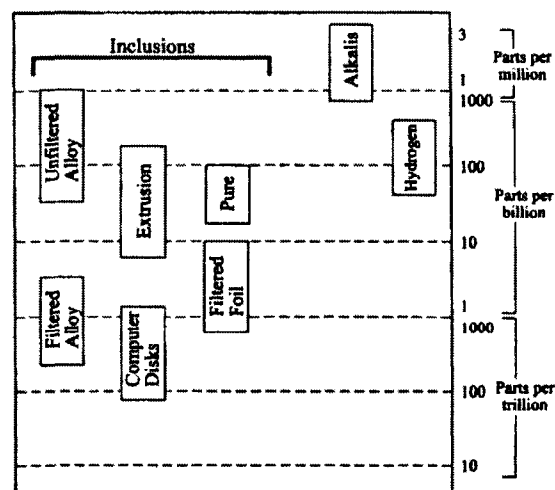


Figure 1.2: Typical Impurity Levels in Some Aluminum Products (Waite, 2002).

The impurities present in the metal are different for primary aluminum and the recycled aluminum products as it is shown in Table 1.1.

Table 1.1: Typical Impurity Levels in the Aluminum from Electrolytic Cells and Recycling Sources (Waite, 2002).

Characteristic	Electrolytic Cells	Recycling
Composition	$\geq 99.7\%$ Al	Alloyed or close to final composition
Hydrogen	0.1-0.3 ppm	0.2-0.6 ppm
Alkali Na	30-150 ppm	$\leq 10$ ppm
Ca	2-5 ppm	5-40 ppm
Li	0-20 ppm	$< 1$ ppm
Inclusions (PoDFA scale)	$1 \text{ mm}^2/\text{kg Al}_4\text{C}_3$	$0.5 < \text{mm}^2/\text{kg} < 5.0$ $\text{Al}_2\text{O}_3, \text{MgO}, \text{MgAl}_2\text{O}_4, \text{Al}_4\text{C}_3, \text{TiB}_2$

Accordingly the employed metal treatment strategy can be different depending on the source. Fig. 1.3 illustrates the general sequence of molten metal processing.

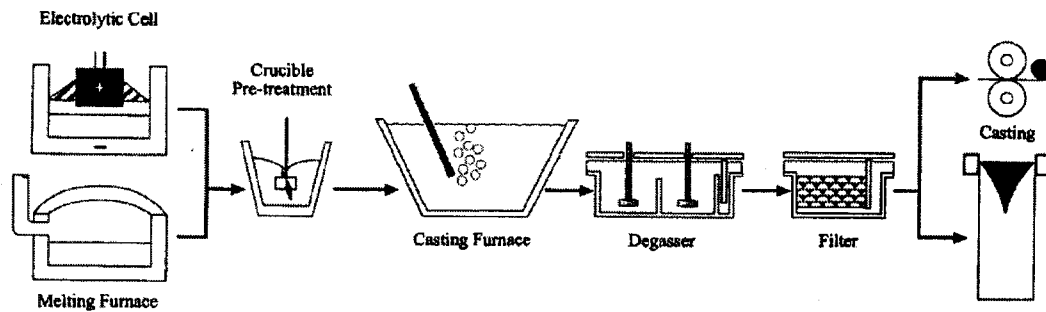


Figure 1.3: An Overview of the Metal Processing Steps (Waite, 2002).

Several crucible based treatment technologies have been developed to remove the alkali metals and inclusions from the metal prior to transfer into the casting furnace. The concept of all these technologies is injecting a reactive flux (mixture of chlorine gas with an inert gas such as argon or nitrogen or a salt flux) into a well-stirred crucible of liquid aluminum.

The most common type of casting furnace is the fossil fuel heated reverberatory design furnace with high surface area to volume ratio to maintain the best heat transfer rate (Waite, 2002). The metal treatment is performed in the furnace similar to the crucible pre-treatment techniques by chlorine or salt fluxing. However due to the shallow bath of metal in the furnace a dispersing system is required to allow longer residence time of the bubbles and increase flux-metal contact area. The injected flux reacts with the alkali impurities and makes solid particles or molten salt droplets which rise in the melt and continue alkali metal exchange. Usually a molten salt layer is employed to cover the melt and prevent the oxidation. This salt layer can also capture the non reacted chloride gases to prevent harmful environmental emissions such as *HCl* gas.

Degasser and filtering steps shown in Fig. 1.3 are two typical categories of in-line metal treatment processes to remove hydrogen and solid inclusions. In the degassing step an inert gas is injected in the melt by using high speed rotary injectors. However by addition of chlorine to the injected inert gas, not only hydrogen and inclusions but also the remaining alkali impurities can be removed by degassing (the alkali removal by chlorine fluxing will be further discussed in the consequent sections). The treated liquid metal then goes through different casting processes depending on the required application.

As it is discussed, there are different kinds of liquid solutions involved in aluminum alloys production steps namely, the cryolitic bath in the reduction cells, metallic mixtures containing impurities and molten salts solutions in the metal processing step and the aluminum alloys in the casting step. Having an accurate knowledge of the transport properties (thermal conductivity, electrical conductance and viscosity) of these solutions at high temperatures is crucial for the efficient design of different steps of the process. Viscosity is an important transport property which is required for the flow simulation calculations in the process. Moreover, from the theoretical stand point, since viscosity is a structural based property, the viscosity knowledge can lead to clearer insight into the behaviour of these liquid mixtures during different steps of the process. However the experimental measurements of viscosity at high temperatures ( $\sim 900^{\circ}\text{C}$  in the reduction cells and  $\sim 700^{\circ}\text{C}$  in the processing steps) are extremely difficult. The difficulties encountered are due to strong reactivity of the melts with container walls and the atmosphere, rapid degradation of the samples, sensitive impurity effects. Due to the relatively low viscosity of the molten salts and liquid metals involved in the process (typically lower than  $\sim 5 \text{ mPa.s}$ ), special care should be taken to avoid the occurrence of turbulency during the viscosity measurements. Accordingly several attempts have been made to obtain the viscosity behaviour of these liquid solutions by modeling approaches. So far rigorous theoretical approaches could not lead to satisfactory results for the viscosity of high temperature and complex industrial systems such as the ones involved in the aluminum production process. Derivation of calculable, rigorous expressions for the viscosity of liquids is difficult since the atomic motions in liquids cannot be precisely



described as a function of time. Consequently several semi-theoretical, semi-empirical approaches have been proposed based on the available experimental data and the observed viscosity behaviour of these systems. The concept of most of these proposed methods is to relate the viscosity to the other measurable physical properties that affect the viscosity. Practically, the fluids encountered in metal processing operations (metals, molten salts and etc.) are Newtonian in behaviour (Szekely, 1979). Therefore, as a Newtonian fluid, the viscosity of these systems is mainly affected by temperature, pressure and in the case of liquid mixtures by the composition. Among the mentioned parameters, temperature and composition have the major contribution to the variation of viscosity. Whereas, at pressures normally used in metals processing operations the viscosity of liquids is independent of pressure (Szekely, 1979).

Most of the proposed models could satisfactorily predict the temperature dependency of viscosity. However only few attempts have been made to explain the composition dependency of viscosity. The proposed composition-dependent models were only applicable to some specific binary systems. They could not be easily extended to other binary systems or multi component liquid mixtures. At the best they could only qualitatively predict the viscosity behavior of multi component systems. However this could not fulfill the increasing demand of viscosity knowledge for industrial purposes. A physically sound viscosity model was required to accurately predict the viscosity behaviour of the multi-component liquid solutions involved in the process. Accordingly a structural based viscosity model has been recently proposed by Robelin and Chartrand (2007) to predict the viscosity behaviour of the cryolitic solutions in the reduction cells.

Their proposed viscosity model could satisfactorily predict the viscosity behaviour of NaF-AlF<sub>3</sub>-CaF<sub>2</sub>-Al<sub>2</sub>O<sub>3</sub> electrolyte in the ranges of composition and temperature of interest by a few parameters. In the present work this model is employed and modified to predict the viscosity behaviour of the liquid solutions involved in the metal processing steps by employing the previously developed density and thermodynamic models for these systems (Chartrand and Pelton, 2001b; Robelin et al., 2007).

## 1.1 Objectives

This master project is a part of VLAB (A Virtual Laboratory for the aluminum industry) project aiming to develop thermodynamic and physical properties databases required by the aluminum industry.

The general objective of this work is to model the viscosity behavior of the liquid solutions in the aluminum production process upon mixing. The main focus is on the molten salt liquid solutions formed during the treatment process. The specific objectives are:

- Modeling the viscosity of molten NaCl-KCl-MgCl<sub>2</sub>-CaCl<sub>2</sub> system and Al-Zn-Si liquid alloy for the whole range of temperature and composition.
- Developing a viscosity database for the liquid solutions involved in the metal processing steps of the aluminum production process.

## 1.2 Methodology

In the following sections after a brief overview of different metal processing steps, the results of a thorough literature review performed regarding the viscosity of liquid

mixtures involved in the process is presented. The experimental viscosity measurement methods are introduced and the proposed viscosity models in the literature are briefly summarized. The viscosity model used in the present work is described and the employed density and thermodynamic models are briefly summarized. A new modification is added to the model for highly short-range ordered systems. The defined unary and binary model parameters are optimized based on the reliable experimental data. A critical review of the available literature data is performed to select the most reliable data sets. Due to the inconsistencies between the reported unary and binary data sets in the literature, correction functions are applied to the data and the corrected binary data sets are employed for the optimizations. The viscosity curves are calculated by using the optimized model parameters. The molar volumes and pair fractions required for the calculations are obtained by FactSage thermochemical software (Bale et al., 2002). The calculated viscosity curves are presented and compared to the experimental data. The optimized model parameters form a database in FactSage 5.6. Employing the developed data base together with the density and thermodynamic databases in FactSage the viscosity calculations in multi component systems are performed and the results are presented.

## **2 Viscosity of Molten Salts and Liquid Aluminum Alloys**

As it is shown previously, there are several liquid solutions involved in the aluminum production process. These solutions can be divided into two categories: molten salts and liquid aluminum alloys. The viscosity of these liquid mixtures is of interest both from the practical and theoretical points of view. From practical stand point, the knowledge of viscosity is important for more accurate design of the processes and from theoretical stand point, for gaining a clearer insight into the behaviour of these liquid mixtures. Viscosity is an important rheological parameter for understanding the hydrodynamics and kinetics of reactions in metal casting. The rate of the rise of gas bubbles and non-metallic inclusions through the molten metal during the metal treatment is primarily related to its viscosity. The  $\text{NaCl-KCl-MgCl}_2\text{-CaCl}_2$  liquid solution is the reaction product during the removal of alkali and alkaline-earth elements in molten aluminum by argon and chlorine injection. The variation of its viscosity as a function of temperature and composition at different stages of the process is important for the efficient design of the process. In the following sections the importance of viscosity knowledge in different metal processing steps is discussed.

### **2.1 Necessity of Viscosity Knowledge in the Aluminum Industry**

#### **2.1.1 Aluminum Treatment Process**

In order to meet the increasing demand of high quality aluminum in the world market place, molten metal quality is the major concern of the cast house. Molten aluminum supplied to the cast house comes from two different sources: electrolytic cells and

remelt/recycle operations. The impurities present in the metal, depending on the source, are different and can affect the metal treatment strategy that is used (Table 1.1). Due to the high quality of the metal required for different applications (Fig. 1.2) the development and implementation of the most appropriate molten metal treatment process is essential. Two of the most undesirable impurities in molten aluminum are alkali and alkaline earth elements. The presence of alkali metals even in levels as parts per million, can cause undesirable properties of the metal. Sodium for example causes cracking during hot rolling. Lithium can accelerate corrosion and create an undesirable black film on foil products. Gas fluxing is the most common technique employed to remove alkali metals. Until recently, the aluminum industry relied exclusively on the use of reactive gases such as chlorine for fluxing. The injected chlorine reacts with the alkali and alkaline earth impurities in the melt and form chlorides as solid particles or liquid droplets which will rise in the liquid alloy and continue to exchange alkali metals. Although the use of chlorine is very efficient in removing alkali metals, it will cause harmful particulate and hydrogen chloride emissions (the non-reacted aluminum chloride gases which are formed during chlorine injection may react with the atmospheric moisture to form HCl gas and  $\text{Al}_2\text{O}_3$  particles). Therefore particular emphasis is placed on minimization of chlorine use. The amount of the employed chlorine is to be accurately optimized to obtain the required efficiency of the process while reducing harmful emissions. However the use of salt fluxes such as the  $\text{MgCl}_2$  containing fluxes for primary aluminum and  $\text{AlF}_3$ ,  $\text{NaAlF}_4$  or the solid chloride fluxes such as  $\text{C}_2\text{Cl}_2$  for recycled aluminum; is becoming more and more common as a replacement of chlorine (Utigard et al., 2001).

The mechanism of the alkali removal by fluxing consists of four major steps: transport of the elements from the bulk molten metal to the metal/flux interface, diffusion of the flux to this interface, transport of elements through this interface, and the chemical reaction between the flux and the alkalis to form chloride salts. As it is shown in Fig 2.1, the chemical reactions involved in this process proceed rapidly due to the very negative Gibbs energies.

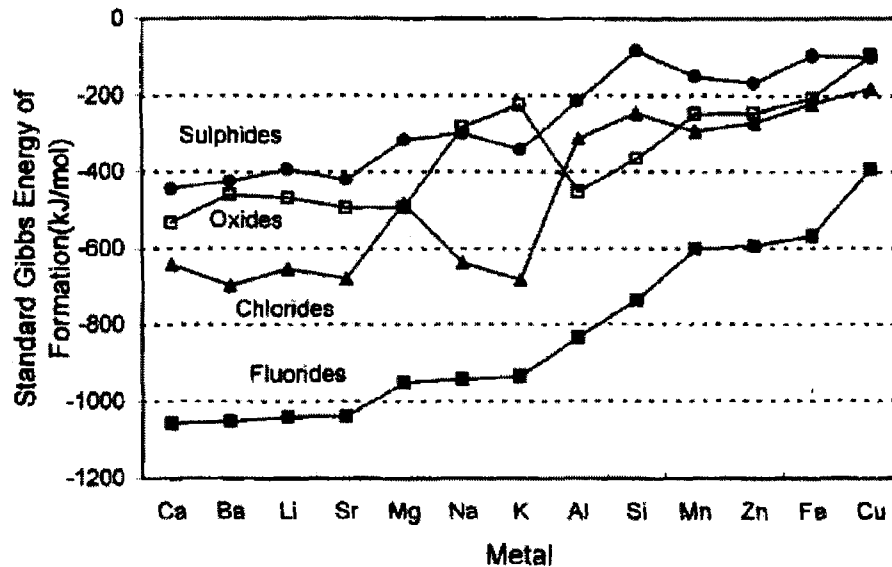


Figure 2.1: Standard Gibbs Energy of Formation of Several Sulphides, Oxides, Chlorides and Fluorides at 723°C per Mole of S, O, Cl<sub>2</sub> and F<sub>2</sub> Respectively (Utigard, 1991).

Therefore the mass transport can be considered as the limiting step of the impurity removal process (Szekely, 1979; Stevens and Yu, 1988; Celik and Doutre, 1989; Sigworth, 2000; Bilodeau et al., 2001). According to Szekely (1979), in the majority of

real systems of practical interest the overall rate at which a dispersed bubble or droplet phase reacts with a continuous melt is not controlled by chemical kinetics but by the physical processes such as diffusion and the nature of the dispersion itself. The growth and detachment of gas bubbles in liquids is affected by several factors, including surface tension, viscosity, liquid inertia and the upstream pressure. These gas bubbles react with the impurities and form molten salts droplets which rise in the melt and continue to exchange alkali metals. The relaxation time of these produced molten salt droplets or the injected salt fluxes can also be an important factor that affects the alkali removal rate. Viscosity of the melt (liquid alloys) and the viscosity of the molten salt droplets are important transport properties that can affect the efficiency of the fluxing. Based on the impurity levels present in the metal and the rate of alkali exchange, the composition of the molten salt droplets varies. Being able to predict the viscosity of these liquid solutions as a function of composition at different steps of the process can improve understanding of the process, more accurate fluid dynamics simulations and as a result more efficient design of the treatment process.

### **2.1.2 Casting**

As it is shown in Fig. 1.3, after passing several metal treatment steps, the treated liquid metal goes through the casting process. Casting is a manufacturing process by which a liquid material is solidified into the required shape. Different casting methods can be employed based on the size and shape of the ingots and the required application. Ingot shapes such as sheet ingots and extrusion billet shown in Fig. 1.1 are usually cast by the direct-chill casting method. In this process, molten metal is poured into a water-cooled

vertical mold. As soon as the metal begins to solidify, the bottom of the mold is lowered and the secondary cooling of the metal is performed by direct contact with water (Smith, 1981). In this method, the metal can be continuously cast into ingots with the desired length.

Viscosity is an important transport property which is required for the fluid flow calculations during different steps of all casting methods. Having the viscosity of different alloys at different compositions and temperatures can lead to more accurate design of the casting process.

## 2.2 Definition of Viscosity

Any transport process in liquids is caused by the gradient of a certain variable such as velocity, temperature or concentration. Momentum transport occurs when a velocity gradient is present in a liquid. By applying a shear force to a liquid, a velocity gradient will be set up which is the result of the fluid resistance to motion (Fig. 2.2). The physical property that characterizes the resistance to flow is called viscosity.

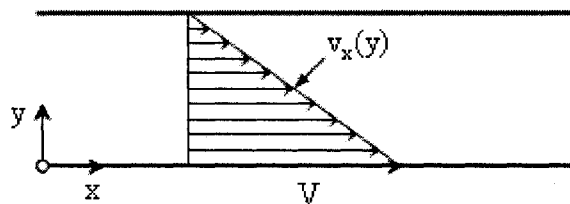


Figure 2.2: Laminar Velocity Profile Generated in a Liquid Between Two Parallel Plates.

In Fig. 2.2, by applying a shear force to the lower plate a velocity gradient is set up between different layers of liquid. The shearing force exerted by the fluid of lesser  $y$  on



the fluid of greater  $y$  in the  $x$  direction on a unit area perpendicular to the  $y$  direction ( $\tau_{yx}$ ) is proportional to the negative value of the velocity gradient ( $\frac{dv_x}{dy}$ ). The constant of proportionality  $\eta$  is a property of fluid, defined to be the viscosity:

$$\tau_{yx} = -\eta \frac{dv_x}{dy} \quad (2.1)$$

This equation is often called Newton's law of viscosity, and the fluids following the mentioned equation are called Newtonian fluids. Eq. (2.1) can be generalized for flows where all velocity components and their gradients are present:

$$\tau = -\eta(\nabla V + (\nabla V)^T) \equiv -\eta \dot{\gamma} \quad (2.2)$$

where  $\tau$ ,  $\nabla V$ ,  $(\nabla V)^T$  and  $\dot{\gamma}$  are stress tensor, velocity gradient tensor, transpose of velocity gradient tensor and shear rate, respectively.

Accordingly, based on Eq. (2.2), the plot of  $\tau$  as a function of  $\dot{\gamma}$  which is known as "flow curve" is a straight line through the origin with a constant slope ( $\eta$ ) considered as the viscosity of the fluid. The mentioned viscosity is a property of fluid which depends only on temperature, pressure and composition. All gases and all liquids composed of small molecules (up to molecular weights of about 5000) are accurately described by Newtonian fluid model (Bird et al., 2002). However there are some structural complex fluids such as polymeric solutions, polymer melts, soap solutions, suspensions, emulsions, pastes and some biological fluids which can not be described by the Newton's law of viscosity. These are called non-Newtonian fluids. Their viscosities depend on the

velocity gradients and they may also display some elastic effects. In the case of fluids with no elastic or memory effects, the “flow curves” are not anymore a straight line. Therefore, Eq. (2.2) has been generalized for non-Newtonian viscous fluids where the viscosity ( $\eta$ ) is a function of shear rate. Accordingly, the generalized Newtonian fluid model can be presented as follows:

$$\tau = -\eta(\nabla \mathbf{V} + (\nabla \mathbf{V})^T) \equiv -\eta \dot{\gamma} \quad \text{with} \quad \eta = \eta(\dot{\gamma}) \quad (2.3)$$

In Fig. 2.3, some simple examples of non-Newtonian behavior are shown. These behaviors can be mainly categorized in two major groups; fluids exhibiting yield stress and fluids without so-called yield stress.

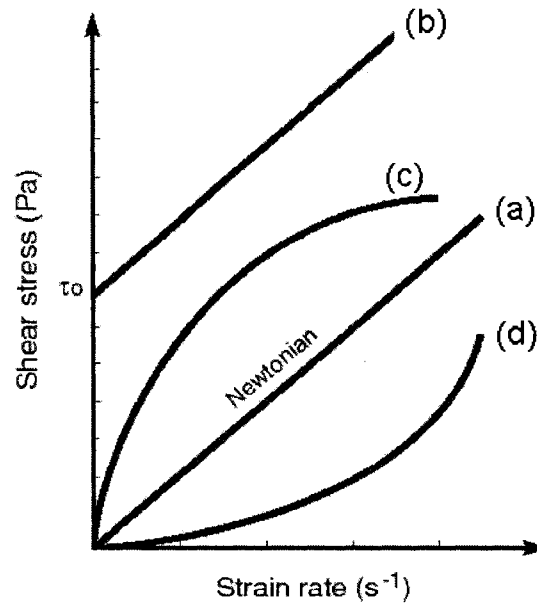


Figure 2.3: “Flow curves” for Some Simple Viscous Fluids: (a) Newtonian fluid, (b) fluid exhibiting yield stress, (c) “shear thinning” or “pseudoplastic” fluid, (d) “shear thickening” or “dilatant” fluid.

Yield stress is the minimum stress level required for the material to flow. Below the mentioned yield stress the material behaves as an elastic solid and no fluid behavior could be observed (Fig. 2.3b). The fluids with such viscous behavior are called “Bingham plastic”. The second category of non-Newtonian fluids keeps its fluidity regardless of the stress level. In certain fluids, the shear stress increases less than in proportion to the shear rate, and therefore their viscosity decreases with shear rate (Fig. 2-3c). These fluids are called “shear thinning” or “pseudoplastic” fluids. On the other hand, in certain fluids the opposite effect can be observed; where the shear stress increases more than in proportion to the shear rate, and consequently the viscosity increases with shear rate (Fig. 2-3d). The mentioned fluids are called “shear thickening” or “dilatant” fluids.

Generally to obtain the viscosity, while dealing with Newtonian fluids, the science of viscosity measurement is called viscometry and the instruments are called viscometers. To study non-Newtonian fluids one has to measure not only the viscosity but also other factors such as normal stresses and the viscoelastic responses. The science of measurement of these properties is called rheometry and the instruments are called rheometers.

Molten salts and liquid metals are believed to be incompressible Newtonian fluids in the low shear rate region (Iida and Guthrie, 1987; Delhommelle and Petravic, 2003; Galamba et al., 2005). However, their behavior at high shear rates is different as it will be discussed in one of the subsequent sections (Section 4.1.1.1). The subject of the present work, concerns the modeling of Newtonian viscosity as a function of temperature and composition of melts in their Newtonian regions (the pressure dependent of the viscosity

is not significant for most systems of metallurgical interest including metals processing operations (Szekely, 1979)). To be consistent with IUPAC's notation, the symbol  $\eta$  for viscosity is used in the whole text. The unit of viscosity in SI system is Pa.s but the mainly used unit for viscosity is poise (c.g.s system).

### 3 Viscosity Measurement Methods for High Temperature

#### Inorganic Liquids

There is a variety of methods to measure the viscosity of liquids. However as it will be shown in the following sections, molten salts and metallic systems studied in the present work have very high melting points of the order of 1000K. Developing a suitable method for the viscosity measurement of these high-temperature, mostly volatile and corrosive melts is not an easy task. Molten salts are considered as very good solvents in several industrial processes and therefore require a proper container and a proper thermocouple to measure those high temperatures without reacting with the sample. A special furnace is needed to maintain the required high temperature during the measurements. The principles of the most frequently used methods for high temperature viscosity measurements are shown in Figure 3-1.

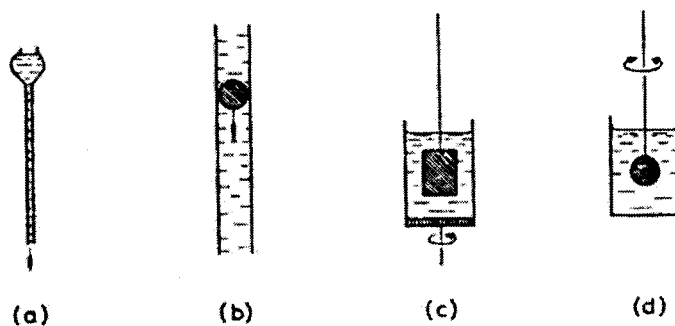


Figure 3.1: Viscosity Measurement Methods: (a) flow through capillary tube, (b) falling body, (c) rotation with constant velocity, (d) oscillating body (Dumas et al., 1970).

In the following sections a brief summary of these measurement methods employed by different laboratories are presented along with the advantages and disadvantages of each method. Serious consideration is given to oscillating body methods which are the most frequent techniques used in the viscosity measurement of molten salts and liquid metals.

### **3.1 Oscillating Body Methods**

Oscillating body methods are the most widely used technique in molten salts and liquid metals viscometry (Janz et al., 1968; Janz et al., 1975; Janz, 1988). All types of oscillating viscometers consist of an axially symmetric body suspended from an elastic stand, where they induce torsional oscillations. The principle underlying the damped oscillational viscosity techniques is applying an initial rotational oscillation to the oscillating body and let it damp by the viscous resistance of liquid. The viscosity resistance of the liquid will cause a logarithmic decrement in the amplitude of oscillation as a function of time and an increase in the period of oscillation. Viscosity can be obtained by measuring these two parameters. Generally an oscillating body viscometer is composed of four fundamental parts: an oscillating part including the oscillating body, suspension system and the oscillation initiator, a heating system (furnace) to maintain the required high temperature, a vacuum system or an inert gas flow to maintain non-reactive atmosphere at high temperatures and a part for detecting the oscillations.

The apparatus and the oscillating body geometries are simple and measurement of the amplitude and period of oscillations are highly accurate. Unfortunately, the mathematical approaches to calculate the viscosity from the observed logarithmic decrement and the

period of the oscillations are in some cases extremely complicated. As it will be further discussed in Section 3.1.3, the high degree of discrepancy observed between different experimental viscosity data, regardless of common experimental errors, can be partly related to the choice of mathematical equation employed (Grouvel and Kestin, 1978; Janz, 1980; Iida and Guthrie, 1987). The oscillating body can be a sphere, cylinder or a filled solid cylinder suspended in the melt or a vessel filled with the melt. In the following chapters each of the mentioned oscillating body methods are briefly discussed.

### **3.1.1 Oscillating Sphere Method**

This method has been widely used for viscosity measurements in molten salts (Murgulescu and Zuca, 1961; 1963; 1965; Bondarenko and Strelets, 1968; Dumas et al., 1970; Zuca and Costin, 1970; Dumas et al., 1973; Brockner et al., 1975; Murgulescu and Misdolea, 1977; Zuca and Borcan, 1984). In this technique, a spherical body is suspended in the melt and rotational oscillation is fed to it. A schematic drawing of the apparatus is shown in Fig. 3.2. The initial oscillation is gradually damped by the viscous resistance of the melt and the logarithmic decrement along with the time periods of the oscillation is accurately recorded.

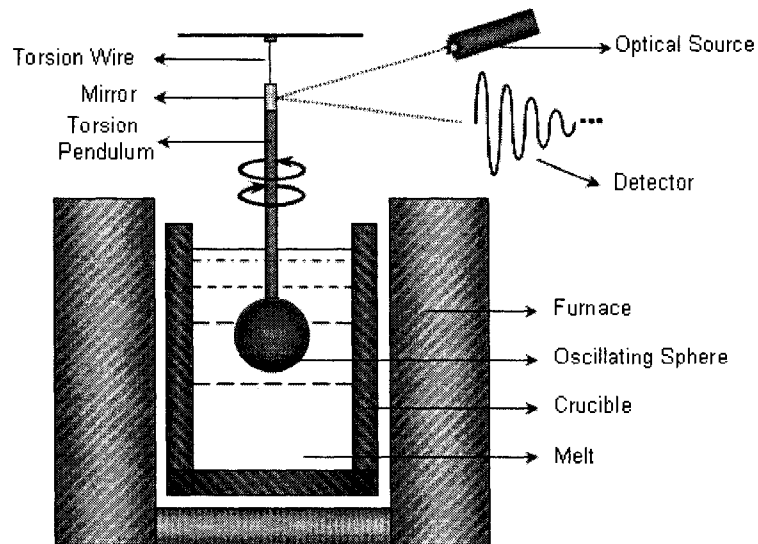


Figure 3.2: The Schematic of an Oscillating Sphere Viscometer.

Fig. 3-3 shows the apparatus used by Dumas et al. (1970) for viscosity measurement of molten salts.

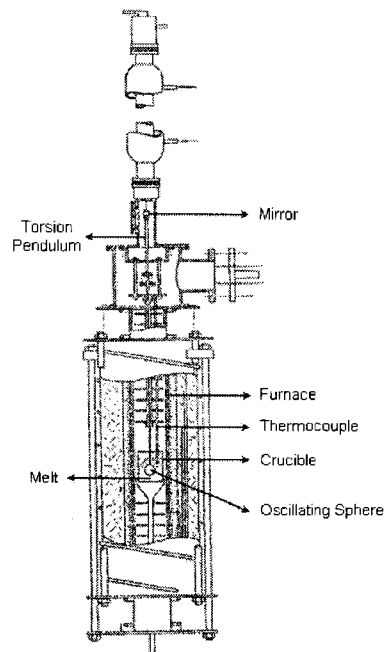


Figure 3.3: The Oscillating Sphere Viscometer used by Dumas et al. (1970).



The mathematical relationship between damping and viscosity has been initially established by Verschaffelt (1916). He assumed the movement of liquid around the sphere to be that of rigid spherical shells performing damped, simple harmonic oscillations around a common z-axis. The liquid was also assumed to exhibit Newtonian behaviour. For small oscillations of the sphere, Verschaffelt considered the following differential equation for the motion of the rigid spherical shells:

$$\frac{\partial^2 \omega}{\partial r^2} + \frac{4}{r} \frac{\partial \omega}{\partial r} - \frac{\rho}{\eta} \frac{\partial \omega}{\partial t} = 0 \quad (3.1)$$

and derived the Eq. (3.2) which gives viscosity as a function of measurable quantities:

$$\eta = \frac{3\Pi I}{4\pi R^3 \theta_0} \left( \frac{1}{2 + Rb_1 + \Sigma} \right)$$

$$\Sigma = \frac{b_1 R + 1}{(b_1 R + 1)^2 + b_1^2 R^2} \quad (3.2)$$

$$b_1 = \sqrt{\frac{\rho\pi}{\eta\theta}}$$

where,  $\eta$  is the viscosity of the liquid,  $\rho$  is the density of liquid,  $R$  is the radius of the sphere,  $I$  is the moment of inertia of the pendulum,  $\theta$  is the period of swing in the liquid,  $\theta_0$  is the period of swing in vacuum,  $\Pi$  is the logarithmic decrement of the oscillation (defined as the logarithm of the ratio of two successive amplitudes of the oscillation).

Solving Eq. (3.2) gives an absolute value for the viscosity. This equation was used by Dumas et al. (1970; 1973) as the working formula for viscosity measurement of molten alkali and alkaline-earth chlorides and their mixtures.

Probable recrystallization of the melt samples on the sphere surface or chemical attack of the sphere surface caused by small amounts of moisture can cause slight changes in the radius of the oscillating sphere during the measurement. As part of the Molten Salts Standard Program<sup>†</sup> to estimate the accuracy of different methods, it was shown that an uncertainty in radius of the sphere imposes a limit to the precision of this technique (Janz, 1980). In molten salt viscosity measurements generally the noble metals such as platinum, gold and their alloys are used for such spheres. The inherent softness of these metals limits the spherical machineability tolerances. Cylinders are simpler to re-machine and can be machined to more exact tolerances than spherical shapes. These considerations led to a shift from sphere to cylinder in oscillating body methods (Dumas et al., 1970; Torklep and Øye, 1979; Janz, 1980).

### **3.1.2 Oscillating Cylinder Method**

This method is employed mostly for molten salts viscometry (Torklep and Øye, 1979; Brockner et al., 1981; Torklep and Øye, 1982). Experimental apparatus used for the oscillating sphere method can be designed in a way that utilizes a cylinder as well as a sphere for the oscillating body. Fig. 3.4 illustrates a schematic drawing of the oscillating cylinder viscometer.

---

<sup>†</sup> The Molten Salts Standard Program initiated in 1973 by G. J. Janz (USA) jointly with S. Zuca (Rumania), was part of a 3 year cooperative research program under the Inter-Academy Agreement and supported by the National Science Foundation (USA) and Ministry of Science and Technology (Rumania)

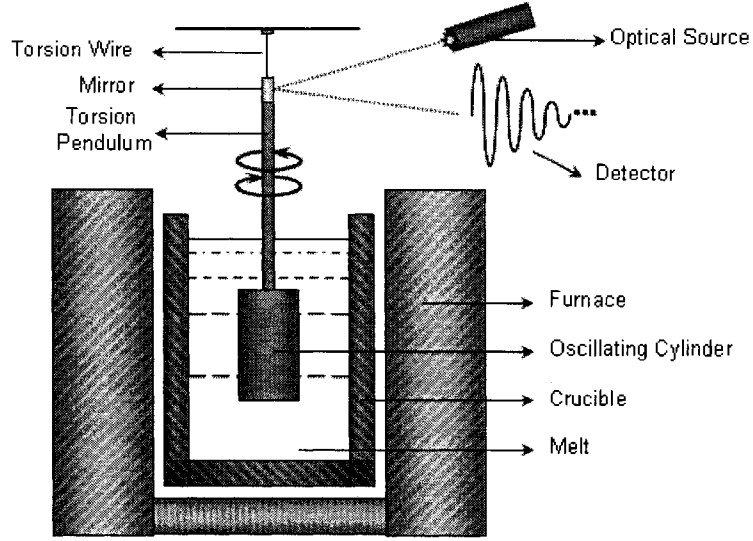


Figure 3.4: The Schematic of an Oscillating Cylinder Viscometer.

Although the cylinder is much simpler to manufacture and re-machine, the theoretical treatment of a cylinder oscillating in liquid is much more difficult to develop than for a sphere: for example, motion of the liquid near the sharp edges of cylinder cannot be easily modeled; therefore finding a general expression which gives a true picture of the liquid motion is not a simple task. By using the general solution given by Azpeitia and Newell (1959), Torklep and Oye (1979) proposed the following working formulas for oscillating cylinder viscometer:

$$(\pi \rho h R^4 / I) [A(\Psi - \Delta q)x^{-1} + Bx^{-2} + Cqx^{-3}] = 2(\Delta - \Delta_0 / \varepsilon) \quad (3.3)$$

$$(\pi \rho h R^4 / I) [A(\Delta \Psi + q)x^{-1} + B\Delta x^{-2} - C\Psi x^{-3}] = 1/\varepsilon^2 - 1 + (\Delta - \Delta_0 / \varepsilon)^2 \quad (3.4)$$

with

$$A = 4 + R/h$$

$$B = 2.407949R/h + 6$$

$$C = 1.89R / h_{1/2} + 1.5$$

$$\varepsilon = \theta_0 / \theta$$

$$\Psi = 1 / \{2[\Delta + (1 + \Delta^2)^{1/2}]\}^{1/2}$$

$$q = 1 / 2\Psi$$

$$x = R(2\pi\rho / \eta\theta)^{1/2}$$

where  $I$  is the total moment of inertia of the oscillating mechanical system,  $R$  is the cylinder radius,  $h_{1/2}$  is the half of the cylinder height,  $\theta$  is the period while the cylinder immersed in liquid,  $\theta_0$  is the period in free atmosphere (gas),  $\rho$  is the density of the liquid,  $\eta$  is the viscosity of the liquid,  $\Delta$  is the total damping observed with the cylinder immersed in the liquid and  $\Delta_0$  is the damping correction term. The damping coefficients ( $\Delta$  &  $\Delta_0$ ) are logarithmic decrements ( $\Pi$ ) per units of  $2\pi$ .

Viscosity can be computed by solving the Eq. (3.3) or Eq. (3.4) for  $x$  by numerical methods. The logarithmic decrement ( $\Pi$ ) and the period ( $\theta$ ) can be obtained by using the basic equation of damped harmonic oscillations to fit the whole range of recorded time intervals:

$$A = A_1 \exp\left(-\frac{\delta t}{\theta}\right) \sin\left(\frac{2\pi t}{\theta}\right) \quad (3.5)$$

where  $A$  is the deflection corresponding to a photodiode position at time  $t$  and  $A_1$  is a constant.

The cylinder used in this method can be either a filled solid cylinder submerged in the liquid or a cup containing the liquid. The former is usually called an oscillating cylinder

viscometer while the latter called an oscillating vessel (cup) viscometer which is more convenient for highly volatile melts (Torklep and Øye, 1979).

### 3.1.3 Oscillating Vessel Method

As it will be shown later in the literature review for the liquid metals, this method is the most frequently used technique for viscosity measurement in liquid metals of interest in the present work. It has also been used by several laboratories for the viscosity measurement of the studied molten salt systems (DeWitt et al., 1974; Ejima et al., 1977; Abe et al., 1980; Ito et al., 1989; Tolbaru et al., 1998). In this method, the oscillating body is a vessel (cup) containing the melt. Fig. 3.5 shows a schematic of the oscillating vessel viscometer.

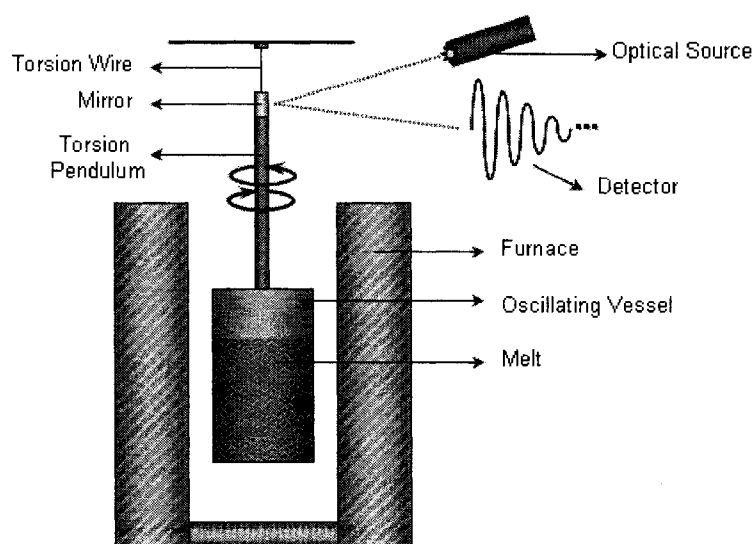


Figure 3.5: The Schematic of an Oscillating Vessel Viscometer.

The initial torsional oscillation applied to the vessel will damp by viscous resistance of the liquid inside the crucible. Fig. 3.6 shows the apparatus used by Brooks et al. (2001) for viscosity measurement of liquid metals.

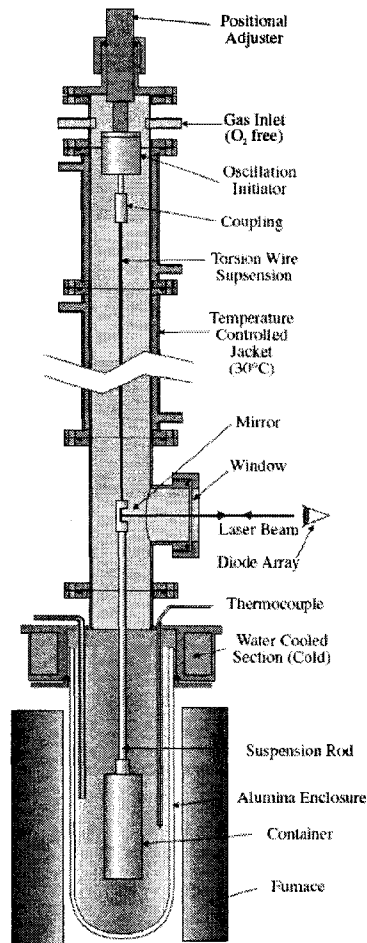


Figure 3.6: The Oscillating Vessel Viscometer (Brooks et al., 2005).

The analytical approach to obtain the working formula of oscillating vessel viscometer is identical to the oscillating cylinder. Therefore working formulas presented for oscillating cylinder viscometers (Eqs. 3.3 and 3.4) are also applicable for oscillating vessels. However there are several approximate working formulas proposed by different authors.

The choice of working formula can affect the accuracy of the viscosity values reported by each laboratory (Janz, 1980; Iida and Guthrie, 1987). The working formulas for the oscillating vessel viscometer proposed by Knappwost (1952), Shvidkovskii (1955) and Roscoe (1958) were reviewed by Iida and Guthrie (1987). They showed that the choice of working formula can be a major source of large discrepancies among experimental viscosity data. They recommended Roscoe's equation as the one providing the most accurate viscosity values (Eq. 3.6).

$$\frac{\Pi}{\rho} = A \left( \frac{\eta}{\rho} \right)^{\frac{1}{2}} - B \left( \frac{\eta}{\rho} \right) + C \left( \frac{\eta}{\rho} \right)^{\frac{3}{2}} \quad (3.6)$$

with

$$A = \frac{\pi^2}{I} \left( 1 + \frac{R}{4H} \right) HR^3 \theta^{\frac{1}{2}}$$

$$B = \frac{\pi}{I} \left( \frac{3}{2} + \frac{4R}{\pi H} \right) HR^2 \theta$$

$$C = \frac{\pi^2}{2I} \left( \frac{3}{8} + \frac{9R}{4H} \right) HR \theta^{\frac{3}{2}}$$

where  $\rho$  is the density of the liquid,  $\eta$  is the viscosity of the liquid,  $\Pi$  is the experimentally determined logarithmic decrement,  $I$  is the moment of inertia of the suspended system,  $R$  is the radius of the vessel,  $H$  is the height of the liquid sample in the vessel and  $\theta$  is the period.

Iida and Guthrie (1987) proposed the addition of a correction factor ( $\zeta$ ) to the original Roscoe's equation to obtain more accurate results under real experimental conditions. Eq. (3.7) is called the corrected Roscoe's formula.

$$\frac{\Pi - \Pi_0}{\rho} = \zeta \left\{ A \left( \frac{\eta}{\rho} \right)^{\frac{1}{2}} - B \left( \frac{\eta}{\rho} \right) + C \left( \frac{\eta}{\rho} \right)^{\frac{3}{2}} \right\} \quad (3.7)$$

where  $\Pi_0$  is a damping correction term proposed by Rothwell (1962) and Thresh (1965). The correction factor ( $\zeta$ ) is due to the end effect depending on different meniscus shapes of liquid and possible slipping phenomena depending on wettability of the liquid. Various studies with different choices of crucible material suggested that the wetting of the crucible can be an important factor affecting the viscosity values (Kimura et al., 1995; Sato et al., 2003). If the liquid does not completely wet the crucible, the resulting slippage between the liquid interface and the crucible wall would provide smaller damping than expected.

### 3.1.3.1 Meniscus Effect in Oscillating Vessel Viscometers

When an oscillating vessel viscometer is used, the cylindrical cup is completely or partially filled with liquid. When the cup is partially filled, the height of the liquid is calculated from the inner diameter of the cup, density and weight of the liquid. There is a slight difference between the calculated height and the actual height caused by the liquid meniscus shape (the actual height is considered to be the depth of the inner wall wetted by the liquid). Depending on the meniscus shape of liquid in the vessel, the actual liquid height is slightly greater or smaller than the calculated one (Fig. 3.6).



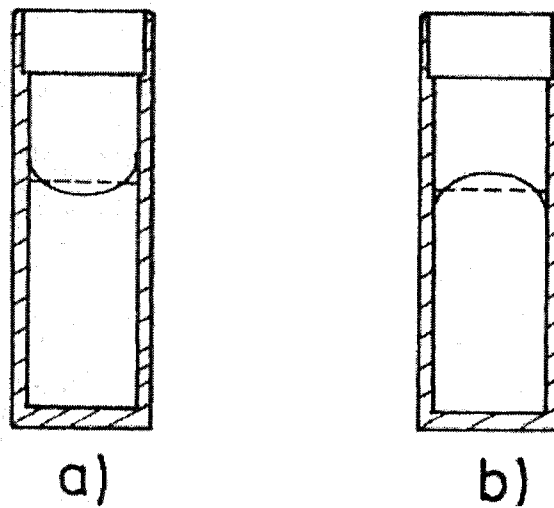


Figure 3.6: Possible Meniscus Shape of Liquid in the Cylindrical Vessel:

(a) concave surface, (b) convex surface, - - - calculated height.

Therefore, applying a correction for the meniscus effect is necessary except for completely filled cups which is extremely difficult to achieve specially in the case of molten salts (Torklep and Øye, 1981). Since this meniscus shape depends only on the surface properties of the liquid and the vessel material, this correction in height would be a fixed value for each individual measurement.

### 3.2 Capillary Method

The capillary method is generally thought to be one of the best methods for viscosity measurement in liquids (Iida and Guthrie, 1987). The principle of this technique is passing a liquid through a narrow circular tube under a given pressure and measuring the efflux time of liquid through the capillary tube. Fig. 3.7 shows a capillary viscometer.

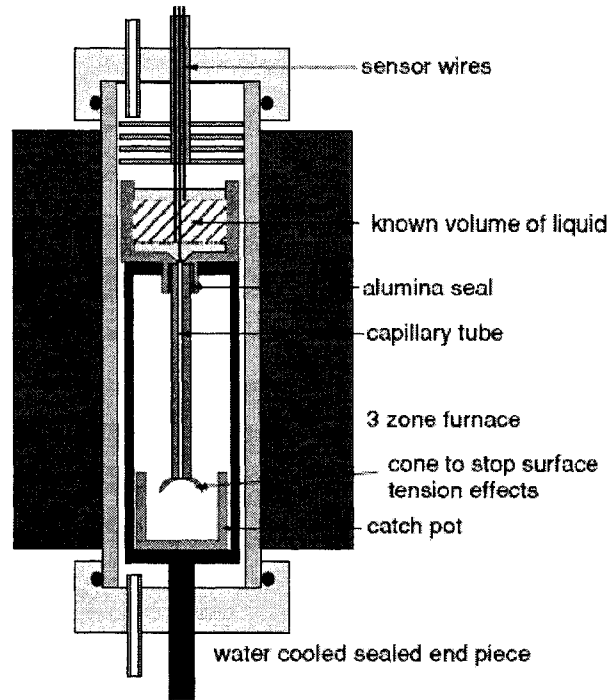


Figure 3.7: The Schematic of a Capillary Viscometer (Brooks et al., 2005).

The time required for a definite volume of liquid to pass through the tube depends on the viscosity of the liquid. The relation between the viscosity and the efflux time for incompressible Newtonian fluids at a given pressure is given by Eq. (3.8) which is often called the Hagen-Poiseuille equation (Bird et al., 2002).

$$\eta = \frac{\pi D^4 \Delta P}{128 QL} \quad (3.8)$$

where,  $\eta$  is the viscosity of the liquid,  $\Delta P$  is the pressure drop along the capillary tube,  $Q$  is the volumetric flow rate,  $D$  and  $L$  are the diameter and length of capillary tube respectively.

In order to obtain the Hagen-Poiseuille equation, the end-effect, the probable wall slip and the alteration in the capillary diameter resulting from slight etching and re-crystallization of melt samples were neglected. Therefore, to apply Eq. (3.8) for viscosity measurements, few corrections are required. These corrections are shown in Eq. (3.9):

$$\eta = \frac{\pi D^4 \Delta P}{128 Q \left[ L + k_2 \left( \frac{D}{2} \right) \right]} - \frac{k_1 \rho Q}{8\pi \left[ L + k_2 \left( \frac{D}{2} \right) \right]} \quad (3.9)$$

where,  $\rho$  is the density of liquid and  $k_1$  &  $k_2$  are constants which can be determined experimentally. “ $k_2 \left( \frac{D}{2} \right)$ ” is called the end-effect correction and the second term in Eq. (3.9) is the kinetic energy correction.

However to apply the Hagen-Poiseuille equation, the condition of low Reynolds number<sup>‡</sup> ( $Re < \text{about } 2100$ ) is required to insure laminar flow. For low viscosity liquids such as molten salts and liquid metals studied in the present work, a fine and long tube is required to satisfy this condition. Besides the material limitation for this special tube, the risk of blockage in capillary tube is also high. Even fine traces of impurities may form gas bubbles or oxide inclusions that may block the tube during the measurement. The blockage of capillary tube has a direct and pronounced effect on the efflux time of liquid. Therefore, clean liquid samples free from any contamination are required for viscosity measurements by this method. These problems together with the difficulties to obtain a long range of constant temperature along the tube length precluded the usage of this

---

<sup>‡</sup>  $Re = \frac{\rho V D}{\eta}$  where  $\rho$  is the density of the fluid,  $V$  is the fluid's velocity,  $D$  is the diameter of the tube and  $\eta$  is the viscosity of the fluid.

method for high temperature measurements. Due to these limitations, this method has been applied to liquids with melting points below 1400-1500 K (Iida and Guthrie, 1987).

### 3.3 Rotational Methods

In rotational methods the viscosity is determined by measuring the torque required to turn a solid object in contact with the liquid. There are several types of viscometers based on the principle of the rotational technique: rotation of a sphere, rotation of a disk and rotation of concentric cylinders (outer cylinder rotated, inner cylinder suspended or outer cylinder fixed, inner cylinder rotated). A schematic of a rotating cylinder viscometer is shown in Fig. 3.8.

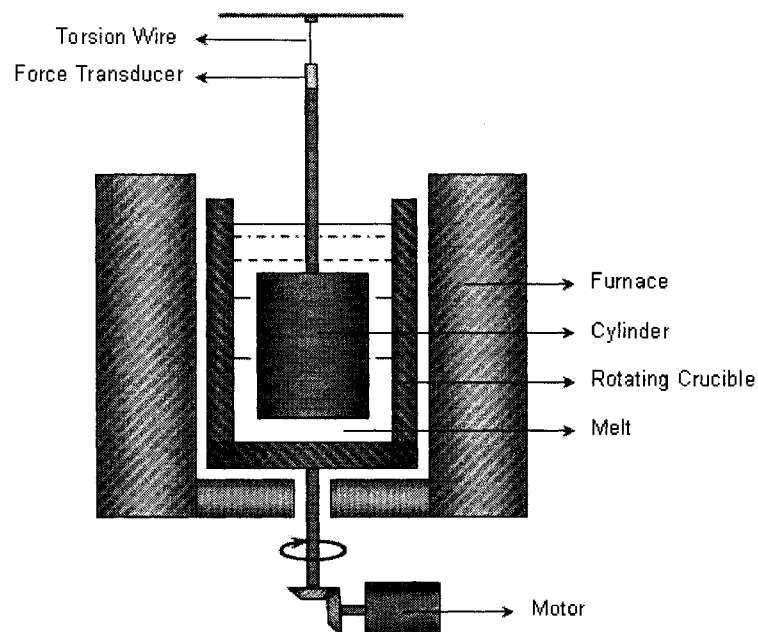


Figure 3.8: The Schematic of a Rotating Cylinder Viscometer (Iida and Guthrie, 1987).

In the rotating cylinder method, the liquid is filling the space between two co-axial cylinders. Viscosity can be obtained by applying a certain angular velocity to the inner or outer cylinder and measuring the torque exerted on the other one. In the case where the outer cylinder rotates, viscosity can be obtained by the following equation (Bird et al., 2002):

$$\eta = \frac{\Gamma(D_o^2 - D_i^2)}{\pi L \omega D_o^2 D_i^2} \quad (3.10)$$

where,  $\eta$  is the viscosity of the liquid,  $\Gamma$  is the torque acting on the inner cylinder,  $L$  is the height of the inner cylinder,  $D_i$  is the diameter of the inner cylinder,  $\omega$  is the angular velocity and  $D_o$  is the diameter of the outer cylinder. Since in deriving Eq. (3.10) the assumption of infinite cylinders was made, a correction for the end effects is required (Jones and Bartlett, 1952).

Bockris and MacKenzie (1959), showed that rotational methods are not suitable for melts with viscosities lower than 10 mPa.s. The application of rotational methods for low-viscosity liquids such as molten salts and liquid metals studied in the present work is technically difficult. In order to obtain the necessary sensitivity to measure low viscosities, the clearance between the stationary and the rotating cylinder has to be made very small and therefore it is difficult to maintain the system coaxially. To obtain accurate viscosity values it is critical that the cylinders rotate axysymmetrically (Brooks et al., 2005). This method has not been used for viscosity measurements of molten chlorides and only a few experimental groups employed this technique for liquid metals (Jones and Bartlett, 1952; Moraru et al., 1997; Hur et al., 2003).

### 3.4 Other Methods

There are other viscometers such as gas bubble viscometer (Friedrichs et al., 1997), electrostatic levitator (Rhim and Ohsaka, 2000; Zhou et al., 2003) and dynamic methods (Roach et al., 2001; Roach and Henein, 2005) which have been employed for viscosity measurement of liquid metals. These methods are either more convenient for high-viscosity liquids or are still under development; therefore they have not been widely used for viscosity measurement of liquid metals.

### 3.5 Choice of Experimental Technique for Molten Salts and Liquid

#### Metals

As it will be shown in the following sections, the molten salts and metallic systems studied in the present work usually have melting points higher than  $\sim 800\text{K}$  and viscosities lower than  $\sim 5\text{ mPa}\cdot\text{s}$ . Only a few viscosity measurement methods are suitable for such high temperature, low viscosity systems. Figure 3-1 summarizes the methods proposed for high temperature viscosity measurements. According to Bockris and MacKenzie (1959), falling body and rotational methods (b and c in Fig. 3.1) are not suitable for melts with viscosities lower than  $10\text{ mPa}\cdot\text{s}$  (see Section 3.3 for details). Due to the relatively low viscosity of the studied molten salts and liquid metals, special care should be taken to avoid the occurrence of turbulence and non-Newtonian behaviour during the measurements. As it will be shown in the present literature review, most of the viscosity measurements for these systems are done by capillary and oscillating body methods (a and d in Fig. 3.1). These two methods are mentioned as the two salient molten

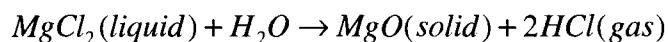
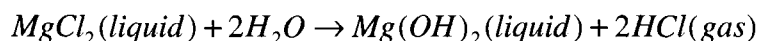
salts viscosity measurement methods, by Janz (1980) in his critical review of the experimental data for molten salts physical properties. The capillary method gives an absolute value for the viscosity without employing complicated equations. However several difficulties such as finding a suitable material for the construction of the capillary tube at high temperature measurements, the alteration in the capillary diameter resulting from slight etching and re-crystallization of the melt samples, the risk of capillary tube blockage by bubbles or oxide inclusions formed during measurements, maintaining a long zone of constant temperature in the furnace precluded the usage of this method. The capillary method has not been recommended for the viscosity measurements at temperatures higher than  $\sim 1300\text{K}$  (Janz, 1980; Iida and Guthrie, 1987).

Considering the results of the present literature review which will be shown later, oscillating body methods are widely used in molten salts and liquid metals viscometry. Relatively small zone of constant temperature, simple and highly accurate measurement of the amplitude and the period of oscillations and wider choices for container material, made these methods convenient for viscosity measurement at high temperatures (Janz, 1980). The oscillating cylinder and oscillating vessel methods have been favored since the cylinders are simpler to re-machine and can be machined to more exact tolerances than a sphere (Dumas et al., 1970; Janz, 1980; Torklep and Øye, 1981). The disadvantages of these methods would appear to be the mathematical complexities of deriving the working formulas which relate the measured parameters to the viscosity. There are a number of mathematical treatments available which appear to yield different

results with the same experimental data (Janz, 1980; Iida and Guthrie, 1987). The advent of computer-assisted techniques though has eased this consideration.

Since the studied liquid metals are mostly volatile at high temperatures, the oscillating vessel method seems to be favored for these systems. As it is previously discussed in Section 3.1.1, in this method, the melt samples are contained in a small closed cup which is proper for highly volatile and corrosive melts. The disadvantage of this method is the unavoidable meniscus effect for partly filled cups (see Section 3.1.3.1). However this effect can be eliminated for completely filled cups which is extremely difficult to achieve with molten salts (Torklep and Øye, 1981). Hence the oscillating cylinder method seems to lead to more accurate viscosity values for molten salt systems (Janz, 1980; Torklep and Øye, 1981).

It is important to point out that due to the high reactivity of the studied melts at high temperatures; there is always the risk of hydrolysis due to even fine traces of moisture. This can lead to the formation of solid oxides, gases or liquid hydroxides which can affect the accuracy of the measurements. Examples of these reactions for molten  $MgCl_2$  are as follows:





## 4 Viscosity Models for Molten Salts and Liquid Metals

There are several approaches to model the viscosity of liquids. Some theoretical approaches based on statistical mechanical theories provide rigorous theoretical expressions for the viscosity. Although these theories may lead to good results for gases, in the case of liquids since the mechanism of the momentum transport is more complicated, they may face several problems. These approaches are usually mathematically complicated and several approximations are required to obtain a simpler equation that can actually lead to a reasonable viscosity value. These approximations are based on several concepts and assumptions which are not necessarily the same for all liquids or liquid mixtures. Therefore these equations cannot lead to satisfactory results compared to the experimental viscosity values and are not simply extendable to multi component systems. These kinds of models are called theoretical models in the present work. As we will see in the following sections, these theoretical models, are mostly concerned about the viscosity of a pure liquid at a given state point. They are not yet capable of explaining the composition dependency of viscosity in liquid mixtures.

In the lack of a practical mathematical expression for liquids which leads to a physically sound viscosity model, several authors proposed different “mechanisms” for viscous flow by assuming a certain liquid model. Others attempted to find a functional relationship between the viscosity and other well defined liquid properties or just simply find an equation which best fits their data. We recall the mentioned types of models, as semi-empirical (semi-theoretical) and empirical models, respectively. As it will be discussed in the following sections, these models are mostly concerned about the temperature

dependency of viscosity. Only a few attempts have been made to explain the viscosity behavior of binary liquid mixtures as a function of composition. However these proposed models are only applicable on some specific binary systems and can not be easily extended to other binary systems or multi component liquid mixtures. At the best they can only give a qualitative prediction of the viscosity behavior for multi component systems. In the following sections after a brief overview of several proposed viscosity models, the composition-dependent viscosity model employed in the present work is presented and modified for highly short-range ordered molten chloride systems. As it will be shown in the following sections, the presented model leads to satisfactory results compared to the experimental data and can be easily extended to multi component systems with a few parameters.

## **4.1 Viscosity Models for Pure Liquids**

### **4.1.1 Theoretical Models**

The mechanism of momentum transport in low molecular weight liquids is different from the one of gases. Viscosity of a gas can be obtained through the classical kinetic theory of gases by assuming that the gas is composed of elastic spheres whose diameters are small compared to their average distance between the molecules. The main role in momentum transport in gases is being played by individual molecules moving randomly between layers of gas with different velocities. However in liquids, due to their higher densities,

usually the average distance between molecules<sup>§</sup> is not much greater than the effective range of intermolecular forces. Therefore the mentioned mechanism for momentum transport is usually overshadowed by the action of intermolecular forces between the nearest neighbours (Reid and Sherwood, 1966). In the statistical mechanical theory of liquids, these interactive forces and energies are assumed to be dominated by the sum of pair interactions. Hence, the viscosity of a liquid can be obtained by defining two basic quantities, the pair distribution functions and the pair potentials. Born and Green (1947) proposed the following equation in terms of these two basic quantities; the pair distribution function  $g(r)$  and the pair potential  $\phi(r)$ :

$$\eta = \frac{2\pi}{15} \left( \frac{m}{\kappa T} \right)^{1/2} n_0^2 \int_0^\infty g(r) \frac{\partial \phi(r)}{\partial r} r^4 dr \quad (4.1)$$

where  $m$  is the mass of liquid components (molecules, atoms or ions),  $\kappa$  is the Boltzmann's constant,  $T$  is the absolute temperature and  $n_0$  is a factor depending on the radial distribution functions. Pair distribution functions can be obtained experimentally using either x-ray, neutron or electron diffractions (Edwards et al., 1978; Biggin and Enderby, 1981; Enderby and Biggin, 1983) or computed by employing Monte Carlo and molecular dynamics simulation techniques (Parrinello and Tosi, 1979). However derivation of calculable, rigorous expressions for these quantities is difficult since the atomic motions in liquids cannot be precisely described as a function of time (Iida and Guthrie, 1987). Consequently several approximate methods based on different concepts

---

<sup>§</sup> For the case of molten chlorides, there are ions that interact with each other and the forces will be interionic forces. For the case of liquid metals there are atoms that interact and the forces would be interatomic forces.

have been proposed in the literature (Longuet-Higgins and Pople, 1956; Rice and Kirkwood, 1959; Forster et al., 1968; Faber, 1972). Some of these expressions have been used to calculate the viscosity values of liquid metals (Bansal, 1973; Bansal, 1973; Kitajima et al., 1976). However they did not lead to satisfactory results from the view point of metallurgical engineering. From a theoretical point of view, the validity of Eq. (4.1) and the accuracy of the calculations for the pair potentials need thorough investigation (Iida and Guthrie, 1987).

For the case of molten salts, the viscosity of some molten alkali halides has been studied by several authors through molecular dynamics simulations. Most of them obtained the radial distribution functions by employing the Born-Mayer-Huggins-Tosi-Fumi (BMHTF) interionic potentials (Born and Mayer, 1932; Huggins and Mayer, 1933; Mayer, 1933; Huggins, 1937; Huggins, 1937; Fumi and Tosi, 1964; Tosi and Fumi, 1964). However these simulated viscosities have been reported only for a single state point. The temperature or density dependence of viscosity has not been the primary focus of these studies (Galamba et al., 2004). In particular we can point to the equilibrium molecular dynamics (EMD) simulation of molten NaCl and KCl performed by Sindzingre and Gillan (1990), non-equilibrium molecular dynamics (NEMD) simulation done by Ciccotti et al. (1976) for six molten alkali halides (LiF, NaCl, NaI, KI, RbCl and RbI) and by Delhomelle and Petravic (2003) for sodium chloride (NaCl). Only Galamba et al. (2004; 2005) investigated the viscosity of NaCl and KCl through both EMD and NEMD simulations at several state points.

The molecular dynamics simulations are still under development and the accuracy of these methods needs to be explored in order to extend these simulations to more complex and industrially important systems. The importance of development of these methods is more emphasized for viscosity determinations at high shear rates which are out of the access of the experimental methods.

#### 4.1.1.1 Viscosity Behaviour of Molten Salts at High Shear Rates

Molten salts as well as most of the Newtonian fluids, exhibit non-Newtonian behaviour at high shear rates. Delhommelle and Petravic (2003) showed that after a certain strain rate, molten salts exhibit shear thinning behaviour. Their viscosity becomes shear rate dependent and decreases with increasing strain rate (Fig. 2.2c). To study the complete rheology of the melt, the viscosity at both Newtonian and non-Newtonian regions, is required. Viscosity at low shear rates (the Newtonian region or zero shear viscosity)  $\eta_0$  can be obtained through experimental methods while the high shear rate viscosities ( $\eta$ ) which are extremely difficult to obtain experimentally, can be calculated through NEMD simulations (Galamba et al., 2005). However, NEMD simulations can only be employed for high shear rate viscosities since at low shear rates the signal-to-noise ratio is very small and difficult to identify for the simulations. The crossover point from Newtonian to Non-Newtonian region is usually at a strain rate that is too high to be accessed by experiment but also too low to be calculated by NEMD simulations (Borzsak et al., 2002). If one could find a relationship to extrapolate the non-Newtonian viscosities ( $\eta$ ) through the Newtonian region, then the NEMD results could be compared with the

experimental data and also EMD results. Several approaches have been proposed in the literature to obtain the Newtonian viscosities ( $\eta_0$ ) from the  $\eta$  NEMD data (Travis et al., 1998; Yang et al., 2000; Borzsak et al., 2002; Delhommelle and Petravic, 2003). Galamba et al. (2005) employed two of these proposed approaches to obtain  $\eta_0$  values from their NEMD viscosity data. One approach was a linear extrapolation using the following equation:

$$\eta = \eta_0 - A\dot{\gamma}^\beta \quad (4.2)$$

with the value of  $\beta$  being 0.5 with respect to the mode-coupling theory prediction for three-dimensional fluids in the limit of zero shear rate (Kawasaki and Gunton, 1973):

$$\lim_{\dot{\gamma} \rightarrow 0} \eta = \eta_0 - A\dot{\gamma}^{0.5} \quad (4.3)$$

The other approach was fitting the NEMD viscosity data to a simplified Carreau equation (Carreau et al., 1997) of the following form:

$$\frac{\eta}{\eta_0} = \left[ 1 + (\lambda\dot{\gamma})^2 \right]^{(n-1)/2} \quad (4.4)$$

where  $\lambda$  is a time constant for the fluid and  $n$  is a parameter describing the slope of the decreasing portion of the  $\eta$  curve.

In Tables 4.1 and 4.2 the extrapolated NEMD results from both approaches are compared with the EMD simulation results and the experimental data for NaCl and KCl pure salts, respectively.

Table 4.1: Newtonian Viscosities for the BMHTF and MWGKL Models of NaCl

Calculated from GK-EMD and NEMD Simulations (Galamba et al., 2005).

T (K)	$\rho$ (g cm <sup>-3</sup> )	<i>Simulations Based on BMHTF Potential Model</i>			<i>Simulations Based on MWGKL Potential Model</i>			<i>Exp.</i>
		$\eta_{\text{Carreau}}$ (mPa.s)	$\eta_{\text{MC}}$ (mPa.s)	$\eta_{\text{GK-EMD}}$ (mPa.s)	$\eta_{\text{Carreau}}$ (mPa.s)	$\eta_{\text{MC}}$ (mPa.s)	$\eta_{\text{GK-EMD}}$ (mPa.s)	$\eta$ (mPa.s)
1100	1.5420	1.129	1.289	1.193	1.154	1.358	1.228	1.00
1200	1.4878	0.906	1.055	0.916	...	...	0.978	0.834
1300	1.4335	0.747	0.852	0.833	...	...	0.859	0.713
1400	1.3793	0.636	0.710	0.702	...	...	0.710	0.624
1500	1.3250	0.547	0.605	0.590	...	...	0.603	0.555

Table 4.2: Newtonian Viscosities for the BMHTF and MWGKL Models of KCl

Calculated from GK-EMD and NEMD Simulations (Galamba et al., 2005).

T (K)	$\rho$ (g cm <sup>-3</sup> )	<i>Simulations Based on BMHTF Potential Model</i>			<i>Simulations Based on MWGKL Potential Model</i>			<i>Exp.</i>
		$\eta_{\text{Carreau}}$ (mPa.s)	$\eta_{\text{MC}}$ (mPa.s)	$\eta_{\text{GK-EMD}}$ (mPa.s)	$\eta_{\text{Carreau}}$ (mPa.s)	$\eta_{\text{MC}}$ (mPa.s)	$\eta_{\text{GK-EMD}}$ (mPa.s)	$\eta$ (mPa.s)
1050	1.5236	1.170	1.36	1.156	1.213	1.29	1.177	1.086
1100	1.4945	1.029	1.20	1.084	...	...	1.058	0.954
1200	1.4362	0.806	0.941	0.838	...	...	0.927	0.759
1250	1.4070	0.730	0.847	0.811	...	...	0.784	0.687
1300	1.3779	0.683	0.774	0.687	...	...	0.708	0.555

where  $\eta_{Carreau}$  and  $\eta_{MC}$  stand for the extrapolated Newtonian viscosity values calculated by fitting the NEMD viscosity data ( $\eta$ ) to Eqs. (4.4) and (4.3), respectively.  $\eta_{GK-EMD}$  stands for the calculated viscosity values by GK-EMD simulations. The experimental data are taken from the NIST 1992 database (Janz, 1992). These results are illustrated in Fig. 4.1.

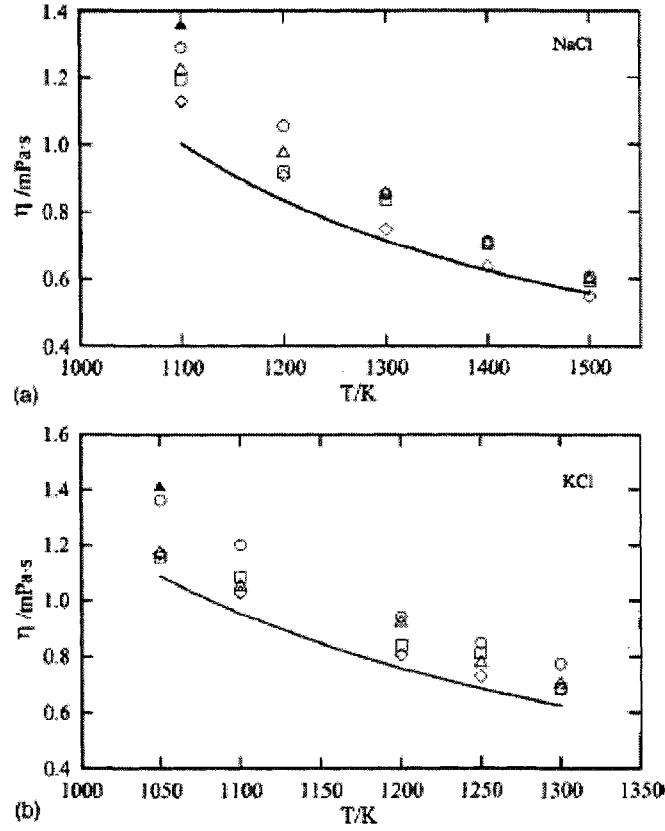


Figure 4.1: Comparison Between the Simulated and Experimental Viscosity Values for (a) NaCl and (b) KCl (at the limit of zero shear rate). Solid Line: Janz (1992);  $\blacktriangle$ GK-EMD-BMHTF;  $\triangle$ GK-EMD MWGKL;  $\blacksquare$ NEMD-BMHTF-MC;  $\blacktriangle$ NEMD-MWGKL-MC;  $\blacklozenge$ NEMD-BMHTF-Carreau; (Galamba et al., 2005).



According to simulations done by Galamba et al. (2005), the crossover point from Newtonian to non-Newtonian behaviour for NaCl and KCl at the given temperatures is expected to be at the shear rates around  $0.2 \times 10^{12} \text{ s}^{-1}$  ( $\log \dot{\gamma} = 2 \text{ ns}^{-1}$ ) as it is illustrated in Figs. 4.2 and 4.3.

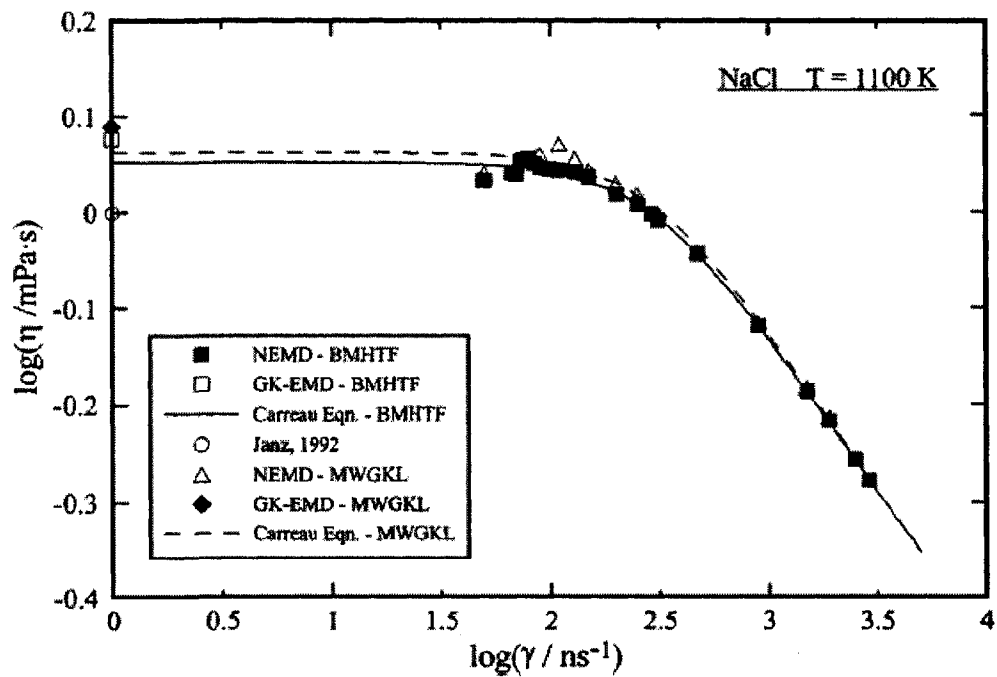


Figure 4.2: Logarithm of the NEMD Shear Viscosity Against the Logarithm of Strain Rate for NaCl at 1100K (Galamba et al., 2005).

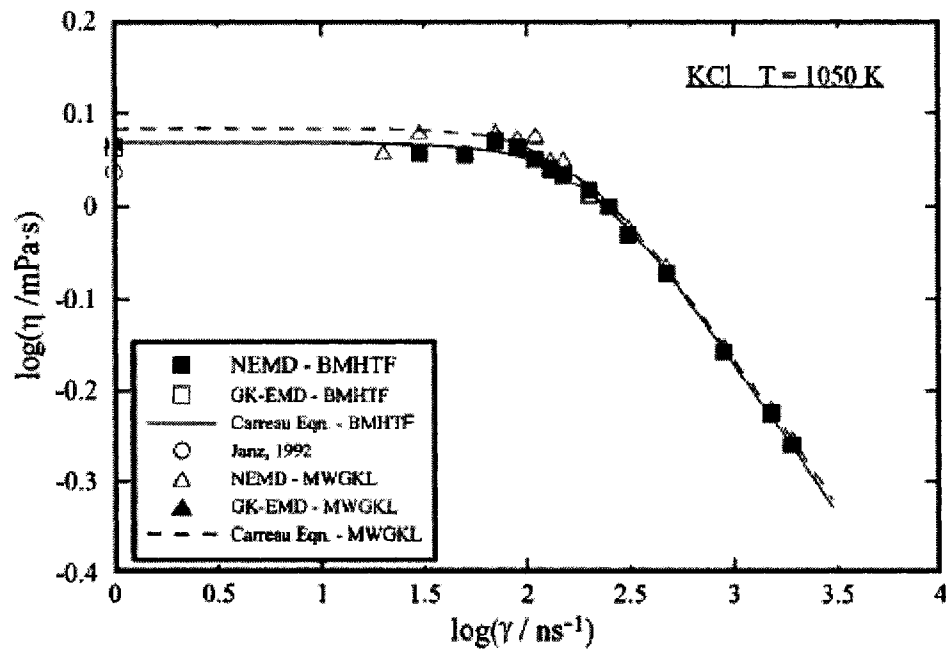


Figure 4.3: Logarithm of The NEMD Shear Viscosity Against the Logarithm of Strain Rate for KCl at 1050K (Galamba et al., 2005).

At the shear rates higher than  $0.2 \times 10^{12} \text{ s}^{-1}$ , the simulated viscosity behaviour turns to shear thinning non-Newtonian behaviour. However as it is shown in Figures 4.4 and 4.5, the simulated crossover point is shifted to the higher shear rates by increasing the temperature.

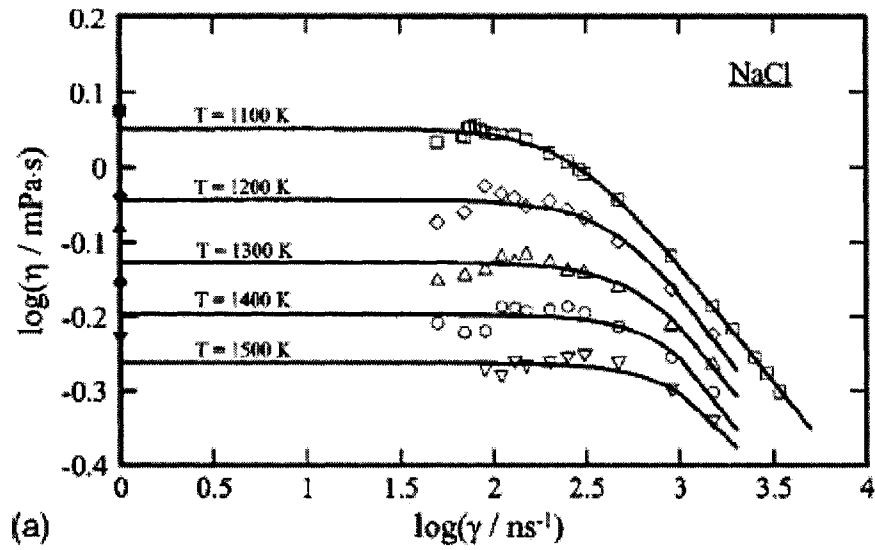


Figure 4.4: Logarithm of the NEMD Shear Viscosity Against the Logarithm of the Strain Rate at Different Temperatures for NaCl (Galamba et al., 2005).

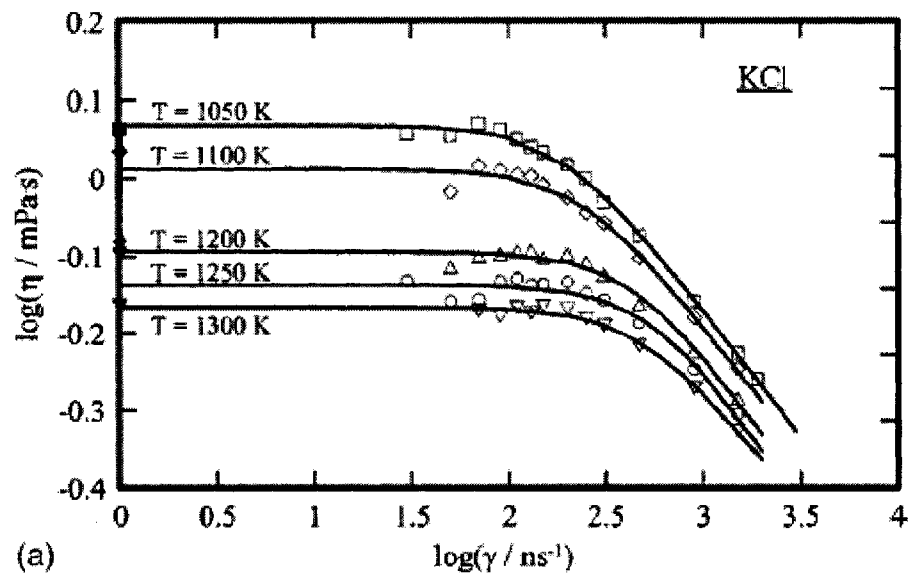


Figure 4.5: Logarithm of the NEMD Shear Viscosity Against the Logarithm of the Strain Rate at Different Temperatures for KCl (Galamba et al., 2005).

According to these simulations, the enlargement of Newtonian region is expected by increasing the temperature Galamba et al. (2005).

#### **4.1.2 Semi-Empirical (Semi-Theoretical) Models**

As it is discussed in the last section, theoretical models are mostly concerned about the viscosity of a pure liquid at a given state point. A few theoretical attempts have been made to study the temperature dependency of the viscosity (Galamba et al., 2004; 2005). However the composition dependency of the viscosity in liquid mixtures has not been yet the primary focus of these studies. The theoretical models are usually mathematically complicated models based on several concepts employing various parameters which are not simply extendable to multi component systems. For the modeling purposes it is impractical to expect an exact mathematical treatment for liquid viscosities. However simply dealing with empirical formulas, cannot give a general result applicable for different systems. Semi- empirical (semi-theoretical) models propose an approach for using the knowledge of molecular structure of the melt along with some adjustable parameters determined most of the time from the experimental data. Well-known examples of this kind of models proposed for liquids are the quasi-crystalline theory of Andrade (1934), the free volume theory of Cohen and Turnbull (1959) and the theory of Eyring (1941) which will be discussed in the following sections. Several authors have developed correlations for the viscosity of pure liquids based on the theory of corresponding states (Pitzer, 1939; Rice and Kirkwood, 1959; Helfand and Rice, 1960). The applicability of this approach for pure ionic salts has been investigated by Reiss et al. (1961), Abe and Nagashima (1981), Young and O'Connell (1971) and Janz et al. (1989)

and for pure liquid metals by Chapman (1966), Pasternak (1972), Wittenberg and Dewitt (1973) and Waseda and Ohtani (1975).

The above mentioned model theories are based on phenomenological parameters which in many cases must be determined experimentally (Iida and Guthrie, 1987).

#### 4.1.2.1 The Quasi-Crystalline Theory of Andrade

Andrade (1934) assumed a quasi-crystalline structure for the liquid in which each atom<sup>\*\*</sup> is confined within a fairly small space and interacts directly only with a few neighbors. The momentum transport from one layer to a neighboring one occurs as a result of atomic vibrations. According to Andrade, the atoms in the liquid (at the melting point) execute vibrations about their equilibrium positions in random directions and periods just as if they were in the solid state. Andrade derived the following equation for the viscosity of simple monatomic liquids close to their melting point.

$$\eta = \frac{4}{3} v \frac{M_A}{a} \quad (4.5)$$

where  $M_A$  is the atomic mass, and  $a$  is the average distance between the atoms.  $v$  is the characteristic frequency of vibration which is defined by Lindemann (1910) as follows:

$$v = C_L \left( \frac{T_m}{M V_M^{2/3}} \right)^{1/2} \quad (4.6)$$

where  $C_L$  is the constant of Lindemann ( $2.8 \times 10^{12}$  in SI units),  $T_m$  is the melting temperature,  $M$  is the molar mass and  $V_M$  is the molar volume at the melting point.

---

<sup>\*\*</sup> Depending on the constituents of liquid, it can be molecules, ions etc.

Assuming  $a = (\text{Atomic Volume})^{1/3}$ , Andrade proposed the following equation for the viscosity at the melting point:

$$\eta|_{T_m} = C_A \frac{(M_A T_m)^{1/2}}{V_M^{2/3}} \quad (4.7)$$

where  $C_A$  is a constant.

Although Andrade's derivation seems unconvincing from the view point of the present theories of liquid, his equation reproduces the experimental viscosity data for liquid metals at their melting points with fairly good agreement (Iida and Guthrie, 1987). Since the concepts of his model were applicable only to temperatures close to the melting point, Eq. (4.7) could not lead to satisfactory results for higher temperatures. Andrade proposed the following equation for the temperature variation of the viscosity:

$$\eta = \frac{A}{V_M^{1/3}} \exp\left(\frac{B}{V_M T}\right) \quad (4.8)$$

where  $A$  and  $B$  are constants,  $V_M$  is the molar volume and  $T$  is the absolute temperature. Although there is no rigorous theoretical explanation for Eq. (4.8), it has been employed by many investigators to fit the experimental viscosity data of liquid metals with a high degree of accuracy (Iida and Guthrie, 1987).

#### 4.1.2.2 The Free Volume Theory of Cohen and Turnbull

According to Cohen and Turnbull (1959), liquid atoms are assumed as hard spheres interacting with only repulsive forces and are confined in cages surrounded by their neighbors. The fluctuation in the local density provides large enough holes to allow the

displacement of the atoms. The momentum transport occurs through the jumps of the atoms into the adjacent holes; hence the viscosity can be calculated as a function of the jump probability. Assuming that the holes are distributed with different sizes within the liquid, the probability of jumps is determined by the chance of finding an adjacent free volume of sufficient size to jump into. A local free volume ( $v_f$ ) is associated with each atom and a distribution of local free volumes is defined as follows:

$$p(v_f) = \frac{\alpha}{\bar{v}_f} \exp\left(-\frac{\alpha v_f}{\bar{v}_f}\right) \quad (4.9)$$

where  $p(v_f)$  is the probability of each atom to find its associated free volume ( $v_f$ ) nearby,  $\bar{v}_f$  is the average free volume per atom and  $\alpha$  is a correction factor (lying between 1/2 and 1) for the overlapping free volumes. Assuming that a minimum volume ( $v^*$ ) is necessary for a jump to occur, the probability of a jump ( $P_v$ ) can be calculated by the following equation:

$$P_v = \int_{v^*}^{\infty} p(v_f) dv_f = \exp\left(-\frac{\alpha v^*}{\bar{v}_f}\right) \quad (4.10)$$

By assuming that the quantity  $v^*$  is close to the atomic volume ( $V_A$ ), the hard sphere viscosity equation is given by Eq. (4.11).

$$\eta = \frac{A}{P_v} = A \exp\left(\frac{\alpha V_A}{\bar{v}_f}\right) \quad (4.11)$$

where  $\eta$  is the viscosity of liquid and  $A$  is a constant. Although the free volume ( $v_f$ ) has both the temperature-dependency and pressure-dependency, the model fails to explain the temperature and pressure dependencies of various liquids (Jhon and Eyring, 1978).

#### 4.1.2.3 The Theory of Eyring

The theory developed by Eyring and coworkers (Glasstone et al., 1941; Eyring et al., 1962; Eyring et al., 1964), gives a qualitative explanation for the mechanism of momentum transfer in liquids. Based on this mechanism, viscosity can be obtained from other physical properties of liquid by means of a few experimental parameters.

In Eyring's theory, the liquid is regarded as a lattice with some sites occupied by molecules and others empty (vacancy or hole). The liquid molecules are constantly in motion within cages made by their nearest neighbours. This cage is characterized by an energy barrier of height  $G_0^*/N_A$  where  $G_0^*$  is the molar viscous activation energy for a molecule to escape from the cage in a liquid at rest and  $N_A$  is the Avogadro's number. According to Eyring, at a time that a molecule gains the required activation energy ( $G_0^*/N_A$ ), it escapes from the cage into an adjacent hole. Thus the molecules move in each of the coordinate directions by jumps of length  $a$  at a frequency  $\nu$  per atom. The frequency is given by the rate equation as follows:

$$\nu = \frac{\kappa T}{h} \exp\left(\frac{-G_0^*}{RT}\right) \quad (4.12)$$

where  $\kappa$  and  $h$  are Boltzman and Planck constants respectively,  $R$  is the gas constant and  $T$  is the absolute temperature. When a shear stress ( $\tau_{yx}$ ) is applied on the liquid, this



frequency will change. If we assume a liquid which is flowing in the  $x$  direction with a velocity gradient  $dv_x/dy$ , the frequency of forward and backward jumps ( $\nu^+$  and  $\nu^-$  respectively) can be defined as follows:

$$\nu^\pm = \frac{\kappa T}{h} \exp\left(\frac{-G^*}{RT}\right) \quad (4.13)$$

$$G^* = G_0^\pm \mp \left(\frac{a}{\delta}\right) \left(\frac{\tau_{yx} V_M}{2}\right) \quad (4.14)$$

where  $G^*$  is the molar viscous activation energy under the applied stress  $\tau_{yx}$ ,  $V_M$  is the molar volume,  $a$  is the distance traveled per jump and  $\delta$  is the distance between the adjacent layers of liquid as it is shown in Fig. 4.6.

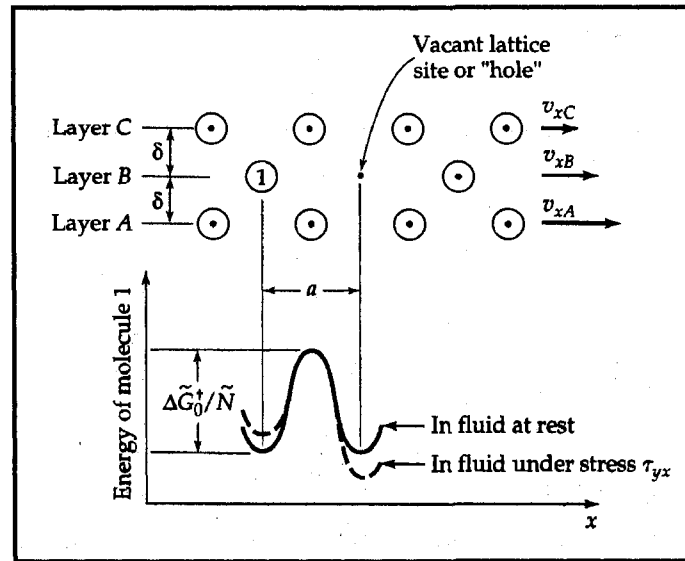


Figure 4.6: Schematic of an Escape Process in the Flow of Liquid (Bird et al., 2002).

The net velocity ( $v_{xA} - v_{xB}$ ) with which molecules in layer  $A$  slip ahead of those in layer  $B$  is the distance traveled per jump ( $a$ ) times the net frequency of forward jumps ( $\nu^+ - \nu^-$ ) as follows:

$$v_{xA} - v_{xB} = a(\nu^+ - \nu^-) \quad (4.15)$$

If the velocity profile considered to be linear over the very small distance  $\delta$  between the layers  $A$  and  $B$ , the velocity gradient can be given by the following equation:

$$-\frac{dv_x}{dy} = \left(\frac{a}{\delta}\right)(\nu^+ - \nu^-) \quad (4.16)$$

Combining Eqs. (4.13), (4.14) and (4.16) gives:

$$-\frac{dv_x}{dy} = \left(\frac{a}{\delta}\right) \left(\frac{\kappa T}{h} \exp\left(\frac{-G_0^*}{RT}\right)\right) \left(2 \sinh \frac{a\tau_{yx} V_M}{2\delta RT}\right) \quad (4.17)$$

Usually  $\frac{a\tau_{yx} V_M}{2\delta RT} \ll 1$  thus by means of a Taylor series<sup>††</sup>, it can replace the term

$\left(\sinh \frac{a\tau_{yx} V_M}{2\delta RT}\right)$  in Eq. (4.17). Then the viscosity can be obtained through the

Newtonian's law of viscosity (Eq. 2.1) as follows:

$$\eta = \left(\frac{\delta}{a}\right)^2 \frac{hN_A}{V_M} \exp\left(\frac{G_0^*}{RT}\right) \quad (4.18)$$

The factor  $\frac{\delta}{a}$  can be taken to be unity without any loss of accuracy since  $G_0^*$  is usually determined empirically to make the equation (4.18) agree with the experimental viscosity data (Bird et al., 2002).

---

<sup>††</sup> Taylor series:  $\sinh x = x + (1/3!)x^3 + (1/5!)x^5 + \dots$

As it will be shown in the next section, the simplified Eyring's equation is similar to the temperature dependence in the Arrhenius form which is used by several authors to fit the experimental viscosity values of various molten salts and liquid metals (Dumas et al., 1973; Brooks et al., 2005).

#### 4.1.3 Empirical Models

Most of the data found for liquid viscosity are presented by an empirical formula proposed by the experimentalists. These empirical formulas give a functional relationship between viscosity and some other physical properties. The most popular empirical formula for liquid viscosity is an Arrhenius-type function of the following form:

$$\eta = A \cdot \exp\left(\frac{E_\eta}{RT}\right) \quad (4.19)$$

where  $A$  and  $E_\eta$  are constants,  $T$  is the absolute temperature and  $R$  is the gas constant.

$E_\eta$  is usually regarded as the activation energy for viscous flow.

This relationship which is similar to the simplified Eyring's equation (Eq. 4.18) has been found for several liquid metals and molten salts over a wide range of temperature (Hertzberg et al., 1980; Iida and Guthrie, 1987; Janz et al., 1989). In order to estimate viscosity values for liquid metals, Grosse (1964; 1964) proposed an approach to relate the constants  $A$  and  $E_\eta$  to well-known parameters of liquid such as molar volume and melting temperature. According to him, the constant  $A$  can be obtained by using Andrade's formula (Eq. 4.7) for the viscosity at melting point:

$$A = \frac{C_A (MT_m)^{1/2}}{V_M^{2/3} \exp(E_\eta / RT_m)} \quad (4.20)$$

He indicated that there is a simple empirical relation between activation energy ( $E_\eta$ ) for liquid metals and their melting point ( $T_m$ ). Iida et al. (Iida et al., 1975) proposed the following relationship for the activation energy of liquid metals:

$$E_\eta = aT_m^b \quad (4.21)$$

where  $a$  and  $b$  are constants. They obtained different numerical values of  $a$  and  $b$  for pure normal metals and semi-metals.

In the case of molten salts, to obtain a better fit of the experimental data, addition of a second-order temperature term to the Arrhenius equation has been proposed by Hertzberg et al. (1980):

$$\eta = A \exp\left(\frac{B}{T} + \frac{C}{T^2}\right) \quad (4.22)$$

where  $A$ ,  $B$  and  $C$  are constants. However, since the parameters  $A$ ,  $B$  and  $C$  are strongly correlated, the conversion problems may appear while estimating the parameters. Hertzberg et al. suggested a re-parameterization to minimize the numerical problems in the model fitting:

$$\eta = a \exp\left[b\left(\frac{1}{T} - \frac{1}{T_{avg.}}\right)\right] \quad (4.23)$$

$$\eta = a \exp\left[b\left(\frac{1}{T} - \frac{1}{T_{avg.}}\right) + c\left(\frac{1000}{T} - \frac{1000}{T_u}\right)^2 - \left(\frac{1000}{T_{avg.}} - \frac{1000}{T_u}\right)^2\right] \quad (4.24)$$

where  $a$ ,  $b$  and  $c$  are much less correlated constants than the constants of Eq. (4.22),  $T_{avg.}$  is chosen as an arbitrary mean temperature and  $T_u$  is an additional arbitrary temperature to obtain the curvature of the fit.

Eqs. (4.23) and (4.24) have been used to describe the temperature dependence of several pure molten alkali and alkaline-earth chlorides (Torklep and Øye, 1979; Brockner et al., 1981; Torklep and Øye, 1982).

## 4.2 Viscosity Models for Binary Liquid Solutions

As it was discussed in the previous sections, several theoretical, semi-empirical and empirical models have been proposed for the viscosity of pure liquids. However due to the increasing demand of the viscosity knowledge for several industrial requirements, it is practical if one could predict the viscosity of more complex and industrially important systems from the properties of the pure components. Among the mentioned viscosity models, the theoretical models were mostly concerned about the viscosity of a pure liquid at a given state point. These theoretical studies proposed mathematically complicated models based on several concepts and approximations which are not necessarily the same for all systems. Usually the extension of these models to higher order systems is not a simple task and requires complicated mathematical approaches. However as we previously discussed in Section 4.1.1, the accuracy of the existing theoretical models still needs to be explored in order to extend them to binary and multi-component systems.

In the lack of a practical theoretical model for the viscosity of liquid mixtures, several attempts have been made to extend the existing semi-empirical and empirical viscosity

models to binary and multi-component systems. However as it was discussed in Section 4.1.1, the viscosity of liquids is dependent partly on the atomic or ionic motions and strongly on the interatomic or interionic forces between nearest neighbors. Depending on the characteristics of the mixtures, the interactions between different species and the bonding energies may undergo several changes upon mixing. Therefore the viscosity of a liquid mixture is expected to be not only temperature dependent but also composition dependent. As it was shown in the previous sections, the existing semi-empirical and empirical models could in some cases satisfactorily describe the temperature dependency of the viscosity for several pure liquids. The addition of composition dependent terms seemed to be a reasonable approach to extend these models to binary and multi-component systems. This is done by a few authors for binary mixtures of molten salts and liquid alloys. However as it will be shown later in this section and in the following section, most of the proposed composition dependent terms are only applicable to some specific binary systems and cannot be simply extended to multi-component systems.

Based on the quasi-crystalline theory of Andrade, Hirai (1992) suggested employing Eqs. (4.19), (4.20) and (4.21) to calculate the viscosity of liquid alloys by replacing the melting temperature by the temperature of liquidus. Hirai calculated the relevant parameters for several liquid alloys and found fairly well results comparing to the experiments. However Hirai's proposed model would imply that the composition dependency of the viscosity isotherms should exhibit the same trend as the liquidus which is not necessarily the case for all alloy systems.

Dumas and co-workers (Dumas et al., 1973; Brockner et al., 1979) employed the Arrhenius empirical equation to describe the viscosity behaviour of binary molten salt systems. They suggested the following Arrhenius equations for the temperature and composition dependencies of the viscosity for ideal mixtures assuming no enthalpy or volume changes upon mixing:

$$\eta_i = A_i \exp(E_i / RT) \quad (4.25)$$

$$\ln \eta = \sum X_i \ln \eta_i \quad (4.26)$$

where  $\eta_i$  and  $X_i$  are the viscosity and mole fraction of component  $i$  respectively,  $\eta$  is the viscosity of liquid mixture and  $A_i$  and  $E_i$  are adjustable parameters for component  $i$ . Assuming the pre-exponential factor in Eq. (4.25) to be equal for all the pure components, Eq. (4.26) can be justified theoretically by Eyring's theory in the following form:

$$\eta = \frac{hN_A}{V_M} \exp\left(\frac{G^*}{RT}\right) \quad (4.27)$$

$$G^* = \sum X_i G_i^* \quad (4.28)$$

where  $h$  is the Planck's constant,  $N_A$  is the Avogadro's number,  $V_M$  is the molar volume and  $G^*$  and  $G_i^*$  are the molar viscous activation energies of liquid mixture and component  $i$  respectively. Dumas et al. (1973) proposed the addition of an excess molar viscous activation energy ( $G_E^*$ ) to Eq. (4.28) for non-ideal mixtures to take into account the activation energy changes upon mixing:

$$G^* = \sum X_i G_i^* + G_E^* \quad (4.29)$$

According to them, the viscosity of a binary mixture with components 1 and 2 is given by the following equation:

$$\eta = \frac{hN_A}{V_M} \exp\left(\frac{X_1 G_1^* + X_2 G_2^* + G_E^*}{RT}\right) \quad (4.30)$$

They obtained the experimental values of  $G_E^*$  for several binary mixtures of alkali and alkaline-earth chlorides and suggested the following simple equation to fit their  $G_E^*$  values (Østvold, 1971; Dumas et al., 1973):

$$G_E^* = X_1 X_2 b^* \quad (4.31)$$

where  $b^*$  is a constant they called the excess parameter. Although their proposed model reproduced their binary data well, it could not easily be extended to multi component systems. For systems with more than two components, they have only qualitatively predicted the viscosity behaviour; no exact relationship has been proposed to predict the viscosity of multi-component systems as a function of temperature and composition.

McAllister (1960) suggested a different approach to take into account the composition dependency of the viscous activation energy of a mixture. He assigned an activation energy and a probability of occurrence to each possible interaction between liquid species (Fig. 4.7 and Table 4.3).



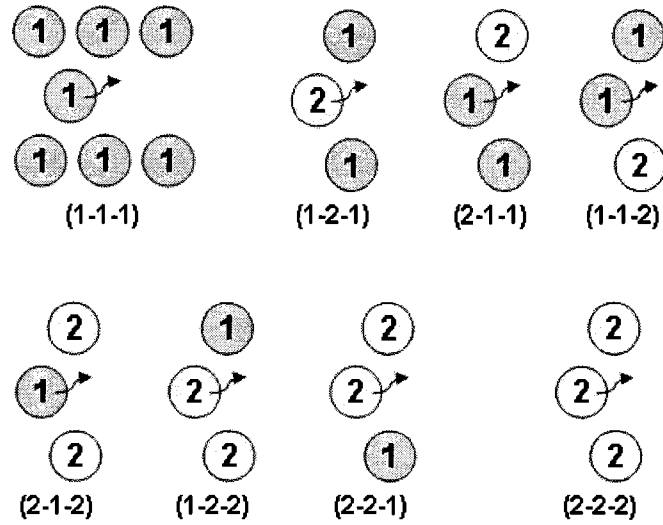


Figure 4.7: Types of Interactions in a Binary Mixture (Assuming a Three-Body Model)

(McAllister, 1960).

Table 4.3: Different Possible Types of Viscosity Interactions in a Binary Mixture

(McAllister, 1960).

Type of interaction	1-1-1	1-2-1	2-1-1 1-1-2	2-1-2	2-2-1 1-2-2	2-2-2
Fraction of total occurrences (assuming random mixing)	$x_1^3$	$x_1^2 x_2$	$2x_1^2 x_2$	$x_1 x_2^2$	$2x_1 x_2^2$	$x_2^3$
Corresponding activation energy	$G_1^*$	$G_{121}^*$	$G_{112}^*$	$G_{212}^*$	$G_{122}^*$	$G_2^*$

McAllister proposed the following equation for the viscous activation energy ( $G^*$ ) of a binary mixture in terms of mole fractions of species ( $X_1$  and  $X_2$ ) and the assigned activation energies:

$$G^* = X_1^3 G_1^* + X_1^2 X_2 G_{121}^* + 2X_1^2 X_2 G_{112}^* + X_1 X_2^2 G_{212}^* + 2X_1 X_2^2 G_{122}^* + X_2^3 G_2^* \quad (4.32)$$

To obtain the probabilities of the interactions shown in Table 4-3, McAllister assumed the random mixing between liquid species, which is only the case for ideal binary systems. Matsumura et al. (1966) applied Eq. (4.32) to NaCl-KCl and LiCl-KCl binary mixtures and obtained the parameters of the viscous activation energies for the mentioned systems. However, random mixing of liquid species is not the case for all liquid mixtures. Moreover applying this model to multi-component systems requires several assumptions and approximations (which are not necessarily similar for all systems) and a variety of empirical parameters to take into account all possible interactions.

#### 4.2.1 Models Based on Viscosity-Thermodynamic Properties Correlations

As it was discussed in the last section, depending on the characteristics of the mixtures, the interactions between different species and bonding energy changes upon mixing may affect the viscosity. Several authors attempted to describe these effects by employing the thermodynamic properties of liquid. Since enthalpy characterizes the bonding energies and entropy represents the configurations of the atoms or ions in liquid, it may be reasonable to expect a correlation between the Gibbs energy of mixing and viscous activation energy.

The excess Gibbs energy (Eq. 4.31) suggested by Dumas and co-workers (Østvold, 1971; Dumas et al., 1973) for binary molten salts is similar to the form of molar excess Gibbs energy ( $G_E$ ) for regular solutions<sup>‡‡</sup>:

$$G_E = \Delta H_m = X_1 X_2 b \quad (4.33)$$

---

<sup>‡‡</sup> For definition of the regular solutions, see Pelton, A. D. (1997)

where  $\Delta H_m$  is the molar enthalpy of mixing. Following a bond force concept, a correlation between  $b^*$  and  $b$  with  $b^*$  having the opposite sign from  $b$ , is expected. Increasing the bond force in mixture ( $b < 0$ ) is expected to lead to positive excess viscosities ( $b^* < 0$ ). Østvold (1971) obtained the mentioned correlation between  $b^*$  and the enthalpy of mixing for  $\text{CaCl}_2\text{-NaCl}$  and  $\text{CaCl}_2\text{-KCl}$  systems. However Dumas et al. (1973) showed that this correlation will break down for systems with large negative enthalpies of mixing ( $b \ll 0$ ) such as the binary mixtures of  $\text{MgCl}_2$  with  $\text{NaCl}$  or  $\text{KCl}$ . For these systems, a surprisingly negative  $b^*$  has been observed. They related this viscosity behaviour of  $\text{MgCl}_2$ -containing binaries, to partly covalent character of  $\text{MgCl}_2$ . The negative  $b^*$  in the  $\text{MgCl}_2$ -rich region could be a result of covalent structural breakdown and in the alkali rich region a result of small enthalpies of mixing having no significant effect on the activation energy (Further discussion about their results is given in Section 5.3.7).

In the case of metallic solutions, Seetharaman and Sichen (1997) suggested an analogy between the viscous activation energy of a liquid mixture and its Gibbs energy of mixing ( $\Delta G_m$ ). The Gibbs energy of mixing for an ideal Raoultian solution can be given by the following equation (Pelton, 1997):

$$\Delta G_m = RT \sum X_i \ln X_i \quad (4.34)$$

They assumed the same ideal form for the viscous activation energy of the solutions they referred to as “regular viscosity systems”. They proposed the following expression for the viscous activation energy of the so called regular viscosity systems:

$$G^* = \sum X_i G_i^* + RT \sum X_i \ln X_i \quad (4.35)$$

where  $G_i^*$  is the viscous activation energy of the pure components that can be a function of temperature:

$$G_i^* = a + bT + cT \ln T \quad (4.36)$$

where parameters  $a$ ,  $b$  and  $c$  can be optimized from available experimental data.

For non-regular viscosity systems, they proposed an excess activation energy represented by a polynomial in the component mole fractions:

$$G_E^* = \sum_{i=1}^{n-1} \sum_{j=i+1}^n X_i X_j L_{i,j} + \sum_{i=1}^{n-2} \sum_{j=i+1}^{n-1} \sum_{k=j+1}^n X_i X_j X_k L_{i,j,k} \quad (4.37)$$

where  $L$  parameters represent the binary interactions and can be expressed as follows:

$$L_{i,j} = A + B(X_i - X_j) + C(X_i - X_j)^2 \quad (4.38)$$

where  $A$ ,  $B$  and  $C$  can be linear functions of temperature:

$$\begin{aligned} A &= A_1 + A_2 \cdot T \\ B &= B_1 + B_2 \cdot T \\ C &= C_1 + C_2 \cdot T \end{aligned} \quad (4.39)$$

The second term in the Eq. (4.37) is required for higher order interactions, when more than two species strongly affect the viscosity. Seetharaman and Sichen (1997) applied their model to several binary metallic systems and reported very good agreement with the experimental data. However to expand their model to more complicated and multi component systems, too many empirical parameters were required. Furthermore the proposed parameters in Eq. (4.37), may not necessarily take into account all the interactions in different multi-component systems with different structural characteristics

such as the systems with high degrees of ordering (see Section 4.3.3 for the description of short range ordering).

The idea of correlating the viscosity to thermodynamic properties such as enthalpy or Gibbs energy of mixing has been followed by several other authors. Moelwyn-Hughes (1961) proposed the following excess viscosity ( $\eta^E$ ) as a function of the enthalpy of mixing ( $\Delta H_m$ ) for a metallic mixture of components 1 and 2 :

$$\eta^E = -2(X_1\eta_1 + X_2\eta_2) \frac{\Delta H_m}{RT} \quad (4.40)$$

with  $X_1$  and  $X_2$ ,  $\eta_1$  and  $\eta_2$  being the mole fractions and viscosities of components 1 and 2 respectively. According to them, the viscosity of a binary alloy ( $\eta$ ) can be obtained by the following equation:

$$\eta = (X_1\eta_1 + X_2\eta_2) + \eta^E \quad (4.41)$$

However the proposed correlation (Eq. 4.40) was not particularly satisfactory for liquid metals according to Iida and Guthrie (1987). They concluded that although the transport coefficients are somehow related to thermodynamic properties, viscosity cannot be formulated in terms of only thermodynamic properties. Other factors such as the atomic sizes and atomic masses of the components may also be important for transport properties. Iida and co-workers (Iida et al., 1976; Morita et al., 1976) proposed the following equation for  $\eta^E$  of alloys in terms of atomic diameters ( $d$ ), atomic masses ( $M_{Ai}$ ) and the activity coefficients ( $\gamma_i$ ) of components:

$$\eta^E = -2(X_1\eta_1 + X_2\eta_2) \left[ \frac{5/2 X_1 X_2 (d_1 - d_2)^2}{X_1 d_1^2 + X_2 d_2^2} + 0.06(X_1 \ln \gamma_1 + X_2 \ln \gamma_2) \right] + 2(X_1\eta_1 + X_2\eta_2) \left[ \left( 1 + \frac{X_1 X_2 (M_{A1}^{1/2} - M_{A2}^{1/2})^2}{(X_1 M_{A1}^{1/2} + X_2 M_{A2}^{1/2})^2} \right) + 1 \right] \quad (4.42)$$

Values calculated from Eq. (4.42) have been compared with the experimental data for several binary alloys. For some regular or nearly regular solutions, good agreement between calculation and experiment obtained (Iida et al., 1976; Morita et al., 1976).

### 4.3 A Viscosity Model for Multi-Component Liquid Solutions

As it was discussed in the previous sections, the existing viscosity models for the liquid mixtures studied in the present work were applicable on some specific binary systems. They could not be easily extended to other binary systems or multi component liquid mixtures. At the best they could only qualitatively predict the viscosity behavior of multi component systems (Dumas et al., 1973). However this could not fulfill the increasing demand of viscosity knowledge for industrial purposes. A physically sound viscosity model was required to accurately predict the viscosity behaviour of several multi-component industrially important systems. Accordingly Robelin and Chartrand (2007) proposed a structural based viscosity model for the cryolitic melts employed in the aluminum industry. Their proposed viscosity model could satisfactorily predict the viscosity behaviour of NaF-AlF<sub>3</sub>-CaF<sub>2</sub>-Al<sub>2</sub>O<sub>3</sub> electrolyte in the ranges of composition and temperature of interest by employing a few parameters (Robelin and Chartrand, 2007). They used a simplified Eyring's equation (Eq. 4.27) to describe the temperature dependency of viscosity. As it was shown in the previous sections, one approach to

define the viscous activation energy of a liquid mixture ( $G^*$ ), was to assume the ideal mixing between components and then define an excess term to take into account the viscous activation energy changes upon mixing. For a binary system, this approach could lead to satisfactory results by employing reliable experimental data. However to extend these models to multi component systems, lengthy equations with a variety of parameters that could only be obtained experimentally were required. To overcome this problem, Robelin and Chartrand (2007) treated the activation energy changes upon mixing, in a different way. They introduced structural units in the melt and then assigned a viscous activation energy to each of these units. The activation energy for viscous flow of the liquid mixture ( $G^*$ ) thus could be calculated by the summation of the activation energies of the viscosity units. Based on the structural picture depicted by the modified quasi-chemical model in quadruplet approximation (Pelton et al., 2001), the structural units of a solution can be quadruplets composed of different constituents of the solution. According to the modified quasichemical model, the solution consists of two sub-lattices. In a salt solution, these sublattices are called anionic and cationic sublattices which are occupied by the anions ( $X, Y, Z, \dots$ ) and the cations ( $A, B, C, \dots$ ), respectively. Each quadruplet in a salt solution consists of two second nearest neighbor (SNN) anions and two SNN cations, the cations and anions being mutual first nearest neighbours (FNN). Some examples of these quadruplets are illustrated in Fig. 4.8.

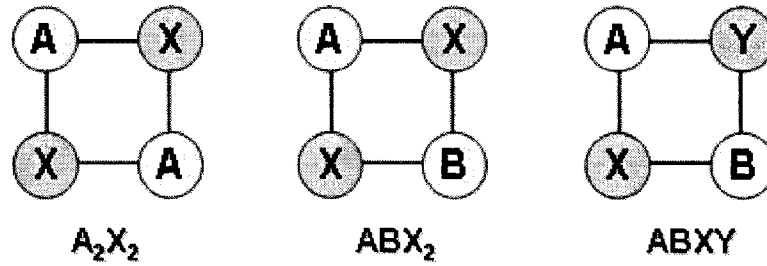


Figure 4.8: Some Quadruplets in an Ionic Solution of Cations ( $A, B, C, \dots$ ) and Anions ( $X, Y, Z, \dots$ ).

The quadruplet mole fractions could be calculated by the thermodynamic database developed in CRCT<sup>§§</sup> for the mentioned system (Chartrand and Pelton, 2002). Based on these concepts, Robelin and Chartrand (2007) proposed the following equation for the viscosity of multi-component systems:

$$\eta = \frac{hN_A}{V_M} \exp \left( \frac{\sum_{quad.} X_{quad.} G_{quad.}^*}{RT} \right) \quad (4.43)$$

where  $\eta$  is the viscosity of the liquid mixture,  $V_M$  is the calculated molar volume of the liquid mixture,  $X_{quad.}$  is the mole fraction of each quadruplet present in the melt (at fixed temperature, pressure and overall mole fractions) and  $G_{quad.}^*$  is the associated viscous activation energy for the corresponding quadruplet.

In this manner, the composition dependency of the activation energy for a liquid mixture could be well expressed through the variation of the quadruplet mole fractions upon

---

<sup>§§</sup> Center for Research in Computational Thermchemistry, École Polytechnique de Montréal, Montréal, Canada. ([www.crct.polymtl.ca](http://www.crct.polymtl.ca))



mixing. The molar volume appeared in the pre-exponential factor of Eq. (4.43), is obtained by the recently developed density model for multi-component liquids (Robelin and Chartrand, 2007) and the  $G^*_{quad.}$  for each quadruplet is given as a linear function of temperature:

$$G^*_{quad.} = c_{quad.} + d_{quad.}T \quad (4.45)$$

where  $c_{quad.}$  and  $d_{quad.}$  are model parameters that have been optimized based on the available experimental data for the related quadruplets. According to Robelin and Chartrand (2007), for the mentioned quaternary system (NaF-AlF<sub>3</sub>-CaF<sub>2</sub>-Al<sub>2</sub>O<sub>3</sub>) considering only the main quadruplets in the ranges of composition and temperature of interest could satisfactorily model the viscosity. Gemme (2004) & Lambotte (2007) applied this viscosity model to several pure liquid metals.

In the present work, the mentioned viscosity model is applied to molten chloride systems and liquid aluminum alloys and the results are compared to the available experimental data. As it will be shown in the following sections, a modification is proposed to the model to better explain the viscosity behavior of highly short-range ordered molten chloride systems. In the following sections a description of the viscosity model is presented along with a brief overview of the corresponding thermodynamic and density models employed for the calculations.

## 5 Description of the Model Employed in the Present Work

As we discussed earlier, a simplified Eyring's equation is used as the starting point of the present viscosity model:

$$\eta = \frac{hN_A}{V_M} \exp\left(\frac{G^*}{RT}\right) \quad (5.1)$$

According to Robelin and Chartrand (2007), the activation energy ( $G^*$ ) for a liquid mixture could be calculated by the summation of the activation energies of the structural units in the melt. As it was discussed previously, these structural units in a salt solution can be quadruplets consisting of two SNN anions and two SNN cations, the cations and anions being mutual FNNs. However for the molten chloride systems studied in the present work, the anionic sublattice is occupied only by the chloride ions (see Section 5.2 for further details). Consequently, all the SNN anions present in the quadruplets, are chloride ions ( $Cl^-$ ). Each quadruplet can be considered as a SNN cation-cation pair ( $A-[Cl]-A$ ,  $B-[Cl]-B$ ,  $A-[Cl]-B$ , ...) and Eq. (4.43) thereby can be re-written in the following form for the studied systems:

$$\eta = \frac{hN_A}{V_M} \exp\left(\frac{\sum X_{ij} G_{ij}^*}{RT}\right) \quad (5.2)$$

The molar volume of the liquid mixture ( $V_M$ ) and the SNN pair fractions ( $X_{ij}$ ) are calculated by the density model and the modified quasichemical model in pair approximation, respectively as it will be described in the subsequent sections.

In this manner, the composition dependency of the activation energy is given by the variation of the SNN pair fractions upon mixing.

The corresponding activation energies ( $G_{ij}^*$ ) for most of the SNN pairs are given by a first order linear function of temperature as follows:

$$G_{ij}^* = c_{ij} + d_{ij}T \quad (5.3)$$

where  $c_{ij}$  and  $d_{ij}$  are called the parameters of the model and can be obtained by the following linear regression among the unary and binary experimental viscosity data:

$$\ln(\eta V_M) - \ln(hN_A) = \frac{X_{ij}}{R} \left( \frac{c_{ij}}{T} + d_{ij} \right) \quad (5.4)$$

The parameters of the model are optimized for the studied systems, by evaluating all the available literature data and employing the most reliable ones. For most of the studied binary systems, these two parameters ( $c_{ij}$  and  $d_{ij}$ ) could very well reproduce the viscosity behaviour. However as it will be shown in Section 6.3.6, for NaCl-MgCl<sub>2</sub> binary system, the present model could not satisfactorily reproduce the experimental data; comparing to the other studied binary systems. As it will be described in the following section, this problem is resolved by proposing a modification to the presented viscosity model.

## 5.1 Modifying the Employed Viscosity Model

After optimizing the model parameters given by Eq. (5.3), for all the binary chloride systems studied in the present work, it follows that for NaCl-MgCl<sub>2</sub> system, the defined activation energies could not satisfactorily reproduce the viscosity behaviour.

NaCl-MgCl<sub>2</sub> is an ionic system with high degree of so called “SNN short range ordering”. As it will be shown later in Section 5.2, depending on the degree of short range ordering, these systems undergo more pronounced configurational and energy changes upon mixing than the other systems. It was concluded that the composition dependency of the viscosity which was given through the variation of SNN pair fractions upon mixing may not be enough to express the viscosity behaviour of highly short range ordered systems. More composition dependent terms were required to accurately express the viscosity behaviour of these systems for the whole range of composition. Accordingly a modified form of the activation energy is proposed where  $G_{ij}^*$  is not only temperature-dependent but also composition-dependent. The Eq. (5.3) thereby can be written in the following form:

$$G_{ij}^* = (G_{ij}^*)^{00} + (G_{ij}^*)^{10} \frac{X_{ii}}{X_{ii} + X_{ij} + X_{jj}} + (G_{ij}^*)^{01} \frac{X_{jj}}{X_{ii} + X_{ij} + X_{jj}} \quad (5.5)$$

with

$$\begin{aligned} (G_{ij}^*)^{00} &= (c_{ij})^{00} + (d_{ij})^{00} T \\ (G_{ij}^*)^{10} &= (c_{ij})^{10} + (d_{ij})^{10} T \\ (G_{ij}^*)^{01} &= (c_{ij})^{01} + (d_{ij})^{01} T \end{aligned} \quad (5.6)$$

where  $(c_{ij})^{00}$ ,  $(d_{ij})^{00}$ ,  $(c_{ij})^{10}$ ,  $(d_{ij})^{10}$ ,  $(c_{ij})^{01}$  and  $(d_{ij})^{01}$  are the modified parameters of the model (clearly the parameters  $(c_{ij})^{10}$ ,  $(d_{ij})^{10}$ ,  $(c_{ij})^{01}$  and  $(d_{ij})^{01}$  will be equal to zero for the pure components).

As it will be shown in Sections 6.2.8 and 6.2.9, this modified form of the activation energy has been employed to model the viscosity behaviour of NaCl-MgCl<sub>2</sub>, RbCl-MgCl<sub>2</sub>

and CsCl-MgCl<sub>2</sub> systems satisfactorily compared to the experimental data. However to model these systems,  $(d_{ij})^{10}$  and  $(d_{ij})^{01}$  were set to zero and the viscosity could be precisely modeled by considering just two more parameters  $(c_{ij})^{10}$  and  $(c_{ij})^{01}$  to the former defined parameters  $((c_{ij})^{00}$  and  $(d_{ij})^{00}$ ).

To justify the proposed modification, two other binary systems with higher degrees of short range ordering, namely RbCl-MgCl<sub>2</sub> and CsCl-MgCl<sub>2</sub>, are studied. As it will be shown in Sections 6.3.7.3 and 6.3.7.4, employing the modified form of  $G^*_{ij}$  could well reproduce the observed maximum in the viscosity isotherms of these systems. However employing the activation energies of the original form proposed by Robelin and Chartrand (2007), could not lead to satisfactory results for these highly short range order systems compared to the experimental data (Further discussion on the results will be presented in Section 6.3.7)

## 5.2 Modified Quasichemical Thermodynamic Model

As it was discussed in the previous section, the quadruplet mole fractions ( $X_{quad.}$ ) and the SNN pair fractions ( $X_{ij}$ ) appearing in the presented viscosity expressions (Eqs. 4.43 and 5.2), can be calculated by the modified quasi-chemical model. The modified quasi-chemical model has been introduced in a series of articles by Pelton and coworkers (Pelton et al., 2000; Pelton and Chartrand, 2001; Pelton et al., 2001; Chartrand and Pelton, 2001a). Chartrand and Pelton (2001b) applied the model to evaluate, optimize and predict the thermodynamic properties and phase equilibria for liquid solutions of alkali

and alkaline-earth chlorides by pair approximation. Molten alkali chlorides-MgCl<sub>2</sub> solutions exhibit structural short-range ordering increasing in importance from LiCl-MgCl<sub>2</sub> to CsCl-MgCl<sub>2</sub>. As it is shown in Figs. 4.9 and 4.10, their enthalpy and entropy of mixing are “V shaped” and “m-shaped” curves respectively, with a minimum close to the composition of maximum ordering.

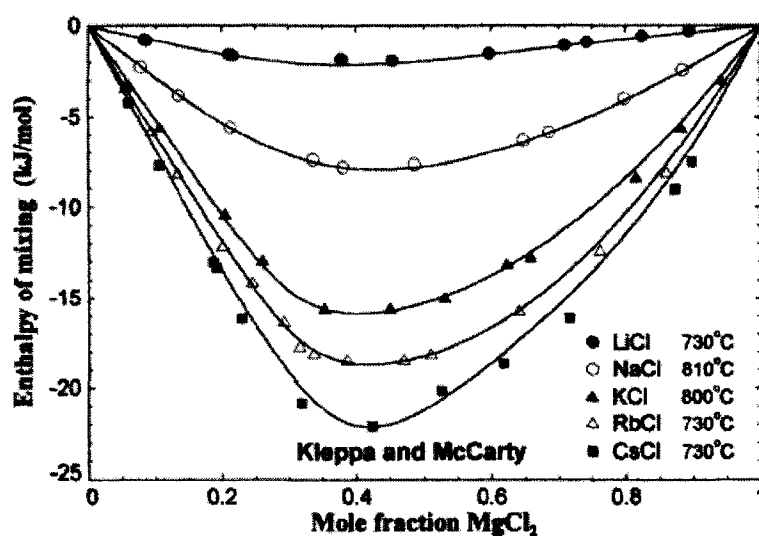


Figure 5.1: Enthalpies of Mixing for the Alkali Chloride-MgCl<sub>2</sub> Liquid Solutions  
Calculated by Chartrand and Pelton (2001b).

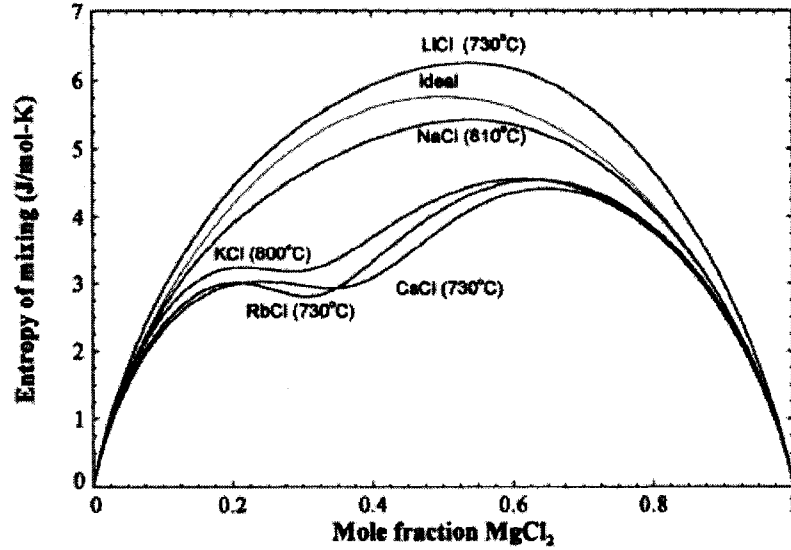
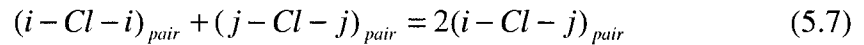


Figure 5.2: Entropy of Mixing for the Alkali Chloride-MgCl<sub>2</sub> Liquid Solutions Calculated by Chartrand and Pelton (2001b).

To treat the cation-cation short-range order in these systems, Chartrand and Pelton (2001b) considered the distribution of SNN cation-cation pairs over the pair sites and assumed the following quasi-chemical reaction between the SNN cation-cation pairs in the melt:



with  $i$  and  $j$  being the cations ( $A, B, C, D, \dots$ ).

When the Gibbs energy change of the above mentioned pair exchange reaction ( $\Delta g_{ij/Cl}$ ) is small, low degree of short-range ordering is observed and the solution can be modeled by assuming the random mixing of cations on the cationic sublattice. As  $\Delta g_{ij/Cl}$  becomes

progressively negative, reaction (5.7) is shifted progressively to the right,  $(i - Cl - j)$  pairs predominate and the solution becomes progressively more ordered. Based on this concept, short-range ordering can be treated by considering the relative numbers of SNN cation-cation pairs in the melt. The Gibbs energy of a multi-component liquid solution thereby is given in terms of the number of pairs and the Gibbs energy changes of pair exchange reactions ( $\Delta g_{ij/Cl}$ ) as follows:

$$G = (n_{A/Cl} g_{A/Cl}^0 + n_{B/Cl} g_{B/Cl}^0 + \dots) - T\Delta S^{config.} + \sum_i \sum_{j>i} (n_{ij/Cl} / 2) \cdot \Delta g_{ij/Cl} \quad (5.8)$$

with the configurational entropy of mixing  $\Delta S^{config.}$  given by the following equation assuming the random distributing of the SNN cation-cation pairs over the pair sites:

$$\Delta S^{config.} = -R(n_{A/Cl} \ln X_{A/Cl} + n_{B/Cl} \ln X_{B/Cl} + \dots) - R \left[ n_{AA/Cl} \ln \left( \frac{X_{AA/Cl}}{Y_A^2} \right) + n_{BB/Cl} \ln \left( \frac{X_{BB/Cl}}{Y_B^2} \right) + \dots + \sum_i \sum_{j>i} n_{ij/Cl} \ln \left( \frac{X_{ij/Cl}}{2Y_i Y_j} \right) \right] \quad (5.9)$$

where  $n_{A/Cl}, n_{B/Cl}, \dots$  are the number of moles of the pure liquid salts ( $A/Cl, B/Cl, \dots$ ),  $g_{A/Cl}^0, g_{B/Cl}^0, \dots$  the molar standard Gibbs energy of the pure salts and  $n_{ij/Cl}$  the number of moles of cation-cation SNN pairs. The overall mole (or site) fractions ( $X_{A/Cl}, X_{B/Cl}, \dots$ ), cation-cation pair fractions ( $X_{ij/Cl}$ ) and “coordination-equivalent” site fractions ( $Y_A, Y_B, \dots$ ) are defined as follows:

$$X_{A/Cl} = n_{A/Cl} / (n_{A/Cl} + n_{B/Cl} + \dots) \quad (5.10)$$

$$X_{B/Cl} = n_{B/Cl} / (n_{A/Cl} + n_{B/Cl} + \dots)$$

$$X_{ij/Cl} = n_{ij/Cl} / \sum n_{ij/Cl} \quad (5.11)$$



$$\begin{aligned} Y_A &= Z_A n_{A/Cl} / (Z_A n_{A/Cl} + Z_B n_{B/Cl} + \dots) \\ Y_B &= Z_B n_{B/Cl} / (Z_A n_{A/Cl} + Z_B n_{B/Cl} + \dots) \end{aligned} \quad (5.12)$$

where  $Z_A, Z_B, \dots$  are the SNN (cation-cation) coordination numbers of  $A, B, \dots$  cations that can be composition dependent in the following manner:

$$\begin{aligned} \frac{1}{Z_A} &= \frac{1}{2n_{AA/Cl} + \sum_{j \neq A} n_{Aj/Cl}} \left( \frac{2n_{AA/Cl}}{Z_{AA}^A} + \sum_{j \neq A} \frac{n_{Aj/Cl}}{Z_{Aj}^A} \right) \\ \frac{1}{Z_B} &= \frac{1}{2n_{BB/Cl} + \sum_{j \neq B} n_{Bj/Cl}} \left( \frac{2n_{BB/Cl}}{Z_{BB}^B} + \sum_{j \neq B} \frac{n_{Bj/Cl}}{Z_{Bj}^B} \right) \end{aligned} \quad (4.13)$$

where  $Z_{Aj}^A$  is the value of  $Z_A$  when all the cation-cation nearest neighbors of  $A$  are  $j$  cations and  $Z_{Bj}^B$  is the value of  $Z_B$  when all the second nearest neighbors of  $B$  are  $j$  cations. Then:

$$\begin{aligned} n_{A/Cl} &= \frac{2n_{AA/Cl}}{Z_{AA}^A} + \sum_{j \neq A} \frac{n_{Aj/Cl}}{Z_{Aj}^A} \\ n_{B/Cl} &= \frac{2n_{BB/Cl}}{Z_{BB}^B} + \sum_{j \neq B} \frac{n_{Bj/Cl}}{Z_{Bj}^B} \end{aligned} \quad (5.14)$$

The last term of the Eq. (5.8) accounts for the excess Gibbs energy caused by the cation-cation short-range order. The empirical parameters of the model ( $\Delta g_{AB/Cl}, \Delta g_{BC/Cl}, \dots$ ) are related to the interactions of SNN pairs on the cationic sublattice and can be expanded as a polynomial in the following form:

$$\begin{aligned} \Delta g_{AB/Cl} &= \Delta g_{AB/Cl}^0 + \sum_{(m+n) \geq 1} q_{AB/Cl}^{mn} \left( \frac{Y_A}{Y_A + Y_B} \right)^m \left( \frac{Y_B}{Y_A + Y_B} \right)^n \\ &\quad + \sum_{\substack{n \geq 0 \\ k \geq 1}} \left( \frac{Y_B}{Y_A + Y_B} \right)^n (q_{AB(C)/Cl}^{0nk} Y_C^k + q_{AB(D)/Cl}^{0nk} Y_D^k + \dots) \end{aligned} \quad (5.15)$$

Where  $\Delta g_{AB/Cl}^0$  and  $q_{AB/Cl}^{mn}$  are composition independent (although possibly temperature-dependent) coefficients obtained from fitting experimental data for binary  $A,B/Cl$  solutions. The remaining terms in Eq. (5.15) are “ternary terms” to take into account the effect of the presence of  $C,D,\dots$  cations upon the energy of reaction (5.7). These ternary terms are zero in the  $A,B/Cl$  binary system.  $\Delta g_{ij/Cl}$  of the other quasichemical pair-exchange reactions can be obtained by the similar approach.

The numbers of moles of cation-cation pairs ( $n_{ij/Cl}$ ) at equilibrium in a given overall composition are calculated by numerical minimization of Gibbs energy (Eq. 5.8), subject to the constraints of Eq. (5.14). This for the quasichemical reaction (5.7) between  $(i - Cl - i)$ ,  $(j - Cl - j)$  and  $(i - Cl - j)$  cation-cation pairs gives:

$$\frac{X_{ij/Cl}^2}{X_{ii/Cl} \cdot X_{jj/Cl}} = 4 \exp\left(\frac{-\Delta g_{ij/Cl}}{RT}\right) \quad (5.16)$$

Which is the equilibrium constant of the mentioned quasichemical reaction. For a given value of  $\Delta g_{ij/Cl}$ , solving Eq. (5.16) together with Eqs. (5.10) and (5.14) gives the equilibrium pair fractions ( $X_{ii}$ ,  $X_{jj}$  and  $X_{ij}$ ).

The modified quasichemical model is shown to be very applicable to molten salt systems involving cation-cation ordering (Chartrand and Pelton, 2001b; Robelin et al., 2004a; 2004b; 2004c; 2006; Lindberg et al., 2007a; 2007b). The model permits a quantitative optimization of all the binary data and could be satisfactorily extrapolated to predict the properties of the multi-component solutions taking into account the mentioned short-range ordering in the melt. Chartrand and Pelton (2001b) obtained all the optimized

parameters of the model for the alkali-alkaline-earth chloride solutions. The similar approach has been applied to the metallic solutions by replacing the chloride ions in the anionic sublattice by the “vacancies”. The optimized parameters for the mentioned salt and metallic solutions are included in the FactSage databases (Bale et al., 2002), where the pair fractions required for the viscosity model can be easily calculated.

### 5.3 Density Model

As we discussed in the previous sections, the molar volume appeared in the pre-exponential factor of the presented viscosity expressions (Eqs. 4.43 and 5.2), can be calculated by the density model recently developed at the CRCT (Robelin and Chartrand, 2007; Robelin et al., 2007).

According to the solution thermodynamics theory (Smith et al., 1996), the molar volume of a solution is defined as the derivative of molar Gibbs energy of solution with respect to pressure, at given temperature and component's mole fractions as follows:

$$V_M = \left( \frac{\partial G}{\partial P} \right)_{T, X_A, X_B, X_C, \dots} \quad (5.17)$$

where  $V_M$  is the molar volume of the solution,  $G$  the molar Gibbs energy of the solution,  $P$  pressure,  $T$  a given temperature and  $X_A, X_B, X_C, \dots$  are the given mole fractions of solution components. Therefore the molar volume can be modeled by introducing the pressure-dependent parameters in the Gibbs energy of solution. Robelin et al. (2007) modeled the molar volume of NaCl-KCl-MgCl<sub>2</sub>-CaCl<sub>2</sub> system by employing the Gibbs energy expression given by the modified quasichemical model in the pair approximation,

for these systems (Eq. 5.8). According to them, the molar Gibbs energy of a pure liquid salt ( $A/Cl$ ) can be written in the following form:

$$\begin{aligned} g^0_{A/Cl}(T, P) &= g^0_{A/Cl}(T, 1 \text{ bar}) + \int_1^P V_{A/Cl}(T).dP \\ &= g^0_{A/Cl}(T, 1 \text{ bar}) + V_{A/Cl}(T).(P - 1) \end{aligned} \quad (5.18)$$

where  $V_{A/Cl}(T)$  is the molar volume of pure liquid  $A/Cl$  at temperature  $T$  and is given as follows:

$$V_{A/Cl}(T) = V_{A/Cl}(T_{ref.}).\exp\left(\int_{T_{ref.}}^T \alpha(T).dT\right) \quad (5.19)$$

where  $T_{ref.}$  is an arbitrary-chosen temperature and  $\alpha(T)$  is the thermal expansion that can be obtained by an optimized fit of the experimental volumetric data using the following temperature function:

$$\alpha(T) = a + bT + cT^{-1} + dT^{-2} \quad (5.20)$$

For a multi-component molten salt system, the solution of Eq.(5.17) together with the Eqs. (5.8) and (5.18) leads to the following equation for the molar volume of the solution:

$$\begin{aligned} V_M &= [n_{A/Cl}.V_{A/Cl}(T) + n_{B/Cl}.V_{B/Cl}(T) + \dots] \\ &+ \sum_i \sum_{j \neq i} \left( \frac{n_{ij/Cl}}{2} \right) \left( \frac{\partial \Delta g_{ij/Cl}}{\partial P} \right)_{T, n_A, n_B, n_C, \dots} \end{aligned} \quad (5.21)$$

where the second term is the excess volume of the mentioned multi-component chloride melt. For a given binary liquid ( $i, j/Cl$ ),  $\Delta g_{ij/Cl}$  can be expanded as a polynomial in the SNN cation-cation pair fractions  $X_{ii/Cl}$  and  $X_{jj/Cl}$  as follows:

$$\begin{aligned}
\Delta g_{ij/Cl} = & \left[ \Delta g_{ij/Cl}^0 + \beta_{ij/Cl}^0 \cdot (p-1) \right] \\
& + \sum_{m \geq 1} \left[ q_{ij/Cl}^{m0} + \beta_{ij/Cl}^{m0} \cdot (p-1) \right] (X_{ii/Cl})^m \\
& + \sum_{n \geq 1} \left[ q_{ij/Cl}^{0n} + \beta_{ij/Cl}^{0n} \cdot (p-1) \right] (X_{jj/Cl})^n
\end{aligned} \tag{5.22}$$

where  $\Delta g_{ij/Cl}^0$ ,  $q_{ij/Cl}^{m0}$  and  $q_{ij/Cl}^{0n}$  are the parameters of the thermodynamic model (see Eq. 5.15).  $\beta_{ij/Cl}^0$ ,  $\beta_{ij/Cl}^{m0}$  and  $\beta_{ij/Cl}^{0n}$  are the parameters of the density model that can be temperature dependent. Similar to the thermodynamic model, the ternary terms can be introduced for higher order systems to better fit the experimental data. However for NaCl-KCl-MgCl<sub>2</sub>-CaCl<sub>2</sub> system, these ternary terms were not required (Robelin et al., 2007).

Robelin et al. (2007) obtained the parameters of the density model by least-squares fitting of the available experimental data for  $i, j/Cl$  binary liquids. Gemme (2004) applied the model to several liquid metallic systems and obtained the optimized parameters of the model. These parameters for the mentioned salt and metallic solutions are included in the FactSage databases (Bale et al., 2002), where the molar volumes required for the viscosity model can be easily calculated.

## 6 Results and Discussion: Molten Salts

In the following sections, the viscosity model presented in Section 5 is applied to the NaCl-KCl-MgCl<sub>2</sub>-CaCl<sub>2</sub> liquid solution. The available literature data for 4 pure components and 6 binary subsystems are collected and reliable data sets are employed to optimize the parameters of the model. The previously developed thermodynamic model (Chartrand and Pelton, 2001b) and density model (Robelin et al., 2007) for this system, are employed to calculate the viscosity values. The calculations are done by using the FactSage thermochemical software (Bale et al., 2002). The calculated viscosity curves are compared with the literature data. The proposed modification to the model for highly ordered systems has been applied to NaCl-MgCl<sub>2</sub> system. To further investigate the viscosity behaviour of highly short-range ordered systems, RbCl-MgCl<sub>2</sub> and CsCl-MgCl<sub>2</sub> systems are also studied and the results are presented.

### 6.1 Pure Molten Salts

#### 6.1.1 General Discussion on Literature Data

As described earlier, the parameters of the viscosity model are optimized based on the available experimental data. A thorough literature review is performed to collect the viscosity data in the literature. Comparing the collected data sets, large discrepancies appeared among the data of different laboratories. In some cases even for the data of the same laboratory these discrepancies were considerably large. This could be the result of several difficulties encountered in the viscosity measurement of high temperature melts (see Section 3 for details). Consequently, a critical evaluation seemed necessary to obtain

the most reliable sets of experimental data. Several factors such as experimental techniques, the number of measurements, the temperature range and the reliability of previous work from any one laboratory, needed to be considered. To start with, the “NSRDS-NBS” and “The Molten Salts Standard Program” critical reviews and evaluated data are used as the starting point. The NSRDS (National Standard Reference Data System) was a program initiated in 1963 by the NBS (National Bureau of Standards) in order to promote, and coordinate systematic data compilation and evaluation activities in all fields of the physical sciences (Brady and Wallenstein, 1964). The results for physical properties (density, surface tension, viscosity and electrical conductivity) of molten salts have been published in several series since 1968 (Janz et al., 1968; 1975; 1988). These publications contain a critical assessment of the existing data for electrical conductance, surface tension, density and viscosity of several pure and binary molten salt systems. Due to the lack of accurate calibration-quality data for the molten salts, several difficulties were being encountered for accuracy estimation in the NSRDS molten salts data compilations. Therefore a parallel program called the Molten Salts Standards Program has been initiated in 1973 by Janz and Zuca (Janz, 1980) to resolve some of these difficulties. NaCl and KNO<sub>3</sub> were selected as the two reference salts for the following properties: density, surface tension, viscosity and electrical conductance. Several laboratories such as “Institute of Inorganic Chemistry, Technical University of Norway, Torndheim, Professor H. A. Øye”, “Center of Physical Chemistry, Bucharest, Rumania, Professor S. Zuca” and “Department of Metallurgy, Tohoku University, Sendai, Japan, Professor T. Ejima”; participated in this program to perform the round-robin series of

measurements. The standard-quality salt samples have been distributed to all laboratories; thus the attention could be focused on technique error-analysis by comparing different experimental techniques employed by different laboratories. The results have been critically examined and provided the accurate calibration-quality data sets that could be used as guidance for the critical evaluation of the experimental data (Janz, 1980). Accordingly several data sets have been upgraded to calibration-quality standards and the complete NSRDS database for the mentioned physical properties has been updated and published in 1988 (Janz, 1988). These recommended data sets are chosen as the reference in the present work and employed to optimize the parameters of the viscosity model for the pure salts. They are highlighted in the presented figures, as “Janz et al., 1988 Recom. Data” and have been compared with the other data sets available in the literature. The measurements performed after 1988 or the ones that have not been considered in NSRDS critical reviews, are also included in the figures. Each figure is accompanied with a table showing the experimental method, conditions and the temperature range for each data set. A brief discussion about the possible errors caused by the choice of experimental technique; and the degree of uncertainty for each data set appearing in the figures is presented in the related sections.

### **6.1.2 NaCl**

As it is discussed in the last section, the viscosity of NaCl, has been accurately measured by different groups participated in the Molten Salts Standards Program. The results are compared in Fig. 6.1 with the data of Murgulescu and Zuca (1963) which was the 1968 NSRDS (Janz et al., 1968) recommended data set for NaCl liquid salt.



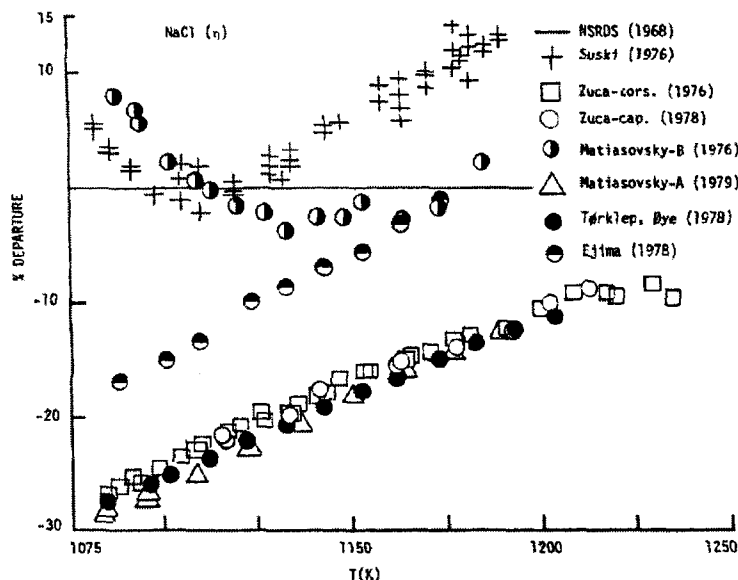


Figure 6.1: The Percent of Departure of NaCl Viscosity Data of Different Participants of Molten Salts Standards Program, from the NSRDS-1968 Recommendation (Janz, 1980).

Janz (1980) critically examined different data sets submitted to Molten Salts Standards Program. Since the quality of NaCl samples were the same for each participating laboratory, the intercomparisons of the two salient molten salts viscosity measurement methods: “capillary and oscillating body techniques”; have been possible (see Section 3 for the details on the experimental methods). The data set of Suski and two data sets of Zuca in Fig. 6.1 were obtained by capillary method while the two data sets of Matiasovsky (A and B), the data sets of Tørklep&Øye and Ejima are obtained by the oscillational body (torsional pendulum) technique (Janz, 1980). The results of the capillary measurements of Zuca were in good agreement (within experimental limits of

accuracies) with the data of oscillational techniques by Matiasovsky-B and Torklep&Øye. It follows that the capillary method is applicable, with good accuracy, in high temperature ranges (1073-1273K). Still a carefully dehydrated salt sample was required to prevent the etching of the capillary tube in the presence of water (as impurity). The accuracy limit of the capillary technique thus was estimated to be  $\sim \pm 1.5\%$  at molten NaCl temperatures (1073-1273K). However, due to several advantages such as the relatively small temperature “flat-zone” required and the wider choice of container material; Janz (1980) recommended the torsional technique for the temperatures higher than  $\sim 773K$ . The disadvantage of the torsional method appeared to be the mathematically complicated working equations required for absolute viscosity measurements. The advent of computer-assisted techniques though has eased this consideration.

To determine the accuracy of the measurements by torsional method, several features have been re-examined as part of the Molten Salts Standards Program. Particularly design features such as torsion wire, torsion pendulum, oscillating bodies (sphere or cylinder); employed by different laboratories; have been considered to estimate the experimental errors. In addition, the factors such as sample quality, irregularities in the shape of the oscillating body and the computational approaches to obtain the viscosity; have also been considered as possible sources of error. According to Janz (1980), the systematic departure of the data of Ejima from those of Torklep&Øye and Matiasovsky-B in Fig. 6.1 may be in large part due to the choice of torsion wire. The torsion wire used by Ejima was made of molybdenum while the ones of Torklep&Øye and Matiasovsky-B were

made of the Kestin alloy which is estimated to significantly reduce the error source (Torklep and Øye, 1979). The Kestin alloy (Pt92% - W8%) has a low internal friction and highly stable elastic constant which makes it a more appropriate material for torsion wires (Torklep and Øye, 1979). The large differences in the earlier and later data sets of Matiasovsky (Matiasovsky-A and Matiasovsky-B in Fig. 6.1) may be related, in large part, to the pendulum design. In the 1976 design, the pendulum had a disk like inertia mass in the hot zone of the furnace. The possible “sail-like” effect of this design would impose additional pendulum movements leading to a precession of the axis of rotation. The secondary flow caused by these movements, affects the rate of damping of the torsional oscillation by the fluid and leads to observed viscosities that are too high. By changing the torsion wire to the Kestin alloy and re-design of the pendulum to remove the inertia mass in the hot zone, Matiasovsky could significantly eliminate the errors of 1976 measurements and report the data set of 1979 (Matiasovsky-B). Further discussion about the other sources of error in torsional techniques caused by the type of oscillating body and the proper working equation for each type etc are given in Section 3.5. According to Janz (1980), the accuracy limits of the oscillating body technique for molten salts estimated to be  $\sim \pm 3\%$  with spherical body and  $\sim \pm 0.2\%$  with cylindrical body. Janz (1980) recommended the torsional technique with immersed cylindrical body, as the most reliable method for viscosity measurements at high temperatures.

Considering all the above mentioned factors, Janz (1980) concluded that the values advanced in the 1968 NSRDS recommendations (Janz et al., 1968), are in serious error ( $\sim 50\%$  at  $1083K$  and  $\sim 10\%$  at  $1273K$ ). The measurements of Torklep and Øye

(1979) by the oscillating cylinder method, were selected as the new recommended data set. Fig. 6.2 illustrates a comparison between this recommended data set and the other viscosity data in the literature for the period 1908-1979.

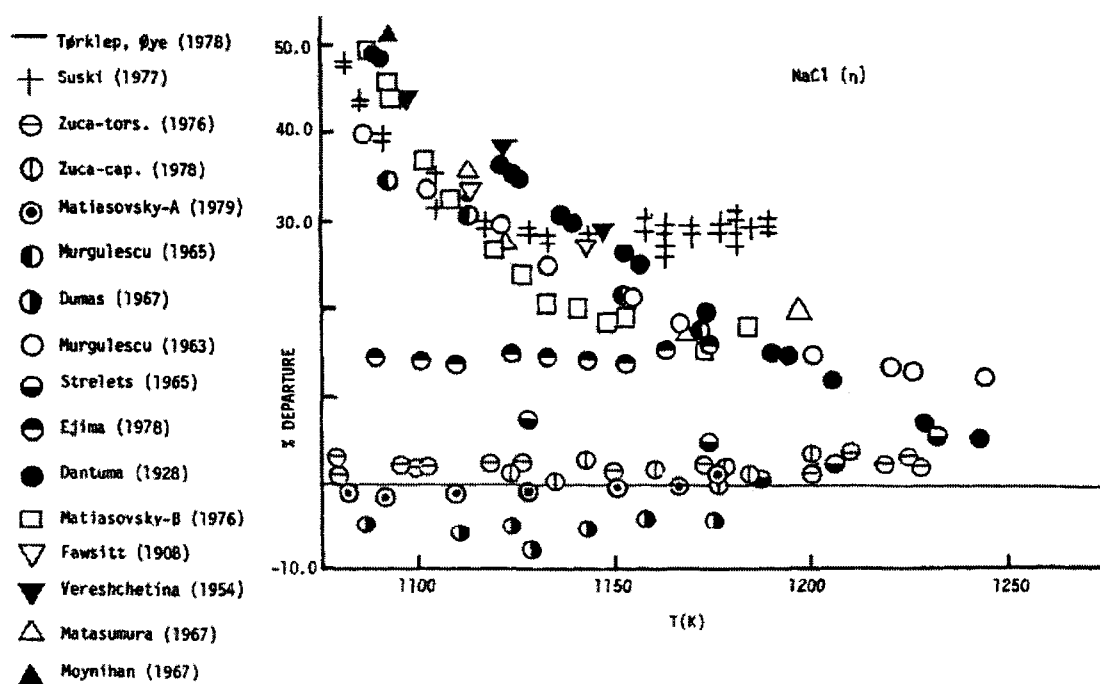


Figure 6.2: NaCl Viscosity Data for the Period 1908-1979, Shown as a Percent Departure Analysis with Torklep and Øye (1978) Data Set as Comparison Standard (Janz, 1980).

The results of the mentioned Standards Program are used as the starting point of the literature review for the viscosity of molten NaCl, in the present work. The data sets reported up to 1979 that has not been appeared in Fig. 6.2, together with the data sets reported after 1979, are illustrated in Fig. 6.3 and compared with the NSRDS

recommendations (Janz et al., 1968; Janz et al., 1975; Janz, 1988) and the result of the optimization in the present work based on the data of Torklep and Øye (1979). This figure is accompanied by Table 6.1 which gives a summary of the experimental methods employed for each measurement and the temperature range of each data set.

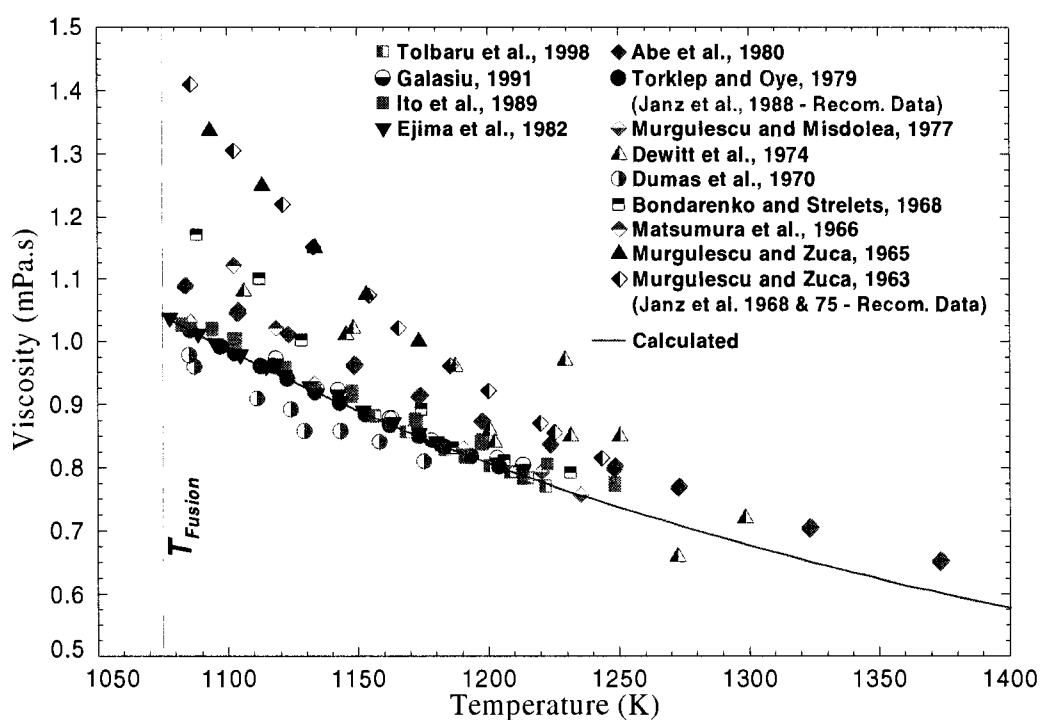


Figure 6.3: Calculated and Experimental Viscosity of Pure Liquid NaCl

Table 6.1: A Summary of the Experimental Methods for the Viscosity Measurements of  
Pure NaCl Reported in the Literature

Author	Year	Experimental Method (Working Equations)	Experimental Conditions	Temperature range [K]
Tolbaru et al.	1998	Oscillating cup (Eq. 3.3)	Pt92%-W8% torsion wire, Inconel X-750 superalloy cup, full cup condition, N <sub>2</sub> atmosphere	1151 – 1222
Galasiu	1991	Capillary (Modified Hagen- Poiseuille, Eq. 3.9)	Quartz capillary tube	1073 – 1223
Ito et al.	1989	Oscillating cup (Mathematical treatment done on the Kestin and Newell (1957) equation)	Pt92%-W8% torsion wire, Heat-resisting SUH3 steel cup, Vacuum atmosphere	1083 – 1248
Ejima et al.	1982	Capillary (Eq. 3.9)	Quartz capillary tube, Calibration done by water	1077 – 1179
Abe et al.	1980	Oscillating cup (Computational procedure based on the Kestin and Newell (1957) equation)	Pt92%-W8% torsion wire, Molybdenum cup, Vacuum atmosphere	1083 – 1473
Torklep & Øye	1979	Oscillating cylinder (Eqs. 3.3 & 3.4)	Pt92%-W8% torsion wire, Pt90%-Ir10% solid cylinder, Pt crucible, N <sub>2</sub> atmosphere, Control measurement by water	1083 – 1203
Murgulescu & Misdolea	1977	Oscillating sphere (Computational procedure based on Eq. 3.2)	Pt92%-W8% torsion wire	1085 – 1235

Dewitt et al.	1974	Oscillating cup (Computational procedure done by wittenberg et al. (1968))	Pt92%-W8% torsion wire, Vacuum atmosphere	1106 – 1298
Dumas et al.	1970	Oscillating sphere (Computational procedure based on Eq. 3.2)	Tungsten torsion wire, Pt90%-Ir10% solid sphere, Pt crucible, N <sub>2</sub> atmosphere, Control measurements by water & KNO <sub>3</sub>	1085 – 1175
Bondarenko & Strelets	1968	Oscillating sphere (-)	Pt sphere, Calibration by water & nitrobenzene & aniline & molten KNO <sub>3</sub> & NaNO <sub>3</sub>	1088 – 1231
Matsumura et al.	1966	Oscillating disc (Using a relation between viscosity and number of oscillation)	Pt disc, Stainless steel wire, Pt crucible	1102 – 1118
Murgulescu & Zuca	1965	Oscillating sphere (-)	Pt sphere, Pt wire, Calibration by water & nitrobenzene & aniline & molten KNO <sub>3</sub> & NaNO <sub>3</sub>	1100 – 1170
Murgulescu & Zuca	1963	Oscillating sphere (Eq. 3.2)	Pt sphere, Pt wire	1083 - 1243

The solid line in Fig. 6.3 shows the results of the present optimization and is obtained by Eqs. (5.2) and (5.3) as it is described in Section 5. Since the only cation cation SNN pairs in the melt are  $Na - Cl - Na$  pairs (shown as  $Na / Cl$ ), we can set  $X_{ij} = X_{Na/Cl} = 1$  and write Eqs. (5.2) and (5.3) for pure liquid NaCl as follows:

$$\eta_{NaCl} = \frac{hN_A}{V_M} \exp\left(\frac{G^*_{Na/Cl}}{RT}\right) \quad (6-1)$$

$$G^*_{Na/Cl} = c_{Na/Cl} + d_{Na/Cl}T \quad (6-2)$$

where  $c_{Na/Cl}$  and  $d_{Na/Cl}$  are the parameters of the model for pure NaCl and can be obtained by a linear regression in the form of Eq. (5-4) as follows:

$$\ln(\eta V_M) - \ln(h N_A) = \frac{c_{Na/Cl}}{R} \cdot \frac{1}{T} + \frac{d_{Na/Cl}}{R} \quad (6-3)$$

The numerical values of  $c_{Na/Cl}$  and  $d_{Na/Cl}$  are given in appendix A in SI units.

As it is observed in Fig. 6.3, most of the data sets reported after 1979 are in good agreement (within experimental limits of accuracies) with the data of Torklep and Øye (1979). Only Abe et al. (1980) reported viscosity values which were systematically higher by about 6% than those of Torklep and Øye (1979). Later Ito et al. (1989) from the same group, performed a redetermination of these viscosity values by considering two possible sources of error, namely, the effect of the meniscus at the liquid surface (see Section 3.1.3.1) and the temperature distribution along the axis of the oscillation system. After applying a minor correction for the meniscus effect and a correction for the temperature, they obtained a new set of data (see Fig. 6-3) which was still uniformly higher than the Torklep and Øye (1979) data set by  $\sim 1\%$  at 1080K and  $\sim 3\%$  at 1200K as estimated by Janz (1991). However the estimated difference between the two data sets lies within the experimental accuracy limits of the oscillating method as it is discussed earlier. According to Janz (1991), the cause of this difference between the two data sets remains undetermined.

### 6.1.3 KCl

The insights gained on the various viscosity measurement techniques through Molten Salts Standards Program, provided guidance for the critical evaluations of the viscosity



data of molten salts. Accordingly, the 1968 and 1975 NSRDS recommendations for pure KCl were updated and published in 1988 (Janz, 1988). The data sets of Dumas et al. (1970), Bondarenko and Strelets (1968), Matsumura et al. (1966), Murgulescu and Zuca (1961; 1965), Brockner et al. (1981) and others have been critically re-examined and evaluated (Janz et al., 1975; Janz, 1988). Considering all the factors mentioned in the last section, the measurements of Brockner, Torklep and Øye (1981) performed with the same viscometer developed by Torklep and Øye (1979) for the Standards Program, were selected as the new recommended data set in 1988 (Janz, 1988). The accuracy of Brockner et al. (1981) data set for KCl was estimated to be similar to that of NaCl ( $\sim \pm 0.2\%$ ) (Torklep and Øye, 1979; Janz, 1988). The 1968 NSRDS recommendation for KCl, which was the data of Murgulescu and Zuca (1961), was superseded with this new data set. The mentioned viscosity measurements evaluated by Janz et al. (1975; 1988) together with the other data reported in the literature are summarized in Table 6.2.

Table 6.2: A Summary of the Experimental Methods for the Viscosity Measurements of Pure KCl Reported in the Literature

Author	Year	Experimental Method (Working Equations)	Experimental Conditions	Temperature range [K]
Moskvitin et al.	1986	Vibrational viscometer (-)	-	1070 – 1080
Ejima et al.	1982	Capillary (Eq. 3.9)	Quartz capillary tube, Calibration done by water	1050 – 1190

Brockner et al.	1981	Oscillating cylinder (Eqs. 3.3 & 3.4)	Pt92%-W8% torsion wire, Pt90%-Ir10% solid cylinder, Pt crucible, N <sub>2</sub> atmosphere, Control measurement by water	1054 – 1175
Ejima et al.	1977	Oscillating vessel (Knappwost (1952) Eq.)	-	1070 – 1160
Dumas et al.	1970	Oscillating sphere (Computational procedure based on Eq. 3.2)	Tungsten torsion wire, Pt90%-Ir10% solid sphere, Pt crucible, N <sub>2</sub> atmosphere, Control measurements by water & KNO <sub>3</sub>	1080 – 1136
Bondarenko & Strelets	1968	Oscillating sphere (-)	Pt sphere, Calibration by water & nitrobenzene & aniline & molten KNO <sub>3</sub> & NaNO <sub>3</sub>	1070 – 1190
Matsumura et al.	1966	Oscillating disc (Using a relation between viscosity and number of oscillation)	Pt disc, Stainless steel wire, Pt crucible	1063 – 1108
Murgulescu & Zuca	1965	Oscillating sphere (-)	Pt sphere, Pt wire, Calibration by water & nitrobenzene & aniline & molten KNO <sub>3</sub> & NaNO <sub>3</sub>	1053 – 1173
Murgulescu & Zuca	1961	Oscillating sphere (Eq. 3.2)	Pt sphere, Pt wire	1056 – 1202

The KCl reported data sets are illustrated in Fig. 6.4 and compared with the result of the present optimization based on the data of Brockner et al. (1981).

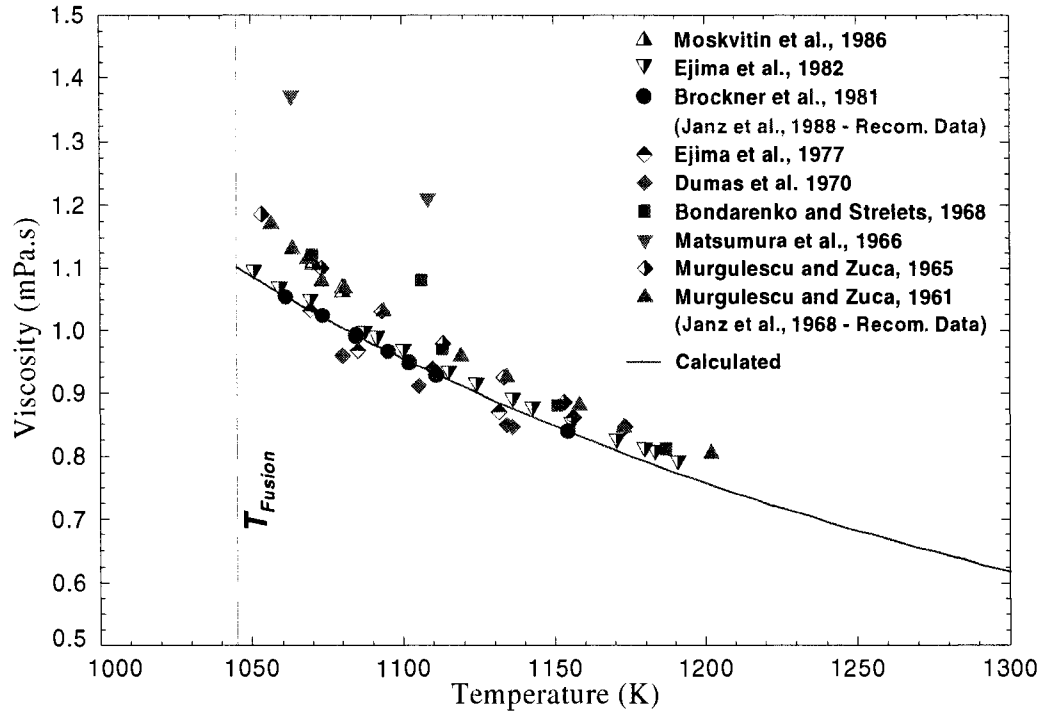


Figure 6.4: Calculated and Experimental Viscosity of Pure Liquid KCl

The solid line in Fig. 6.4 shows the results of the present optimization and is obtained similar to that of NaCl (see Section 6.1.2). The numerical values of  $c_{K/Cl}$  and  $d_{K/Cl}$ , the optimized parameters of the model for pure liquid KCl, are given in Appendix A in SI units. As it is observed in Fig. 6-4, the viscosity measurements of Ejima et al. (1977) by oscillating vessel method and Ejima et al. (1982) by capillary method are in good agreement (within experimental limits of accuracies) with the calculated line based on the data of Brockner et al. (1981).

#### 6.1.4 $\text{MgCl}_2$

For  $\text{MgCl}_2$  pure liquid, Janz et al. (1975) critically re-examined the measurements of Bondarenko and Strelets (1968) and Dumas et al. (1970) by oscillating sphere method and recommended both mentioned sets of data in 1975 NSRDS publication. Janz et al. estimated the accuracy limits of these measurements to be  $\sim \pm 2\%$ . Later in 1988, by considering the results of Molten Salts standards Program, the data set of Torklep and Øye (1982) has been recommended with the estimated accuracy of  $\sim \pm 1\%$  (Janz, 1988). These measurements were performed by the oscillating cylinder viscometer developed earlier (Torklep and Øye, 1979) for the Molten Salts Standards Program measurements. To ensure the purity of the  $\text{MgCl}_2$  samples, after an initial treatment with HCl, samples were melted and again treated with HCl then filtered and distilled twice on a vacuum line. The salt samples were transported to the viscometer in closed vessels and the measurements performed under nitrogen atmosphere. Torklep and Øye (1982) considered their results with the oscillating cylinder to be superior to the ones of Dumas et al. (1970) with the oscillating sphere.

The measurements evaluated by Janz et al. (1975) together with the measurements reported after 1975, are summarized in Table 6.3.

Table 6.3: A Summary of the Experimental Methods for the Viscosity Measurements of  
Pure  $\text{MgCl}_2$  Reported in the Literature

Author	Year	Experimental Method (Working Equations)	Experimental Conditions	Temperature range [K]
Torklep & Øye	1982	Oscillating cylinder (Eqs. 3.3 & 3.4)	Pt92%-W8% torsion wire, Pt90%-Ir10% solid cylinder, Pt crucible, $\text{N}_2$ atmosphere, Control measurement by water	993 – 1172
Ejima et al.	1977	Oscillating vessel (Knappwost (1952) Eq.)	-	1006 – 1132
Dumas et al.	1970	Oscillating sphere (Computational procedure based on Eq. 3.2)	Tungsten torsion wire, Pt90%-Ir10% solid sphere, Pt crucible, $\text{N}_2$ atmosphere, Control measurements by water & $\text{KNO}_3$	995 – 1118
Bondarenko & Strelets	1968	Oscillating sphere (-)	Pt sphere, Calibration by water & nitrobenzene & aniline & molten $\text{KNO}_3$ & $\text{NaNO}_3$	1003 – 1143

These data sets are compared in Fig. 6.5 with the result of the present optimization based on the data of Torklep and Øye (1982).

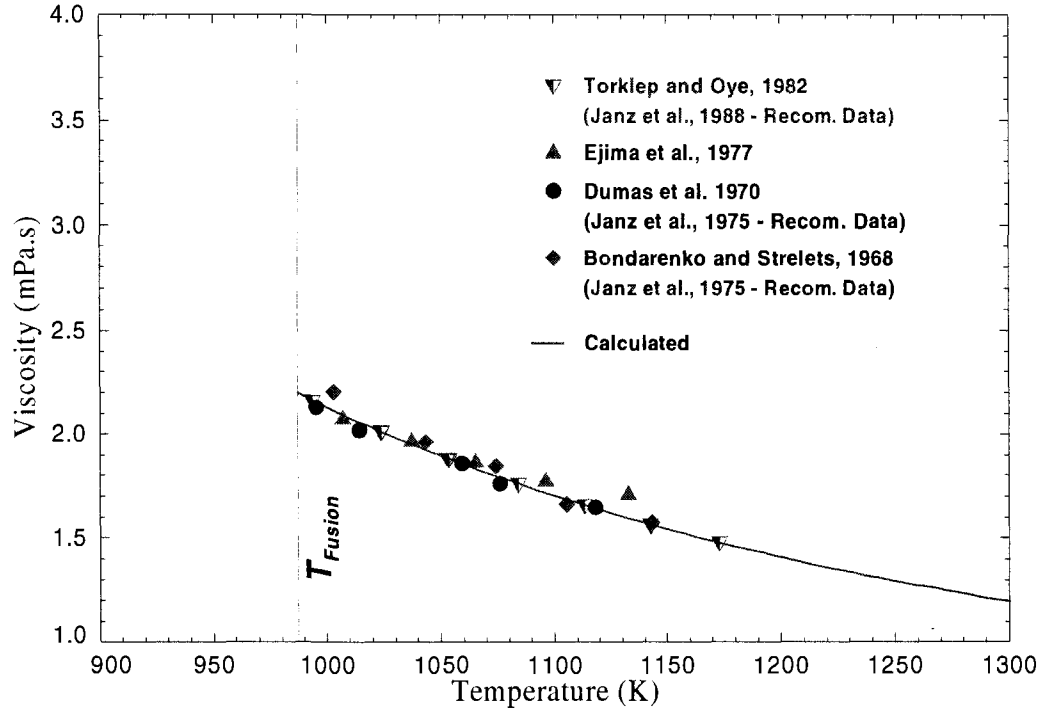


Figure 6.5: Calculated and Experimental Viscosity of Pure  $\text{MgCl}_2$

The solid line in Fig. 6-5 shows the results of the present optimization and is obtained similar to that of  $\text{NaCl}$  (see Section 6.1.2). The numerical values of  $c_{\text{Mg/Cl}}$  and  $d_{\text{Mg/Cl}}$ , the optimized parameters of the model for pure liquid  $\text{MgCl}_2$ , are given in Appendix A in SI units. As it is observed in Fig. 6-5, the measurements of Ejima et al. (1977) by oscillating vessel method are in good agreement (within experimental limits of accuracies) with the calculated line based on the data of Torklep and Øye (1982).

### 6.1.5 $\text{CaCl}_2$

For  $\text{CaCl}_2$  pure liquid, Janz et al. (1975) critically re-examined the measurements of Barzakovskii (1940), Vereshchetina and Luzhnaya (1954) and Zuca and Costin (1970). The data of Zuca and Costin (1970) based on the oscillating sphere method were selected as the most reliable one in 1975 NSRDS recommendations with  $\sim \pm 1\%$  estimated accuracy. Later in 1988, based on the results of the Molten Salts Standards Program, this data set has been superseded by the measurements of Torklep and Øye (1982) which were also recommended for  $\text{MgCl}_2$  as it was discussed in the last section. The NSRDS recommended measurements together with the other measurements reported in the literature are summarized in Table 6.4

Table 6.4: A Summary of the Experimental Methods for the Viscosity Measurements of Pure  $\text{CaCl}_2$  Reported in the Literature

Author	Year	Experimental Method (Working Equations)	Experimental Conditions	Temperature range [K]
Torklep & Øye	1982	Oscillating cylinder (Eqs. 3.3 & 3.4)	Pt92%-W8% torsion wire, Pt90%-Ir10% solid cylinder, Pt crucible, $\text{N}_2$ atmosphere, Control measurement by water	1014 – 1238
Ejima et al.	1977	Oscillating vessel (Knappwost (1952) Eq.)	-	1061 – 1145

Dumas et al.	1973	Oscillating sphere (Computational procedure based on Eq. 3.2)	Tungsten torsion wire, Pt90%-Ir10% solid sphere, Pt crucible, N <sub>2</sub> atmosphere, Control measurements by water & KNO <sub>3</sub> & KCl	1068 – 1129
Zuca & Costin	1970	Oscillating sphere (Eq. 3.2)	Pt sphere, Pt wire, N <sub>2</sub> atmosphere	1057 – 1221

These data sets are compared in Fig. 6.6 with the result of the present optimization based on the data of Torklep and Øye (1982).



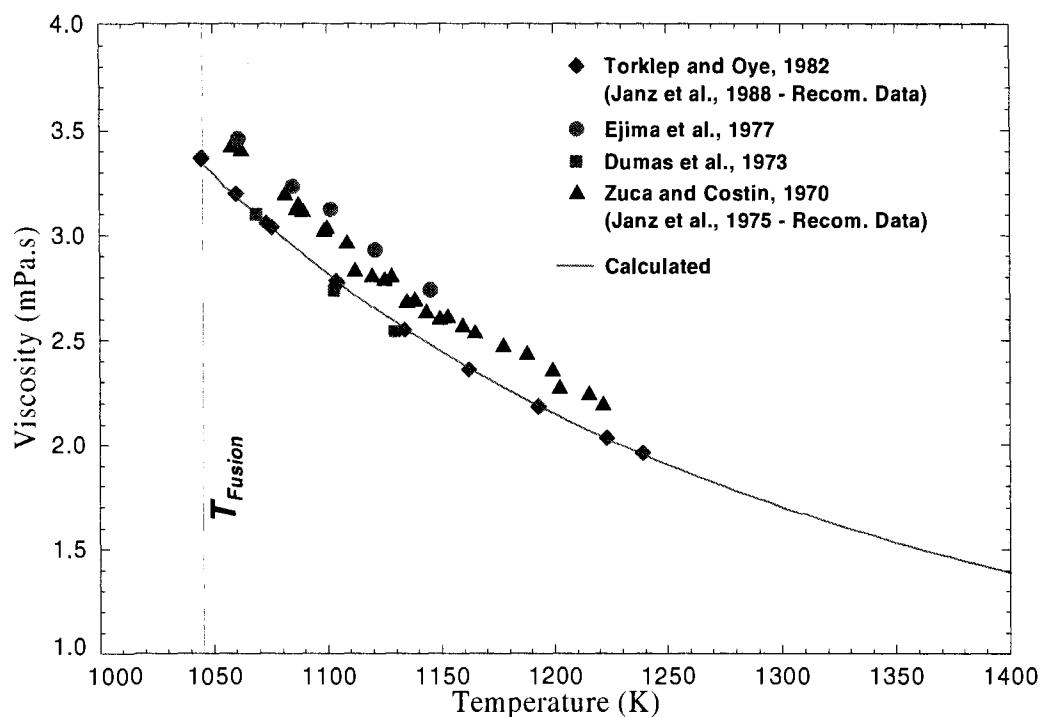


Figure 6.6: Calculated and Experimental Viscosity of Pure  $\text{CaCl}_2$ .

The solid line in Fig. 6.6 shows the results of the present optimization and is obtained similar to that of  $\text{NaCl}$  (see Section 6.1.2). The numerical values of  $c_{\text{Ca/Cl}}$  and  $d_{\text{Ca/Cl}}$ , the optimized parameters of the model for pure liquid  $\text{CaCl}_2$ , are given in Appendix A in SI units. As it is observed in Fig. 6.6, the measurements of Ejima et al. (1977) which were in good agreement with the calculated lines of  $\text{KCl}$  and  $\text{MgCl}_2$ , in the case of  $\text{CaCl}_2$  were higher than the recommended values and closer to the superseded values of Zuca and Costin (1970).

As it is shown in Fig. 6.7, the calculated viscosities of pure NaCl, KCl,  $\text{MgCl}_2$  and  $\text{CaCl}_2$  between 300K and 1900K extrapolated well below and above the melting points of the pure salts.

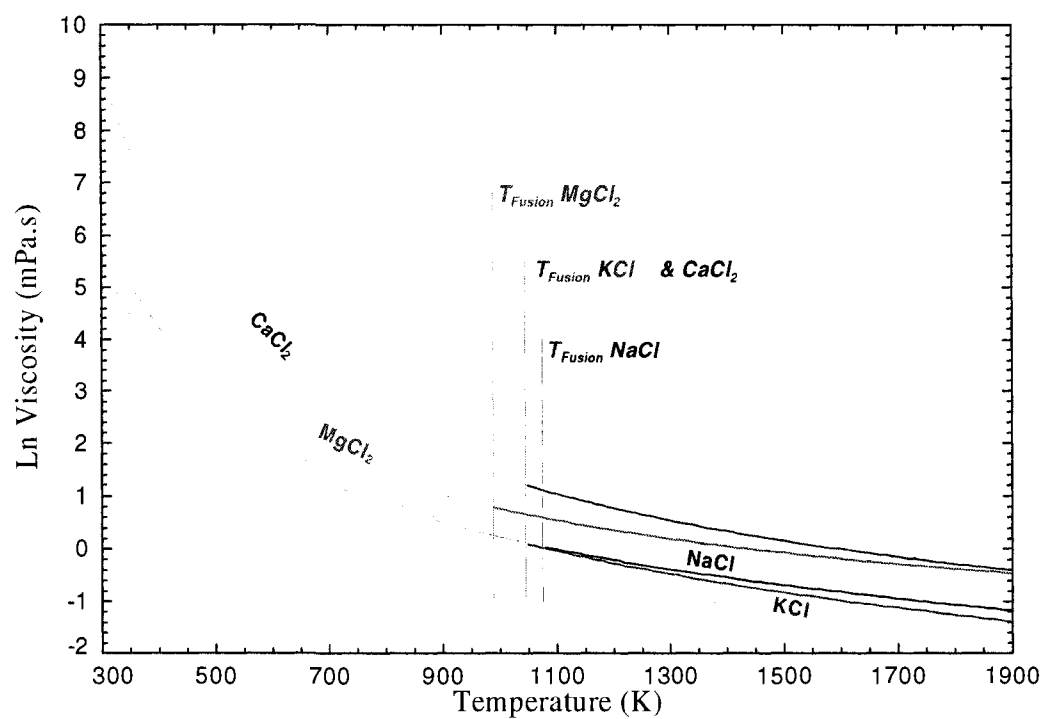


Figure 6.7: The Extrapolation of the Viscosity Curves Calculated by the Model Parameters for NaCl, KCl,  $\text{MgCl}_2$  and  $\text{CaCl}_2$  Pure Salts Below Their Melting Points.

## **6.2 Binary Molten Salts**

### **6.2.1 General Discussion on Literature Data**

To obtain the optimized parameters of the model for binary systems, a thorough literature review is performed to collect the binary viscosity data. As we will see in the upcoming sections, likewise the unary data, large discrepancies are observed between the collected binary data. The most frequently used method for the binary measurements, was the oscillating body technique (Murgulescu and Zuca, 1965; Dumas et al., 1973; Ejima et al., 1977; Zuca and Borcan, 1984). As it is discussed in the last sections, the results of the Molten Salts Standards Program (Janz, 1980) showed several error sources in viscosity measurements by this technique leading to large discrepancies among the reported literature data. Particularly design features such as torsion wire, torsion pendulum and oscillating bodies (sphere or cylinder); together with the sample quality, irregularities in the shape of the oscillating body and the computational approaches to obtain the viscosity have been considered as possible sources of error. Later Torklep and Øye (1982) showed that the numerous conflicts between reported viscosity measurements by oscillating sphere method, can be ascribed to radius calibration errors. Brockner et al. (1981) mentioned the gas bubbles adhering to the oscillation body, as another source of error (1981), that can explain significant discrepancies of more than 10 % in reported viscosity values. This error becomes more important at alternating decreasing temperature. According to Brockner et al. (1981), when melts are cooled from a high temperature, the reduced gas solubility results in gas bubbles adhering to the oscillating body. Such

bubbles affect both the moment of inertia and the friction and lead to erroneous results which are too high. The similar effects are observed if the melt contains solid particles that adhere to the oscillating body.

Based on the above mentioned considerations and the significant shifts of the 1988 NSRDS recommendations for pure salts; (up to 50% in the case of NaCl, comparing to the former recommendations); similar upgraded data sets were expected for binary systems. Despite the expectation to observe the similar shift between 1975 and 1988 recommendations for the binary systems containing these pure salts, the binary recommendations in 1988 remain unchanged for several systems. As an example, the 1975 NSRDS recommended data set for NaCl-KCl binary system, was the data of Murgulescu and Zuca (1965). This data set is again recommended in 1988 NSRDS publication as the most reliable data set for NaCl-KCl viscosity. According to this data set, the corresponding unary viscosity values (at  $X_{NaCl} = 1$  and  $X_{KCl} = 1$ ) are equal to that of Murgulescu and Zuca (1963) for pure NaCl; and Murgulescu and Zuca (1961) for pure KCl. As it is discussed in Sections 6.1.1 and 6.1.2 and illustrated in Figs. 6.3 and 6.4, the results of the Molten Salts Standards Program showed that the Murgulescu and Zuca (1961; 1963) data sets were in serious error. These data sets have been significantly shifted to lower values in the 1988 NSRDS recommendations for pure salts (Janz, 1980; 1988). It seems that the shift observed in the unary recommended data has not been considered in the binary data evaluation. This inconsistency between the recommended unary and binary data in 1988 NSRDS recommendations was observed for most of the binary systems studied in the present work. To resolve this problem and obtain upgraded

binary viscosity values consistent with the recommended unary data, it could be reasonable to apply a systematic correction. As it is described in the upcoming section, these corrections are calculated for the binary data sets based on the estimated error of their corresponding pure components. The so called “Corrected” data sets are the ones employed to calculate the binary parameters of the model. They appeared as “Corrected” in the figures for binary systems. In the following sections, the experimental literature data reported for the binary systems are summarized and the results of our optimizations are presented. The temperature-dependency and composition-dependency of the viscosity, given by the model, for each binary system are illustrated in separate figures and compared with the literature data.

### **6.2.2 Data Correction**

To calculate the correction factor required for each binary data set, the first step is to estimate the error of its corresponding pure components. As an example, the NaCl-KCl data of Murgulescu and Zuca (1965) at a given temperature is shown in Fig. 6.8 along with its corresponding pure data; Murgulescu and Zuca (1963) for pure NaCl; and Murgulescu and Zuca (1961) for pure KCl.

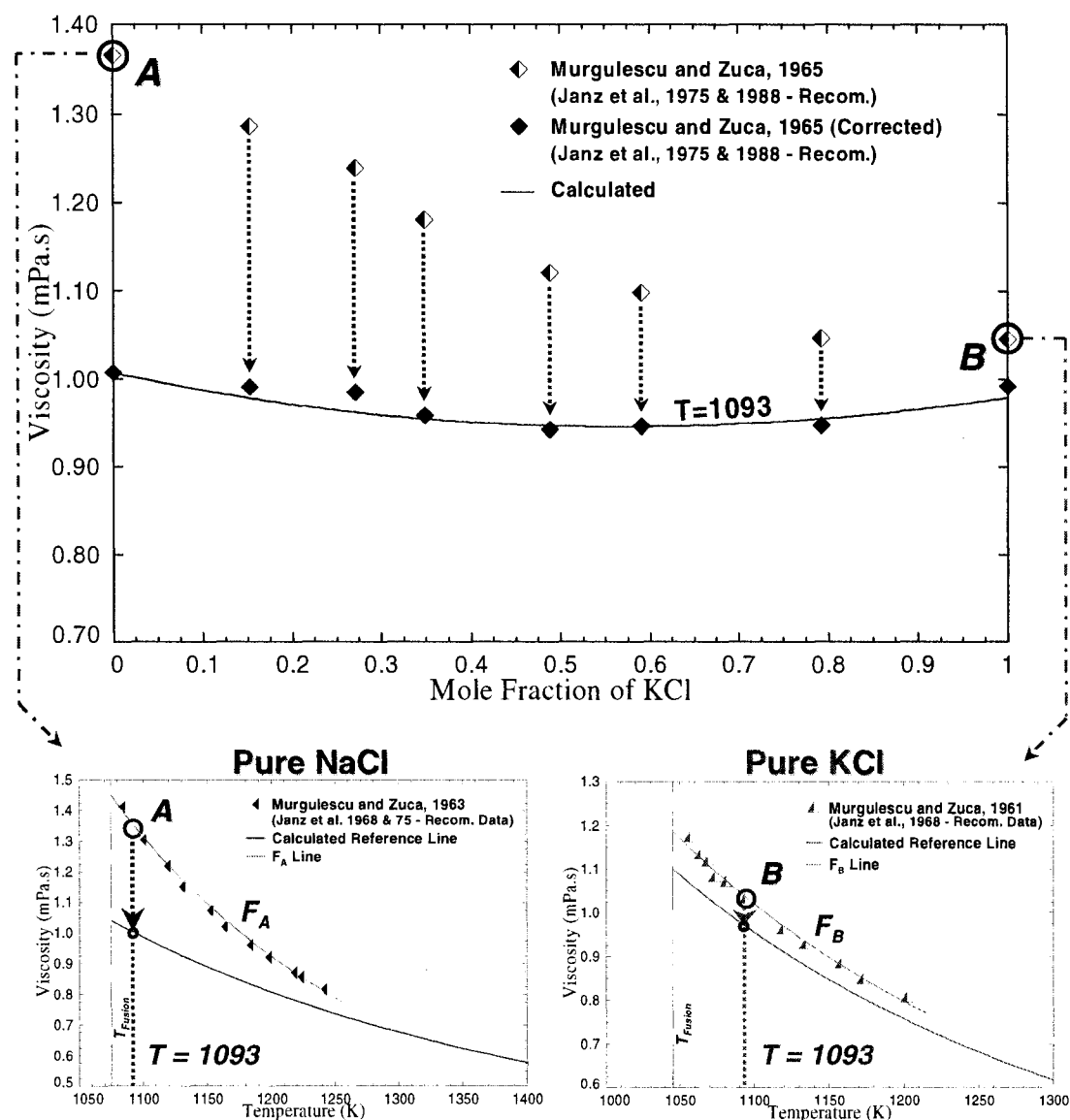


Figure 6.8: The Correction Applied to the Binary Data of Murgulescu and Zuca (1965) for NaCl-KCl System at a Given Temperature, Based on the Estimated Error of its Corresponding Pure Data Sets.

In the Fig. 6.8,  $F_A$  is an exponential function in the form of Eq. (6.1) fitted to the Murgulescu and Zuca (1963) data set for pure NaCl,  $F_B$  is the similar fit of Murgulescu and Zuca (1961) data set for pure KCl and the reference lines in Fig. 6.8 are the fits given by the optimized parameters of the model as it is described in Sections 6.1.1 and 6.1.2. The errors of the Murgulescu and Zuca (1961; 1963) data sets are obtained by estimating the distances between  $F_B$ ,  $F_A$  and the reference lines of KCl and NaCl, respectively. Accordingly the mentioned data sets can be corrected by the error functions of the following forms:

$$\begin{aligned}\Delta_{NaCl}^{Mur-Zuca-63} &= \frac{F_A - F_{NaCl}}{F_A} = 1 - \frac{\frac{hN_A}{V_M} \exp(\frac{c_{NaCl} + d_{NaCl}T}{RT})}{\frac{hN_A}{V_M} \exp(\frac{c_A + d_A T}{RT})} \\ &= 1 - \exp\left[\frac{(c_{NaCl} - c_A) + (d_{NaCl} - d_A)T}{RT}\right]\end{aligned}\quad (6.4)$$

$$\begin{aligned}\Delta_{KCl}^{Mur-Zuca-61} &= \frac{F_B - F_{KCl}}{F_B} = 1 - \frac{\frac{hN_A}{V_M} \exp(\frac{c_{KCl} + d_{KCl}T}{RT})}{\frac{hN_A}{V_M} \exp(\frac{c_B + d_B T}{RT})} \\ &= 1 - \exp\left[\frac{(c_{KCl} - c_B) + (d_{KCl} - d_B)T}{RT}\right]\end{aligned}\quad (6.5)$$

where  $\Delta_{NaCl}^{Mur-Zuca-63}$  is the error function of Murgulescu and Zuca (1963) data set for pure NaCl,  $\Delta_{KCl}^{Mur-Zuca-61}$  is the error function of Murgulescu and Zuca (1961) data set for pure KCl,  $c_{Na/Cl}$ ,  $d_{Na/Cl}$ ,  $c_{K/Cl}$  and  $d_{K/Cl}$  are the optimized parameters of the model for pure NaCl and pure KCl (given in Appendix A),  $c_A$  and  $d_A$  are the parameters of the activation energy (Eq. 6.2) obtained by fitting the data set of Murgulescu and Zuca (1963) for pure NaCl and  $c_B$  and  $d_B$  are the parameters of the Murgulescu and Zuca (1961) fit for pure KCl. Similar error functions are obtained for all the unary literature data corresponding to the studied binary data sets and listed in Appendix C. The corrected data sets are illustrated in Figs. 6.9 to 6.12 for each pure component.

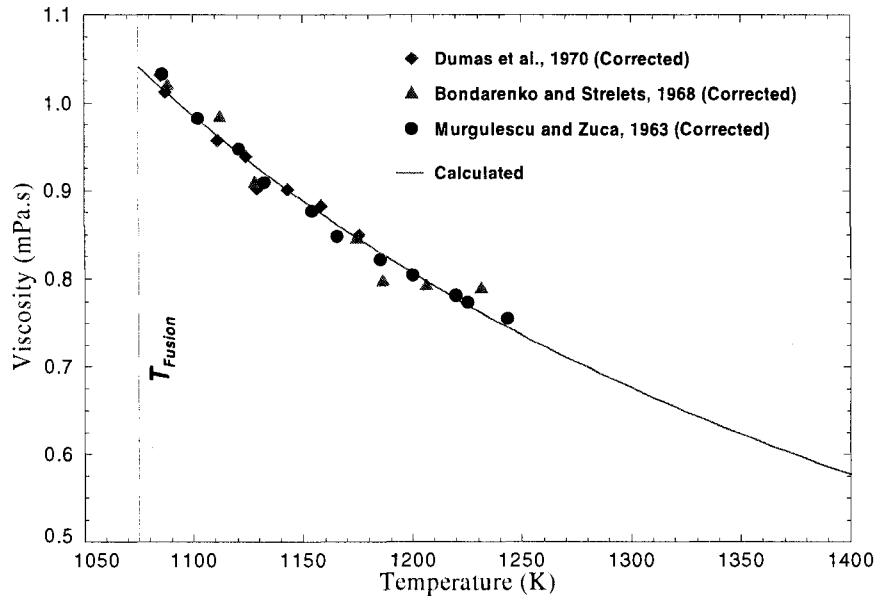


Figure 6.9: The Corrected Data Sets for Pure NaCl.



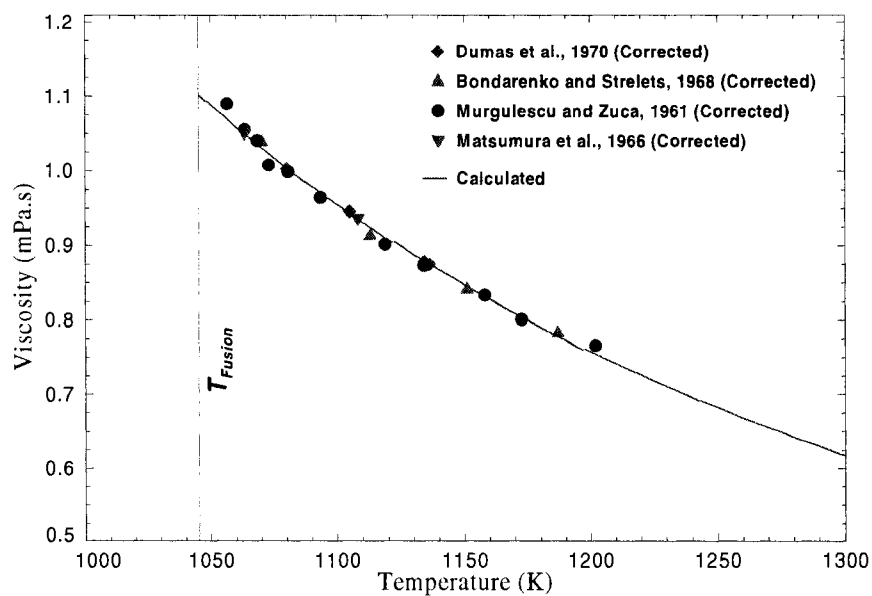


Figure 6.10: The Corrected Data Sets for Pure KCl.

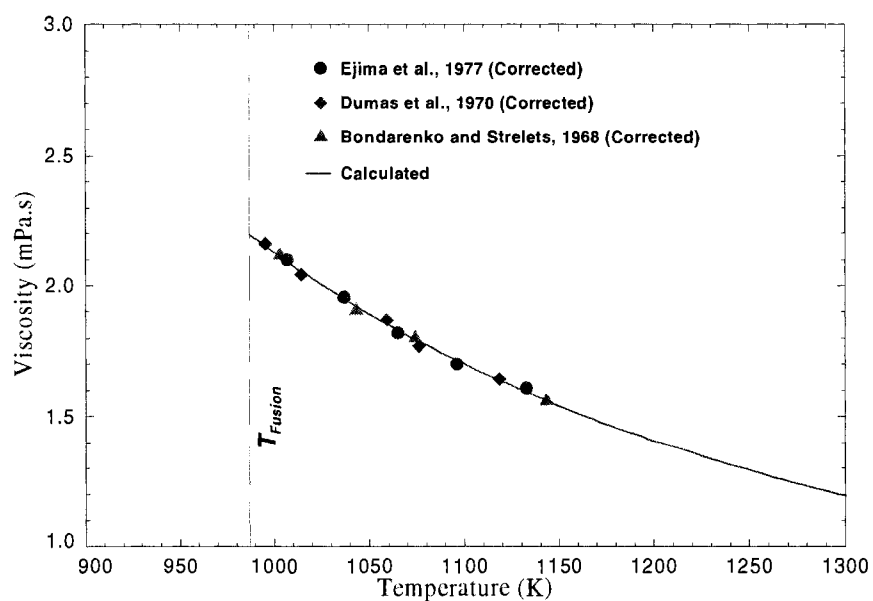


Figure 6.11: The Corrected Data Sets for Pure MgCl<sub>2</sub>.

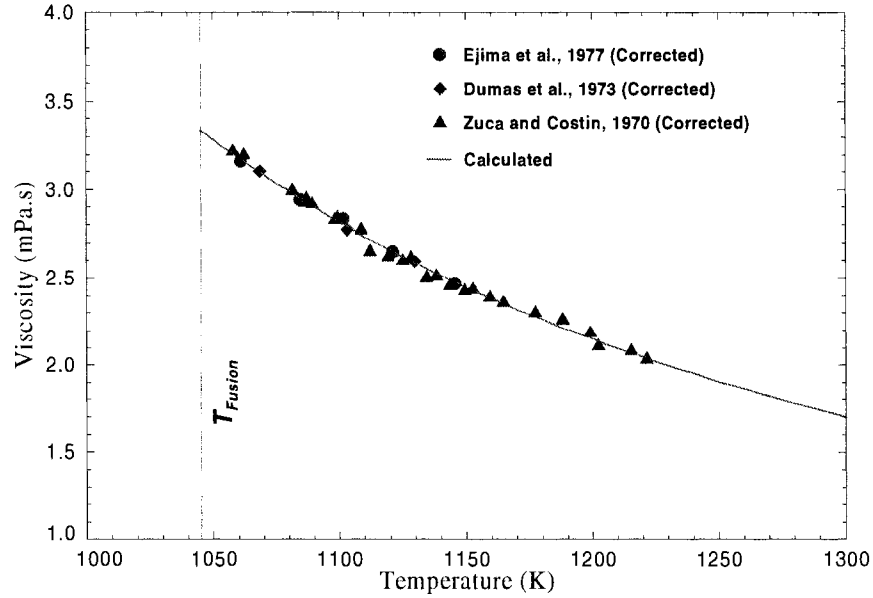


Figure 6.12: The Corrected Data Sets for Pure  $\text{CaCl}_2$ .

After estimating the error of pure data sets, the second step is to obtain a systematic error function for the corresponding binary data sets. This systematic error function could be any function of unary correction factors which could best correct the binary data. However due to the lack of reliable binary measurements and enough information about the accuracy estimation of high temperature viscosity measurements; it is decided to employ a simple linear error function for the binary systems. The binary correction functions thereby are obtained by a linear additivity relation between the pure error functions and the mole fractions of the components as follows:

$$\Delta_{Na-K}^{Mur-Zuca-65} = X_{NaCl} \cdot \Delta_{NaCl}^{Mur-Zuca-63} + X_{KCl} \cdot \Delta_{KCl}^{Mur-Zuca-61} \quad (6.6)$$

where  $\Delta_{Na-K}^{Mur-Zuca-65}$  is the error function of Murgulescu and Zuca (1965) binary data set,  $X_{NaCl}$  is the mole fraction of NaCl and  $X_{KCl}$  is the mole fraction of KCl. The binary data set of Murgulescu and Zuca (1965) is corrected by multiplying the reported viscosity values to  $1 - \Delta_{Na-K}^{Mur-Zuca-65}$ . As it is illustrated in Fig. 6.8 for a given temperature, the corrected binary data are shifted to lower values consistent with the corresponding unary values. All the binary data sets that appear in the figures of the following sections are corrected in the similar manner to be consistent with the recommended unary data.

### 6.2.3 NaCl-KCl

The literature data for NaCl-KCl binary system are summarized in Table 6.5.

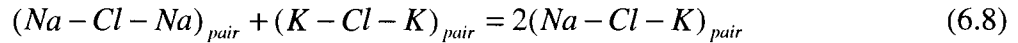
Table 6.5: A Summary of the Experimental Methods for the Viscosity Measurements of NaCl-KCl Reported in the Literature.

Author	Year	Experimental Method (Working Equations)	Experimental Conditions	KCl [Mol%]	Temperature Range [K]
Murgulescu & Zuca	1965	Oscillating sphere (-)	Pt sphere, Pt wire, Calibration by water, nitrobenzene, aniline, molten $KNO_3$ & $NaNO_3$	0 – 100	993 – 1173
Matsumura et al.	1966	Oscillating disc (Using a relation between viscosity and number of oscillation)	Pt disc, Stainless steel wire, Pt crucible	0 – 100	992 – 1118
Bondarenko et al.	1966	Oscillating sphere (-)	Pt sphere, Calibration by water, nitrobenzene, aniline, molten $KNO_3$ & $NaNO_3$	20.7, 44, 70.2, 100	988 – 1187

Several data sets such as (Murgulescu and Zuca, 1965; Bondarenko, 1966; Matsumura et al., 1966), have been evaluated in 1975 NSRDS critical review (Janz et al., 1975). The measurements of Murgulescu and Zuca (1965) by the oscillating sphere method has been recommended as the most reliable data set. The mentioned data set was again recommended in 1988 NSRDS publication (Janz, 1988), despite the significant shifts of its corresponding unary data sets. As it was described in the previous section, this data set is corrected, due to the inconsistency with its corresponding recommended unary data (see Appendix C for the numerical values of the corrections). The corrected data set is employed to optimize the binary parameters of the model in the present work. As it is previously discussed in Section 5, the binary parameters of the model can be obtained by a linear regression in the form of Eq. (5.4) among the binary experimental viscosity data as follows:

$$\ln(\eta V_M) - \ln(hN_A) = \frac{X_{NaK/Cl}}{R} \left( \frac{c_{NaK/Cl}}{T} + d_{NaK/Cl} \right) \quad (6.7)$$

where  $\eta$  is the experimental viscosity value at a given temperature and composition,  $V_M$  is the molar volume of the binary solution given by the density model as a function of temperature and composition of the melt (see Section 5.3),  $c_{NaK/Cl}$  and  $d_{NaK/Cl}$  are the binary parameters of the model and  $X_{NaK/Cl}$  is the mole fraction of the (Na – Cl – K) SNN pairs. Assuming the following quasicheical reaction between the SNN pairs in the melt:



The mole fractions of the pairs can be calculated by the modified quasichemical model in pair approximation, as it is discussed in Section (5.2).

The numerical values of  $c_{NaK/Cl}$  and  $d_{NaK/Cl}$  are given in Appendix A. Accordingly, the viscosity of NaCl-KCl binary solution can be calculated by Eq. (5.2) in terms of the mole fractions of the SNN pairs and unary and binary activation energies as follows:

$$\eta = \frac{hN_A}{V_M} \exp\left(\frac{X_{NaNa/Cl}G^*_{Na/Cl} + X_{KK/Cl}G^*_{K/Cl} + X_{NaK/Cl}G^*_{NaK/Cl}}{RT}\right) \quad (6.9)$$

with the activation energies given by the optimized parameters of the model as follows:

$$\begin{aligned} G^*_{Na/Cl} &= c_{Na/Cl} + d_{Na/Cl}T \\ G^*_{K/Cl} &= c_{K/Cl} + d_{K/Cl}T \\ G^*_{NaK/Cl} &= c_{NaK/Cl} + d_{NaK/Cl}T \end{aligned} \quad (6.10)$$

(see Appendix A for the numerical values of the parameters)

The calculated viscosity isotherms and isocomposition lines obtained by Eq. (6.9) are illustrated in Figs. 6.13 and 6.14.

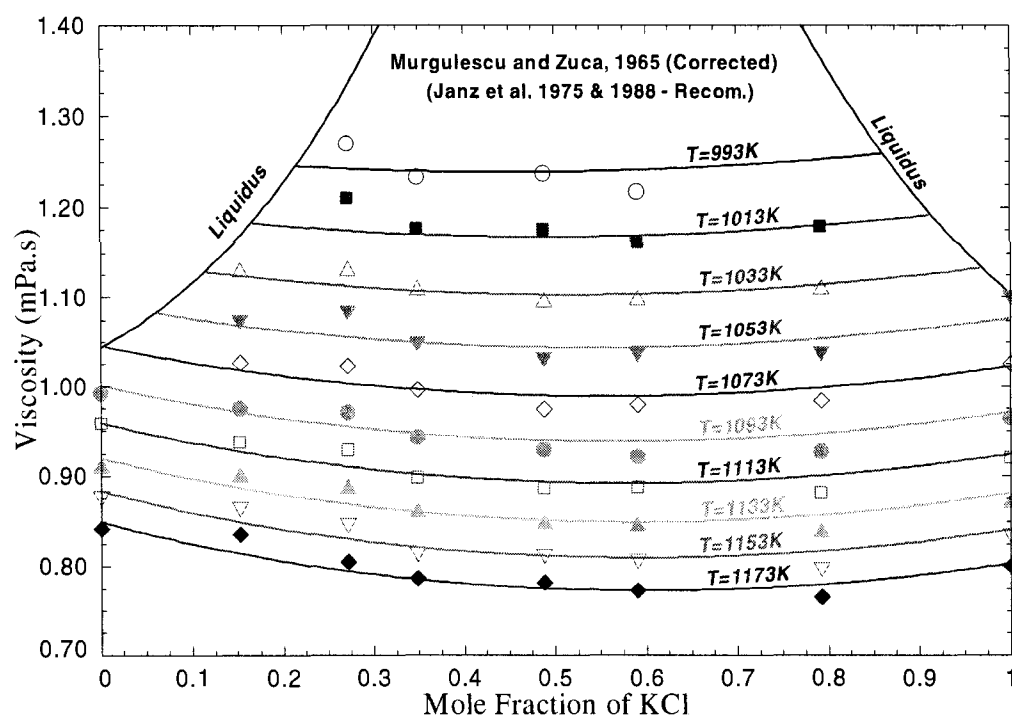


Figure 6.13: Calculated and Experimental Viscosity of NaCl-KCl Melt at Various Temperatures.

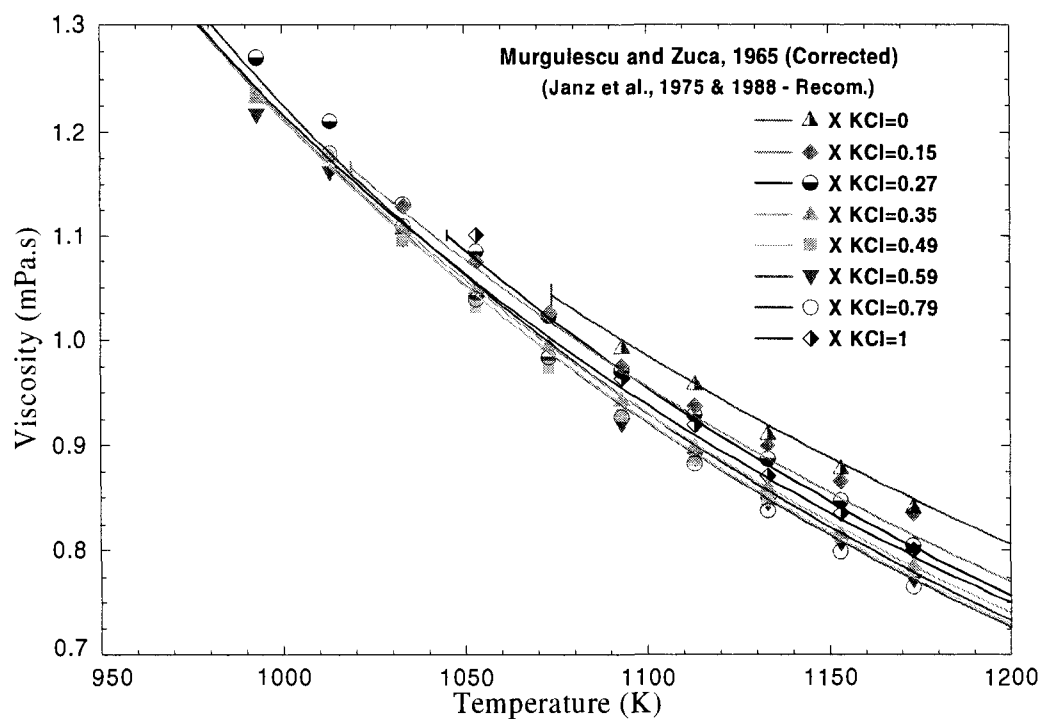


Figure 6.14: Calculated and Experimental Viscosity of NaCl-KCl Melt at Various Mole Fractions of KCl.

Fig. 6.15 illustrates a comparison between the calculated viscosity isotherms and the literature data which are not used to obtain the parameters of the model.

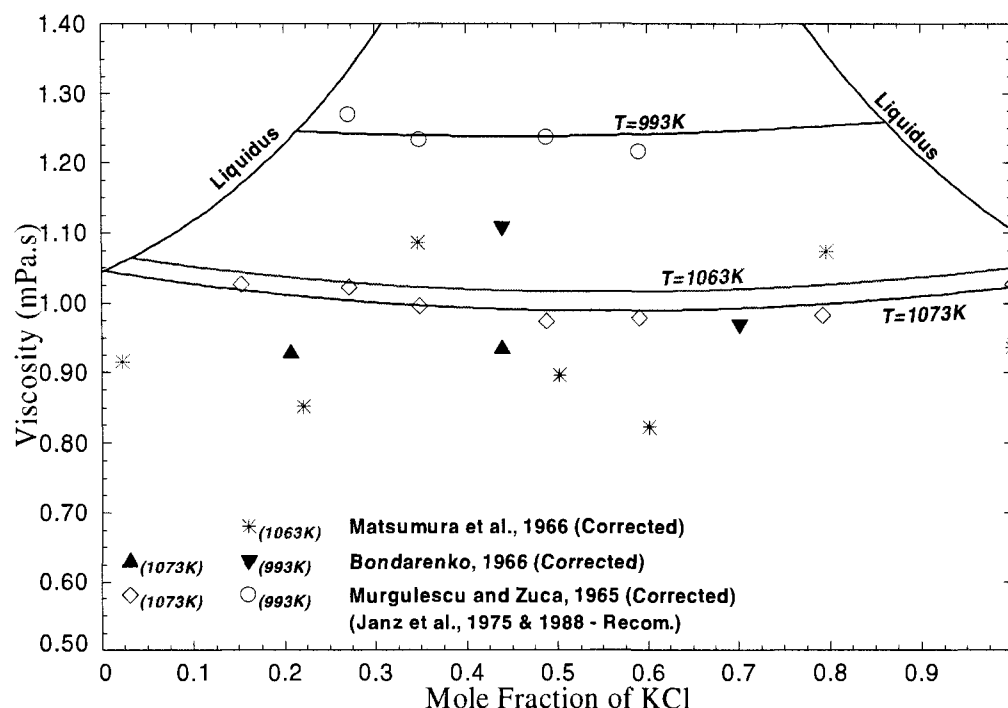


Figure 6.15: A Comparison Between the Calculated Viscosity Isotherms and the Experimental Data of NaCl-KCl Melt.

As it is shown in Fig. 6.13, the addition of KCl to pure liquid NaCl, does not significantly affect the viscosity. Since both pure salts have almost similar viscosity values and similar ionic structure, the viscosity isotherms are almost linear with a slight negative deviation. This can be called an ideal viscosity behavior upon mixing, which is consistent with the thermodynamic definition of this binary system. From the thermodynamic point of view, since  $Na^+$  and  $K^+$  cations are almost identical (ionic radiuses of  $Na^+$  and  $K^+$  cations are  $1.02\text{\AA}$  and  $1.38\text{\AA}$  respectively), there will be negligible change in bonding energy or



volume upon mixing. Consequently the Gibbs energy change of the quasichemical reaction (6.8) is small, low degree of short-range ordering is observed and the equilibrium SNN pair fractions can be calculated by assuming a random distribution of cations on the cationic sublattice (see Section 5.2 for the thermodynamic model). Since these equilibrium pair fractions are employed to calculate the viscous activation energy of the binary solution, the structural behavior of the system can be properly manifested in the present viscosity model.

#### **6.2.4 $\text{CaCl}_2\text{-MgCl}_2$**

According to the present literature review, two data sets have been reported for the viscosity of  $\text{CaCl}_2\text{-MgCl}_2$  binary system. The measurements of Fan et al. (2004) by rotating cylinder method and the measurements of Dumas et al. (1973) by the oscillating sphere method. It was no recommendation for the viscosity of this system in 1975 and 1988 NSRDS publications (Janz et al., 1975; Janz, 1988). The data set of Dumas et al. (1973) is mentioned as one of the unevaluated systems for the viscosity in 1975 NSRDS publication.

As it is illustrated in Fig. 6.16, the scattered viscosity values reported by Fan et al. (2004) are too high, compared to the ones of Dumas et al. (1973).

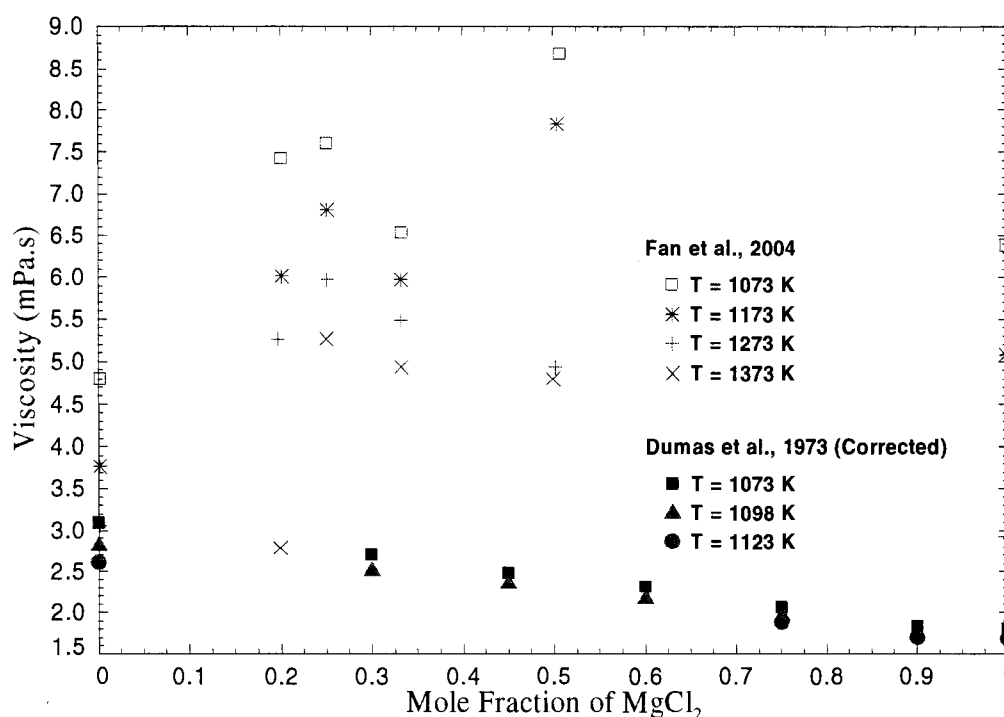


Figure 6.16: A Comparison Between the Binary Data of Dumas et al. (1973) and Fan et al. (2004) for CaCl<sub>2</sub>-MgCl<sub>2</sub> Melt.

As it was previously discussed in Section 3.3, to obtain accurate viscosity values by the rotational technique, it is critical that the cylinders rotate axisymmetrically. Maintaining this condition for low viscosity liquids is technically difficult due to the small clearance required between the stationary and the rotating cylinder. Accordingly, the scattered high viscosity values of Fan et al. (2004), can be a result of the experimental errors. Due to the lack of information regarding the experimental conditions of Fan et al. (2004) measurements, the experimental error of the measurements could not be estimated. On

the other hand, the systematic corrections applied for the other binary data sets were not applicable to the Fan et al. (2004) rotational measurements; since those corrections were based on the estimated error of oscillating methods. Therefore the mentioned data set has not been considered in the optimization of binary parameters in the present work. The binary parameters of the model for this system are obtained by employing the Dumas et al. (1973) binary data set. As it is illustrated in Figs 6.5 and 6.6, the corresponding unary measurements of Dumas et al. (1973) for pure  $\text{CaCl}_2$  and pure  $\text{MgCl}_2$  show good agreement (within experimental limits of accuracies) with the recommendations for the pure salts. In the case of pure  $\text{MgCl}_2$ , the reported viscosity values are similar to the ones of Dumas et al. (1970) which are recommended in 1975 NSRDS publication with the estimated accuracy of  $\sim \pm 2\%$  (Janz et al., 1975). According to Dumas et al. (1973), the apparatus, the technique and the computational procedure employed to obtain the binary viscosity values are the same as Dumas et al. (1970) measurements for pure salts. The  $\text{CaCl}_2$  and  $\text{MgCl}_2$  salt crystals were carefully purified and treated with  $\text{HCl}$  gas and mechanically mixed in a dry-box. The salt mixture was then placed in a Pyrex container fitted with a valve which allowed the transfer of salts to the viscosity crucible without exposure to air. According to Dumas et al. (1973), this transfer mechanism was also used for adding the pure salts to the first prepared melts in order to perform the binary measurements in different compositions.

Based on the above mentioned considerations and the high accuracy of the measurements performed by Dumas, Øye and co-workers for the Molten Salts Standards Program (Janz, 1980) with the similar technique (employing oscillating cylinder instead of sphere in the

same viscometer), the data set of Dumas et al. (1973) was considered as a reliable data set (Further discussion on the reliability of the measurements of this group will be given in the next section). However a minor systematic correction is applied to this data set due to the minor inconsistency of its corresponding unary viscosity values with the recommended values (see Section 6.2.2). The related correction functions are given in Appendix C. This corrected data set is employed to calculate the parameters of the model for  $\text{CaCl}_2\text{-MgCl}_2$  system. The binary parameters of the model ( $c_{\text{CaMg/Cl}}$  and  $d_{\text{CaMg/Cl}}$ ) are calculated similar to that of  $\text{NaCl-KCl}$  as it is described in Section 6.2.3 (See Appendix A for the numerical values of the parameters).

The calculated viscosity isotherms and isocomposition lines are illustrated in Figs. 6.17 and 6.18 and compared with the experimental data.

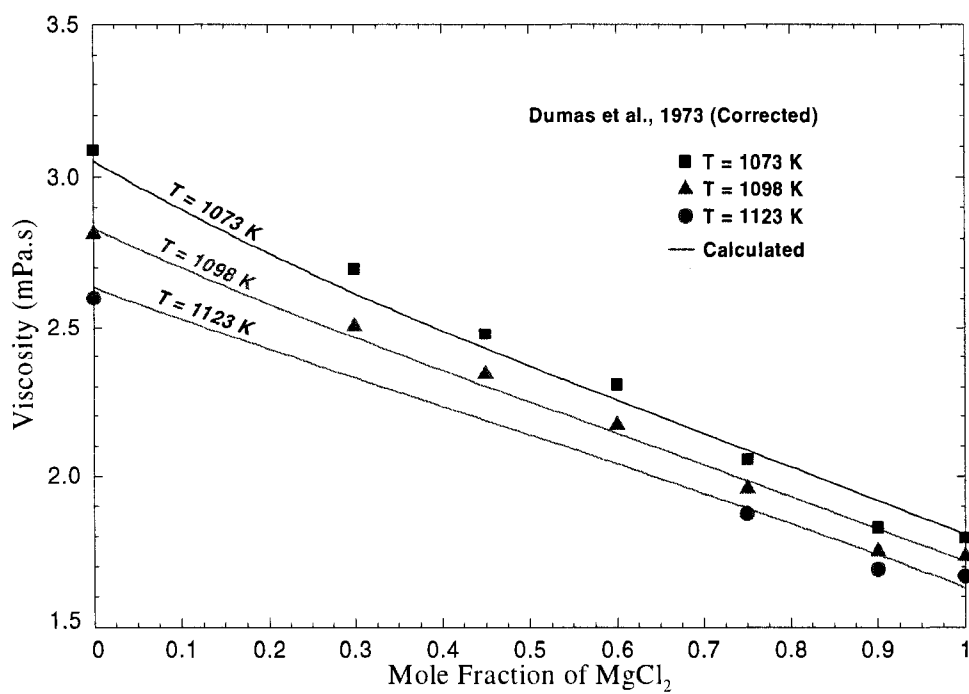


Figure 6.17: Calculated and Experimental Viscosity of  $\text{CaCl}_2\text{-MgCl}_2$  Melt at Various Temperatures.

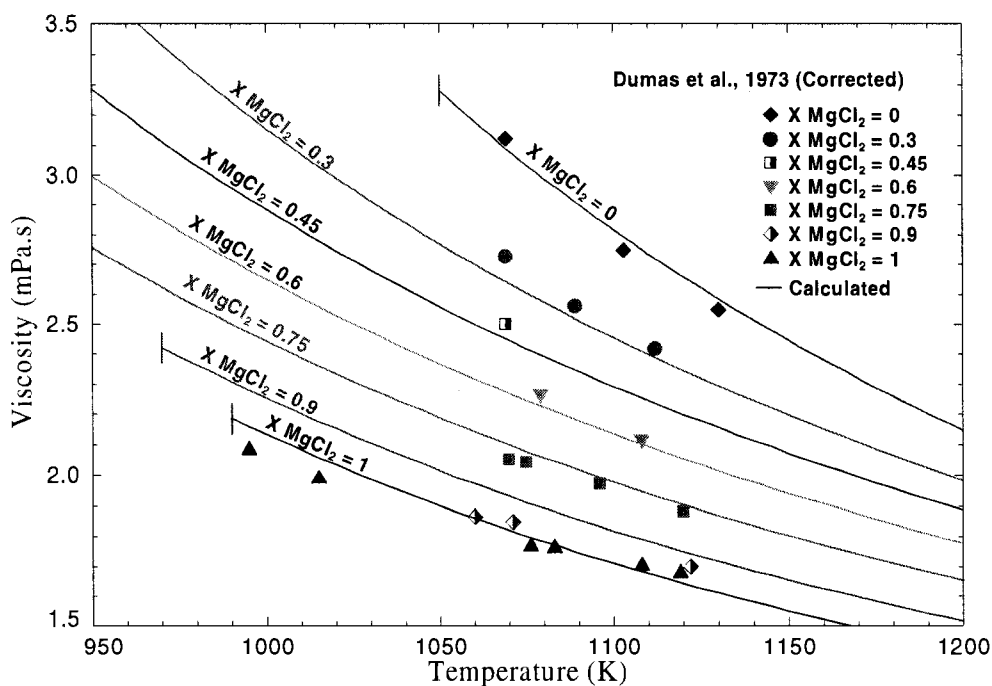


Figure 6.18: Calculated and Experimental Viscosity of  $\text{CaCl}_2\text{-MgCl}_2$  Melt at Various Mole Fractions of  $\text{MgCl}_2$ .

As it is shown in Fig. 6.17, a linear decrease in the viscosity of liquid solution is observed upon the addition of  $\text{MgCl}_2$  due to its lower viscosity. Likewise the case of  $\text{NaCl-KCl}$  binary solution, a so called ideal viscosity behavior for this binary system, is manifested in the viscosity isotherms obtained by the model.

### 6.2.5 $\text{KCl-CaCl}_2$

A summary of the literature data reported for this binary system is given in Table 6.6.

Table 6.6: A Summary of the Experimental Methods for the Viscosity Measurements of KCl-CaCl<sub>2</sub> Reported in the Literature.

Author	Year	Experimental Method (Working Equations)	Experimental Conditions	KCl [Mol %]	Temperature Range [K]
Dumas et al.	1973	Oscillating sphere (Computational procedure based on Eq. 3.2)	Tungsten torsion wire, Pt90%-Ir10% solid sphere, Pt crucible, N <sub>2</sub> atmosphere, Control measurements by water & KNO <sub>3</sub> & KCl	0 – 90	1023 – 1123
Ejima et al.	1977	Oscillating vessel (Knappwost, 1952)	-	0 – 100	988 – 1153
Zuca & Borcan	1984	Oscillating sphere (Eq. 3.2)	Pt sphere, Pt wire, N <sub>2</sub> atmosphere	25 – 85	1070 - 1248

There was no recommendation for the viscosity of this system in 1975 and 1988 NSRDS publications (Janz et al., 1975; Janz, 1988). The data set of Dumas et al. (1973) is mentioned as one of the unevaluated systems for the viscosity in 1975 NSRDS publication. As it was previously discussed in Section 6.1.2, the results of the Molten Salts Standards Program later confirmed the high accuracy of the measurements performed by this laboratory (Janz, 1980). According to Torklep and Øye (1979), the

oscillating sphere viscometer which were used for several years in their laboratory (Dumas et al., 1970; Dumas et al., 1973; Brockner et al., 1975), has been re-designed for the measurements of the Standards Program to replace the oscillating sphere, by a cylinder. Since cylinders could be re-machined to more exact tolerances than the spheres, this modification could lead to more accurate viscosity values (Janz, 1980). Accordingly, by estimating a correction factor to take into account these modifications, the measurements of this group by the oscillating sphere, are used as reliable sets of data in the present work. The systematic correction applied to the data set of Dumas et al. (1973) for KCl-CaCl<sub>2</sub> binary system, is obtained based on the error estimated for its corresponding unary data (the corresponding data set for pure KCl was similar to the one of Dumas et al. (1970)). The corrected data sets are illustrated in Figs. 6.10 and 6.12 and related numerical values of the correction functions are given in Appendix C. The binary parameters of the model ( $c_{KCa/Cl}$  and  $d_{KCa/Cl}$ ) are calculated based on the mentioned corrected data set of Dumas et al. (1973), in the similar manner explained in Section 6.2.3 (See Appendix A for the numerical values of the parameters). The calculated viscosity isotherms and isocomposition lines are illustrated in Figs. 6.19 and 6.20 and compared with the corrected experimental data.



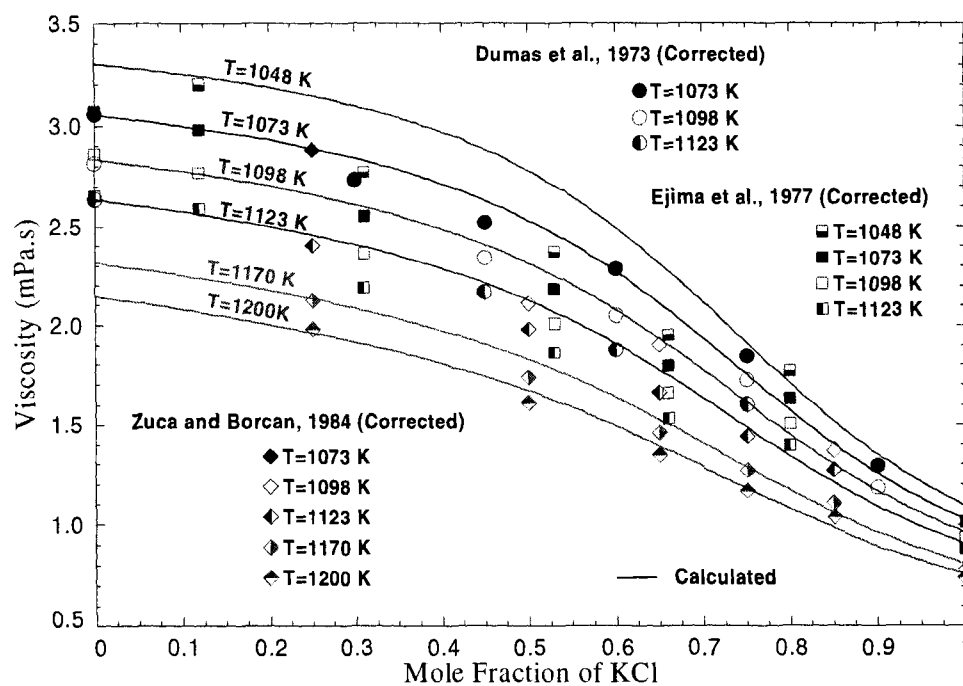


Figure 6.19: Calculated and Experimental Viscosity of KCl-CaCl<sub>2</sub> Melt at Various Temperatures.

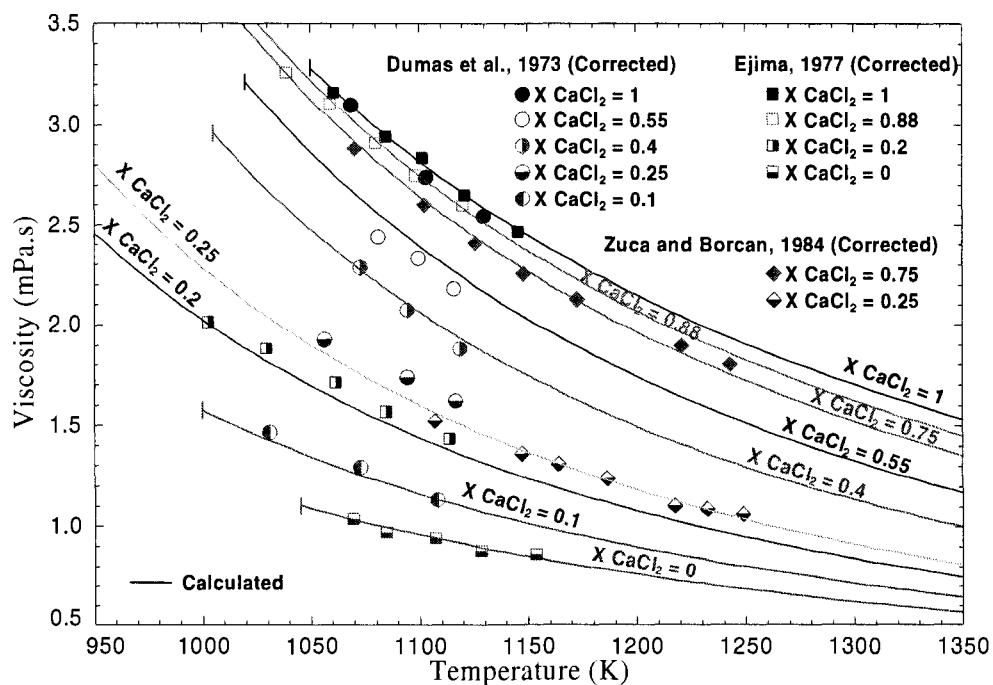


Figure 6.20: Calculated and Experimental Viscosity of KCl-CaCl<sub>2</sub> Melt at Various Mole Fractions of CaCl<sub>2</sub>.

The data sets of Zuca and Borcan (1984) and Ejima et al. (1977) illustrated in the figure, are corrected in the same manner described for Dumas et al. (1973) data set. Since the viscosity values of the corresponding pure components have not been reported in Zuca and Borcan (1984) publication, their earlier measurements in 1961 for pure KCl and in 1970 for pure CaCl<sub>2</sub> with the same technique (Murgulescu and Zuca, 1961; Zuca and Costin, 1970) are used to estimate the required correction functions. According to Zuca and Borcan (1984), the corresponding unary data sets are in very good agreement (within

$\pm 1\%$ ) with their 1961 and 1970 measurements for pure KCl and pure  $\text{CaCl}_2$  respectively (see Figs. 6.10 and 6.12 for corrected pure data sets and Appendix C for the numerical values).

#### **6.2.6 NaCl- $\text{CaCl}_2$**

The data sets of Barzakovskii (1940) and Vereshchetina and Luzhnaya (1954) have been re-examined in 1975 NSRDS critical review (Janz et al., 1975). The measurements of Vereshchetina and Luzhnaya (1954) by the oscillating sphere method has been recommended as the most reliable data set. However the data set of Dumas et al. (1973) has been mentioned in the same publication (Janz et al., 1975), as one of the unevaluated systems. Based on the considerations previously described in Sections 6.2.4 and 6.2.5, the measurements of Dumas et al. (1973) were selected as a reliable data set for NaCl- $\text{CaCl}_2$  binary system. However, similar to the  $\text{MgCl}_2$ - $\text{CaCl}_2$  and KCl- $\text{CaCl}_2$  binary systems, a correction factor is defined for this data set to take into account the accuracy limits imposed by the oscillating sphere method. The systematic correction applied to the data set of Dumas et al. (1973) for NaCl- $\text{CaCl}_2$  binary system, is obtained based on the error estimated for its corresponding unary data (the corresponding data set for pure NaCl was similar to the one of Dumas et al. (1970)). The corrected data sets are illustrated in Figs 6.9 and 6.12 and related numerical values of the correction functions are given in Appendix C. Another set of data reported for this system was the one of Zuca and Borcan (1984) (see Table 6.6 for the summary of experimental conditions). After applying the systematic corrections (similar to that of KCl- $\text{CaCl}_2$ ) on the data set of Zuca and Borcan (1984), it follows that the viscosity values reported are consistent with the data set of

Dumas et al. (1973). Therefore both mentioned corrected data sets are employed simultaneously to optimize the parameters of the model for NaCl-CaCl<sub>2</sub> binary system. The binary parameters of the model ( $c_{NaCl/Cl}$  and  $d_{NaCl/Cl}$ ) are calculated in the similar manner explained in Section 6.2.3 (see Appendix A for the numerical values of the parameters). The calculated viscosity isotherms and isocomposition lines are illustrated in Figs. 6.21 and 6.22 and compared with the corrected experimental data.

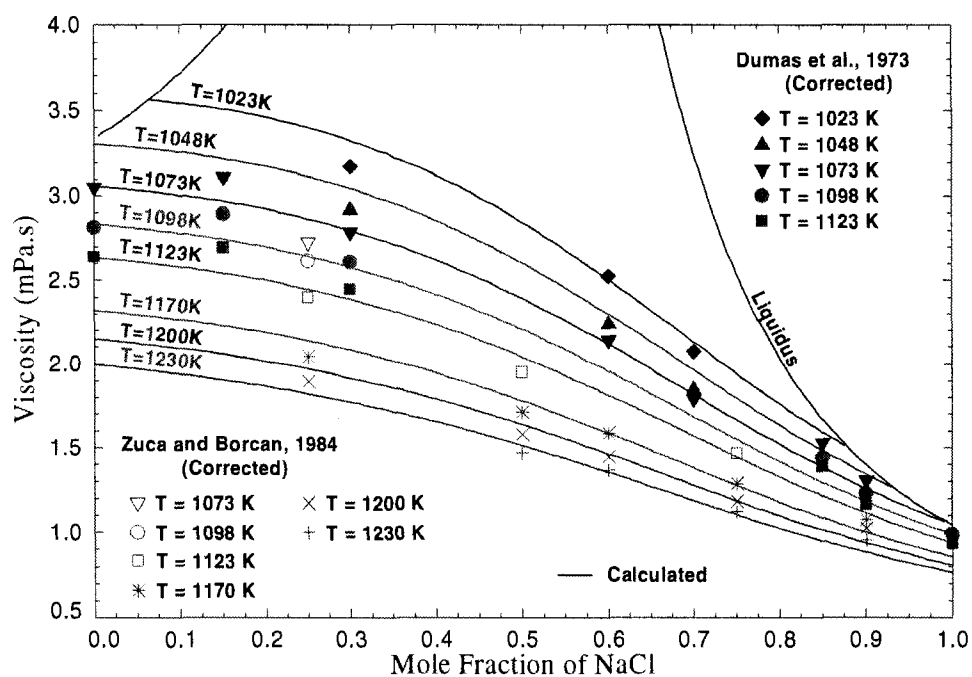


Figure 6.21: Calculated and Experimental Viscosity of NaCl-CaCl<sub>2</sub> Melt at Various Temperatures.

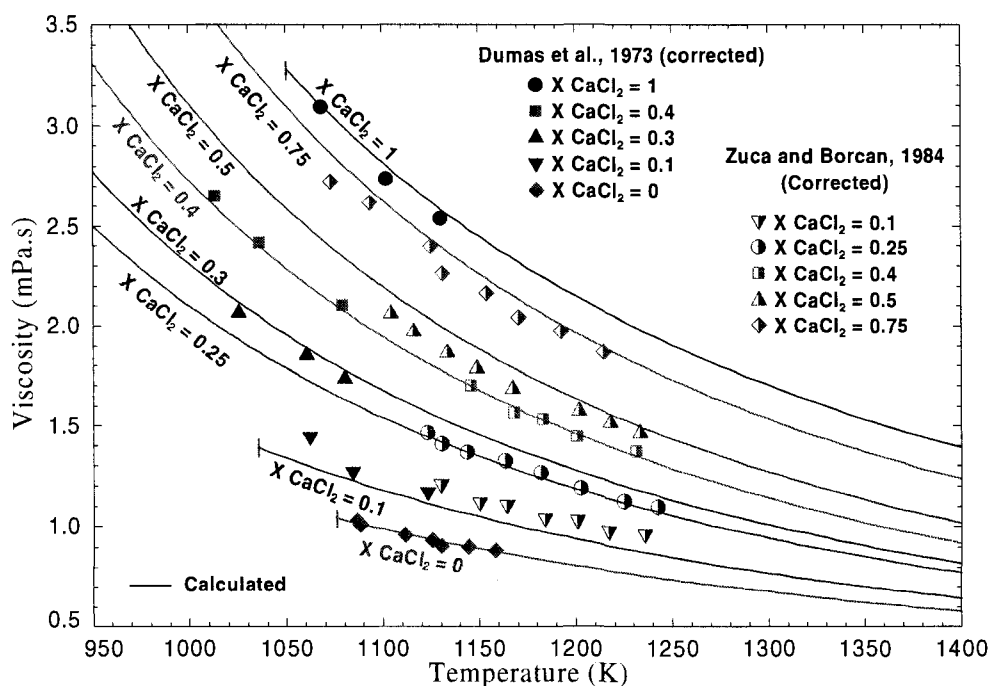


Figure 6.22: Calculated and Experimental Viscosity of NaCl-CaCl<sub>2</sub> Melt at Various Mole Fractions of CaCl<sub>2</sub>.

### 6.2.7 KCl-MgCl<sub>2</sub>

In the 1975 NSRDS critical review, several reported data sets for this system have been re-examined and the measurements of Bondarenko and Strelets (1968) were recommended as the most reliable data set (Janz et al., 1975). However similar to the previous systems, the data set of Dumas et al. (1973) has been mentioned as one of the unevaluated systems. A summary of the mentioned measurements together with another data reported in the literature is given in Table 6.7.

Table 6.7: A Summary of the Experimental Methods for the Viscosity Measurements of KCl-MgCl<sub>2</sub> Reported in the Literature.

Author	Year	Experimental Method (Working Equations)	Experimental Conditions	KCl [Mol%]	Temperature Range [K]
Bondarenko & Strelets	1968	Oscillating sphere (-)	Pt sphere, Calibration by water & nitrobenzene & aniline & molten KNO <sub>3</sub> & NaNO <sub>3</sub>	0 – 100	973 – 1373
Dumas et al.	1973	Oscillating sphere (Computational procedure based on Eq. 3.2)	Tungsten torsion wire, Pt90%-Ir10% solid sphere, Pt crucible, N <sub>2</sub> atmosphere, Control measurements by water & KNO <sub>3</sub> & KCl	0 – 15, 50 – 100	998 – 1148
Ejima et al.	1977	Oscillating vessel (Knappwost, 1952)	-	0 – 100	863 – 1153

Based on the considerations previously described in Sections 6.2.4 and 6.2.5, the measurements of Dumas et al. (1973) were selected as a reliable data set for KCl-MgCl<sub>2</sub> system. Similar to the other systems, a systematic correction has been applied to this data set, based on the error estimated for its corresponding unary data. (the corresponding data sets for pure KCl and pure MgCl<sub>2</sub> were similar to the ones of Dumas et al. (1970) as illustrated in Figs. 6.4 and 6.5). The corrected data sets are shown in Figs 6.9 and 6.11 and related numerical values of the correction functions are given in Appendix C. These corrected data are employed to optimize the parameters of the model for KCl-MgCl<sub>2</sub> binary system. The binary parameters of the model ( $c_{KMg/Cl}$  and  $d_{KMg/Cl}$ ) are calculated in

the similar manner explained in Section 6.2.3 (see Appendix A for the numerical values of the parameters). The calculated viscosity isotherms and isocomposition lines are illustrated in Figs. 6.23 and 6.24 and compared with the corrected experimental data.

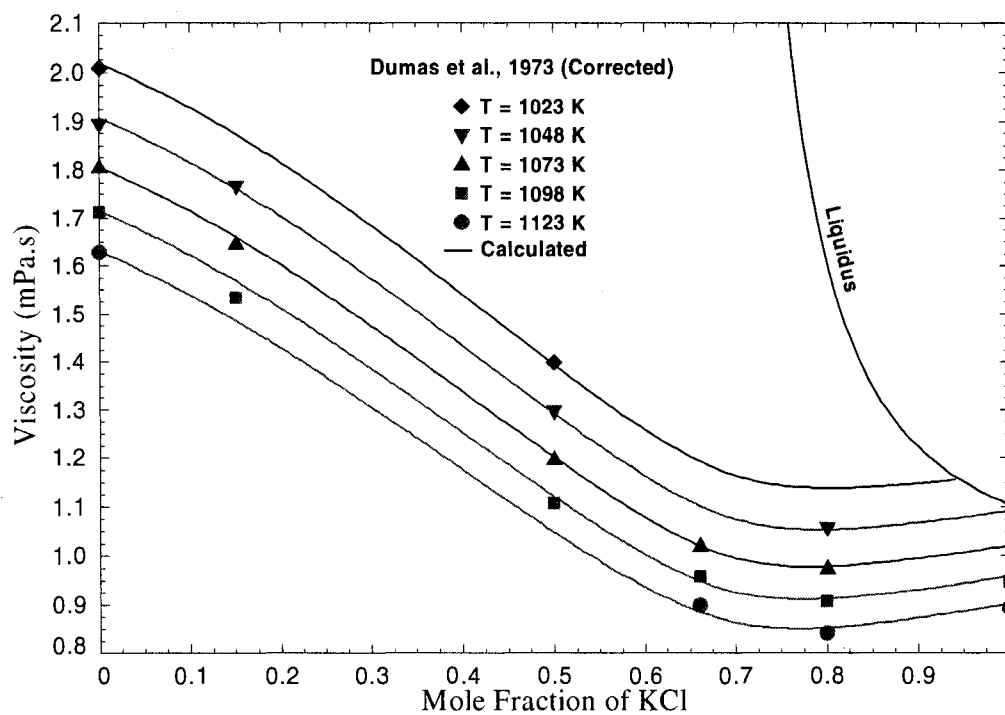


Figure 6.23: Calculated and Experimental Viscosity of KCl-MgCl<sub>2</sub> Melt at Various Temperatures.

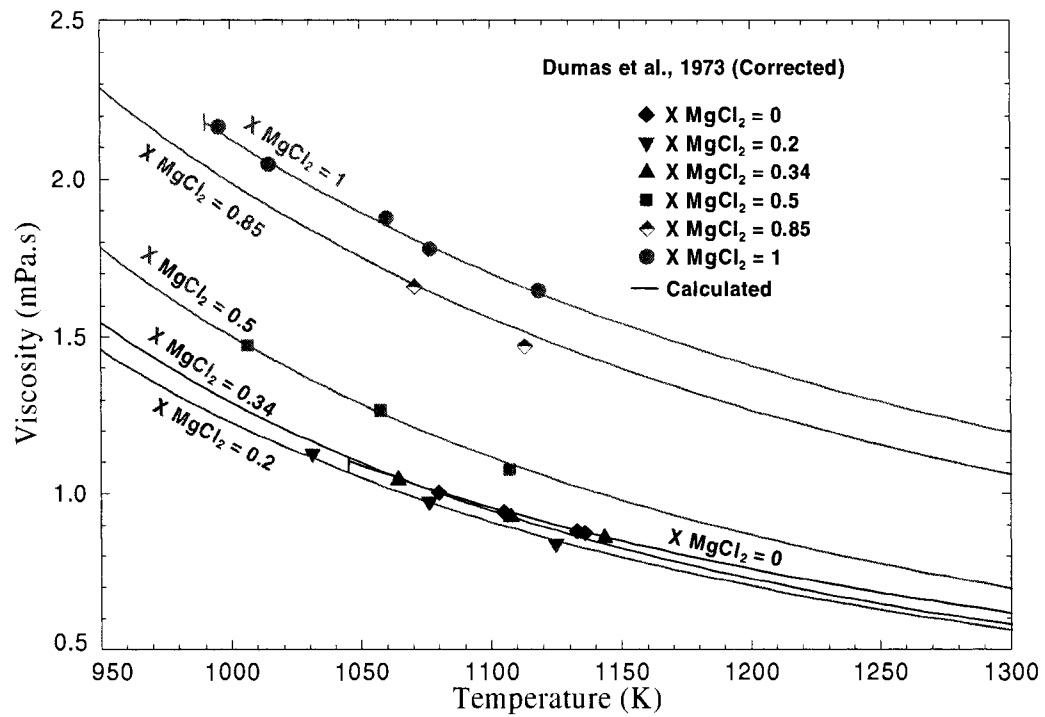


Figure 6.24: Calculated and Experimental Viscosity of KCl-MgCl<sub>2</sub> Melt at Various Mole Fractions of MgCl<sub>2</sub>.

Fig. 6.25 illustrates a comparison between the calculated viscosity isotherms and the literature data which are not used to obtain the parameters of the model.



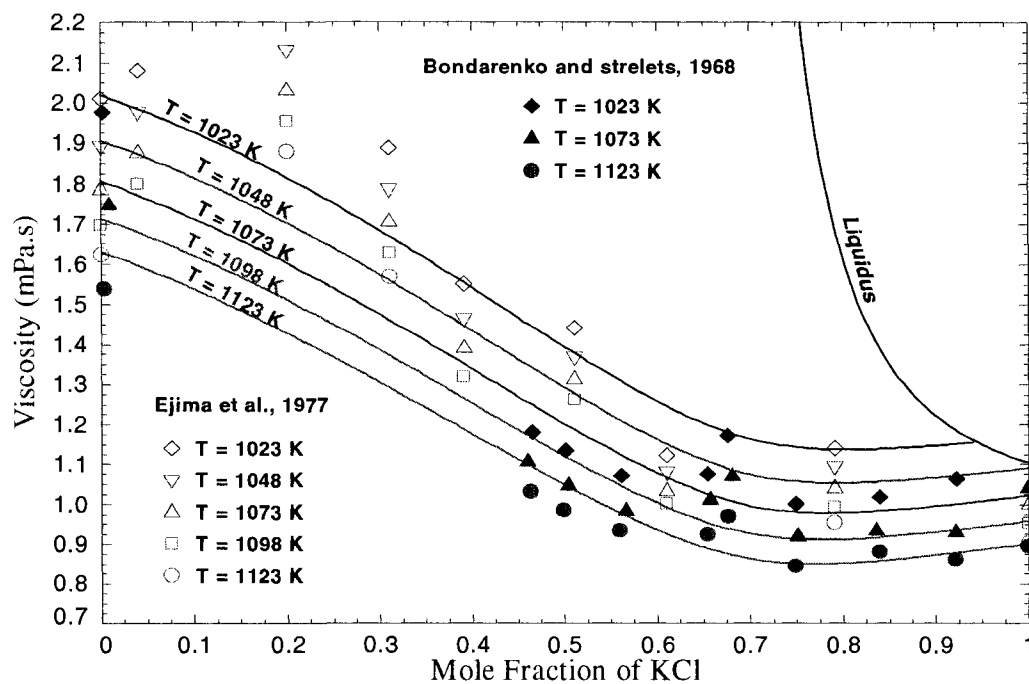


Figure 6.25: A Comparison Between the Calculated Viscosity Isotherms and the Experimental Data of KCl-MgCl<sub>2</sub> Melt.

The correction functions of the illustrated data sets are given in Appendix C.

As it is previously described in Section 5.2, liquid KCl-MgCl<sub>2</sub> solutions exhibit “V shaped” and “m-shaped” enthalpy and entropy of mixing respectively with a minimum

near  $X_{KCl} = \frac{2}{3}$  (see Figs. 4.9 and 4.10). This indicates maximum short range ordering of

$K^+$  and  $Mg^{2+}$  ions on the cationic sublattice at this composition (Chartrand and Pelton, 2001b). Since the short range ordering leads to strengthening of the bond forces, as a common sense, one expects an increase in the viscosity of the melt at the compositions

close to the maximum short range ordering. Surprisingly, as illustrated in Fig. 6.23, the calculated viscosity isotherms and the experimental data of Dumas et al. (1970), indicate a slight minimum close to this composition. As it is shown in the next section, the similar behavior is observed for NaCl-MgCl<sub>2</sub> system. Dumas et al. (1973) related this viscosity behavior to the so called structural breakdown of the melt. According to them, the partly covalent structure of MgCl<sub>2</sub> melt, will breakdown by addition of KCl. This structural breakdown, will lead to lower viscosity values. According to Dumas et al. (1973), the observed minimum of the viscosity isotherms in KCl rich region could be a result of this structural breakdown. As it will be shown later in Section 6.2.9, according to the structural studies reported for alkali chloride-MgCl<sub>2</sub> systems, this interpretation of the viscosity behavior seems reasonable.

#### **6.2.8 NaCl-MgCl<sub>2</sub>**

Data sets of Strelets et al. (1953; 1955) and Bondarenko and Strelets (1965) have been re-examined in the 1975 NSRDS critical review and the data set of Bondarenko and Strelets (1965) by the oscillating sphere method, was recommended as the most reliable data set (Janz et al., 1975). However similar to the previous systems, the data set of Dumas et al. (1973) has not been evaluated in 1975 NSRDS publication. (see Table 6.7 for the experimental conditions). Based on the considerations described for previous binary systems, the measurements of Dumas et al. (1973) were selected as a reliable data set for NaCl-MgCl<sub>2</sub> system. A systematic correction has been applied to this data set, based on the error estimated for its corresponding unary data (the corresponding data sets for pure NaCl and pure MgCl<sub>2</sub> were similar to the ones of Dumas et al. (1970) illustrated in Figs.

6.3 and 6.5). The corrected data sets are shown in Figs 6.9 and 6.11 and related numerical values of the correction functions are given in Appendix C. These corrected data were employed to optimize the parameters of the model for NaCl-MgCl<sub>2</sub> binary system. The binary parameters of the model ( $c_{NaMg/Cl}$  and  $d_{NaMg/Cl}$ ) primarily were calculated in the similar manner explained in Section 6.3.1. The calculated viscosity isotherms and isocomposition lines are illustrated in Figs. 6.26 and 6.27 and compared with the corrected experimental data.

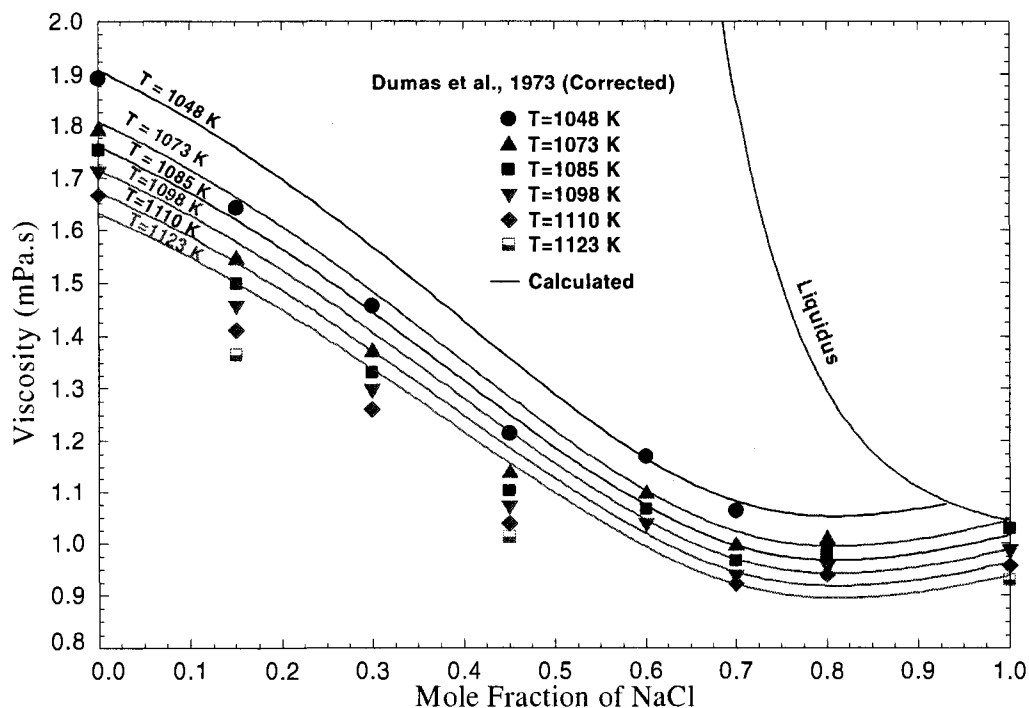


Figure 6.26: A Comparison Between the Experimental and Calculated Viscosity of NaCl-MgCl<sub>2</sub> Melt at Various Temperatures (Employing the Initial Form of the Model).

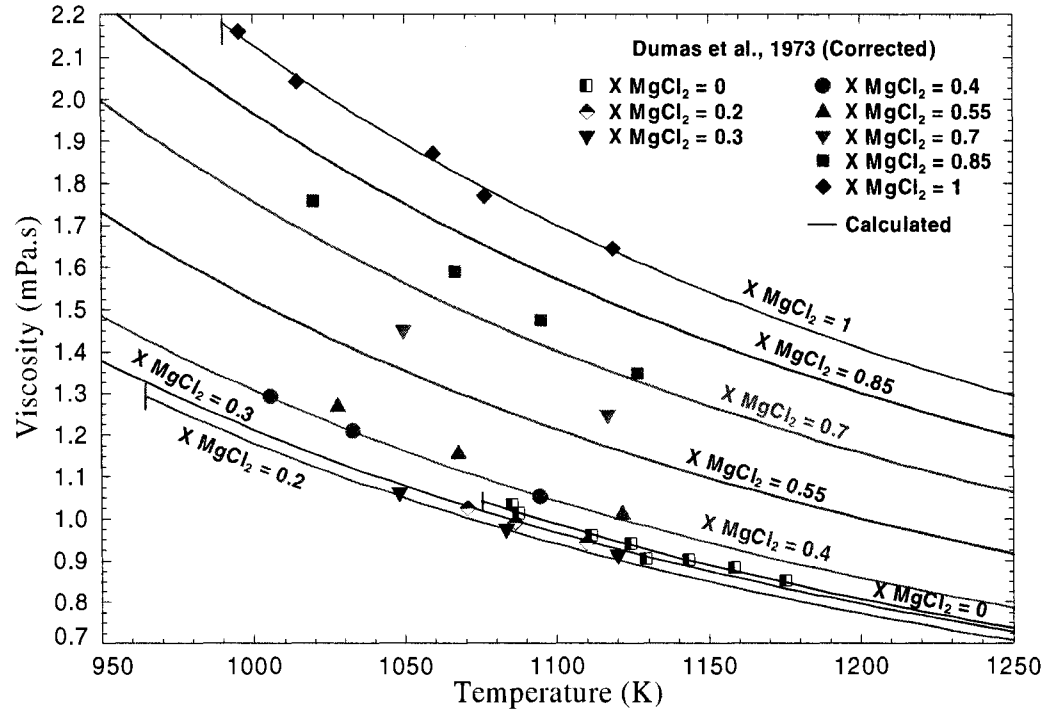


Figure 6.27: A Comparison Between the Experimental and Calculated Viscosity of NaCl-  
MgCl<sub>2</sub> Melt at Various Mole Fraction of MgCl<sub>2</sub> (Employing the Initial Form of the  
Model).

As it is illustrated in Figs. 6.26 and 6.27, it follows that the calculated viscosity curves by the initial form of the model, could not satisfactorily reproduce the experimental data for the whole range of temperature and composition. Accordingly based on the considerations described previously in Section 5.1, a modified form of the activation energy is proposed (Eq. 5.5) where  $G_{ij}^*$  is not only temperature-dependent but also

composition-dependent. Based on the proposed modification, the activation energy of NaCl-MgCl<sub>2</sub> binary system ( $G^*$ ) takes the following form:

$$G^* = X_{NaNa/Cl} G_{Na/Cl}^* + X_{MgMg/Cl} G_{Mg/Cl}^* + X_{NaMg/Cl} G_{NaMg/Cl}^* \quad (6.11)$$

where  $G_{Na/Cl}^*$  and  $G_{Mg/Cl}^*$  are the corresponding activation energies of the pure NaCl and pure MgCl<sub>2</sub> which are defined previously as a linear function of temperature (Eq. 5.3 with the numerical values of the parameters given in Appendix A).  $G_{NaMg/Cl}^*$  is defined in the modified form given by Eq. (5.5) as follows:

$$\begin{aligned} G_{NaMg/Cl}^* = & (G_{NaMg/Cl}^*)^{00} + (G_{NaMg/Cl}^*)^{10} \frac{X_{NaNa/Cl}}{X_{NaNa/Cl} + X_{NaMg/Cl} + X_{MgMg/Cl}} \\ & + (G_{NaMg/Cl}^*)^{01} \frac{X_{MgMg/Cl}}{X_{NaNa/Cl} + X_{NaMg/Cl} + X_{MgMg/Cl}} \end{aligned} \quad (6.12)$$

with the activation energies given by the modified parameters of the model as follows:

$$\begin{aligned} (G_{NaMg/Cl}^*)^{00} &= (c_{NaMg/Cl})^{00} + (d_{NaMg/Cl})^{00} T \\ (G_{NaMg/Cl}^*)^{10} &= (c_{NaMg/Cl})^{10} + (d_{NaMg/Cl})^{10} T \\ (G_{NaMg/Cl}^*)^{01} &= (c_{NaMg/Cl})^{01} + (d_{NaMg/Cl})^{01} T \end{aligned} \quad (6.13)$$

The numerical values of the modified parameters are given in Appendix B ( $(d_{NaMg/Cl})^{10}$  and  $(d_{NaMg/Cl})^{01}$  are set to zero for this system).

Fig. 6.28 shows a comparison between the experimental data and the viscosity isotherm calculated by the initial model and the modified model at a given temperature.

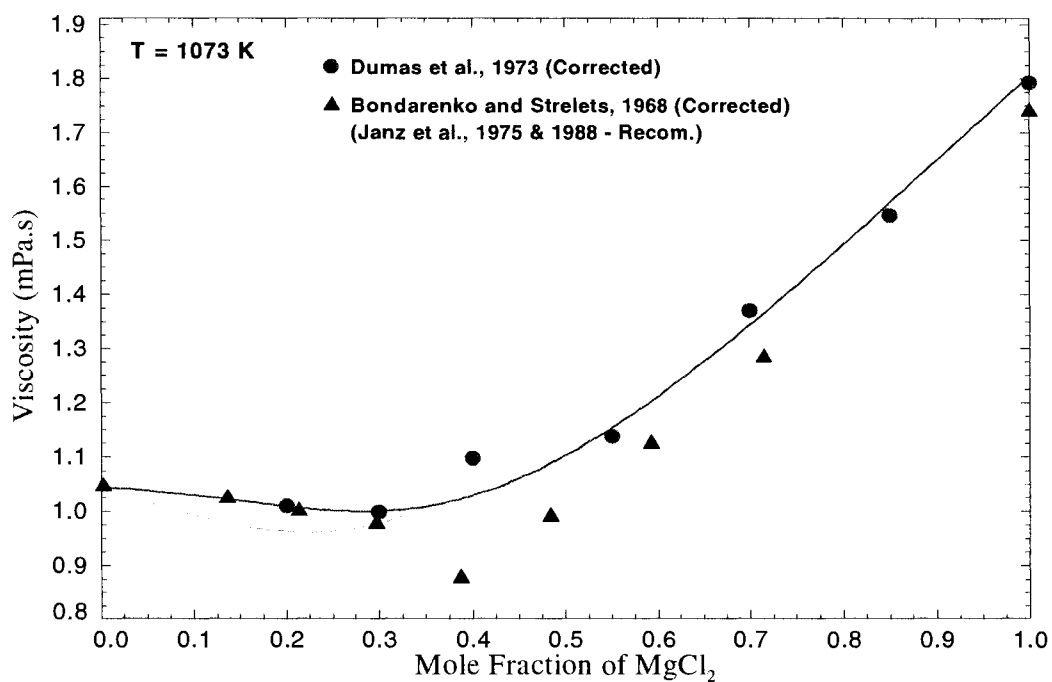


Figure 6.28: A Comparison Between the Experimental Data and the Viscosity Isotherm Calculated by the Initial Form (the dashed line) and the Modified Form (the solid line) of the Model at 1073 K.

As it is shown in Fig. 6.28, employing the modified form of the activation energy with more composition-dependent terms is better reproducing the viscosity behavior. This is shown for other viscosity isotherms illustrated in Figs. 6.29 and 6.30.

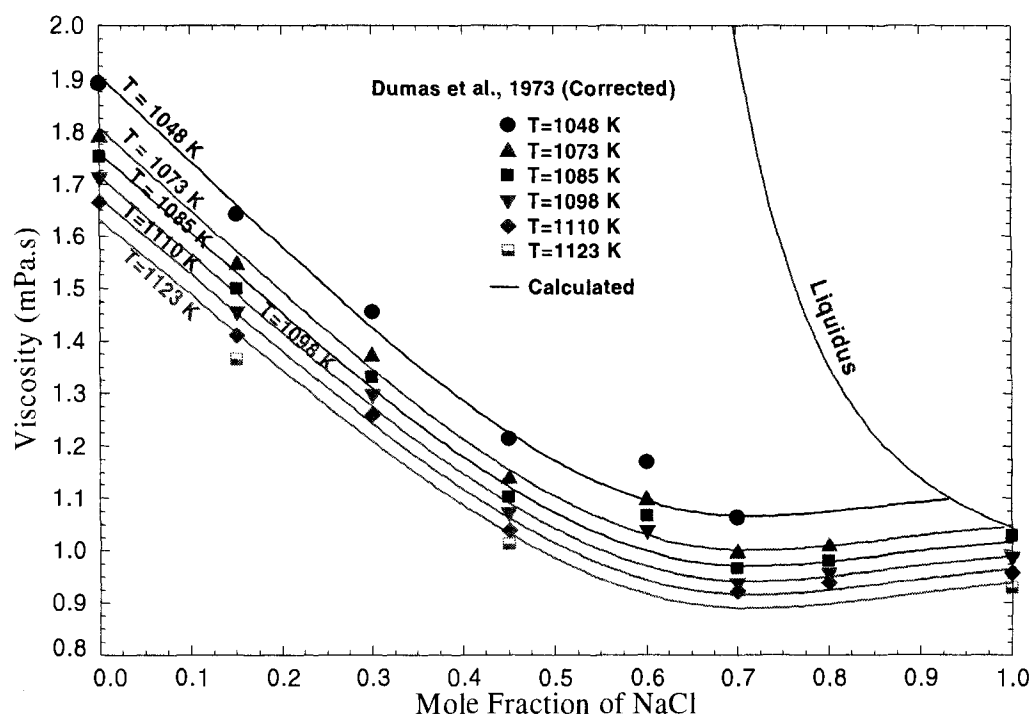


Figure 6.29: Calculated and Experimental Viscosity of NaCl-MgCl<sub>2</sub> Melt at Various Temperatures (Employing the Modified Form of the Model).

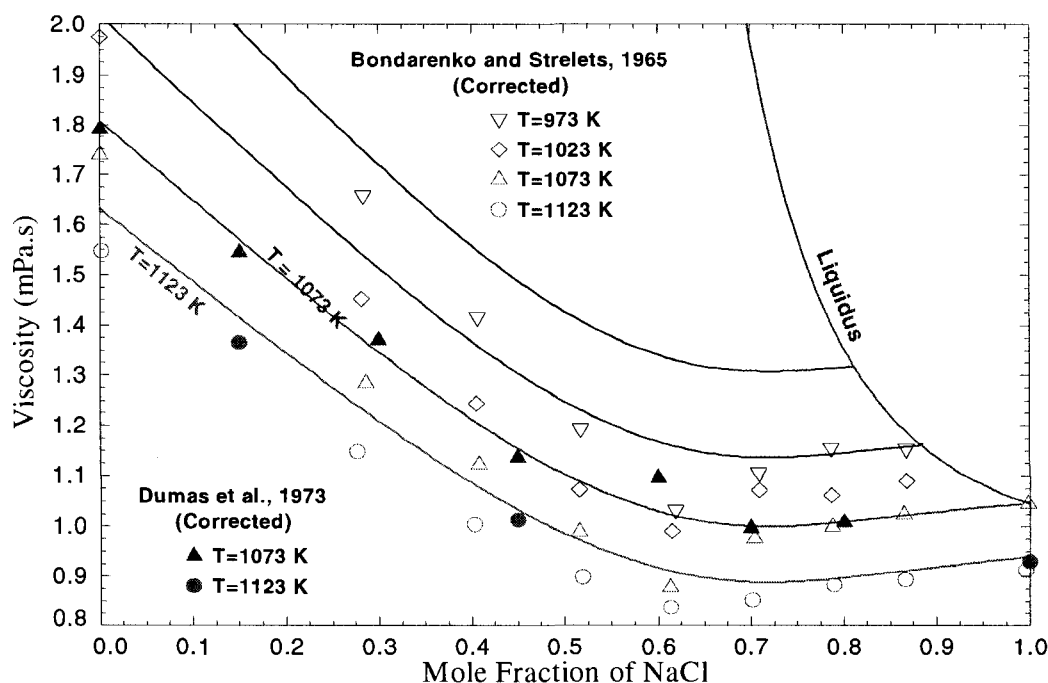


Figure 6.30: A Comparison Between the Calculated Viscosity Isotherms of NaCl-MgCl<sub>2</sub> by the Modified Form of the Model and the Experimental Data.

The correction functions of the illustrated data sets are given in Appendix C (the corresponding unary data sets of Bondarenko and Strelets (1965) measurements were similar to the ones reported by Bondarenko and Strelets (1968)).

As it is illustrated in Figs. 6.29 and 6.30, the re-calculated viscosity isotherms by the modified form of the activation energy are satisfactorily reproducing the viscosity behavior, compared to the experimental data. It will be shown in the following sections that the proposed modification to the model could successfully reproduce the viscosity



behavior of other highly short range ordered systems, namely RbCl-MgCl<sub>2</sub> and CsCl-MgCl<sub>2</sub>.

### 6.2.9 Further Discussion on the Results

As it is previously described in Section 5.2 and illustrated in Figs. 4.9 and 4.10, the highest structural short-range ordering is observed in the RbCl-MgCl<sub>2</sub> and CsCl-MgCl<sub>2</sub> systems. To further investigate the viscosity behavior of highly-short range ordered systems and justify the proposed modification to the model, the viscosity behavior of RbCl-MgCl<sub>2</sub> and CsCl-MgCl<sub>2</sub> are also studied in the following sections. The modified form of the model is employed to calculate the viscosity isotherms of these systems. It follows that the expected viscosity increase at composition of the maximum short range ordering, which was not observed for KCl-MgCl<sub>2</sub> and NaCl-MgCl<sub>2</sub> systems, finally shows up for these binary systems as it will be shown in Figs. 6.33 and 6.34, this difference in behavior between the mentioned systems can be explained by considering the structure of these melts.

#### 6.2.9.1 The Structure of Alkali Chloride-MgCl<sub>2</sub> Melts

Alkali chlorides in their solid state have typically ionic lattices. However MgCl<sub>2</sub> is partly covalent and crystallizes in layer structures. The solid state structure of MgCl<sub>2</sub> is of the CdCl<sub>2</sub> type which is a layer structure made up of cubic close-packed chloride ions, with magnesium ions filling all the octahedral sites between every other layer, thereby forming a rhombohedrally centered hexagonal structure themselves (Wells, 1962; Bloom, 1967). When alkali chlorides melt, the ions formerly fixed in the rigid lattices become free to

move and form an ionic liquid. However the Raman spectroscopic studies of  $\text{MgCl}_2$  melts have shown a partly covalent structure for molten  $\text{MgCl}_2$ . Evidence was found for the existence of a polymeric species  $[\text{MgCl}_2]_p$  with a structure resembling that of the solid  $\text{MgCl}_2$  (Balasubrahmanyam, 1966; Maroni and Cairns, 1969; Maroni et al., 1971; Capwell, 1972; Huang and Brooker, 1976; Kazmierczak et al., 1998). Such a rigid three dimensional structure tends to break up by addition of alkali chlorides to pure  $\text{MgCl}_2$ . This can explain the sharp decrease in viscosity isotherms of  $\text{MgCl}_2\text{-KCl}$  and  $\text{MgCl}_2\text{-NaCl}$  melts upon addition of alkali chlorides. Addition of more alkali chloride to the melt will lead to the formation of tetrahedral complex anions like  $\text{MgCl}_4^{2-}$  (Balasubrahmanyam, 1966; Maroni and Cairns, 1969; Maroni et al., 1971; Dai et al., 1995). However according to Kazmierczak et al.(1998), the kinetic stability and dissociation of those complexes depend on the ionic radius of the alkali cations. Kazmierczak et al. showed that the  $\text{MgCl}_4^{2-}$  complex is more stable in the presence of the bigger alkali cations. This can give a clue to understand the difference in behaviour between the  $\text{NaCl-MgCl}_2$  and  $\text{KCl-MgCl}_2$  systems in contrast with the  $\text{RbCl-MgCl}_2$  and  $\text{CsCl-MgCl}_2$  systems. As Dumas et al. (1973) and Zuca et al. (1991) have also mentioned, the relaxation time of the  $\text{MgCl}_4^{2-}$  complexes may be so much shorter in the  $\text{NaCl}$  and  $\text{KCl}$  containing melts that it is not manifested in the viscosity. Therefore the maximum in viscosity isotherms that shows up for  $\text{RbCl}$  and  $\text{CsCl}$  containing melts, is not observed for the  $\text{NaCl-MgCl}_2$  and  $\text{KCl-MgCl}_2$  systems.

### 6.2.9.2 RbCl

The NSRDS recommended data in 1968 (Janz et al., 1968) for pure liquid RbCl, was the measurements of Murgulescu and Zuca (1963). However as it was previously discussed, similar to the other pure components considering the results of the Molten Salts standards Program, the data set of Brockner et al. (1981) has been recommended later in 1988 NSRDS publication with the estimated accuracy of  $\sim \pm 1\%$  (Janz, 1988). Brockner et al. (1981) performed their measurements with the same viscometer developed by Torklep and Øye (1979) for the Standards Program. A brief overview of their measurement method together with the other measurements reported in the literature for this system is given in Table 6.8.

Table 6.8: A Summary of the Experimental Methods for the Viscosity Measurements of Pure RbCl Reported in the Literature.

Author	Year	Experimental Method (Working Equations)	Experimental Conditions	Temperature range [K]
Veliyulin et al.	1995	Oscillating cylinder (Eqs. 3.3 & 3.4)	Pt92%-W8% torsion wire, Pt90%-Ir10% solid cylinder, Pt crucible, N <sub>2</sub> atmosphere	1065 – 1193
Ejima et al.	1982	Capillary (Eq. 3.9)	Quartz capillary tube, Calibration done by water	1000 – 1182

Brockner et al.	1981	Oscillating cylinder (Eqs. 3.3 & 3.4)	Pt92%-W8% torsion wire, Pt90%-Ir10% solid cylinder, Pt crucible, N <sub>2</sub> atmosphere, Control measurement by water	996 – 1134
Dumas et al.	1973	Oscillating sphere (Computational procedure based on eq. 3.2)	Tungsten torsion wire, Pt90%-Ir10% solid sphere, Pt crucible, N <sub>2</sub> atmosphere, Control measurements by water & KNO <sub>3</sub> & KCl	1034 – 1083
Murgulescu & Zuca	1963	Oscillating sphere (Eq. 3.2)	Pt sphere, Pt wire	1005 - 1148

The listed data sets are compared in Fig. 6.31 with the result of the present optimization based on the data of Brockner et al. (1981).

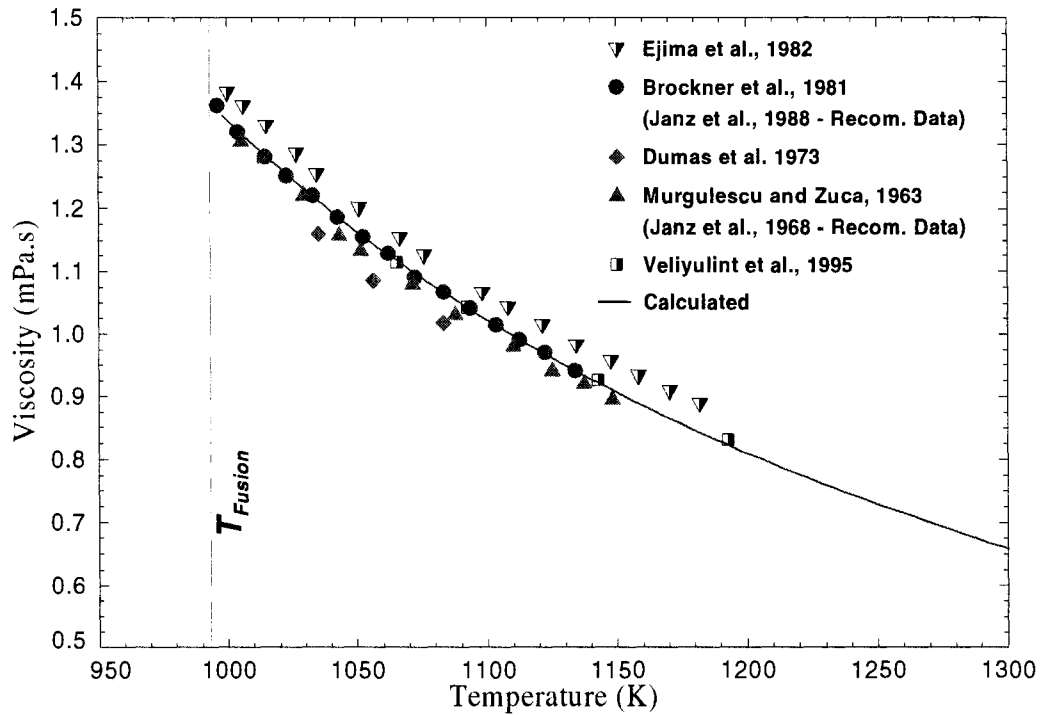


Figure 6.31: Calculated and Experimental Viscosity of Pure RbCl

The solid line in Fig. 6.31 shows the results of the present optimization and is obtained similar to that of NaCl (see Section 6.1.2). The numerical values of  $c_{Rb/Cl}$  and  $d_{Rb/Cl}$ , the optimized parameters of the model for pure liquid RbCl, are given in Appendix A in SI units.

### 6.2.9.3 CsCl

For pure liquid CsCl, Janz et al.(1968) recommended the measurements of Murgulescu and Zuca (1963) as the most reliable data set. Later in 1975 NSRDS publication (Janz et

al., 1975), several data sets have been re-examined for this system (Smirnov and Khokhlov, 1967; Smirnov and Khokhlov, 1969; Vasu, 1969; Zuca, 1973) and the measurements of Zuca (1973) has been recommended as the most reliable data set with the estimated error of  $\pm 3\%$ . However based on the results of the Molten Salts Standards Program, this recommended data set has been replaced by the data set of Brockner et al. (1981) in the NSRDS 1988 publication (Janz, 1988). These recommended data sets together with the other data sets reported in the literature are summarized in Table 6.9.

Table 6.9: A Summary of the Experimental Methods for the Viscosity Measurements of Pure CsCl Reported in the Literature.

Author	Year	Experimental Method (Working Equations)	Experimental Conditions	Temperature range [K]
Ejima et al.	1982	Capillary (Eq. 3.9)	Quartz capillary tube, Calibration done by water	933 – 1183
Brockner et al.	1981	Oscillating cylinder (Eqs. 3.3 & 3.4)	Pt92%-W8% torsion wire, Pt90%-Ir10% solid cylinder, Pt crucible, N <sub>2</sub> atmosphere, Control measurement by water	923 – 1086
Dumas et al.	1973	Oscillating sphere (Computational procedure based on eq. 3.2)	Tungsten torsion wire, Pt90%-Ir10% solid sphere, Pt crucible, N <sub>2</sub> atmosphere, Control measurements by water & KNO <sub>3</sub> & KCl	1028 – 1075
Zuca	1973	Oscillating sphere (-)	-	950 – 1086

Murgulescu & Zuca	1963	Oscillating sphere (Eq. 3.2)	Pt sphere, Pt wire	927 - 1110
-------------------	------	---------------------------------	--------------------	------------

The listed data sets are compared in Fig. 6.32 with the result of the present optimization based on the data of Brockner et al. (1981).

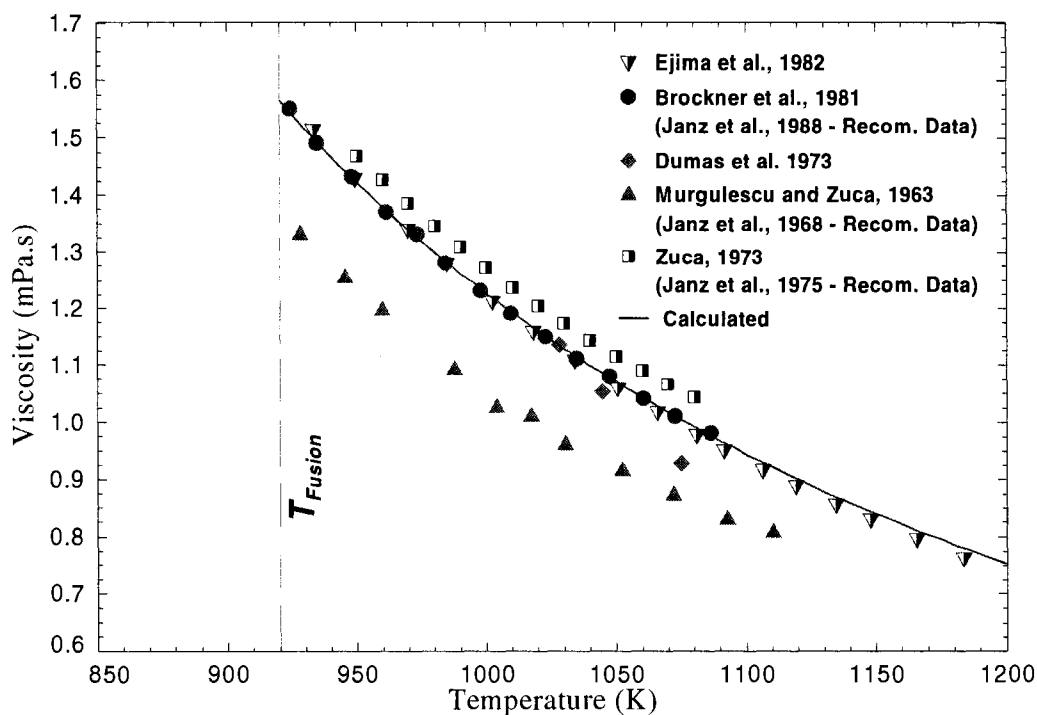


Figure 6.32: Calculated and Experimental Viscosity of Pure CsCl

The solid line in Fig. 6.32 shows the results of the present optimization and is obtained similar to that of NaCl (see Section 6.1.2). The numerical values of  $c_{Cs/Cl}$  and  $d_{Cs/Cl}$ , the optimized parameters of the model for pure liquid CsCl, are given in Appendix A in SI

units. As it is illustrated in Fig 6.32 the reported data set of Ejima et al.(1982) is in good agreement (within the experimental limits of accuracy) with the calculated line.

#### 6.2.9.4 RbCl-MgCl<sub>2</sub>

According to the present literature review, the data set of Dumas et al. (1973) by the oscillating sphere method has been reported for the viscosity of RbCl-MgCl<sub>2</sub> binary system (see Table 6.6 for the summary of the experimental method and conditions). There was no recommendation for the viscosity of this system in 1975 and 1988 NSRDS publications (Janz et al., 1975; Janz, 1988). The data set of Dumas et al. (1973) is mentioned as one of the unevaluated systems for the viscosity in 1975 NSRDS publication. Based on the considerations previously described in Sections 6.2.4 and 6.2.5, the measurements of Dumas et al. (1973) is selected as a reliable data set for RbCl-MgCl<sub>2</sub> binary system. However, similar to the other binary systems, a correction factor is defined for this data set to take into account the accuracy limits imposed by the oscillating sphere method. The systematic correction applied to the data set of Dumas et al. (1973) for NaCl-CaCl<sub>2</sub> binary system, is obtained based on the error estimated for its corresponding unary data (the corresponding data set for pure MgCl<sub>2</sub> was similar to the one of Dumas et al. (1970) illustrated in Fig. 6.5). The numerical values of the correction functions are given in Appendix C. Similar to NaCl-MgCl<sub>2</sub> system, the modified form of the activation energy (Eqs. 6.11, 6.12 and 6.13) is employed to model the viscosity behavior of this system. The mentioned corrected data set is employed to optimize  $(c_{RbMg/Cl})^{00}$ ,  $(d_{RbMg/Cl})^{00}$ ,  $(c_{RbMg/Cl})^{10}$  and  $(c_{RbMg/Cl})^{01}$ ; the modified parameters of the



model ( $(d_{RbMg/Cl})^{10}$  and  $(d_{RbMg/Cl})^{01}$  are set to zero for this system). The numerical values of the parameters are given in Appendix B. The calculated viscosity isotherms are illustrated in Fig. 6.33 and compared with the experimental data.

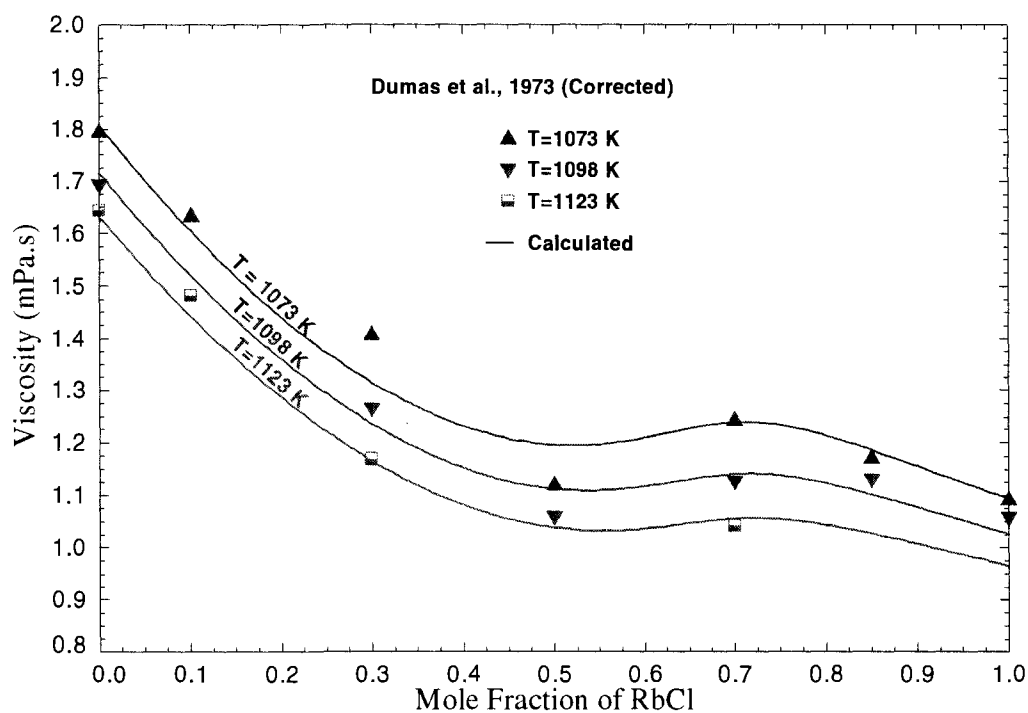


Figure 6.33: Calculated and Experimental Viscosity of RbCl-MgCl<sub>2</sub> Melt at Various Temperatures (Employing the Modified Form of the Model).

As it is shown in the figure, a maximum is observed close to the composition of maximum short range ordering. As it was previously discussed in Section 6.2.9, this maximum can be due to the strengthening of the bond forces in the melt close to this composition. Introducing the composition dependent activation energies by the modified

form of the model, could precisely reproduce the specific viscosity behavior of this highly short range ordered system.

#### 6.2.9.5 CsCl-MgCl<sub>2</sub>

According to the present literature review, the data set of Dumas et al. (1973) by the oscillating sphere method has been reported for the viscosity of CsCl-MgCl<sub>2</sub> binary system (see Table 6.6 for the summary of the experimental method and conditions). Similar to the RbCl- MgCl<sub>2</sub> system, there was no recommendation for the viscosity of this system in 1975 and 1988 NSRDS publications (Janz et al., 1975; Janz, 1988) and the data set of Dumas et al. (1973) is mentioned as one of the unevaluated systems. After applying a systematic correction based on the error estimated for its corresponding unary data, this data set is employed to optimize  $(c_{CsMg/Cl})^{00}$ ,  $(d_{CsMg/Cl})^{00}$ ,  $(c_{CsMg/Cl})^{10}$  and  $(c_{CsMg/Cl})^{01}$ ; the modified parameters of the model ( $(d_{CsMg/Cl})^{10}$  and  $(d_{CsMg/Cl})^{01}$  are set to zero for this system). The numerical values of the parameters are given in Appendix B. The calculated viscosity isotherms are illustrated in Fig. 6.34 and compared with the experimental data.

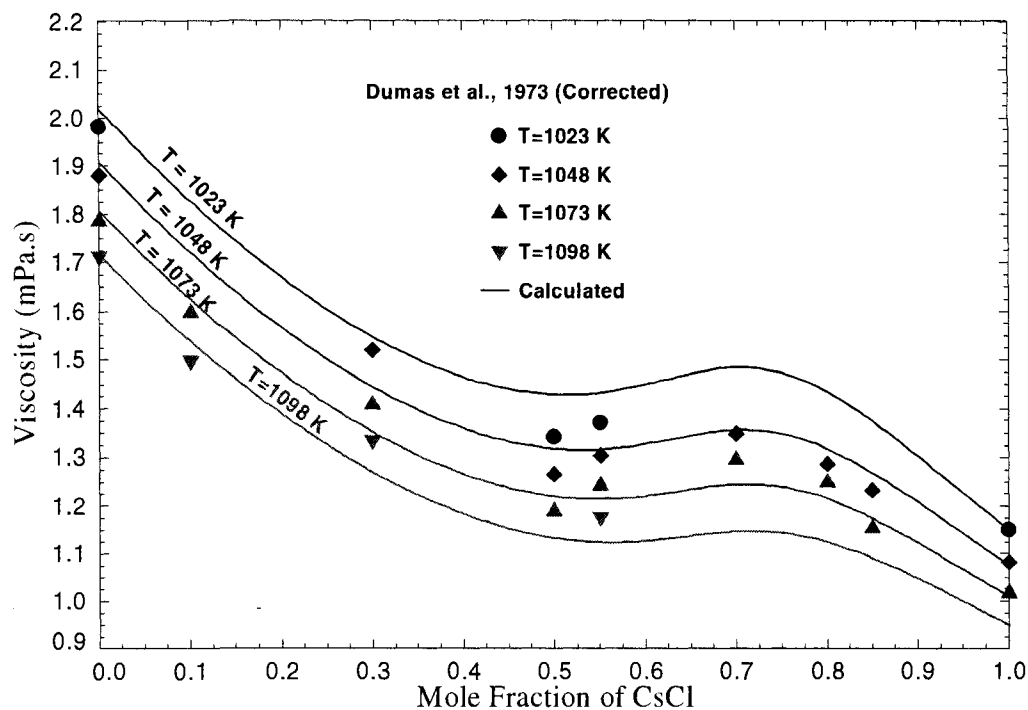


Figure 6.34: Calculated and Experimental Viscosity of CsCl-MgCl<sub>2</sub> Melt at Various Temperatures (Employing the Modified Form of the Model).

As it is shown in the figure, since this system has the highest degree of short range order among all the other alkali chloride-MgCl<sub>2</sub> systems, the observed maximum close to the composition of short range ordering is more highlighted compared to the other binary systems.

### 6.3 Multi-Component Molten Salts

As it was described previously in Section 5, the presented model can be simply employed to calculate the viscosity of multi component systems by having the related unary and binary activation energies. In the previous sections, all the activation energy parameters required for the NaCl-KCl-MgCl<sub>2</sub>-CaCl<sub>2</sub> multi-component system, were optimized based on the available experimental data. For NaCl-MgCl<sub>2</sub> binary parameters, a modified form of the activation energy was proposed and the composition dependent parameters were added to the model. Employing the above mentioned parameters given in Appendixes A and B, the viscosity of the NaCl-KCl-MgCl<sub>2</sub>-CaCl<sub>2</sub> system can be calculated for the whole range of temperature and composition by Eq. (5.2) as follows:

$$\eta = \frac{hN_A}{V_M} \exp\left(\frac{\sum X_{ij} G_{ij}^*}{RT}\right) = \frac{hN_A}{V_M} \exp\left(\frac{X_{NaNa/Cl} G_{Na/Cl}^* + X_{KK/Cl} G_{K/Cl}^* + X_{MgMg/Cl} G_{Mg/Cl}^* + X_{CaCa/Cl} G_{Ca/Cl}^* + X_{NaK/Cl} G_{NaK/Cl}^* + X_{NaMg/Cl} G_{NaMg/Cl}^* + X_{NaCa/Cl} G_{NaCa/Cl}^* + X_{KMg/Cl} G_{KMg/Cl}^* + X_{KCa/Cl} G_{KCa/Cl}^* + X_{MgCa/Cl} G_{MgCa/Cl}^*}{RT}\right) \quad (6.14)$$

where the SNN pair fractions ( $X_{ij}$ ) are calculated by the modified quasichemical thermodynamic model in pair approximation, the molar volume of the multi-component system ( $V_M$ ) is calculated by the density model (see Section 5.3) and unary and binary activation energies ( $G_{ij}^*$ ) are given by the parameters of the model as follows:

$$\begin{aligned}
G^*_{Na/Cl} &= c_{Na/Cl} + d_{Na/Cl}T \\
G^*_{K/Cl} &= c_{K/Cl} + d_{K/Cl}T \\
G^*_{Mg/Cl} &= c_{Na/Cl} + d_{Na/Cl}T \\
G^*_{Ca/Cl} &= c_{K/Cl} + d_{K/Cl}T \\
G^*_{NaK/Cl} &= c_{NaK/Cl} + d_{NaK/Cl}T \\
G^*_{NaCa/Cl} &= c_{NaCa/Cl} + d_{NaCa/Cl}T \\
G^*_{KMg/Cl} &= c_{KMg/Cl} + d_{KMg/Cl}T \\
G^*_{KCa/Cl} &= c_{KCa/Cl} + d_{KCa/Cl}T \\
G^*_{MgCa/Cl} &= c_{MgCa/Cl} + d_{MgCa/Cl}T \\
G^*_{NaMg/Cl} &= (c_{NaK/Cl})^{00} + (d_{NaK/Cl})^{00}T + (c_{NaMg/Cl})^{10} \frac{X_{NaNa/Cl}}{X_{NaNa/Cl} + X_{NaMg/Cl} + X_{MgMg/Cl}} \\
&\quad + (c_{NaMg/Cl})^{01} \frac{X_{MgMg/Cl}}{X_{NaNa/Cl} + X_{NaMg/Cl} + X_{MgMg/Cl}}
\end{aligned}$$

with the numerical values of the parameters ( $c$  and  $d$ ) given in the Appendixes A and B. To our knowledge, this is the first time that the viscosity of NaCl-KCl-MgCl<sub>2</sub>-CaCl<sub>2</sub> quaternary system can be precisely predicted by a model for the whole range of temperature and composition. The viscosity calculations for this system can be done by employing the thermodynamic and density model through the 22 optimized parameters of the model (8 parameters for the pure components activation energies and 14 parameters for the binaries).

To determine the accuracy of the model for ternary and multi-component systems, a literature review is performed to collect the reported viscosity data. Unfortunately only a few experiments have been reported in the literature for these molten salt systems. For NaCl-KCl-MgCl<sub>2</sub> ternary system, 3 sets of experimental data have been reported (Berenblit, 1937; Bondarenko, 1966; Maurits, 1967). There was no standard quality data

for the multi-component systems; therefore to estimate the accuracy of the reported measurements, their corresponding unary data sets are compared to the standard pure component viscosity values in 1988 NSRDS publication (Janz, 1988). The results are shown in Fig. 6.35 (The corresponding pure component data sets of Maurits (1967) were similar to the ones of Berenblit (1937)).

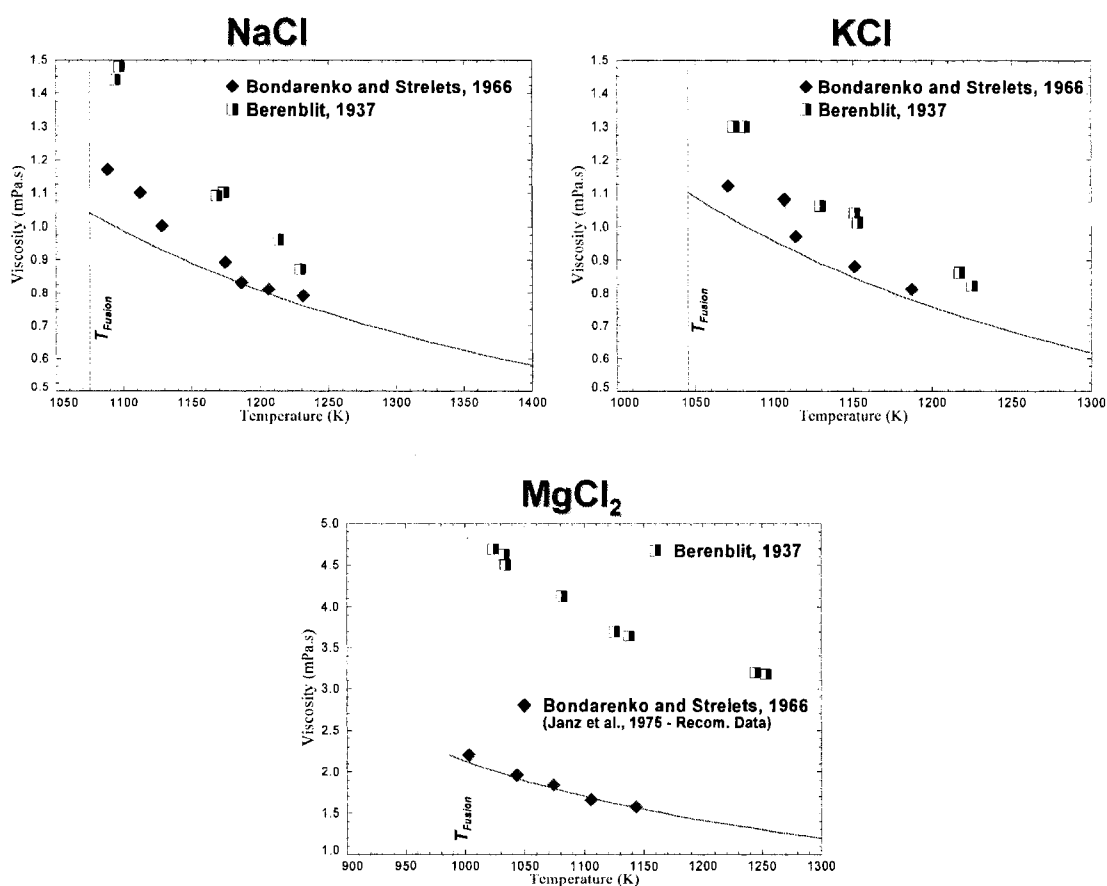


Figure 6.35: A Comparison Between the Corresponding Pure NaCl, KCl and MgCl<sub>2</sub> Data Sets of Berenblit (1937) and Bondarenko (1966) and the 1988 NSRDS (Janz, 1988) Recommended Viscosity Values (the solid lines).

It follows that the reported data sets of Berenblit (1937) and Maurits (1967) are in serious error compared to the standard values. For the case of  $\text{MgCl}_2$ , the estimated error is about 100% which is too large to be systematically corrected similar to the corrections that have been previously applied to the binary systems. These measurements have been excluded from the optimizations of the binary and unary parameters in the present work. The reported ternary data of Bondarenko (1966) have been systematically corrected (see Section 6.2.2 for details) and compared to the calculations done by the model in Figs. 6.36 to 6.39. The corresponding pure component data sets are similar to the ones of Bondarenko and Strelets (1968) for which the related correction functions are given in Appendix C.

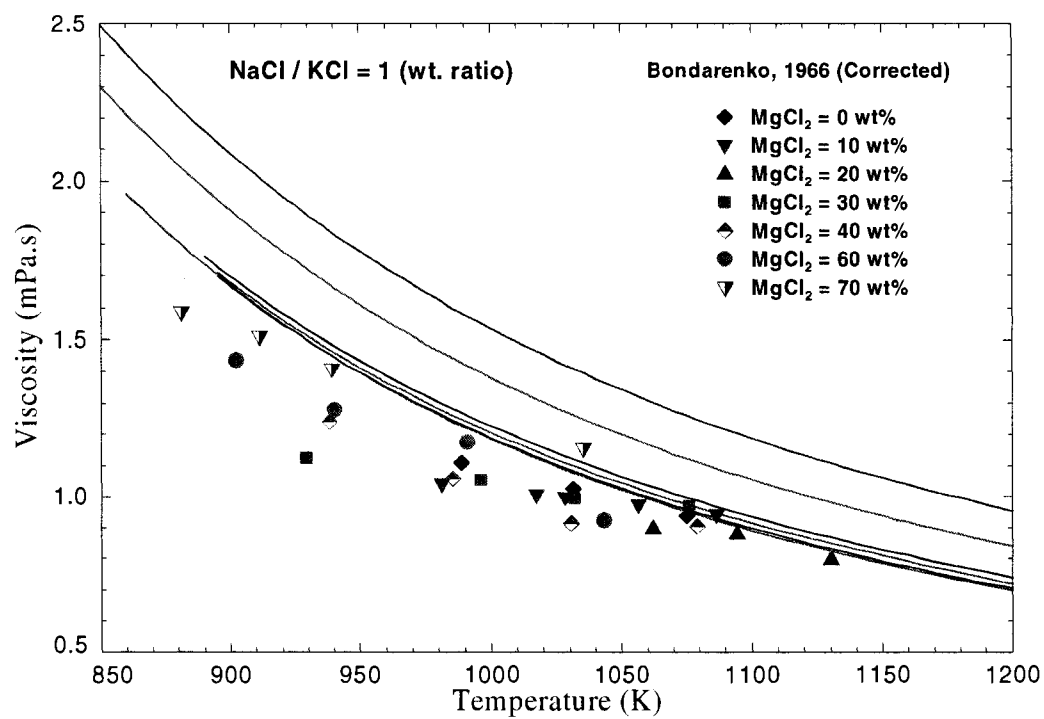


Figure 6.36: Calculated and Experimental Viscosity of NaCl-KCl- $\text{MgCl}_2$  Ternary System at Various Weight Percents of  $\text{MgCl}_2$  with the Weight Ratio of NaCl/KCl Equal to 1.



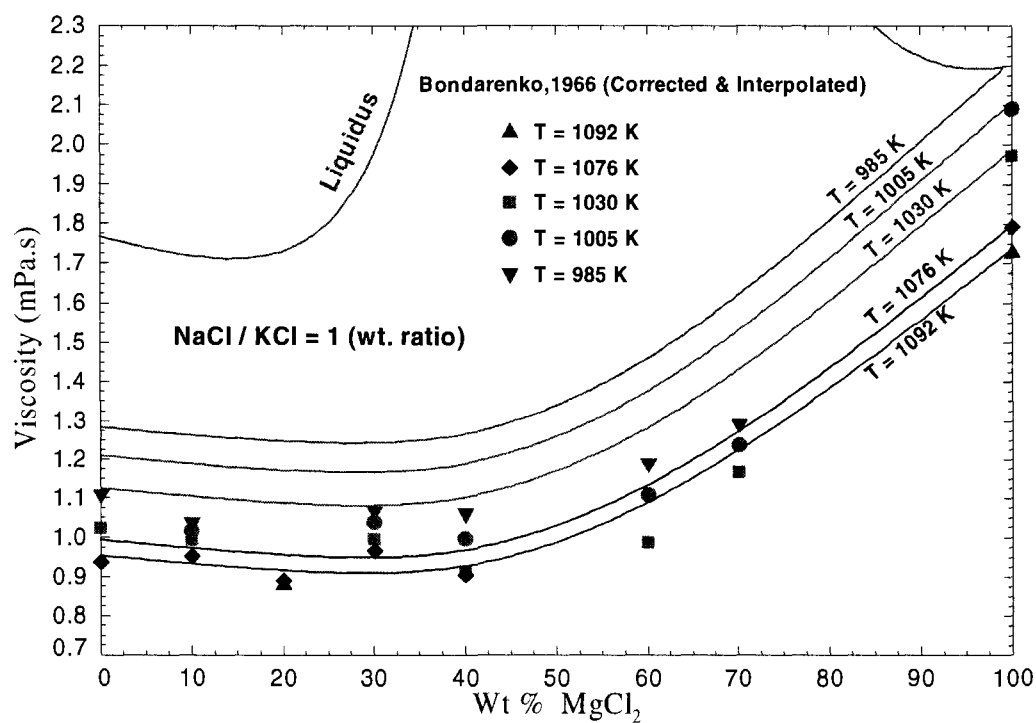


Figure 6.37: Calculated and Experimental Viscosity of NaCl-KCl- $\text{MgCl}_2$  Ternary System at Various Temperatures with the Weight Ratio of NaCl/KCl Equal to 1.

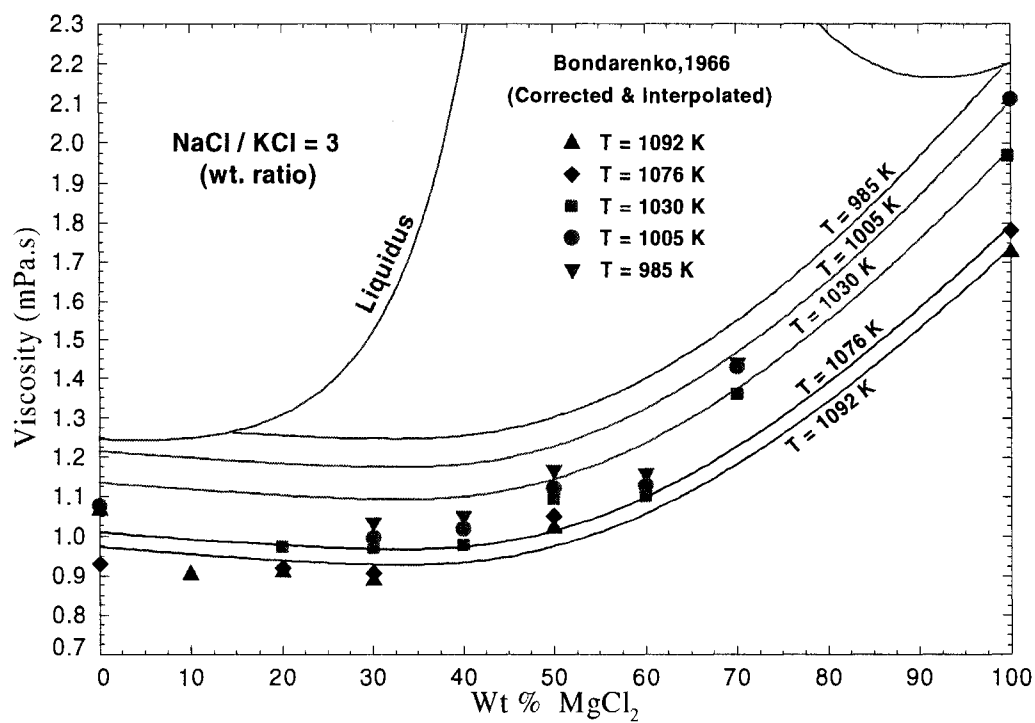


Figure 6.38: Calculated and Experimental Viscosity of NaCl-KCl-MgCl<sub>2</sub> Ternary System at Various Temperatures with the Weight Ratio of NaCl/KCl Equal to 3.

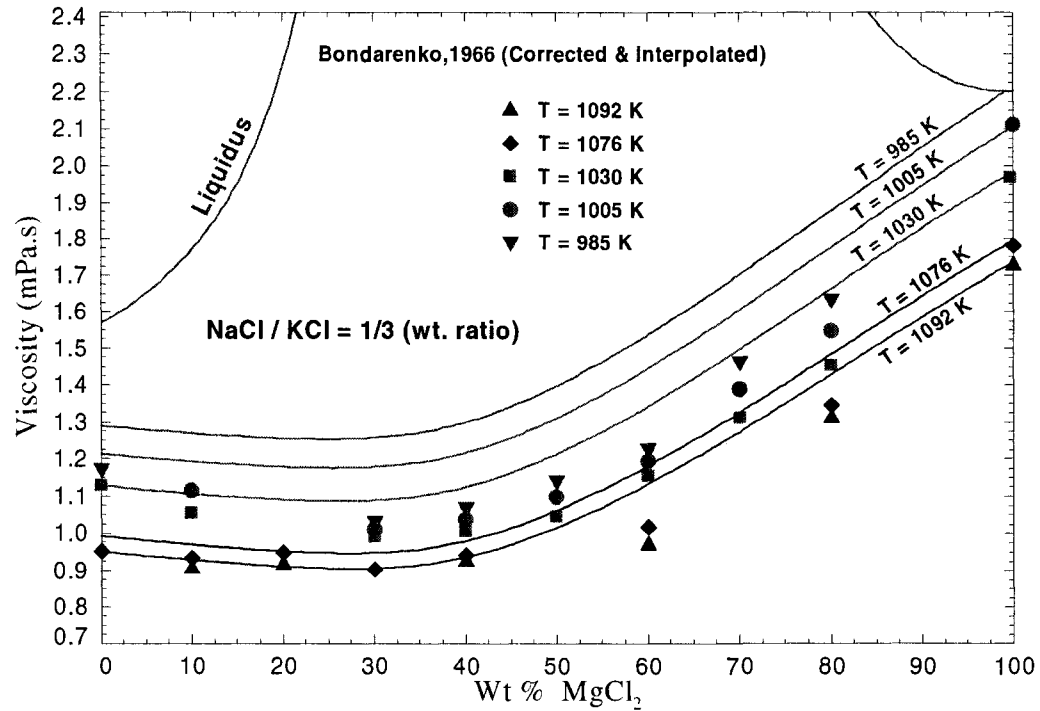


Figure 6.39: Calculated and Experimental Viscosity of NaCl-KCl-MgCl<sub>2</sub> Ternary System at Various Temperatures with the Weight Ratio of NaCl/KCl Equal to 1/3.

However similar to its corresponding unary and binary data (see Figs 6.35, 6.15, 6.25 and 6.30), the ternary data of Bondarenko (1966) are scattered for the temperatures lower than  $\sim 1100\text{K}$ . As it is shown in the Figs. 6.35 to 6.38, they show better agreement with the calculated lines at higher temperatures ( $T = 1076\text{K}$  and  $T = 1092\text{K}$  in Figs. 6.37 to 6.39).

The ternary viscosity curves predicted by the model are consistent with the viscosity behaviours observed for the binary systems in the previous sections. Similar to the KCl-

$\text{MgCl}_2$  and  $\text{NaCl-MgCl}_2$  binary systems ( Figs 6.23 and 6.29), although the viscosity of pure  $\text{MgCl}_2$  is higher than the  $\text{NaCl}$  and  $\text{KCl}$  viscosities, the addition of  $\text{MgCl}_2$  to the  $\text{NaCl-KCl}$  mixture actually results in a slight decrease in the viscosity at the composition ranges lower than  $\sim 30$  Wt%  $\text{MgCl}_2$ . This behaviour has been qualitatively predicted by Dumas et al. (1973) for the industrially interesting composition ranges (5-20 Wt%  $\text{MgCl}_2$ ). On the other hand, the addition of  $\text{NaCl-KCl}$  mixture to the pure  $\text{MgCl}_2$  will result in a significant decrease in viscosity. This decrease was previously observed for the binary mixtures of  $\text{NaCl-MgCl}_2$  and  $\text{KCl-MgCl}_2$  (Figs 6.23 and 6.29) upon the addition of  $\text{NaCl}$  and  $\text{KCl}$  to pure  $\text{MgCl}_2$ . Changing the composition of the  $\text{NaCl-KCl}$  mixture however seems to result in very small changes in viscosity especially for the industrially interesting composition ranges (5 to 20 Wt%  $\text{MgCl}_2$ ) as it is shown in Fig. 6.40 for a given temperature.

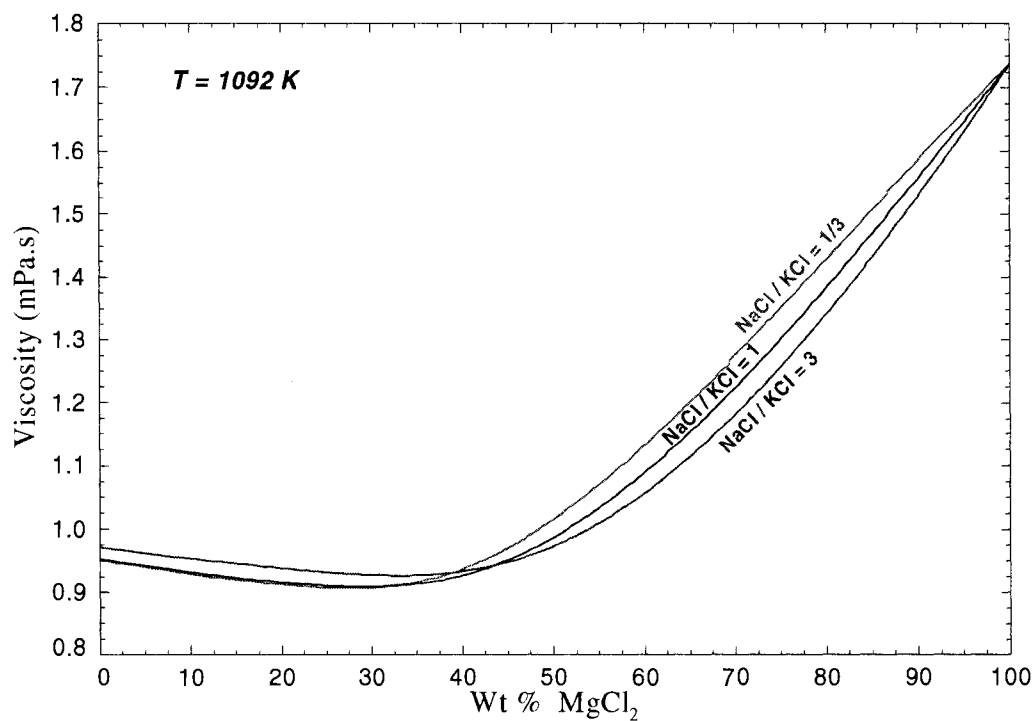


Figure 6.40: A Comparison Between the Calculated Viscosity Isotherms ( $T = 1092 \text{ K}$ ) of NaCl-KCl- $\text{MgCl}_2$  Ternary System at various Weight Ratios of NaCl/KCl.

This behaviour seems reasonable since NaCl and KCl have nearly equal viscosities and similar liquid structure. It was previously shown for the binary mixtures of NaCl- $\text{MgCl}_2$  and KCl- $\text{MgCl}_2$  and also NaCl- $\text{CaCl}_2$  and KCl- $\text{CaCl}_2$ ; that the exchange of NaCl for KCl results in small changes in viscosity. Similar viscosity behavior is qualitatively predicted by Dumas et al. (1973) for a quaternary mixture of NaCl-KCl- $\text{MgCl}_2$ - $\text{CaCl}_2$ . According to them, the exchange of NaCl for KCl in a quaternary mixture is expected not to affect the viscosity significantly.

However, the only data reported for the quaternary system is the one of Zuca (1991) for a limited range of composition and temperature. This data set is systematically corrected based on the estimated error of its corresponding pure data sets (see Section 6.2.2 for details). According to Zuca (1991), the corresponding pure data sets are in agreement with the data set of Murgulescu and Zuca (1963) for NaCl, the data set of Murgulescu and Zuca (1961) for KCl, the data set of Dumas et al. (1970) for  $\text{MgCl}_2$  and the data set of Zuca and Costin (1970) for  $\text{CaCl}_2$  (see Section 6.2.2 for the calculation of the estimated errors and Appendix C for the numerical values of the correction functions). These corrected data are compared with the calculated values given by the model in Table 6.10 and Fig. 6.41.

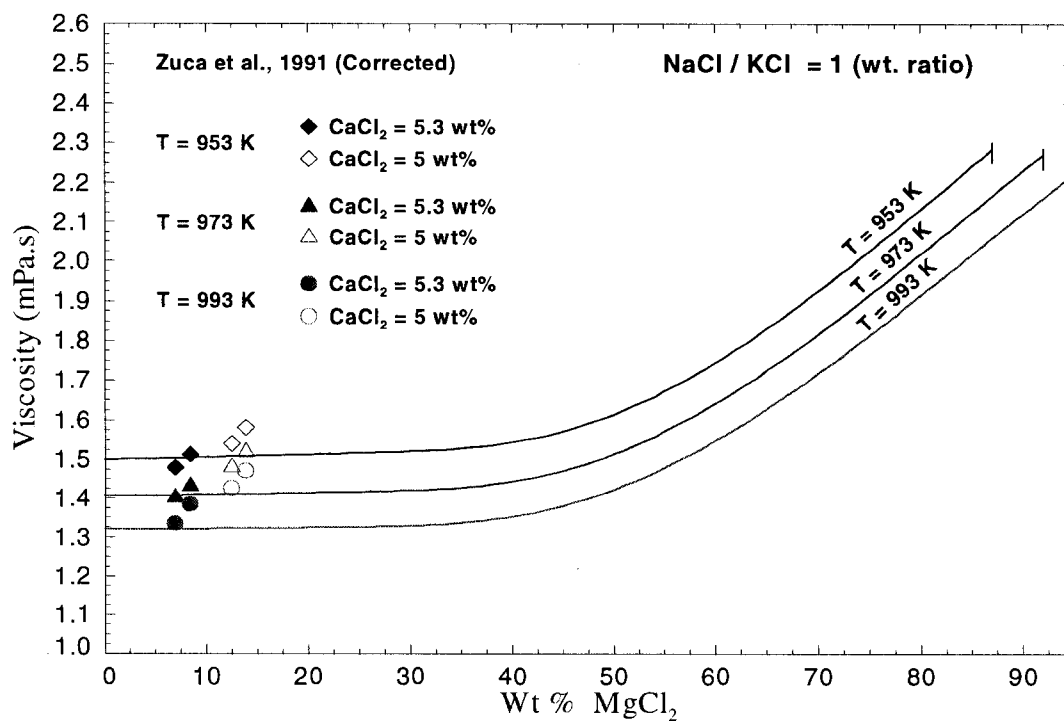


Figure 6.41: Calculated and Experimental Viscosity of NaCl-KCl-MgCl<sub>2</sub>-CaCl<sub>2</sub> System at Various Temperatures for Given Weight Percents of CaCl<sub>2</sub> and the Weight Ratio of NaCl/KCl Equal to 1.

Table 6.10: A Comparison Between the Calculated Viscosity Values and the Experimental Data of Zuca et al. (1991) for NaCl-KCl-MgCl<sub>2</sub>-CaCl<sub>2</sub> System.

T (K)	Composition (wt%)				Experimental $\eta$ (mPa.s) (Corrected)	Calculated $\eta$ (mPa.s)	Shift (%)
	NaCl	KCl	MgCl <sub>2</sub>	CaCl <sub>2</sub>			
953	43.9	43.9	6.9	5.3	1.479	1.510	-2.101
	43.2	43.2	8.3	5.3	1.513	1.511	0.104
	41.3	41.3	12.4	5	1.540	1.507	2.116
	40.6	40.6	13.8	5	1.581	1.508	4.596

973	43.9	43.9	6.9	5.3	1.402	1.414	-0.823
	43.2	43.2	8.3	5.3	1.431	1.414	1.190
	41.3	41.3	12.4	5	1.480	1.410	4.768
	40.6	40.6	13.8	5	1.520	1.411	7.168
993	43.9	43.9	6.9	5.3	1.335	1.327	0.629
	43.2	43.2	8.3	5.3	1.383	1.327	4.087
	41.3	41.3	12.4	5	1.425	1.322	7.246
	40.6	40.6	13.8	5	1.468	1.322	9.937

The quaternary viscosity behavior predicted by the model is consistent with the binary and ternary viscosity behaviors which are previously discussed. As it is shown in Fig 6.41, The addition of  $\text{MgCl}_2$  to the mixture results in small changes in viscosity for the composition ranges lower than  $\sim 30$  Wt%  $\text{MgCl}_2$ . On the other hand for the  $\text{MgCl}_2$  rich region, a significant decrease in the viscosity is predicted by decreasing the  $\text{MgCl}_2$  composition in the melt.

Since  $\text{CaCl}_2$  has the highest viscosity among the other pure components, the addition of  $\text{CaCl}_2$  to the ternary mixture of  $\text{NaCl-KCl-MgCl}_2$  is expected to increase the viscosity. This is illustrated in Fig. 6.42 for various weight percents of  $\text{CaCl}_2$ .



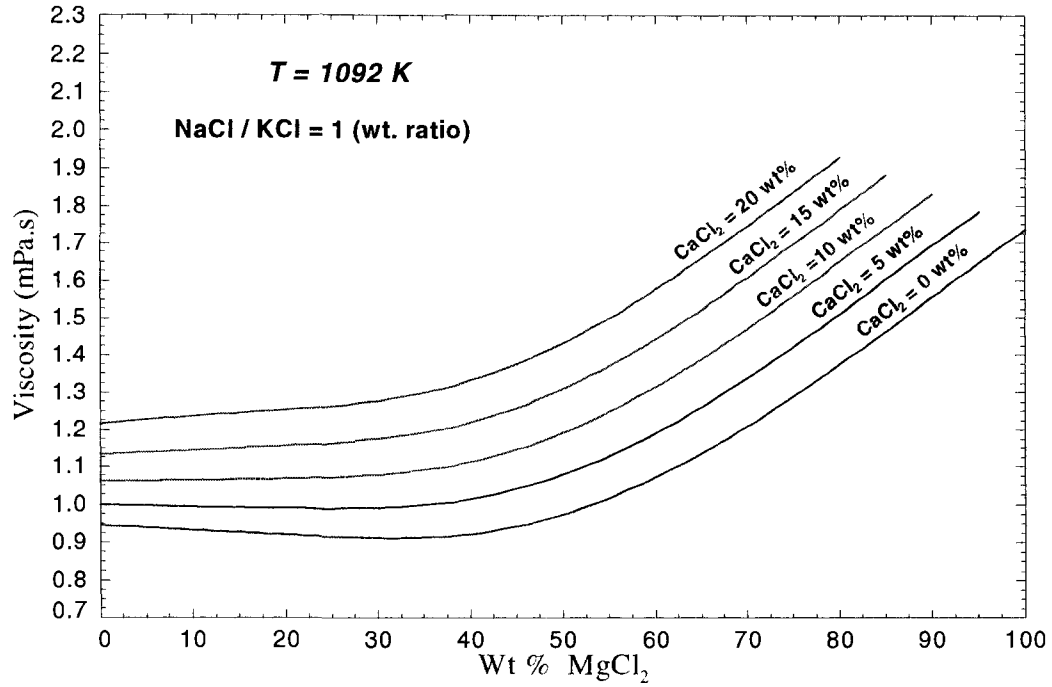


Figure 6.42: Calculated and Experimental Viscosity of NaCl-KCl-MgCl<sub>2</sub>-CaCl<sub>2</sub> System at Various Weight Percents of CaCl<sub>2</sub> and the Weight Ratio of NaCl/KCl Equal to 1 for a Given Temperature.

A similar viscosity behaviour upon the addition of CaCl<sub>2</sub> has been qualitatively predicted by Dumas et al. (1973). However Dumas et al. did not present any justification about this behavior in their paper.

## 7 Results and Discussion: Liquid Metals

In the following sections, the viscosity model presented in Section 5 is applied to obtain the viscosity of Al-Zn and Al-Si binary alloys. The model has been previously employed by Gemme (2004) to calculate the viscosity of pure Al, pure Zn and Al-Zn alloy. However instead of the linear temperature dependence given by Eq. 5.3, he proposed the following equation for the temperature dependence of the activation energy for liquid metals:

$$G^* = c + dT \ln T + \frac{e}{T^2} \quad (7.1)$$

Accordingly Gemme (2004) obtained the parameters  $c$ ,  $d$  and  $e$  for pure Al, pure Zn and Al-Zn alloy. Later Lambotte (2007) performed a thorough literature review and collected the available experimental data for pure liquid metals, namely Al, Zn, Si, Cu and Mg. He proposed the following temperature dependence for the activation energy:

$$G^* = c + dT + \frac{e}{T} + \frac{f}{T^2} \quad (7.2)$$

and obtained the parameters  $c$ ,  $d$ ,  $e$  and  $f$  for the mentioned pure metals by employing the most reliable data sets. However due to the very low values of the calculated  $e$  and  $f$  parameters and the high melting temperature of the metals (higher than 800K), the last two terms of the Eq. (7.2) are negligible and the parameters  $c$  and  $d$  can satisfactorily reproduce the experimental data. In the present work, the parameters  $c$  and  $d$  obtained by Lambotte (2007) for pure Al and pure Si are employed as the unary parameters of the

model. These parameters are re-optimized for pure Zn as it will be discussed in the subsequent sections.

To obtain the binary parameters of the model, the available literature data for the binary systems are collected and reliable data sets are employed to optimize the parameters. The density model previously developed for liquid metals (Gemme, 2004), is employed to calculate the required molar volumes. The calculations for the molar volumes and pair fractions are done by using the FactSage thermochemical software (Bale et al., 2002). The calculated viscosity curves are compared to the literature data.

## **7.1 Pure Liquid Metals**

### **7.1.1 General Discussion on Literature Data**

As described earlier in Section 5, the parameters of the viscosity model are optimized based on the available experimental data. A thorough literature review has been previously performed by Lambotte (2007) and the available data for the studied pure metals namely Al, Zn and Si, were collected. As it will be shown in the following sections, a comparison between the collected data sets shows large discrepancies among the reported experimental data. This could be the result of certain difficulties encountered in the viscosity measurement of high temperature, low-viscosity, reactive and volatile melts (see Section 3.5). Consequently, a critical evaluation was necessary to obtain the most reliable sets of experimental data. This is done by Lambotte (2007) for the pure liquid metals studied in the present work. Several factors such as experimental techniques, the reliability of the employed working equations and other different sources

of errors have been considered in his critical review of the experimental data. Based on the results of the mentioned literature review, the reliable data sets are selected to optimize the unary parameters of the viscosity model. These data sets are shown in the related figures in the following sections and are compared with the viscosity curves calculated by the model. Each figure is accompanied with a table showing the experimental method, conditions and the temperature range for each data set.

### 7.1.2 Al

The data reported for the pure aluminum are listed in Table 7.1 with a summary of the employed experimental method and conditions for each measurement.

Table 7.1: A Summary of the Experimental Methods for the Viscosity Measurements of Pure Liquid Al Reported in the Literature (Lambotte, 2007).

Author, (Year)	Experimental Method (Working Equations)	Experimental Conditions	Temperature Range [K]
Polyak and Sergeev, (1941)	Oscillating sphere (Verschaffelt equation, Eq. 3.2)	Steel sphere with ZnO coating, protecting the liquid using a flux	943 – 1073
Sergeev and Polyak, (1947)	Oscillating sphere (Verschaffelt equation, Eq. 3.2)	Steel sphere with ZnO coating	943 – 1073
Jones and Bartlett, (1952)	Rotational cylinder (Poynting & Thomson, (1947) equation)	Graphite cylinder, inert gas atmosphere, Al purity: 99.55%	933 – 1123
Yao and Kondic, (1952)	Oscillating pendulum (Empirical equation)	Calibration with water, high purity Al: 99.9935%, Argon (Ar) atmosphere	933 – 1073
Gebhardt et al., (1953)	Oscillating vessel (Modified Knappwost, 1952 equation)	Graphite vessel, calibration with Tin (Sn) and Mercury (Hg), high purity Al: 99.996%	933 – 1173

Sato and Munakata, (1955)	Oscillating vessel (Similar mathematical procedure as Roscoe, 1958)	Graphite vessel	973 – 1173
Shvidkovskii, (1955)	Oscillating vessel (Mathematical treatment proposed by the author)	Book in Russian language (book not available), Data reported by Glazov and Ghistyakov, (1958)	933 – 1063
Alvargonzales and Kondic, (1956)	Oscillating vessel (Similar mathematical treatment as Roscoe, 1958)	Graphite vessel, calibration with Lead (Pb) and Zinc (Zn), Ar 99.8% atmosphere	933 – 1033
Glazov and Ghistyakov, (1958)	Oscillating vessel	High purity Al: 99.996%	933 – 1223
Goryaga and Nosyreva, (1958)	Oscillating vessel (Shvidkovskii, 1955 equation)	Graphite vessel	933 – 1173
Korol'kov, (1959)	Oscillating vessel (Shvidkovskii, 1955 equation)		933 – 1103
Gebhardt and Detering, (1959)	Oscillating vessel (Modified Knappwost, 1952 equation)	Graphite vessel, calibration with Sn and Hg, high purity Al: 99.996%	933 – 1173
Koledov and Lyubimov, (1962)	Oscillating vessel (Shvidkovskii, 1955 equation)	Graphite vessel, high purity Al: 99.99%	933 – 1173
Rothwell, (1962)	Oscillating hollow sphere	Graphite sphere, Ar atmosphere	933 – 1103
Lihl et al., (1964)	Oscillating vessel (Modified Knappwost, 1952 equation)	Alumina vessel, calibration with Sn and Zn, high purity Al: 99.995%	933 – 1173
Eretnov and Lyubimov, (1966)	Oscillating vessel (Shvidkovskii, 1955 equation)	High purity Al: 99.9%, purified Helium (He) atmosphere	1373 – 1573
Koledov, (1966)	Oscillating vessel (Shvidkovskii, 1955 equation)	Graphite vessel, Al with four different purities: from 99.8% to 99.99%	933 – 1298
Vignau et al., (1967)	Oscillating vessel (Mathematical treatment based on the works of Shvidkovskii, 1955)	Graphite vessel, high purity Al: 99.996%	933 – 1073
Lihl and Schwaiger, (1967)	Oscillating vessel (Modified Knappwost, 1952 equation)	Alumina vessel, calibration with different metals, high purity Al: 99.99%	933 – 1173
Kononenko et al., (1969)	Oscillating vessel (Knappwost, 1952)	Graphite vessel, calibration with Hg, high purity Al:	933 – 1303

	equation)	99.99%	
Levin, (1971)	Oscillating vessel (Shvidkovskii, 1955 equation)	High purity Al: 99.99%	973 – 1823
Levin et al., (1972)	Oscillating vessel (Shvidkovskii, 1955 equation)	High purity Al: 99.99%	1373 – 1823
Arsent'ev and Polyakova, (1977)	Oscillating vessel (Shvidkovskii, 1955 equation)	Alumina vessel, He atmosphere, Al with different purities: from 98% to 99.99%	943 – 1273
Fridlyander and Kolpachev, (1980)	Oscillating vessel (Shvidkovskii, 1955 equation)	High purity Al: 99.99%, No raw data, article not used	
Kisun'ko et al., (1983)	Oscillating vessel (Shvidkovskii, 1955 equation)	High purity Al: 99.99%	948 – 1173
Zamyatin et al., (1986)	Oscillating vessel (Shvidkovskii, 1955 equation)	Beryllium oxide (BeO) vessel, high purity Al: 99.99%	933 – 1373
Yamasaki et al., (1993)	Oscillating vessel (Roscoe, 1958 equation)	Alumina vessel, high purity Al: 99.99%, He atmosphere	933 – 1073
Herwig and Hoyer, (1994)	Oscillating vessel (Roscoe, 1958 equation)	Alumina vessel, high purity Al: 99.999%, Ar atmosphere mixed with 5% H <sub>2</sub>	933 – 1423
Friedrichs et al., (1997)	Falling ball viscometer	Alumina crucible, SiO <sub>2</sub> capillary for producing the balls, Al purity: 99.9%, Ar atmosphere	1063 – 1123
Moraru et al., (1997)	Rotational cylinder	Ceramic crucible, high purity Al: 99.99%, effect of ultra-sound studied	933 – 1033
Novokhatvskii et al., (1999)	Oscillating vessel (Shvidkovskii, 1955 equation)	Three types of vessel: (alumina, Zirconium oxide, Beryllium oxide), high purity Al: 99.99%	943 – 1193
Sun et al., (2000)	Oscillating vessel	Alumina vessel, high purity Al: 99.999%	933 – 1373
Roach et al., (2001)	Dynamic method	Graphite smelter, high purity Al: 99.95%, Ar or N <sub>2</sub> atmosphere	973 – 1173
Wang and Overfelt,	Oscillating vessel	Graphite vessel with a	953 – 1113

(2002)	(Mathematical treatment proposed by the author)	Boron nitride (BN) coating, Al purity: 99.995%	
Mills, 2002	Oscillating vessel (Roscoe, 1958 equation)	Alumina vessel, high purity Al: 99.995% (Data reported by Assael et al., (2006))	
Hur et al., (2003)	Rotational cylinder	Graphite crucible and cylinder, commercial Al	933 – 1223
Kofanov et al., (2004)	Oscillating vessel	High purity Al: 99.999%	943 – 1323
Sato, (2004)	Oscillating vessel (Roscoe, 1958 equation)	Data in logarithmic scale (impossible to extract the data due to overlapping with Magnesium and Lead Data)	
Roach and Henein, (2005)	Dynamic method	Graphite crucible, Argon (Ar) atmosphere, Al purity: 99.95%	973 – 1173

The most reliable data sets have been selected by Lambotte (2007) and employed to optimize the unary model parameters. He used the temperature dependence given by Eq. (7.2) with 4 parameters to define the activation energy ( $G^*$ ) for pure liquid metals. However as it was mentioned earlier due to the very low values of the calculated  $e$  and  $f$  parameters and the high melting temperature of aluminum ( $T=927.89\text{K}$ ), the last two terms of the Eq. (7.2) are negligible and the parameters  $c$  and  $d$  can satisfactorily reproduce the experimental data. This is similar to the activation energy previously defined for pure molten salts. The viscosity of liquid aluminum thereby can be obtained similar to the pure molten salts with two parameters as follows:

$$\eta_{Al} = \frac{hN_A}{V_M} \exp\left(\frac{G^*_{Al}}{RT}\right) \quad (7-3)$$

$$G^*_{Al} = c_{Al} + d_{Al} \cdot T \quad (7-4)$$

where  $c_{Al}$  and  $d_{Al}$  are the parameters of the model for pure liquid Al. The numerical values of the parameters are given in Appendix A in SI units. The calculated viscosity curve is compared with the experimental data in Figs. 7.1 and 7.2.

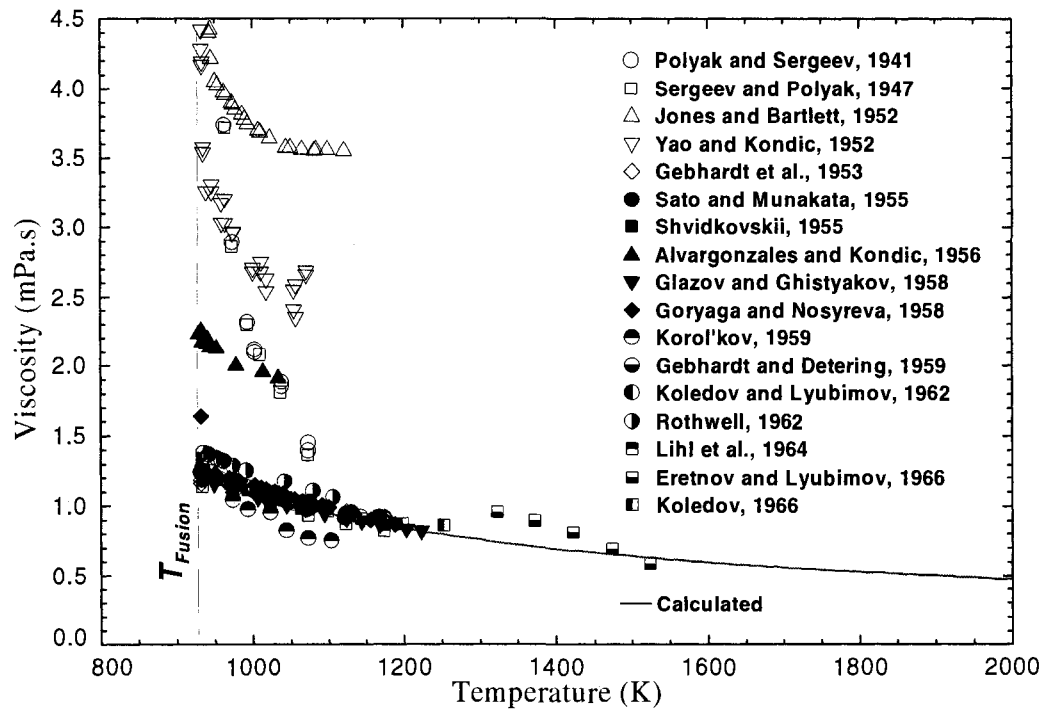


Figure 7.1: Calculated and Experimental Viscosity of Pure Liquid Al (Up to 1966).



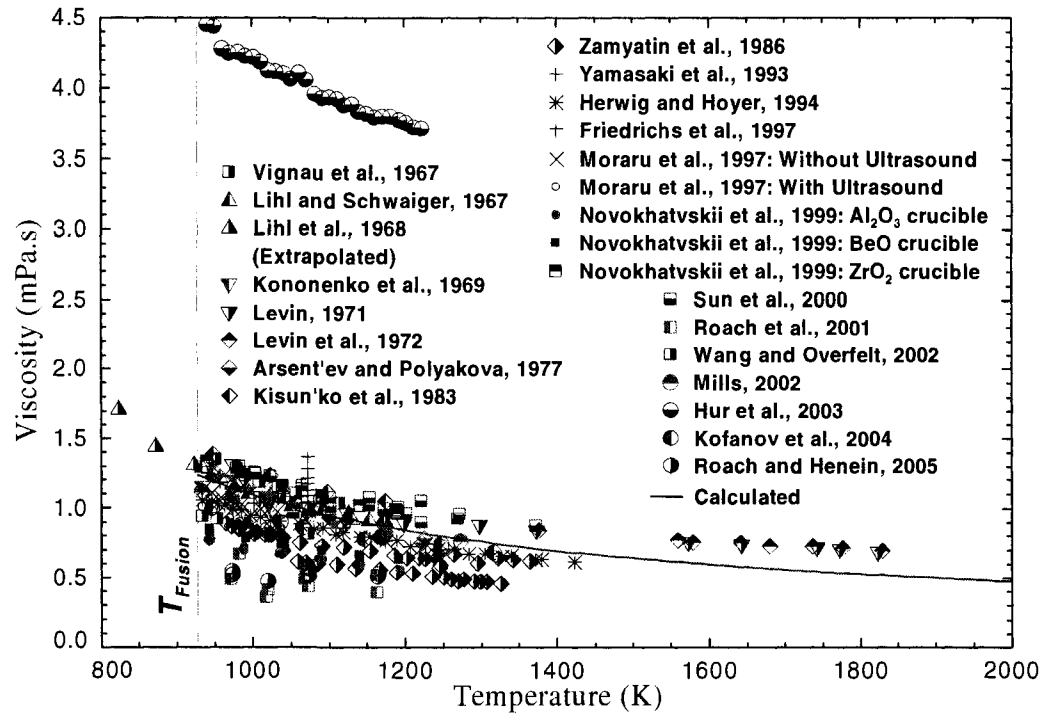


Figure 7.2: Calculated and Experimental Viscosity of Pure Liquid Al (After 1966).

### 7.1.3 Zn

The data reported for the pure zinc are listed in Table 7.2 with a summary of the employed experimental method and conditions for each measurement.

Table 7.2: A Summary of the Experimental Methods for the Viscosity Measurements of Pure Liquid Zn Reported in the Literature (Lambotte, 2007).

Author, (Year)	Experimental Method (Working Equations)	Experimental Conditions	Temperature Range [K]
Gering and Sauerwald, (1935)	Horizontal capillary viscometer	Argon (Ar) used as a gas, highest available purity was reported (Zinc of Kahlbaum purity), Supremax glass by Schott as capillary tube	723 – 973
Hopkins and Toye, (1950)	Oscillating vessel (Using similar mathematical treatment as Roscoe, 1958)	Calibration with organic liquid and Tin (Sn), Alumina ( $\text{Al}_2\text{O}_3$ ) vessel, $\text{H}_2$ atmosphere, high purity Zinc.	703 – 753
Yao and Kondic, (1952)	Oscillating pendulum (Empirical equation)	Calibration with water, high purity Zinc (Zn): 99.9962%, Ar used as a gas	693 – 873
Gebhardt et al., (1954)	Oscillating vessel (Modified Knappwost, 1952 equation)	Calibration with Mercury (Hg) and Sn, Graphite vessel, high purity Zn	773 – 973
Sato and Munakata, (1955)	Oscillating vessel (Similar mathematical procedure as Roscoe, 1958)	Graphite vessel	713 – 853
Yao, (1956)	Oscillating vessel (Knappwost, 1952 equation)	Calibration with organic liquid, Alumina vessel	693 – 1013
Goryaga and Nosyreva, (1958)	Oscillating vessel (Shvidkovskii, 1955 equation)	Graphite vessel, Zinc purified by the author using Schott filter	693 – 973
Gebhardt and Detering, (1959)	Oscillating vessel (Knappwost, 1952 equation)	Graphite vessel, high purity Zn: 99.996%	723 – 973
Korol'kov, (1959)	Oscillating vessel (Shvidkovskii, 1955	---	703 – 923

equation)			
Ofte and Wittenberg, (1963)	Oscillating vessel (Roscoe, 1958 equation)	Tantalum vessel, high purity Zn: 99.99%	693 – 1093
Thresh, (1965)	Oscillating vessel (Roscoe, 1958 equation)	Graphite vessel, calibration with Hg, high purity Zinc: 99.99%	693 – 773
Menz et al., (1966)	Capillary viscometer, double capillary system	Glass tube immersed in a molten salt	753 – 953
Lihl et al., (1968)	Oscillating vessel (Knappwost, 1952 equation)	Alumina vessel, calibration with Tin (Sn), Ar atmosphere	913 – 1173
Sinha and Miller, (1970)	Oscillating vessel (Roscoe, 1958 equation)	Graphite vessel	723 – 793
Harding and Davis, (1975)	Oscillating vessel (Roscoe, 1958 equation)	Graphite vessel, calibration by varying the inertia of the assembly, high purity Zn: 99.99%	693 – 823
Lida et al., (1980)	Oscillating vessel (Modified Roscoe, 1958 equation)	Non-suspended graphite vessel lied on an oscillating assembly, Zn purity: 99.9%	693 – 993

According to Lambotte (2007) the data sets of Gering and Sauerwald (1935), Goryaga and Nosyreva (1958) and Iida et al. (1980) seem to provide the most reliable experimental data. Based on these data sets, the unary parameters of the model are re-optimized for pure Zn. Employing these parameters, the viscosity of liquid zinc is calculated by Eqs. 7.3 and 7.4 and compared with the experimental data in Fig 7.3.

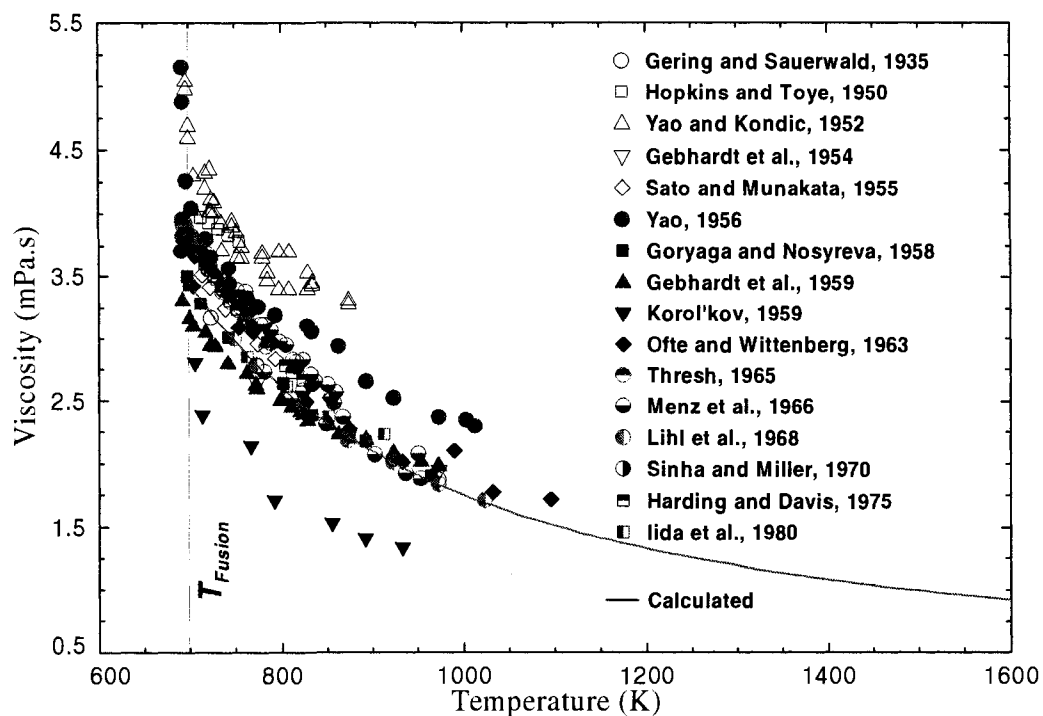


Figure 7.3: Calculated and Experimental Viscosity of Pure Liquid Zn.

The numerical values of the re-optimized parameters ( $c_{Zn}$  and  $d_{Zn}$ ) are given in Appendix A.

#### 7.1.4 Si

The data reported for the pure silicon are listed in Table 7.3 with a summary of the employed experimental method and conditions for each measurement.

Table 7.3: A Summary of the Experimental Methods for the Viscosity Measurements of Pure Liquid Si Reported in the Literature (Lambotte, 2007).

Author, (Year)	Experimental Method (Working Equations)	Experimental Conditions	Temperature Range [K]
Glazov, (1962)	Oscillating vessel	Alumina ( $\text{Al}_2\text{O}_3$ ) vessel	1693 – 1873
Baum et al., (1967)	Oscillating vessel (Shvidkovskii, 1955 equation)	Alumina vessel, high purity Si: 99.99%	1693 – 2093
Kakimoto, 1989	Oscillating vessel (Roscoe, 1958 equation)	Boron nitride (BN) vessel (reported by Kimura et al., (1995))	1698 – 1833
Kimura et al., (1995)	Oscillating vessel (Shvidkovskii, 1955 equation)	Two types of vessels (SiC and PbN), a polycrystalline Si used.	1693 – 1893
Sato, 1998	Oscillating vessel (Roscoe, 1958 equation)	Graphite (C) vessel, other conditions reported by Rhim and Ohsaka, (2000)	1693 – 1903
Rhim and Ohsaka, (2000)	Electrostatic levitation	Pure Si	1593(supercooled) – 1753
Sato et al., (2003)	Oscillating vessel (Roscoe, 1958 equation)	Seven types of vessels (graphite, SiC, alumina, $\text{Si}_3\text{N}_4$ , BN, quartz ( $\text{SiO}_2$ ) and 92% $\text{ZrO}_2$ -8% $\text{Y}_2\text{O}_3$ )	1656(supercooled) – 1893
Zhou et al., (2003)	Electrostatic levitation	High purity Si: 99.999%	1633(supercooled) – 1843

The most reliable data sets have been selected by Lambotte (2007) and employed to optimize the unary model parameters. Similar to the pure aluminum, the two parameters  $c$  and  $d$  of Eq. 7.2, could satisfactorily reproduce the experimental data. The numerical values of the parameters ( $c_{\text{Si}}$  and  $d_{\text{Si}}$ ) are given in Appendix A. Accordingly the viscosity of liquid silicon is calculated by Eqs. 7.3 and 7.4 and compared with the experimental data in Fig 7.4.

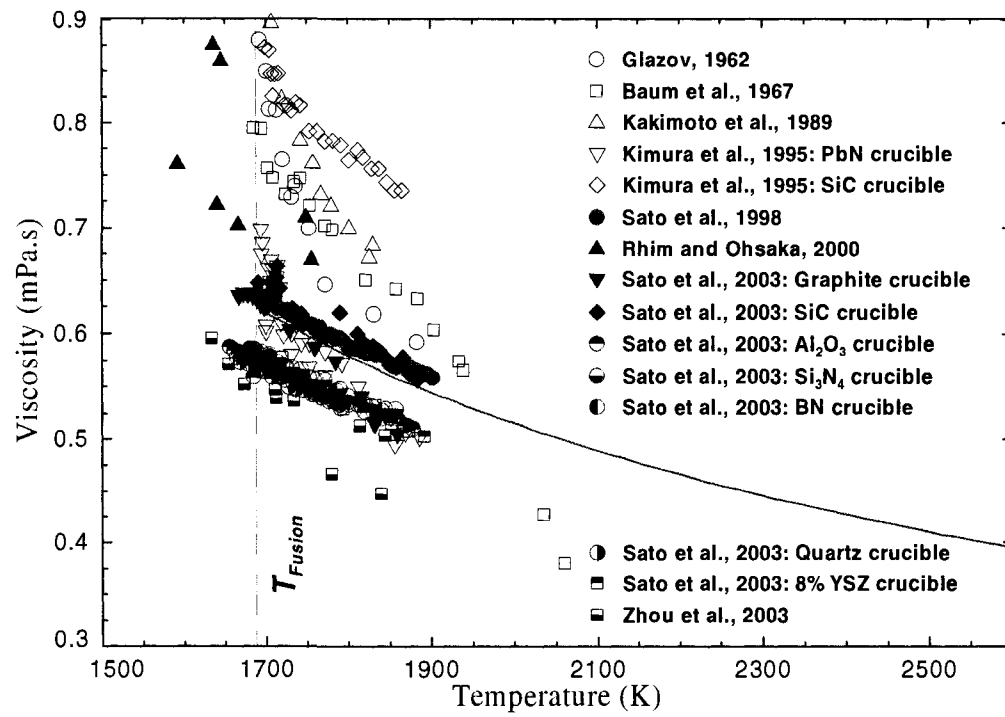


Figure 7.4: Calculated and Experimental Viscosity of Pure Liquid Si.

As it is shown in Fig. 7.5, the calculated viscosities of pure Al, Zn and Si between 300K and 2000K extrapolated well below and above the melting points of the pure metals.

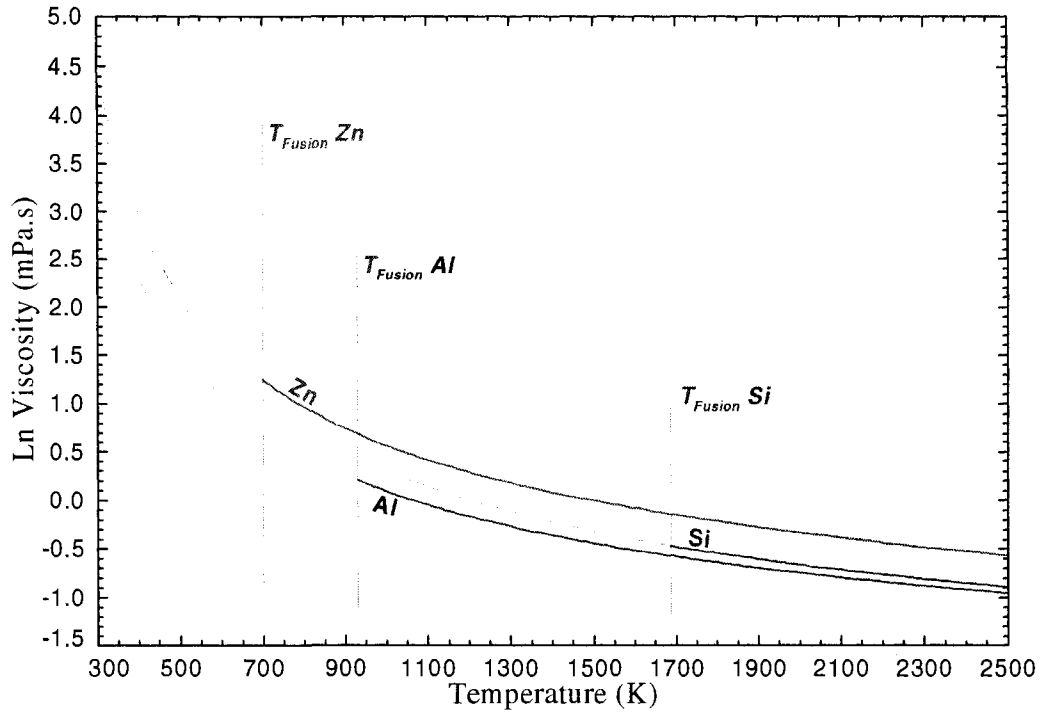


Figure 7.5: The Extrapolation of the Viscosity Curves Calculated by the Model

Parameters for Al, Zn and Si Pure Metals Below Their Melting Points.

## 7.2 Binary Liquid Metals

### 7.2.1 General Discussion on Literature Data

For the two binary systems studied in the present work, namely Al-Zn and Al-Si, a literature review is performed and the available literature data are collected and critically

reviewed. The reported binary data sets are evaluated based on the estimated accuracy of their corresponding unary data sets. Similar to the studied molten salt systems, systematic corrections are applied to the binary data based on the estimated error of their corresponding pure data sets (see Section 6.2.2). The error estimation for the molten salts was based on the standard quality unary data sets recommended in NSRDS publications. However for the pure liquid metals, there were larger discrepancies among the data and no such standard quality data set was reported. Since the calculated viscosity curves for pure metals are obtained by a statistical approach between the most reliable data sets; the similar systematic errors applied to the molten salts systems could not be accurately calculated for liquid metals. The estimated corrections within the accuracy limits of the employed experimental methods ( $\leq \sim 5\%$ ) thereby are not applied to liquid alloys. Only the corrections larger than 5% are systematically applied to the binary data sets. The binary parameters of the model are then optimized based on the corrected experimental data. The calculated binary viscosity curves are compared to the literature data for each system.

### **7.2.2 Al-Zn**

According to the present literature review, following data sets have been reported for the viscosity of Al-Zn binary system. The measurements of Jones and Bartlett (1952) by the rotating cylinder method and the measurements of Lihl et al. (1968) and Gebhardt and Detering (1959) by the oscillating vessel method. As it is illustrated in Fig. 7.6, the viscosity values reported by Jones and Bartlett (1952) by the rotational method are too



high, compared to the ones of Lihl et al. (1968) and Gebhardt and Detering (1959) (see Table 7.1 for the details of the experimental conditions).

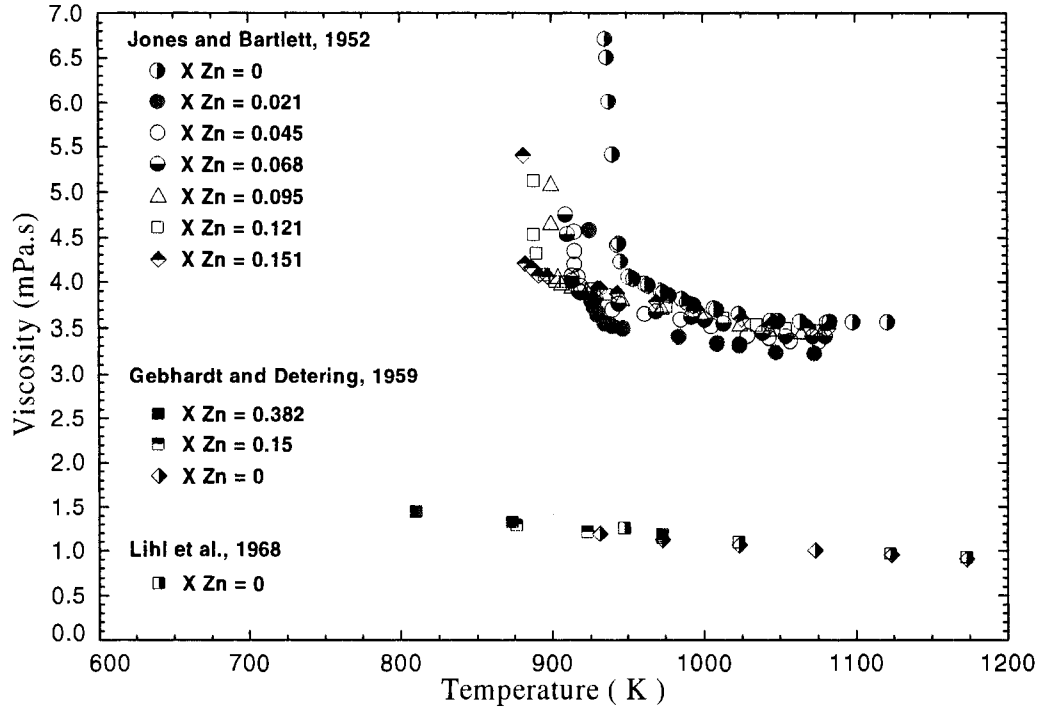


Figure 7.6: A Comparison Between the Data Set of Jones and Bartlett (1952) (Rotating Cylinder Method) and the Viscosity Data of Lihl et al. (1968) and Gebhardt and Detering (1959) (Oscillating Vessel Method) for Al-Zn Binary System.

As it was previously discussed in Section 3.3, obtaining accurate viscosity values by the rotational technique is technically difficult for the low viscosity liquids. Bockris and MacKenzie (1959), showed that rotational methods are not suitable for melts with viscosities lower than 10 mPa.s. According to the presented literature review for molten

salts and liquid metals, among all the measurements performed for these low viscosity liquids, only a few experimental groups employed the rotational technique. Most of the measurements for the studied liquid metals are done by the oscillating vessel method which is proper for highly volatile and corrosive melts at high temperatures (see Section 3.5 for the details on the choice of experimental methods).

Based on the motioned considerations, the high viscosity values of Jones and Bartlett (1952) by the rotating cylinder method, can be a result of the inaccuracy of the employed experimental technique. The systematic corrections similar to the ones applied on molten salts (based on the estimated error of the corresponding unary data sets) were not applicable to the Jones and Bartlett (1952) rotational measurements; since those corrections were based on the estimated error of the oscillating methods. However applying a correction to this data set does not seem reasonable since the shift of the data estimated to be over 100 %. Therefore the mentioned data set has not been considered in the optimization of binary parameters in the present work. The binary parameters of the model for this system are obtained by employing the measurements of Lihl et al. (1968) and Gebhardt and Detering (1959) by the oscillating vessel method. A comparison between the corresponding unary data sets of these measurements and the calculated lines for pure Al and pure Zn (Figs. 7.1, 7.2 and 7.3) shows a minor inconsistency between the data. As it is discussed in the previous section, the inconsistencies are mostly within the experimental limits of accuracy. However a correction factor is applied on the measurements of Gebhardt and Detering (1959) due to the estimated error for the pure zinc. The numerical values of the applied correction functions are given in Appendix C.

This corrected data set (1959) and the one of Lihl et al. (1968) are employed to optimize the parameters of the model for Al-Zn binary system. The numerical values of the binary parameters of the model ( $c_{Al/Zn}$  and  $d_{Al/Zn}$ ) are given in Appendix A. The viscosity of the Al-Zn binary system thereby can be calculated by the optimized parameters of the model as follows:

$$\eta = \frac{hN_A}{V_M} \exp\left(\frac{X_{AlAl}G_{Al}^* + X_{ZnZn}G_{Zn}^* + X_{AlZn}G_{Al/Zn}^*}{RT}\right) \quad (7.5)$$

with the activation energies given by the optimized parameters of the model as follows:

$$\begin{aligned} G_{Al}^* &= c_{Al} + d_{Al}T \\ G_{Zn}^* &= c_{Zn} + d_{Zn}T \\ G_{Al/Zn}^* &= c_{Al/Zn} + d_{Al/Zn}T \end{aligned} \quad (7.6)$$

where the molar volume of the binary system ( $V_M$ ) and the pair fractions ( $X_{AlAl}$ ,  $X_{ZnZn}$  and  $X_{AlZn}$ ) are calculated by FactSage thermochemical software (Bale et al., 2002) as a function of temperature and composition of the melt.

The calculated viscosity isotherms and isocomposition lines obtained by Eq. (7.5) are illustrated in Figs. 7.7 and 7.8 and compared with the experimental data.

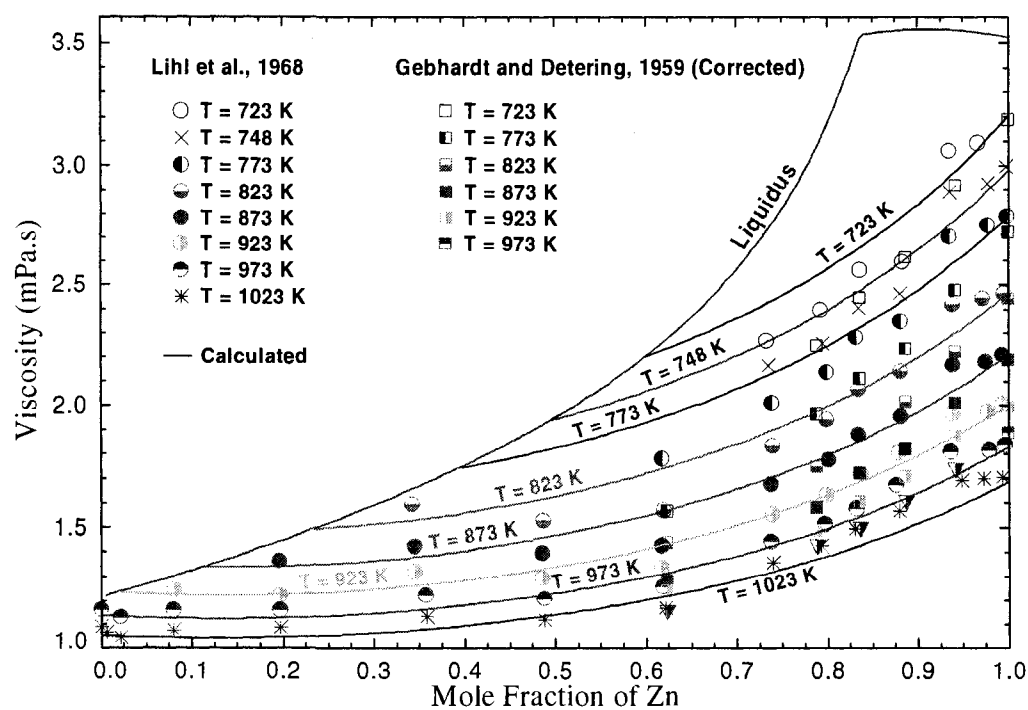


Figure 7.7: Calculated and Experimental Viscosity of Al-Zn Melt at Various Temperatures.

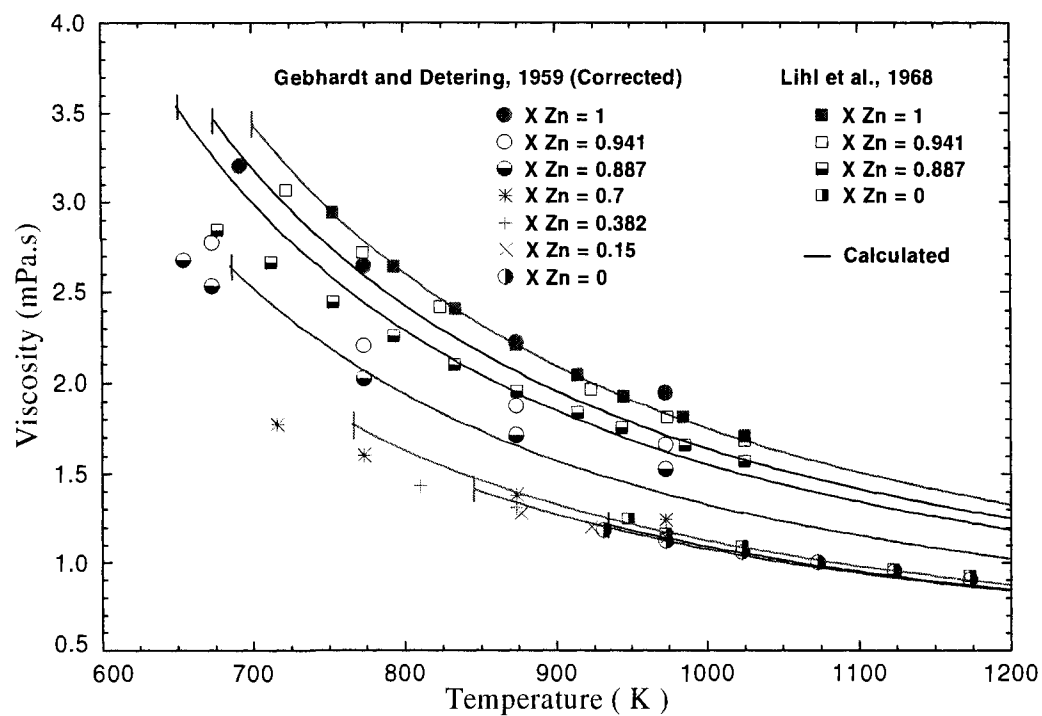


Figure 7.8: Calculated and Experimental Viscosity of Al-Zn Melt at Various Mole Fractions of Zn.

### 7.2.3 Al-Si

A summary of the data sets reported for Al-Zn binary system is presented in Table 7.4.

Table 7.4: A Summary of the Experimental Methods for the Viscosity Measurements of Al-Si Binary System Reported in the Literature.

Author, (Year)	Experimental Method (Working Equations)	Experimental Conditions	Si [Wt%]	Temperature Range [K]
Sergeev and Polyak,(1947)	Oscillating sphere (Verschaffelt equation, Eq. 3.2)	Steel sphere, Steel wire, Calibration by water & C <sub>6</sub> H <sub>6</sub>	0 – 19	973
Jones and Bartlett, (1952)	Rotational cylinder (Poynting & Thomson, (1947) equation)	Graphite cylinder, inert gas atmosphere, Al purity: 99.55%	0-18.6	850 - 1123
Gebhardt and Detering, (1959)	Oscillating vessel (Modified Knappwost, 1952 equation)	Graphite vessel, calibration with Sn and Hg, high purity Al: 99.996%	0 – 23	923 – 1173
Vignau, (1968)	Oscillating vessel (Mathematical treatment based on the works of Shvidkovskii, 1955)	Graphite vessel, high purity Al and Si: 99.996%, protecting the liquid using a carnallite based flux	5 - 15	903 – 1173
Lihl et al., (1968)	Oscillating vessel (Modified Knappwost, 1952 equation)	Alumina vessel, calibration with different metals, high purity Al: 99.99%	0-23.4	823 – 1173
Geng et al., (2005)	Oscillating vessel (empirical equation by the author)	High purity Al: (99.7%) and Si (99.99%)	5, 12.5, 16 and 20	983-1313

As it is shown in Table 7.4, the available measurements of binary Al-Si alloys are performed in the Al-rich region. None of the mentioned authors reported a unary data set

for pure silicon<sup>\*\*\*</sup>. Only the unary data sets for pure Al have been reported in these publications. Accordingly the systematic corrections applied on the other binary systems, are estimated based on the estimated error of the pure Al unary data set for Al-Si binary system.

A comparison between the data of pure Al reported by Sergeev and Polyak (1947) and the optimized line calculated by the model (Fig. 7.1) shows high discrepancies (higher than 100% at the temperatures close to the melting point). Furthermore this data set is reported only at a given temperature and the temperature dependency of the viscosity has not been measured in this publication. Therefore the binary data of Sergeev and Polyak (1947) has not been considered for the optimization of the binary model parameters.

As it is illustrated in Fig. 7.9, the binary data reported by Jones and Bartlett (1952) by the rotational method are too high, compared to the ones of Lihl et al. (1968) and Gebhardt and Detering (1959).

---

<sup>\*\*\*</sup> Pure Si has a very high melting point (1687.41K) and is highly reactive. Viscosity measurements of this high-temperature and reactive melt is extremely difficult and requires a specially designed viscometer. See Sato et al., (2003)

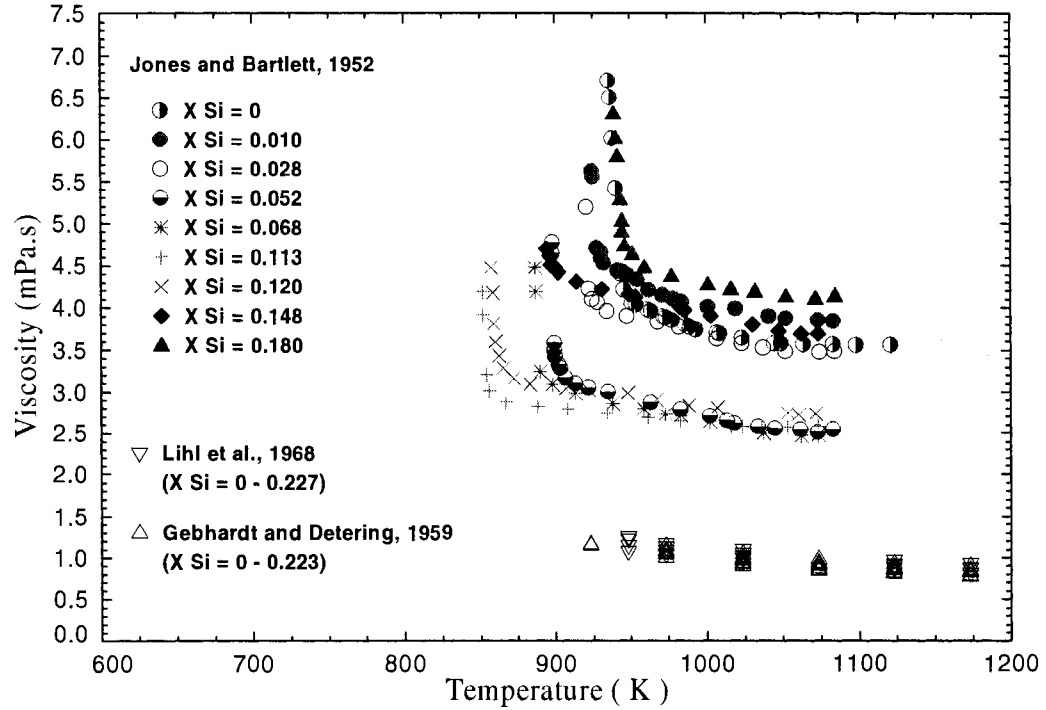


Figure 7.9: A Comparison Between the Data Set of Jones and Bartlett (1952) (Rotating Cylinder Method) and the Viscosity Data of Lihl et al. (1968) and Gebhardt and Detering (1959) (Oscillating Vessel Method) for Al-Si Binary System.

As it was previously discussed in the previous section for Al-Zn system, the high viscosity values of Jones and Bartlett (1952) by the rotating cylinder method are excluded in the optimization of binary parameters in the present work.

As it is mentioned in Table 7.4, Vignau (1968) employed a carnallite based flux protection layer to prevent the oxidation of aluminum during the measurements. This extra layer on the surface of the samples could result in experimental errors during the



measurements. The similar method has been employed for the measurements of pure Al by this author. A comparison between its corresponding data set for pure Al and the optimized line in Fig 7.2, shows lower viscosity values than the other reported data. Accordingly the data set of Vignau (1968) has been corrected based on the estimated error of its corresponding data set for pure Al. The numerical value of the applied correction function is given in Appendix C.

A comparison between the corresponding unary data set of Geng et al. (2005) measurements for pure Al (Sun et al., 2000) shows the viscosity values higher than the optimized viscosity curve (Fig 7.2). A correction factor was required to shift the data down to the lower optimized values. However as illustrated in Fig 7.10, the binary data set reported by Geng et al. (2005) shows lower binary viscosity values compared to the other reported data sets.

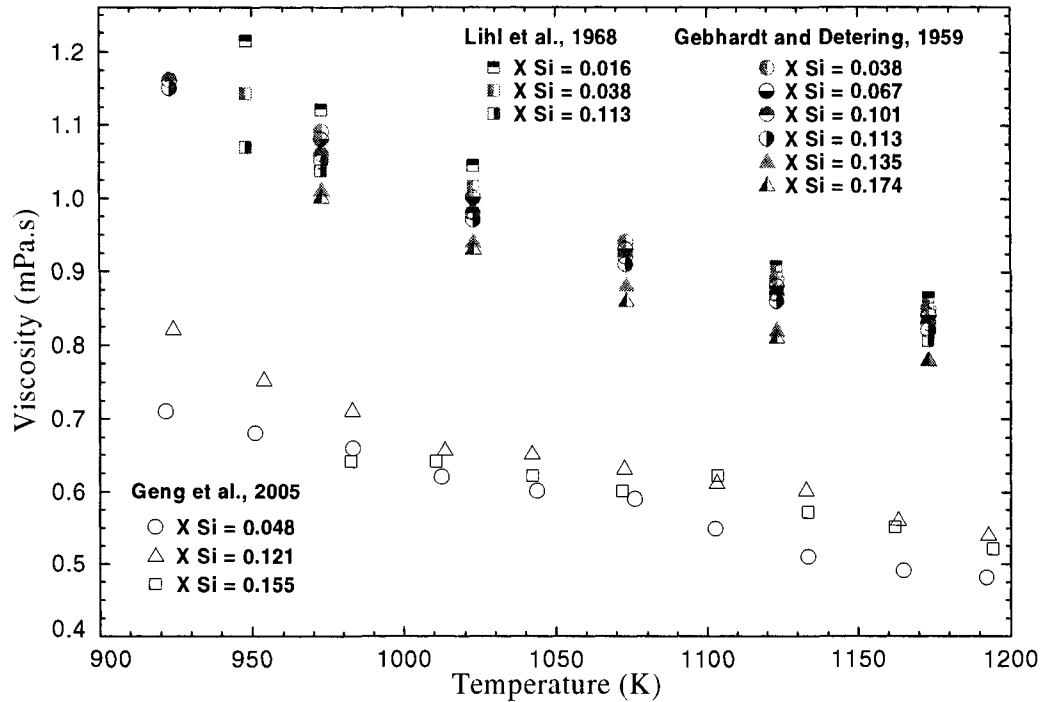


Figure 7.10: A Comparison Between the Data Set of Geng et al. (2005) and the Viscosity Data of Lihl et al. (1968) and Gebhardt and Detering (1959) (Oscillating Vessel Method) for Al-Si Binary System.

Due to the lack of information regarding the experimental conditions of Fan et al. (2004) measurements, the cause of this inconsistency between the unary and binary data could not be explained. However applying a systematic correction based on the estimated error for the pure Al data set will result in much lower viscosity values for the binary data of Geng et al. (2005). Accordingly this data set is not considered in the optimization of the binary parameters.

Based on the above mentioned considerations, the binary parameters of the model for Al-Si system are obtained based on the measurements of Lihl et al. (1968) and Gebhardt and Detering (1959) by the oscillating vessel method. The numerical values of the parameters ( $c_{Al/Si}$  and  $d_{Al/Si}$ ) are given in Appendix A. A comparison between the corresponding pure Al data sets of these measurements and the calculated lines for pure Al (Figs. 7.1, 7.2) shows a minor inconsistency between the data. However as it is discussed in the previous section, these inconsistencies are less than 5% (within the experimental limits of accuracy). Therefore the corrections are not applied on these binary data.

The viscosity of Al-Si binary system then can be calculated by employing the unary and binary parameters of the model by Eq. (7.5). The calculated viscosity isotherms and isocomposition curves are illustrated in Figs. 7.11 and 7.12 and compared with the experimental data.

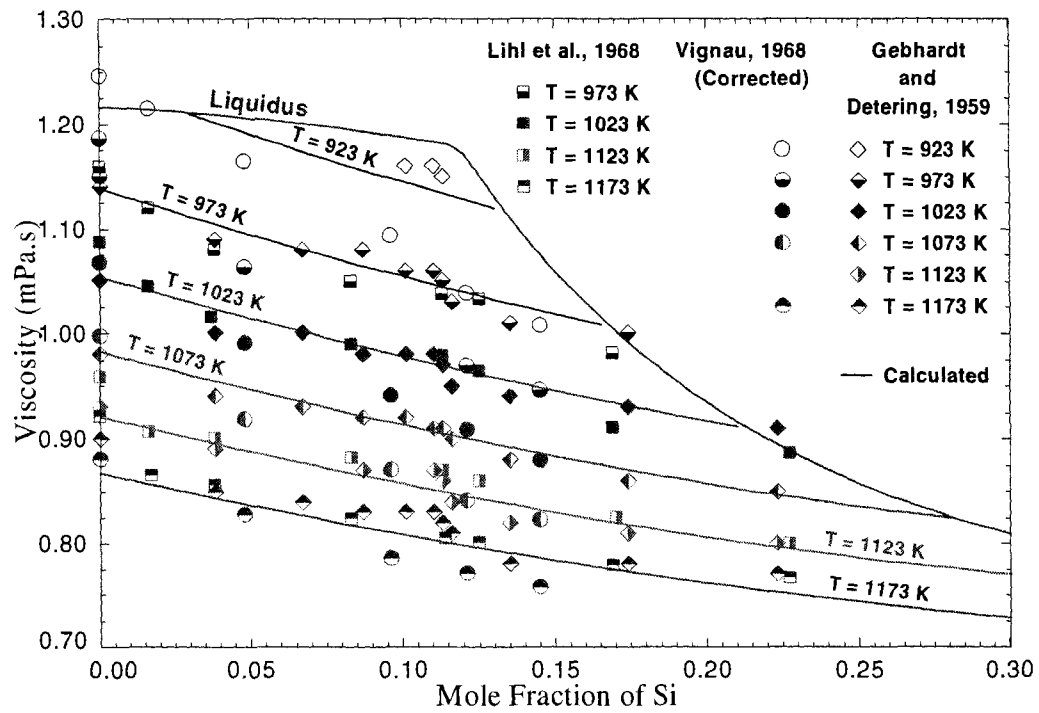


Figure 7.11: Calculated and Experimental Viscosity of Al-Si Melt at Various Temperatures.

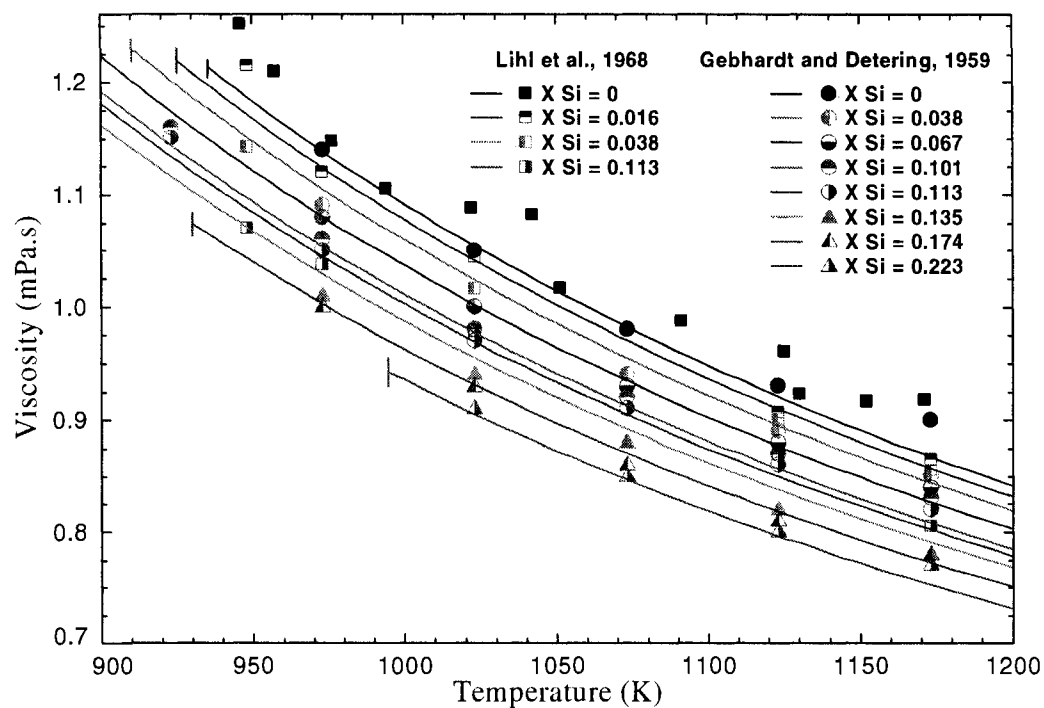


Figure 7.12: Calculated and Experimental Viscosity of Al-Si Melt at Various Mole Fractions of Si.

## **8 Example of the Application of the Model in Aluminum Treatment Process**

As it is previously discussed in Section 2.1.1, gas fluxing is the most common technique employed to remove alkali and alkaline earth impurities from the aluminum alloys. Usually a mixture of chlorine and an inert gas such as argon (which is used as a carrier for chlorine) is injected in the bottom of the melt. The injected chlorine reacts with the alkali and alkaline earth impurities in the melt and forms chlorides as solid particles or liquid droplets which will rise in the liquid alloy and continue to exchange alkali metals. However as it is discussed in Section 2.1.1, due to several environmental problems, the use of salt fluxes as a replacement for chlorine is becoming more common. One of the salt fluxes that can be employed for fluxing is a mixture of KCl and  $\text{MgCl}_2$  salts.

By employing the presented viscosity model and the developed viscosity database, the viscosity of liquid solutions involved in this process can be calculated at different temperatures and compositions. An example of these calculations done by FactSage thermochemical software (Bale et al., 2002) is given in this section at  $720^\circ\text{C}$  (which is the typical temperature used for the treatment process) for an Al-Zn-Si alloy containing ppm amounts of alkali and alkaline earth impurities. To remove these impurities, a mixture of chlorine and argon gas and KCl-MgCl<sub>2</sub> solid powder is injected in the melt. The hypothetical properties of the liquid alloy and the injected flux assumed in this example are given in Table 8.1.

Table 8.1: Hypothetical Properties of the Liquid Al-Zn-Si Alloy and the Injected Cl<sub>2</sub>-Ar and KCl-MgCl<sub>2</sub> Flux Employed for the Example of the Treatment Process.

Liquid Al Alloy		Injected Flux*	
Component	Amount	Component	Amount
Al	~ 94 wt. %	Cl <sub>2</sub> (gas)	0.02 mole
Si	5 wt. %	Ar (gas)	1.9 mole
Zn	1 wt. %	KMgCl <sub>3</sub> (solid)	0.08 mole
Mg	1000 ppm		
Na	350 ppm		
Ca	50 ppm		
K	5 ppm		
<b>Total:</b>	<b>1 metric ton</b>	<b>Total:</b>	<b>192 mole</b> <b>(~4.4 m<sup>3</sup> at STP**)</b>

\* Injected at 100 steps; each step 2 mole (~0.16 m<sup>3</sup>)

\*\* Standard Temperature and Pressure (273.15K & 100kPa)

The given amount of reactive flux with the given composition is injected through the liquid alloy in 100 steps. The flux reacts with the alkali and alkaline earth impurities and forms the solid or liquid salts which can be later removed from the melt. This leads to reduction of the amounts of alkali and alkaline earth impurities in the treated alloy. Fig 8.1 shows the amount of impurities as a function of the volume of the injected flux.

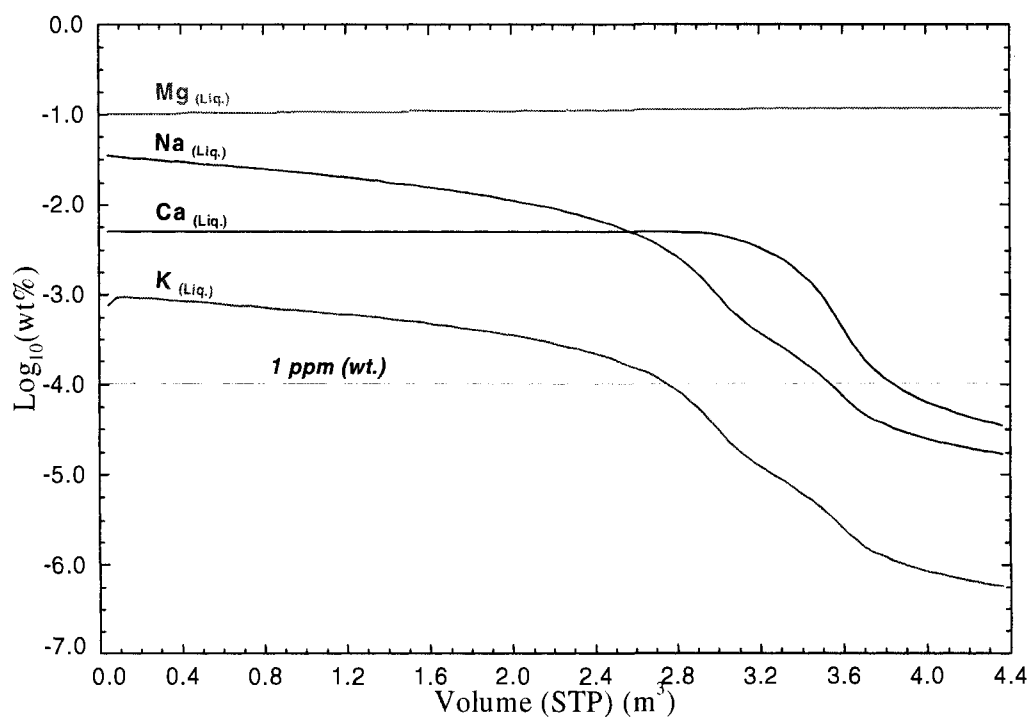


Figure 8.1: The Amount of Alkali and Alkaline Earth Impurities per Metric Ton of Alloy During a Hypothetical Treatment Process as a Function of the Volume of the Injected Flux at Standard Temperature and Pressure.

As it is shown in Fig 8.1, the composition of the undesirable alkali and alkaline earth impurities such as Na, K and Ca are reduced to less than 1 ppm after fluxing. The reaction products formed during the injection are shown in Fig. 8.2.



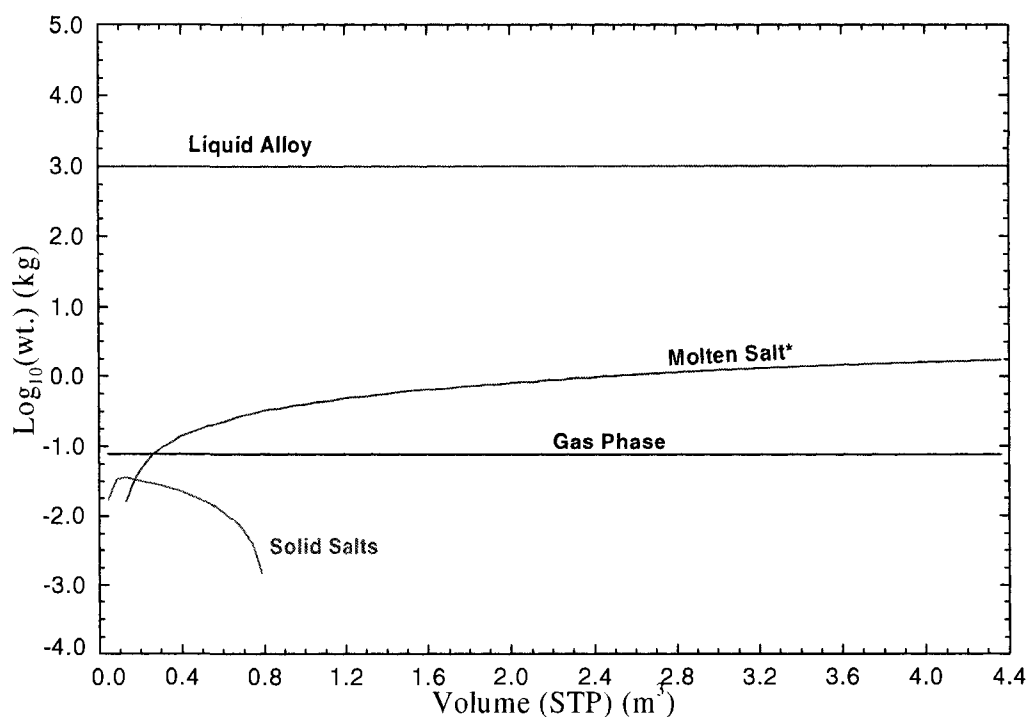


Figure 8.2: The Reaction Products per Metric Ton of Alloy During a Hypothetical Treatment Process as a Function of the Volume of the Injected Flux at Standard Temperature and Pressure.

The molten salt solution formed during the process (marked with a star in Fig. 8.2) is a mixture of NaCl, KCl, CaCl<sub>2</sub> and MgCl<sub>2</sub> pure liquid salts with different compositions as it is illustrated in Fig. 8.3.

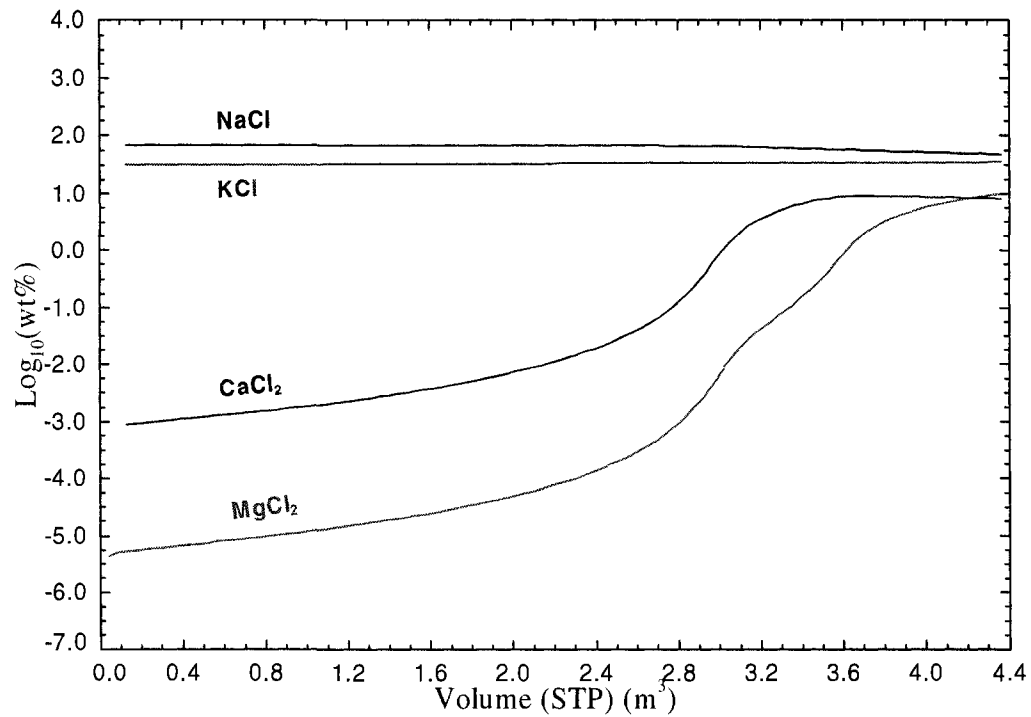


Figure 8.3: The Liquid Salts Formed per Metric Ton of Alloy During a Hypothetical Treatment Process as a Function of the Volume of the Injected Flux at Standard Temperature and Pressure.

The viscosity of the produced molten salt solution shown in Fig. 8.2 and 8.3 can be calculated by the presented viscosity model at different steps of the process at various compositions as it is illustrated in Fig. 8.4.

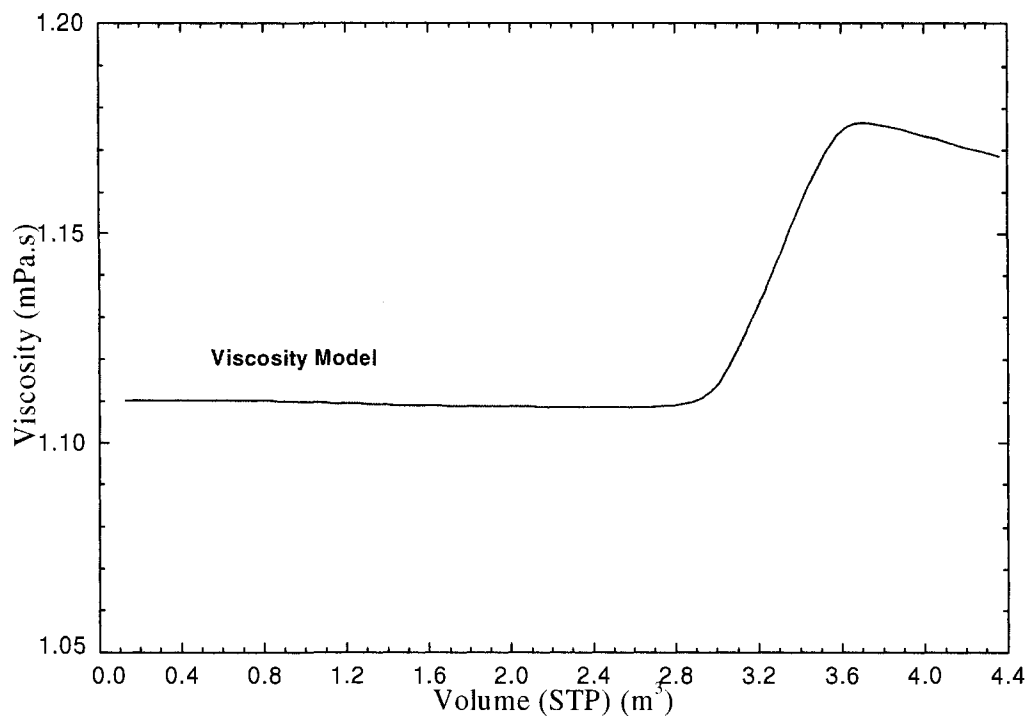


Figure 8.4: The Viscosity of the Multi-Component Molten Salt Solution Formed During a Hypothetical Treatment Process as a Function of the Volume of the Injected Flux at Standard Temperature and Pressure.

Due to the amounts of impurities present in the melt and the composition of the injected flux, the calculated viscosity curve may have different shapes.

In the presented example, the composition of the liquid alloy was assumed to be constant; however the model could calculate the viscosity of the liquid alloys at different compositions of the alloying elements.

## 9 Conclusions and Future Work

This master project is a part of VLAB (A Virtual Laboratory for the aluminum industry) project aiming to develop thermodynamic and physical properties databases required by the aluminum industry. These databases can be accessed through the FactSage thermochemical software to perform multi-component thermodynamic and physical property calculations for the processes involved in the aluminum industry. In particular, the viscosity model presented in this work was used to develop a viscosity database for molten salts and liquid metals.

The objective of this master project was to model the viscosity of multi-component liquid solutions formed during the treatment and casting of liquid aluminum and its alloys namely, NaCl-KCl-MgCl<sub>2</sub>-CaCl<sub>2</sub> molten salt system and Al-Zn-Si alloy, upon mixing.

A structural viscosity model is presented that can employ the previously developed density and thermodynamic models (Chartrand and Pelton, 2001b; Robelin et al., 2007) to predict the viscosity of multi-component systems as a function of temperature and composition. A modification is proposed to the model to better reproduce the viscosity behavior of highly short-range ordered systems as a function of composition.

The temperature dependency of the viscosity in this model is given by an Eyring type exponential equation. The activation energy for viscous flow of a multi-component system is given by the summation of the activation energies of the SNN pairs present in the melt. The composition dependency of the viscosity for a liquid mixture is thereby expressed in the viscous activation energy term through the variation of the SNN pair fractions upon mixing (the SNN pair fractions being calculated by the thermodynamic

model). The defined activation energies for the SNN pairs are the parameters of the model given as linear functions of temperature. However for highly short-range ordered systems, the model is modified by introducing composition dependent terms in the activation energy as well as the temperature dependent terms. The model parameters are optimized based on the reliable experimental data collected through a critical review of the literature data. Due to the inconsistencies between the reported unary and binary data sets in the literature, correction functions are applied to the data and the corrected binary data sets are employed for the optimizations.

The calculated viscosity curves by the model could well reproduce the viscosity behavior predicted by the experiments for simple binary systems: NaCl-KCl, MgCl<sub>2</sub>-CaCl<sub>2</sub>, NaCl-CaCl<sub>2</sub> and KCl- CaCl<sub>2</sub> as well as the highly short-range ordered systems: NaCl- MgCl<sub>2</sub>, KCl- MgCl<sub>2</sub>, RbCl- MgCl<sub>2</sub> and CsCl- MgCl<sub>2</sub>. There were few experimental data in the literature for multi-component molten salt systems, however the predictions of the model for NaCl-KCl-MgCl<sub>2</sub>-CaCl<sub>2</sub> system compare reasonably well with the available experimental data reported for a limited range of composition and temperature. The viscosity curves calculated by the model well reproduce the experimental data reported for the Al-Zn and Al-Si binary alloys.

In resume, the model leads to very satisfactory results for the molten chloride mixtures and liquid aluminum alloys studied in the present work. The viscosity behaviour of these systems is well understood through the presented results. The proposed modification for the highly short-range ordered systems could well reproduce the viscosity behavior of

these systems. The optimized model parameters are employed to develop a database for the viscosity calculations of the studied molten salts and liquid alloys. This database is included in the FactSage 5.6 data bases where the viscosity of multi-component molten salts and binary aluminum alloys can be calculated through the presented viscosity model by simultaneously employing the thermodynamic and density models.

The present viscosity database can be extended to make possible the viscosity calculations for more complicated systems including different salts and metallic elements.

In the present work, the model parameters are obtained by employing the available experimental data. Due to several difficulties encountered in viscosity measurements of high temperature reactive melts, it would be convenient if one could correlate the viscosity to the already modeled thermodynamic properties. The possibility of correlating the defined viscous activation energies to the thermodynamic properties such as enthalpy of mixing is to be discovered in the future research programs. However several other factors such as the effect of the kinetic stability of the species in the melt should also be considered.

It is important to point out that the present viscosity model is applicable for the incompressible Newtonian liquids where the viscosity is only a function of temperature and composition. However the model can be extended to non-Newtonian regions (where the viscosity becomes shear rate-dependent) by means of a proper shear rate-viscosity correlation. The model can also be employed to obtain the viscosity of slurries containing

solid particles (suspensions) through further investigation of the effect of the solid inclusions on the viscosity behavior of these liquid solutions.

In conclusion this master project was contributed to the development of a database for the viscosity of the liquid solutions involved in the aluminum production process, namely molten alkali and alkaline earth chlorides and aluminum alloys. By employing this database simultaneously with the thermodynamic and density databases in FactSage 5.6, the viscosity calculations for these multi-component solutions can be performed in a fully consistent manner.

## 10 References

- Abe, Y., Kosugiyama, O., & Nagashima, A. (1980). Viscosity measurements on sodium chloride in the temperature range 1083-1473 K. *Berichte der Bunsen-Gesellschaft*, 84(11), 1178-84.
- Abe, Y., & Nagashima, A. (1981). The principle of corresponding states for alkali halides viscosity. *Journal of Chemical Physics*, 75(8), 3977-85.
- Alvargonzales, J. M. N., & Kondic, V. (1956). Viscosity study on molten metals and alloys. *Instituto del Hierro y del Acero, Madrid [Publicaciones]*, 9, 953-70.
- Andrade, E. N. d. (1934). Theory of viscosity of liquids. *Philosophical Magazine (1798-1977)*, 17, 497-511, 698-732.
- Arsent'ev, P. P., & Polyakova, K. I. (1977). Viscosity of molten aluminum. *Izvestiya Akademii Nauk SSSR, Metally*, (2), 65-70.
- Assael, M. J., Kakosimos, K., Banish, R. M., Brillo, J., Egry, I., Brooks, R., Qusted, P. N., Mills, K. C., Nagashima, A., Sato, Y., & Wakeham, W. A. (2006). Reference data for the density and viscosity of liquid aluminum and liquid iron. *Journal of Physical and Chemical Reference Data*, 35(1), 285-300.
- Azpeitia, A. G., & Newell, G. F. (1959). Theory of oscillation-type viscometers. IV. A thick disk. *Zeitschrift fuer Angewandte Mathematik und Physik*, 10, 15-34.
- Balasubrahmanyam, K. (1966). Raman spectra of liquid  $\text{MgCl}_2$  and liquid  $\text{MgCl}_2$ -sbd.KCl system. *Journal of Chemical Physics*, 44(9), 3270-3.
- Bale, C. W., Chartrand, P., Degterov, S. A., Eriksson, G., Hack, K., Ben Mahfoud, R., Melancon, J., Pelton, A. D., & Petersen, S. (2002). FactSage thermochemical software and databases. *CALPHAD: Computer Coupling of Phase Diagrams and Thermochemistry*, 26(2), 189-228.
- Bansal, R. (1973). Frequency moments and viscosities of liquid aluminum. *Journal of Physics C: Solid State Physics*, 6(21), 3071-6.
- Bansal, R. (1973). Frequency moments and viscosities of liquid sodium. *Journal of Physics C: Solid State Physics*, 6(7), 1204-12.



- Barzakovskii, V. P. (1940). The density, viscosity, electric conductivity and surface tension of some binary salt systems in the fused state. *Bull. acad. sci. U. R. S. S., Classe sci. chim.*, 825-31 (in German, 831).
- Baum, B. A., Gel'd, P. V., & Kocherov, P. V. (1967). Viscosity of silicon and chromium and its silicides. *Izvestiya Akademii Nauk SSSR, Metally*, (1), 62-9.
- Berenblit, V. M. (1937). Viscosity of the system potassium chloride-magnesium chloride-sodium chloride. *Trudy Vses. Alyum.-Magn. Inst.*, (No. 14), 25-36.
- Biggin, S., & Enderby, J. E. (1981). The structure of molten calcium chloride. *Journal of Physics C: Solid State Physics*, 14(25), 3577-83.
- Bilodeau, J.-F., Lakroni, C., & Kocaeffe, Y. (2001). Modeling of rotary injection process for molten aluminum processing. *Light Metals (Warrendale, PA, United States)*, 1009-1015.
- Bird, R. B., Stewart, W. E., & Lightfoot, E. N. (2002). *Transport phenomena* (2nd). New York: J. Wiley.
- Bloom, H. (1967). *The Chemistry of Molten Salts, An Introduction to the Physical and Inorganic Chemistry of Molten Salts and Salt Vapors*.
- Bockris, J. O. M., White, J. L., Mackenzie, J. D., & Editors (1959). *Physicochemical Measurements at High Temperatures*.
- Bondarenko, N. V. (1966). Viscosity of melts of the magnesium chloride-sodium chloride-potassium chloride system. *Zhurnal Prikladnoi Khimii (Sankt-Peterburg, Russian Federation)*, 39(12), 2684-90.
- Bondarenko, N. V., & Strelets, K. L. (1965). Viscosity of melts in the system  $\text{MgCl}_2$ - $\text{NaCl}$ - $\text{BaCl}_2$ . *Zhurnal Prikladnoi Khimii (Sankt-Peterburg, Russian Federation)*, 38(6), 1273-9.
- Bondarenko, N. V., & Strelets, K. L. (1968). Viscosity of melts of some chloride systems. *Fizicheskaya Khimiya i Elektrokimiya Rasplavlennykh Solei i Shlakov, Trudy Vsesoyuznogo Soveshchaniya po Fizicheskoi Khimii i Elektrokhimii Rasplavlennykh Solei i Shlakov*, 95-104.
- Born, M., & Green, H. S. (1947). A general kinetic theory of liquids. III. Dynamical properties. *Proc. Roy. Soc. (London)*, A190, 455-74.
- Born, M., & Mayer, J. E. (1932). The lattice theory of ion crystals. *Zeitschrift fuer Physik*, 75, 1-18.

- Borzsak, I., Cummings, P. T., & Evans, D. J. (2002). Shear viscosity of a simple fluid over a wide range of strain rates. *Molecular Physics*, 100(16), 2735-2738.
- Brady, E. L., & Wallenstein, M. B. (1964). *National Standard Reference Data System Plan of Operation (National Bureau of Standards Reference Data Series, NSRDS-NBS 1)*.
- Brockner, W., Grjotheim, K., Ohta, T., & Øye, H. A. (1975). High-temperature viscometer for fluid liquids. II. Viscosities of the alkali chlorides. *Berichte der Bunsen-Gesellschaft*, 79(4), 344-7.
- Brockner, W., Toerklep, K., & Oeye, H. A. (1981). Viscosity of molten alkali chlorides. *Journal of Chemical and Engineering Data*, 26(3), 250-3.
- Brockner, W., Toerklep, K., & Øye, H. A. (1979). Viscosity of sodium fluoride-aluminum fluoride melt mixtures. *Berichte der Bunsen-Gesellschaft*, 83(1), 12-19.
- Brooks, R. F., Day, A. P., Andon, R. J. L., Chapman, L. A., Mills, K. C., & Quested, P. N. (2001). Measurement of viscosities of metals and alloys with an oscillating viscometer. *High Temperatures - High Pressures*, 33(1), 73-82.
- Brooks, R. F., Dinsdale, A. T., & Quested, P. N. (2005). The measurement of viscosity of alloys-a review of methods, data and models. *Measurement Science and Technology*, 16(2), 354-362.
- Capwell, R. J. (1972). Raman spectra of crystalline and molten magnesium chloride. *Chemical Physics Letters*, 12(3), 443-6.
- Carreau, P. J., De Kee, D. C. R., Chhabra, R. P., & Editors (1997). *Rheology of Polymeric Systems: Principles and Application*.
- Celik, C., & Dautre, D. (1989). Theoretical and experimental investigation of furnace chlorine fluxing. *Light Metals (Warrendale, PA, United States)*, 793-800.
- Chapman, T. W. (1966). The viscosity of liquid metals. *AIChE Journal*, 12(2), 395-400.
- Chartrand, P., & Pelton, A. D. (2001a). The modified quasi-chemical model: Part III. Two sublattices. *Metallurgical and Materials Transactions A: Physical Metallurgy and Materials Science*, 32(6), 1397-1407.
- Chartrand, P., & Pelton, A. D. (2001b). Thermodynamic evaluation and optimization of the LiCl-NaCl-KCl-RbCl-CsCl-MgCl<sub>2</sub>-CaCl<sub>2</sub> system using the modified quasi-

- chemical model. *Metallurgical and Materials Transactions a-Physical Metallurgy and Materials Science*, 32(6), 1361-1383.
- Chartrand, P., & Pelton, A. D. (2002). A predictive thermodynamic model for the Al-NaF-AlF<sub>3</sub>-CaF<sub>2</sub>-Al<sub>2</sub>O<sub>3</sub> system. *Light Metals (Warrendale, PA, United States)*, 245-252.
- Ciccotti, G., Jacucci, G., & McDonald, I. R. (1976). Transport properties of molten alkali halides. *Physical Review A: Atomic, Molecular, and Optical Physics*, 13(1), 426-36.
- Cohen, M. H., & Turnbull, D. (1959). Molecular transport in liquids and glasses. *Journal of Chemical Physics*, 31, 1164-9.
- Dai, S., Begun, G. M., Young, J. P., & Mamantov, G. (1995). Application of chemometric methods in Raman spectroscopic studies of molten salt system containing MgCl<sub>2</sub>-KCl: experimental evidence for existence of Mg<sub>2</sub>Cl<sub>7</sub><sup>3-</sup> dimer and its Raman spectrum. *Journal of Raman Spectroscopy*, 26(10), 929-32.
- Delhomelle, J., & Petravic, J. (2003). Shear viscosity of molten sodium chloride. *Journal of Chemical Physics*, 118(6), 2783-2791.
- DeWitt, R., Wittenberg, L. J., & Cantor, S. (1974). Viscosity of molten sodium chloride, sodium tetrafluoroborate, and potassium tetrafluoroborate. *Physics and Chemistry of Liquids*, 4(2-3), 113-23.
- Dumas, D., Fjeld, B., Grjotheim, K., & Øye, H. A. (1973). Viscosities of some binary mixtures between magnesium chloride, calcium chloride, and alkali chlorides. *Acta Chemica Scandinavica (1947-1973)*, 27(1), 319-28.
- Dumas, D., Grjotheim, K., Hogdahl, B., & Øye, H. A. (1970). Theory of oscillating bodies and its utilization for determination of high-temperature viscosities. *Acta Chemica Scandinavica (1947-1973)*, 24(2), 510-30.
- Edwards, F. G., Howe, R. A., Enderby, J. E., & Page, D. I. (1978). The structure of molten barium chloride. *Journal of Physics C: Solid State Physics*, 11(6), 1053-7.
- Ejima, T., Iwasaki, K., & Saito, G. (1977). Viscosity of magnesium chloride-potassium chloride and calcium chloride-potassium chloride binary melts. *Nippon Kinzoku Gakkaishi*, 41(8), 784-91.
- Ejima, T., Shimakage, K., Sato, Y., Okuda, H., Kumada, N., & Ishigaki, A. (1982). Viscosity measurement of alkali chlorides with capillary viscometer. *Nippon Kagaku Kaishi*, (6), 961-8.

- Enderby, J. E., & Biggin, S. (1983). Structural investigations of molten salts by diffraction methods. *Advances in Molten Salt Chemistry*, 5, 1-25.
- Eretnov, K. I., & Lyubimov, A. P. (1966). Viscosity of a molten copper alloys. *Izvestiya Vysshikh Uchebnykh Zavedenii, Tsvetnaya Metallurgiya*, 9(1), 119-23.
- Eyring, H., Henderson, D., & Ree, T. (1962). Thermodynamic and transport properties of liquids. *Progr. Intern. Res. Thermodyn. Transport Properties Papers, Symp. Thermophys. Properties, 2nd, Princeton, N.J.*, 340-51.
- Eyring, H., Henderson, D., Stover, B. J., & Eyring, E. M. (1964). *Statistical Mechanics and Dynamics*.
- Faber, T. E. (1972). *Introduction to the Theory of Liquid Metals*.
- Fan, J.-f., Yuan, Z.-f., Li, J., & Xu, C. (2004). Viscosity properties of molten  $\text{CaCl}_2\text{-MgCl}_2$  system. *Zhongguo Youse Jinshu Xuebao*, 14(10), 1759-1762.
- Forster, D., Martin, P. C., & Yip, S. (1968). Moment method approximation for the viscosity of simple liquids: application to argon. *Physical Review*, 170(1), 160-3.
- Fridlyander, I. N., & Kolpachev, A. A. (1980). Toughness of high-purity aluminum. *Izvestiya Akademii Nauk SSSR, Metally*, (4), 38-41.
- Friedrichs, H. A., Ronkow, L. W., & Zhou, Y. (1997). Measurement of viscosity, density, and surface tension of metal melts. *Steel Research*, 68(5), 209-214.
- Fumi, F. G., & Tosi, M. P. (1964). Ionic sizes and Born repulsive parameters in the  $\text{NaCl}$ -type alkali halides. I. Huggins-Mayer and Pauling forms. *Journal of Physics and Chemistry of Solids*, 25(1), 31-43.
- Galamba, N., Nieto de Castro, C. A., & Ely, J. F. (2004). Molecular Dynamics Simulation of the Shear Viscosity of Molten Alkali Halides. *Journal of Physical Chemistry B*, 108(11), 3658-3662.
- Galamba, N., Nieto de Castro, C. A., & Ely, J. F. (2005). Shear viscosity of molten alkali halides from equilibrium and nonequilibrium molecular-dynamics simulations. *Journal of Chemical Physics*, 122(22), 224501/1-224501/9.
- Gebhardt, E., Becker, M., & Dorner, S. (1953). Properties of metallic melts. VII. Viscosity of molten aluminum and its alloys. *Zeitschrift fuer Metallkunde*, 44, 510-14.

- Gebhardt, E., Becker, M., & Dorner, S. (1954). Properties of metallic melts. IX. Viscosity of molten Al-Zn alloys. *Zeitschrift fuer Metallkunde*, 45, 83-5.
- Gebhardt, E., & Detering, K. (1959). Properties of metallic melts. XVI. Internal friction of an aluminum alloy eutectic. *Zeitschrift fuer Metallkunde*, 50, 379-85.
- Gemme, F. (2004). *Étude des propriétés physico-chimiques des alliages liquides d'aluminium*. Rapport de project de Maîtrise, École Polytechnique de Montréal, Montréal, Canada.
- Geng, H. R., Wang, R., Yang, Z. X., Chen, J. H., Sun, C. J., & Wang, Y. (2005). Temperature dependence of viscosity of Al-Si alloy melts. *Acta Metallurgica Sinica (English Letters)*, 18(2), 159-163.
- Gering, K., & Sauerwald, F. (1935). The internal friction of molten metals and alloys. VI. The internal friction of Pb, Cd, Zn, Ag, Sn, K, Na and the question of structural viscosity of amalgams. *Z. anorg. allgem. Chem.*, 223, 204-8.
- Glasstone, S., Laidler, K. J., & Eyring, H. (1941). *The Theory of Rate Processes. The Kinetics of Chemical Reactions, Viscosity, Diffusion and Electrochemical Phenomena*.
- Glazov, V. M. (1962). Viscosity and electrical conductivity of liquid silicon. *Izvestiya Akademii Nauk SSSR, Otdelenie Tekhnicheskikh Nauk, Metallurgiya i Toplivo*, (No. 5), 110-16.
- Glazov, V. M., & Ghistyakov, Y. D. (1958). The temperature relation of the viscosity of aluminum. *Izvest. Akad. Nauk S.S.S.R., Otdel. Tekh. Nauk*, (No. 7), 141-3.
- Goryaga, G. I., & Nosyreva, I. A. (1958). Viscosity of molten zinc, aluminum, cadmium, and antimony. *Vestnik Moskovskogo Universiteta, Seriya Matematiki, Mekhaniki, Astronomii, Fiziki, Khimii*, 13(No. 6), 59-64.
- Gross, P. H., & Zimmerman, H. K. (1964). Properties of the liquid state. II. Description of viscosity over the entire liquid range. *Rheologica Acta*, 3(4), 290-4.
- Gross, P. H., & Zimmerman, H. K. (1964). Properties of the liquid state. III. General relationship between viscosity, density, and temperature. *Rheologica Acta*, 3(4), 294-9.
- Grouvel, J. M., & Kestin, J. (1978). *J. Appl. Sci. Res*, 34, 427.
- Harding, M. P., & Davis, A. J. (1975). Viscosity of liquid lead, zinc, and zinc-based diecasting alloys. *Journal of the Australian Institute of Metals*, 20(3), 150-7.

- Helfand, E., & Rice, S. A. (1960). Principle of corresponding states for transport properties. *Journal of Chemical Physics*, 32, 1642-4.
- Hertzberg, T., Torklep, K., & Øye, H. A. (1980). Viscosity of molten sodium fluoride-aluminum fluoride-aluminum oxide-calcium fluoride mixtures. Selecting and fitting models in a complex system. *Light Metals (Warrendale, PA, United States)*, 159-70.
- Herwig, F., & Hoyer, W. (1994). Viscosity investigations on liquid alloys of the monotectic system aluminum-indium. *Zeitschrift fuer Metallkunde*, 85(6), 388-90.
- Hirai, M. (1992). Estimation of viscosities of liquid alloys. *Tetsu to Hagane*, 78(3), 399-406.
- Hopkins, M. R., & Toye, T. C. (1950). The determination of the viscosity of molten metals. *Proceedings of the Physical Society, London*, 63B, 773-82.
- Huang, C.-H., & Brooker, M. H. (1976). Raman spectrum of molten magnesium chloride. *Chemical Physics Letters*, 43(1), 180-2.
- Huggins, M. L. (1937). The calculation of intermolecular forces and energies. *Physical Review*, 51, 379.
- Huggins, M. L. (1937). Lattice energies, equilibrium distances, compressibilities and characteristic frequencies of alkali halide crystals. *Journal of Chemical Physics*, 5, 143-8.
- Huggins, M. L., & Mayer, J. E. (1933). Interatomic distances in crystals of the alkali halides. *Journal of Chemical Physics*, 1, 643-6.
- Hur, B.-Y., Park, S.-H., & Hiroshi, A. (2003). Viscosity and surface tension of Al and effects of additional element. *Materials Science Forum*, 439(Eco-Materials Processing & Design), 51-56.
- Hur, B.-Y., Park, S.-H., & Hiroshi, A. (2003). Viscosity and surface tension of Al and effects of additional element. (439, 51-56). Gyungpodae, South Korea: Trans Tech Publications Ltd.
- Iida, T., & Guthrie, R. I. L. (1987). *The Physical Properties of Liquid Metals*.
- Iida, T., Morita, Z., & Takeuchi, S. (1975). Viscosity measurements of pure liquid metals by the capillary method. *Nippon Kinzoku Gakkaishi*, 39(11), 1169-75.

- Iida, T., Satoh, A., Ishiura, S., Ishiguro, S., & Morita, Z. (1980). An investigation on the viscosity determination of liquid metals by the oscillating vessel method. *Nippon Kinzoku Gakkaishi*, 44(4), 443-52.
- Iida, T., Ueda, M., & Morita, Z. (1976). Excess viscosity of liquid alloys and the atomic interaction of their constituents. *Tetsu to Hagane*, 62(9), 1169-78.
- International-Aluminium-Institute. (2000). "WORLD-ALUMINIUM.ORG, Home of the International Aluminium Institute." from <http://www.world-aluminum.org/production/index.html>.
- Ito, T., Kojima, N., & Nagashima, A. (1989). Redetermination of the viscosity of molten sodium chloride at elevated temperatures. *International Journal of Thermophysics*, 10(4), 819-31.
- Janz, G. J. (1980). Molten salts data as reference standards for density, surface tension, viscosity, and electrical conductance: potassium nitrate and sodium chloride. *Journal of Physical and Chemical Reference Data*, 9(4), 791-829.
- Janz, G. J. (1988). Thermodynamic and transport properties for molten salts: correlation equations for critically evaluated density, surface tension, electrical conductance, and viscosity data. *Journal of Physical and Chemical Reference Data, Supplement*, 17(2), 309 pp.
- Janz, G. J. (1991). High-temperature calibration quality data: molten salts and metals. *Materials Science Forum*, 73-75(Molten Salt Chem. Technol.), 707-14.
- Janz, G. J. (1992). *NIST Properties of Molten Salts Database (NIST SRD 27, Boulder)*.
- Janz, G. J., Dampier, F. W., Lakshminarayanan, G. R., Lorenz, P. K., & Tomkins, R. P. T. (1968). Molten salts. I. Electrical conductance, density, and viscosity data, Molten Salts Data Center, Rensselaer Polytech. Inst., Troy, NY, USA.: 139 pp.
- Janz, G. J., Tomkins, R. P. T., Allen, C. B., Downey, J. R., Jr., Gardner, G. L., Krebs, U., & Singer, S. K. (1975). Molten salts: Volume 4, Part 2, Chlorides and mixtures. Electrical conductance, density, viscosity, and surface tension data. *Journal of Physical and Chemical Reference Data*, 4(4), 871-1178.
- Janz, G. J., Yamamura, T., & Hansen, M. D. (1989). Corresponding-states data correlations and molten salts viscosities. *International Journal of Thermophysics*, 10(1), 159-71.
- Jhon, M. S., & Eyring, H. (1978). A model of the liquid state. Three-phase partition functions. *Theoretical Chemistry (New York)*, 3, 55-141.

- Jones, W. R. D., & Bartlett, W. L. (1952). The viscosity of aluminum and binary aluminum alloys. *Journal of the Institute of Metals*, 81, 145-52; Paper No 1426.
- Kawasaki, K., & Gunton, J. D. (1973). Theory of nonlinear transport processes. Nonlinear shear viscosity and normal stress effects. *Physical Review A: Atomic, Molecular, and Optical Physics*, 8(4), 2048-64.
- Kazmierczak, J., Kiswa, A., Borresen, B., Haarberg, G. M., & Tunold, R. (1998). Kinetics and mechanism of the magnesium electrode reaction in molten MgCl<sub>2</sub>-KCl binary mixtures. *Proceedings - Electrochemical Society*, 98-11 (Molten Salts XI), 114-127.
- Kestin, J., & Newell, G. F. (1957). Theory of oscillating-type viscometers: the oscillating cup. I. *Zeitschrift fuer Angewandte Mathematik und Physik*, 8, 433-49.
- Kimura, S., Sasaki, H., & Terashima, K. (1995). Properties of Si melt near melting point. *Ceramic Transactions*, 60 (Crystal Growth of Novel Electronic Materials), 69-82.
- Kisun'ko, V. Z., Novokhatskii, I. A., Beloborodov, A. Z., Bychkov, Y. B., & Pogorelov, A. I. (1983). Toughness of secondary aluminum alloys with silicon, manganese, copper, and magnesium. *Tsvetnye Metally (Moscow, Russian Federation)*, (1), 74-6.
- Kitajima, M., Saito, K., & Shimoji, M. (1976). Shear viscosity of liquid sodium-potassium alloys. *Transactions of the Japan Institute of Metals*, 17(9), 582-7.
- Knappwost, A. (1952). High-temperature viscometry by the rotating-tube method. *Z. physik. Chem.*, 200, 81-9.
- Kofanov, S. A., Kofanov, S. A., Chikova, O. A., & Popel, P. S. (2004). Viscosity of Al-Ni-liquid alloys. *Rasplavy*, (3), 30-37.
- Koledov, L. A. (1966). Viscosity of pure aluminum. *Izvestiya Vysshikh Uchebnykh Zavedenii, Tsvetnaya Metallurgiya*, 9(4), 111-13.
- Koledov, L. A., & Lyubimov, A. P. (1962). Effect of small additions of iron on the viscosity and electric resistance of liquid aluminum. *Izvestiya Vysshikh Uchebnykh Zavedenii, Chernaya Metallurgiya*, 5(No. 11), 140-5.
- Kononenko, V. I., Yatsenko, S. P., Rubinshtein, G. M., & Privalov, I. M. (1969). Viscosity and electrical resistivity of molten aluminum. *Teplofizika Vysokikh Temperatur*, 7(2), 265-8.



- Korol'kov, A. M. (1959). The viscosity of liquid metals. *Izvestiya Akademii Nauk SSSR, Otdelenie Tekhnicheskikh Nauk, Metallurgiya i Toplivo*, (No. 5), 123-6.
- Lambotte, G. (2007). *Modélisation de la viscosité de l'aluminium et de ses alliages*. Rapport de examen de synthèse, École Polytechnique de Montréal, Montréal, Canada.
- Lambotte, G. (2007). *Modélisation de la viscosité de l'aluminium et de ses alliages*. Rapport de examen de synthèse, École Polytechnique de Montréal, Montréal, Canada.
- Levin, E. S. (1971). Polytherms of the viscosity and self-diffusion of molten aluminum. *Izvestiya Akademii Nauk SSSR, Metally*, (5), 72-8.
- Levin, E. S., Shetrushevskii, M. S., Gel'd, P. V., & Ayushina, G. D. (1972). Viscosity and energy of interatomic interaction in molten iron-aluminum alloys. *Zhurnal Fizicheskoi Khimii*, 46(9), 2210-13.
- Lihl, F., Nachtigall, E., & Pointner, G. (1964). Measurement of the viscosity of fused aluminum. *Metall (Berlin, 1914-34)*, 18, 1054-64.
- Lihl, F., Nachtigall, E., & Schwaiger, A. (1968). Viscosity measurements on binary aluminum alloys containing silicon, zinc, copper, and magnesium. *Zeitschrift fuer Metallkunde*, 59(3), 213-19.
- Lihl, F., & Schwaiger, A. (1967). Transitions in liquid aluminum. *Zeitschrift fuer Metallkunde*, 58(11), 777-9.
- Lindberg, D., Backman, R., & Chartrand, P. (2007a). Thermodynamic evaluation and optimization of the (Na<sub>2</sub>CO<sub>3</sub> + Na<sub>2</sub>SO<sub>4</sub> + Na<sub>2</sub>S+K<sub>2</sub>CO<sub>3</sub> + K<sub>2</sub>SO<sub>4</sub> + K<sub>2</sub>S) system. *Journal of Chemical Thermodynamics*, 39(6), 942-960.
- Lindberg, D., Backman, R., & Chartrand, P. (2007b). Thermodynamic evaluation and optimization of the (NaCl + Na<sub>2</sub>SO<sub>4</sub> + Na<sub>2</sub>CO<sub>3</sub> + KCl + K<sub>2</sub>SO<sub>4</sub> + K<sub>2</sub>CO<sub>3</sub>) system. *Journal of Chemical Thermodynamics*, 39(7), 1001-1021.
- Lindemann, F. A. (1910). The Calculation of Molecular Vibration Frequencies. *Physik. Z.*, 11, 609-12.
- Longuet-Higgins, H. C., & Pople, J. A. (1956). Transport properties of a dense fluid of hard spheres. *Journal of Chemical Physics*, 25, 884-9.
- Maroni, V. A., & Cairns, E. J. (1969). Raman spectroscopy of fused salts and studies of some halide-containing systems. *Molten Salts, Symp.*, 231-89.

- Maroni, V. A., Hathaway, E. J., & Cairns, E. J. (1971). Structural studies of magnesium halide-potassium halide melts by Raman spectroscopy. *Journal of Physical Chemistry*, 75(1), 155-9.
- Matsumura, Y., Mizuno, M., & Nishihara, K. (1966). The viscosity of the fused salts mixtures. *Memoirs of the Faculty of Engineering, Kyoto University*, 28(4), 404-12.
- Maurits, A. A. (1967). Viscosity of molten salts of the potassium chloride-sodium chloride-calcium chloride-magnesium chloride system with a weight ratio of potassium chloride:sodium chloride of 8:1. *Zhurnal Prikladnoi Khimii (Sankt-Peterburg, Russian Federation)*, 40(1), 48-55.
- Mayer, J. E. (1933). Dispersion and polarizability and the van der Waals potential in the alkali halides. *Journal of Chemical Physics*, 1, 270-9.
- McAllister, R. A. (1960). The viscosity of liquid mixtures. *AIChE Journal*, 6, 427-31.
- Menz, W., Sauerwald, F., & Fischer, K. (1966). Viscosity measurements. XVII. The new double capillary viscometer and a critical survey of new measurements of eta values for pure metals. *Acta Metallurgica*, 14(11), 1617-23.
- Moelwyn-Hughes, E. A. (1961). *Physical Chemistry*. 2nd ed.
- Moraru, L., Tudose, C., & Vlad, M. (1997). The viscosity of melted aluminum and aluminum-12% silicon eutectic alloy in ultrasonic field. *Romanian Journal of Physics*, 42(9-10), 755-762.
- Morita, Z., Iida, T., & Ueda, M. (1976). The excess viscosity of liquid binary alloys. *Conference Series - Institute of Physics*, 30(Liq. Met., Invited Contrib. Pap. Int. Conf., 3rd, 1976), 600-6.
- Murgulescu, I. G., & Misdolea, C. (1977). A relation for the viscosity of ionic liquids. *Revue Roumaine de Chimie*, 22(11-12), 1433-9.
- Murgulescu, I. G., & Zuca, S. (1961). Viscosity of some simple molten salts. *Zeitschrift fuer Physikalische Chemie (Leipzig)*, 218, 379-91.
- Murgulescu, I. G., & Zuca, S. (1963). Viscosity of some molten salts. II. *Zeitschrift fuer Physikalische Chemie (Leipzig)*, 222(5/6), 300-4.

- Murgulescu, I. G., & Zuca, S. (1965). Viscosity of binary mixtures of molten salts. The systems: KCl + NaCl, KCl + KBr, PbBr<sub>2</sub> + KBr. *Studii si Cercetari de Chimie*, 14(2), 115-25.
- Novokhatvskii, I. A., Yaroshenko, I. V., Kisun'ko, V. Z., & Pogorelov, A. I. (1999). Cluster adsorption and viscous flows of liquid metals in near-wall layers. *Zhurnal Fizicheskoi Khimii*, 73(9), 1629-1633.
- Ofte, D., & Wittenberg, L. J. (1963). Viscosity of bismuth, lead, and zinc to 1000 Deg. *Transactions of the American Institute of Mining, Metallurgical and Petroleum Engineers*, 227, 706-11.
- Østvold, T. (1971). Thesis, University of Trondheim, Trondheim, Norway.
- Parrinello, M., & Tosi, M. P. (1979). Structure and dynamics of simple ionic liquids. *Rivista del Nuovo Cimento della Societa Italiana di Fisica*, 2(6), 69 pp.
- Pasternak, A. D. (1972). Liquid metal transport properties. *Physics and Chemistry of Liquids*, 3(1), 41-53.
- Pelton, A. D. (1997). Solution models. *Advanced Physical Chemistry for Process Metallurgy*, 87-117.
- Pelton, A. D., & Chartrand, P. (2001). The modified quasi-chemical model: Part II. Multicomponent solutions. *Metallurgical and Materials Transactions A: Physical Metallurgy and Materials Science*, 32A(6), 1355-1360.
- Pelton, A. D., Chartrand, P., & Eriksson, G. (2001). The modified quasi-chemical model: Part IV. Two-sublattice quadruplet approximation. *Metallurgical and Materials Transactions A: Physical Metallurgy and Materials Science*, 32(6), 1409-1416.
- Pelton, A. D., Degterov, S. A., Eriksson, G., Robelin, C., & Dessureault, Y. (2000). The modified quasichemical model I - binary solutions. *Metallurgical and Materials Transactions B: Process Metallurgy and Materials Processing Science*, 31B(4), 651-659.
- Pitzer, K. S. (1939). Corresponding states for perfect liquids. *Journal of Chemical Physics*, 7, 583-90.
- Polyak, E. V., & Sergeev, S. V. (1941). Determination of the viscosity of molten aluminum and its alloys. *Doklady Akademii Nauk SSSR, Seriya A*, 30, 137-9.
- Poynting, J. H., & Thomson, J. J. (1947). *Properties of Matter* (14th ). London: Charles Griffin & Co.

- Reid, R. C., & Sherwood, T. K. (1966). *The Properties of Gases and Liquids*.
- Reiss, H., Mayer, S. W., & Katz, J. (1961). Law of corresponding states for fused salts. *Journal of Chemical Physics*, 35, 820-6.
- Rhim, W. K. W. K., & Ohsaka, K. (2000). Thermophysical properties measurement of molten silicon by high-temperature electrostatic levitator: density, volume expansion, specific heat capacity, emissivity, surface tension and viscosity. *Journal of Crystal Growth*, 208(1-4), 313-321.
- Rice, S. A., & Kirkwood, J. G. (1959). An approximate theory of transport in dense media. *Journal of Chemical Physics*, 31, 901-8.
- Roach, S. J., & Henein, H. (2005). A new method to dynamically measure the surface tension, viscosity, and density of melts. *Metallurgical and Materials Transactions B: Process Metallurgy and Materials Processing Science*, 36B(5), 667-676.
- Roach, S. J., & Henein, H. (2005). A new method to dynamically measure the surface tension, viscosity, and density of melts. *Metallurgical and Materials Transactions B (Process Metallurgy and Materials Processing Science)*, 36B(5), 667-76.
- Roach, S. J., Henein, H., & Owens, D. C. (2001). A new technique to measure dynamically the surface tension, viscosity and density of molten metals. *Light Metals (Warrendale, PA, United States)*, 1285-1291.
- Robelin, C., & Chartrand, P. (2007). A density model based on the modified quasichemical model and applied to the NaF-AlF<sub>3</sub>-CaF<sub>2</sub>-Al<sub>2</sub>O<sub>3</sub> electrolyte. *Metallurgical and Materials Transactions B: Process Metallurgy and Materials Processing Science*, 38B(6), 881-892.
- Robelin, C., & Chartrand, P. (2007). Predictive models for the density and viscosity of the NaF-AlF<sub>3</sub>-CaF<sub>2</sub>-Al<sub>2</sub>O<sub>3</sub> electrolyte. *Light Metals (Warrendale, PA, United States)*, 565-570.
- Robelin, C., Chartrand, P., & Eriksson, G. (2007). A density model for multicomponent liquids based on the modified quasichemical model: application to the NaCl-KCl-MgCl<sub>2</sub>-CaCl<sub>2</sub> system. *Metallurgical and Materials Transactions B: Process Metallurgy and Materials Processing Science*, 38B(6), 869-879.
- Robelin, C., Chartrand, P., & Pelton, A. D. (2004a). Thermodynamic evaluation and optimization of the (NaCl + KCl + AlCl<sub>3</sub>) system. *Journal of Chemical Thermodynamics*, 36(8), 683-699.

- Robelin, C., Chartrand, P., & Pelton, A. D. (2004b). Thermodynamic evaluation and optimization of the (MgCl<sub>2</sub> + CaCl<sub>2</sub> + MnCl<sub>2</sub> + FeCl<sub>2</sub> + CoCl<sub>2</sub> + NiCl<sub>2</sub>) system. *Journal of Chemical Thermodynamics*, 36(9), 793-808.
- Robelin, C., Chartrand, P., & Pelton, A. D. (2004c). Thermodynamic evaluation and optimization of the (NaCl + KCl + MgCl<sub>2</sub> + CaCl<sub>2</sub> + MnCl<sub>2</sub> + FeCl<sub>2</sub> + CoCl<sub>2</sub> + NiCl<sub>2</sub>) system. *Journal of Chemical Thermodynamics*, 36(9), 809-828.
- Robelin, C., Chartrand, P., & Pelton, A. D. (2006). A thermodynamic database for AlCl<sub>3</sub>-based molten salt systems. *Proceedings - Electrochemical Society, 2004-24(Molten Salts XIV)*, 108-121.
- Roscoe, R. (1958). Viscosity determination by the oscillating vessel method. I. Theoretical considerations. *Proceedings of the Physical Society, London*, 72, 576-84.
- Rothwell, E. (1962). A precise determination of the viscosity of liquid tin, lead, bismuth, and aluminum by an absolute method. *Journal of the Institute of Metals*, 90, 389-94.
- Sato, T., & Munakata, S. (1955). The viscosity of molten metals and alloys. II. The viscosity coefficients of molten cadmium-zinc, cadmium-bismuth, and cadmium-tin alloys and the measurement of densities of molten metals and alloys. *Bull. Research Inst. Mineral Dressing and Met.*, 11, 11-16.
- Sato, Y. (2004). Viscosity of molten metals and the method for viscosity measurement. *Molten Salts*, 47(3), 132-139.
- Sato, Y., Kameda, Y., Nagasawa, T., Sakamoto, T., Moriguchi, S., Yamamura, T., & Waseda, Y. (2003). Viscosity of molten silicon and the factors affecting measurement. *Journal of Crystal Growth*, 249(3-4), 404-415.
- Seetharaman, S., & Sichen, D. (1997). Viscosities of high temperature systems - a modeling approach. *ISIJ International*, 37(2), 109-118.
- Sergeev, S. V., & Polyak, E. V. (1947). Determination of the viscosity of molten alloys and its applications. *Zavodskaya Laboratoriya*, 13, 336-44.
- Shvidkovskii, E. G. (1955). *Nekotorye voprosy вязкости расплавленных металлов (Some Questions on the Viscosity of Molten Metals)*.
- Sigworth, G. K. (2000). Gas fluxing of molten aluminum Part 2: Removal of alkali metals. *Light Metals (Warrendale, Pennsylvania)*, 773-778.

- Sindzingre, P., & Gillan, M. J. (1990). A computer simulation study of transport coefficients in alkali halides. *Journal of Physics: Condensed Matter*, 2(33), 7033-42.
- Sinha, A., & Miller, E. (1970). Evidence of clustering in liquid zinc-antimony alloys from viscosity measurements. *Metallurgical Transactions*, 1(5), 1365-70.
- Smirnov, M. V., & Khokhlov, V. A. (1967). Viscosity of molten cesium chloride-lithium chloride mixtures. *Trudy Instituta Elektrokhimii, Ural'skii Filial, Akademiya Nauk SSSR*, No. 10, 31-4.
- Smirnov, M. V., & Khokhlov, V. A. (1969). Viscosity of fused cesium chloride-barium dichloride salt mixtures. *Trudy Instituta Elektrokhimii, Ural'skii Filial, Akademiya Nauk SSSR*, No. 12, 45-9.
- Smith, J. M., Van Ness, H. C., & Abbott, M. M. (1996). *McGraw Hill Chemical Engineering Series: Introduction to Chemical Engineering Thermodynamics*. 5th Ed.
- Smith, W. F. (1981). *Structure and Properties of Engineering Alloys*.
- Stevens, J. G., & Yu, H. (1988). Mechanisms of sodium, calcium and hydrogen removal from an aluminum melt in a stirred tank reactor - the Alcoa 622 process. *Light Metals (Warrendale, PA, United States)*, 437-43.
- Strelets, K. L., Taits, A. Y., & Gulyanitzkii, B. S. (1953). *Metallurgie des Magnesiums*.
- Strelets, K. L., Zhudneva, V. N., & Reznikov, I. L. (1955). Viscosity of fused salts in the isoconcentration polytherm (10 wt. %  $\text{MgCl}_2$ ) of the system  $\text{MgCl}_2\text{-CaCl}_2\text{-KCl-NaCl}$ . *Zhurnal Prikladnoi Khimii (Sankt-Peterburg, Russian Federation)*, 28, 643-51.
- Sun, M., Geng, H., Bian, X., & Liu, Y. (2000). The simulation of the viscosity of liquid aluminum using the tight-binding potential. *Materials Science Forum*, 331-337(Pt. 1, Aluminium Alloys: Their Physical and Mechanical Properties), 337-342.
- Szekely, J. (1979). *Fluid Flow Phenomena in Metals Processing*.
- Thresh, H. R. (1965). Viscosity of liquid zinc by oscillating a cylindrical vessel. *Transactions of the American Institute of Mining, Metallurgical and Petroleum Engineers*, 233(1), 79-88.

- Toerklep, K., & Oeye, H. A. (1979). An absolute oscillating-cylinder (or cup) viscometer for high temperatures. *Journal of Physics E: Scientific Instruments*, 12(9), 875-85.
- Tolbaru, D., Borcan, R., & Zuca, S. (1998). Viscosity measurements on molten salts with an oscillating cup viscometer. Viscosity of molten KNO<sub>3</sub> and NaCl. *Berichte der Bunsen-Gesellschaft*, 102(10), 1387-1392.
- Torklep, K., & Øye, H. A. (1979). An absolute oscillating-cylinder (or cup) viscometer for high temperatures. *Journal of Physics E: Scientific Instruments*, 12(9), 875-85.
- Torklep, K., & Øye, H. A. (1982). Viscosity of molten alkaline-earth chlorides. *Journal of Chemical and Engineering Data*, 27(4), 387-91.
- Torklep, K. E., & Øye, H. A. (1981). Some comments on the viscosity of NaCl and determination of viscosity in general. *Ber. Bunsenges. Phys. Chem.*, 85, 814-815.
- Tosi, M. P., & Fumi, F. G. (1964). Ionic sizes and Born repulsive parameters in the NaCl-type alkali halides. II. Generalized Huggins-Mayer forms. *Journal of Physics and Chemistry of Solids*, 25(1), 45-52.
- Travis, K. P., Searles, D. J., & Evans, D. J. (1998). Strain rate dependent properties of a simple fluid. *Molecular Physics*, 95(2), 195-202.
- Utigard, T. (1991). Thermodynamic considerations of aluminum refining and fluxing. *Extr., Refin., Fabr. Light Met., Proc. Int. Symp.*, 4th, 353-65.
- Utigard, T. A., Roy, R. R., & Friesen, K. (2001). The roles of molten salts in the treatment of aluminum. *Canadian Metallurgical Quarterly*, 40(3), 327-334.
- Vasu, G. (1969). Mechanism of viscous flow in ionic liquids. *Revue Roumaine de Chimie*, 14(2), 167-71.
- Vereshchetina, I. P., & Luzhnaya, N. P. (1954). Conductivity, viscosity, and density of fusions of binary salt systems with simple eutectic. *Izvest. Sektora Fiz.-Khim. Anal., Inst. Obshchei i Neorg. Khim., Akad. Nauk S.S.S.R.*, 25, 188-207.
- Verschaffelt, J. E. (1916). The viscosity of liquefied gases. I. The rotational oscillations of a sphere in a viscous liquid. *Proc. Akad. Wetenschappen*, 18, 840-56.
- Vignau, J. M. (1968). Viscosity and castability of aluminum and aluminum-silicon alloys. *Metaux: Corrosion-Industrie*, 43(511), 93-108.

- Vignau, J. M., Azou, P., & Bastien, P. (1967). Viscosity of aluminum and aluminum-silicon alloys; the effect of alumina film. *Comptes Rendus des Seances de l'Academie des Sciences, Serie C: Sciences Chimiques*, 264(2), 174-7.
- Waite, P. (2002). A technical perspective on Molten aluminum processing. *Light Metals (Warrendale, PA, United States)*, 841-848.
- Wang, D., & Overfelt, R. A. (2002). Oscillating Cup Viscosity Measurements of Aluminum Alloys: A201, A319 and A356. *International Journal of Thermophysics*, 23(4), 1063-1076.
- Waseda, Y., & Ohtani, M. (1975). Estimation of viscosity coefficients, self-diffusion coefficients, and surface tension of molten metals by the principle of corresponding states. *Tetsu to Hagane*, 61(1), 46-53.
- Wells, A. F. (1962). *Structural Inorganic Chemistry*. 3rd ed.
- Wittenberg, L. J., & DeWitt, R. (1973). Viscosity of liquid rare-earth and actinide metals. *Prop. Liquid Metals. Proc. Int. Conf., 2nd*, 555-60.
- Wittenberg, L. J., Ofte, D., & Curtiss, C. F. (1968). Fluid flow of liquid plutonium alloys in an oscillating-cup viscometer. *Journal of Chemical Physics*, 48(7), 3253-60.
- Yamasaki, T., Kanatani, S., Ogino, Y., & Inoue, A. (1993). Viscosity measurements for liquid aluminum-nickel-lanthanum and aluminum-nickel-Mm (Mm: Mischmetal) alloys by an oscillating crucible method. *Journal of Non-Crystalline Solids*, 156-158(Pt. 1), 441-4.
- Yang, Y., Pakkanen, T. A., & Rowley, R. L. (2000). Nonequilibrium molecular dynamics simulations of shear viscosity: isoamyl alcohol, n-butyl acetate, and their mixtures. *International Journal of Thermophysics*, 21(3), 703-717.
- Yao, T.-P. (1956). Viscosity of metallic melts. *Giesserei Tech.-Wiss. Beih. Giessereiw. u. Metallk.*, 837-51.
- Yao, T. P., & Kondic, V. (1952). The viscosity of molten tin, lead, zinc, aluminum, and some of their alloys. *Journal of the Institute of Metals*, 81, 17-24, Paper No 1410.
- Young, R. E., & O'Connell, J. P. (1971). Empirical corresponding states correlation of densities and transport properties of 1-1 alkali metal molten salts. *Industrial & Engineering Chemistry Fundamentals*, 10(3), 418-23.



- Zamyatin, V. M., Nasyirov, Y. A., Klassen, N. I., Bazin, Y. A., & Baum, B. A. (1986). The anomalies of the viscosity polytherms of molten aluminum-copper alloys. *Zhurnal Fizicheskoi Khimii*, 60(1), 243-5.
- Zhou, Z., Mukherjee, S., & Rhim, W.-K. (2003). Measurement of thermophysical properties of molten silicon using an upgraded electrostatic levitator. *Journal of Crystal Growth*, 257(3-4), 350-358.
- Zuca, S. (1973). Private communication to Janz, G.J. reported in 1975 NSRDS publication.
- Zuca, S., & Borcan, R. (1984). Viscosity of certain charge-unsymmetrical molten chloride mixtures: calcium chloride-(sodium, potassium, rubidium, cesium) chloride. *Revue Roumaine de Chimie*, 29(3), 233-9.
- Zuca, S., & Costin, R. (1970). Viscosity of some molten alkaline-earth chlorides. *Revue Roumaine de Chimie*, 15(12), 1831-7.
- Zuca, S., Olteanu, M., Borcan, R., Popescu, A. M., & Ciochina, M. (1991). Electrical conductivity, density, and viscosity of molten magnesium chloride-calcium chloride-2-sodium chloride-potassium chloride quaternary system. *Chemical Papers*, 45(5), 585-92.

## Appendix A: Numerical Values of the Model Parameters

$$G^* = c + dT \text{ (J/mol)}$$

Molten Salts	Liquid Metals
Unary Parameters	
$c_{Ca/Cl} = 2.749795E + 04$ $d_{Ca/Cl} = 2.4387E + 01$  $c_{Cs/Cl} = 2.029795E + 04$ $d_{Cs/Cl} = 2.3383E + 01$  $c_{K/Cl} = 2.109947E + 04$ $d_{K/Cl} = 2.0575E + 01$  $c_{Mg/Cl} = 1.878405E + 04$ $d_{Mg/Cl} = 2.8722E + 01$	$c_{Al} = 1.177691E + 04$ $d_{Al} = 1.6840E + 01$  $c_{Si} = 1.437059E + 04$ $d_{Si} = 1.5120E + 01$  $c_{Zn} = 1.229861E + 04$ $d_{Zn} = 1.9460E + 01$
$c_{Na/Cl} = 1.807487E + 04$ $d_{Na/Cl} = 2.1305E + 01$  $c_{Rb/Cl} = 2.101379E + 04$ $d_{Rb/Cl} = 2.2215E + 01$	
Binary Parameters	
$c_{CaMg/Cl} = 1.442345E + 04$ $d_{CaMg/Cl} = 3.4416E + 01$  $c_{KCa/Cl} = 3.645222E + 04$ $d_{KCa/Cl} = 1.4420E + 01$  $c_{KMg/Cl} = 2.885035E + 04$ $d_{KMg/Cl} = 1.3395E + 01$	$c_{AlSi} = 1.000000E + 04$ $d_{AlSi} = 1.4700E + 01$  $c_{AlZn} = 1.050000E + 04$ $d_{AlZn} = 1.7000E + 01$

$$c_{NaCa/Cl} = 3.330974E + 04$$

$$d_{NaCa/Cl} = 1.6528E + 01$$

$$c_{NaK/Cl} = 2.372506E + 04$$

$$d_{NaK/Cl} = 1.6602E + 01$$

$$c_{NaMg/Cl} = 2.293613E + 04$$

$$d_{NaMg/Cl} = 1.6541E + 01$$

## Appendix B: Numerical Values of the Modified Model

### Parameters

$$G^*_{ij} = (G^*_{ij})^{00} + (G^*_{ij})^{10} \frac{X_{ii}}{X_{ii} + X_{ij} + X_{jj}} + (G^*_{ij})^{01} \frac{X_{jj}}{X_{ii} + X_{ij} + X_{jj}}$$

$$(G^*_{ij})^{00} = (c_{ij})^{00} + (d_{ij})^{00}T$$

$$(G^*_{ij})^{10} = (c_{ij})^{10} + (d_{ij})^{10}T$$

$$(G^*_{ij})^{01} = (c_{ij})^{01} + (d_{ij})^{01}T$$

NaCl-MgCl <sub>2</sub>		
$(c_{NaMg/Cl})^{00} = 2.293613E + 04$ $(d_{NaMg/Cl})^{00} = 1.6541E + 01$	$(c_{NaMg/Cl})^{10} = 2000$ $(d_{NaMg/Cl})^{10} = 0$	$(c_{NaMg/Cl})^{01} = -3000$ $(d_{NaMg/Cl})^{01} = 0$
RbCl-MgCl <sub>2</sub>		
$(c_{RbMg/Cl})^{00} = 3.3000000E + 04$ $(d_{RbMg/Cl})^{00} = 1.2500E + 01$	$(c_{RbMg/Cl})^{10} = 1000$ $(d_{RbMg/Cl})^{10} = 0$	$(c_{RbMg/Cl})^{01} = -8000$ $(d_{RbMg/Cl})^{01} = 0$
CsCl-MgCl <sub>2</sub>		
$(c_{CsMg/Cl})^{00} = 3.3000000E + 04$ $(d_{CsMg/Cl})^{00} = 1.3000E + 01$	$(c_{CsMg/Cl})^{10} = 3000$ $(d_{CsMg/Cl})^{10} = 0$	$(c_{CsMg/Cl})^{01} = -6000$ $(d_{CsMg/Cl})^{01} = 0$

## Appendix C: Numerical Values of the Correction Functions

$$\Delta_{\text{component}}^{\text{Author-year}} = 1 - \exp\left[\frac{a + bT}{RT}\right]$$

Author	Year	Component	a	b
Dumas et al.	1970	NaCl	7.254E+02	-2.141E-01
Bondarenko & Strelets	1968	NaCl	-1.063E+03	8.628E+00
Murgulescu & Zuca	1963	NaCl	-1.683E+04	1.290E+01
Ejima et al.	1977	KCl	-2.037E+03	3.119E+00
Dumas et al.	1970	KCl	1.688E+03	-1.212E+00
Bondarenko & Strelets	1968	KCl	-3.927E+03	3.032E+00
Matsumura et al.	1966	KCl	-2.133E+03	-2.116E-01
Murgulescu & Zuca	1961	KCl	-1.628E+03	9.319E-01
Ejima et al.	1977	MgCl <sub>2</sub>	5.732E+03	-5.575E+00
Dumas et al.	1970	MgCl <sub>2</sub>	1.102E+03	-9.778E-01
Bondarenko & Strelets	1968	MgCl <sub>2</sub>	-2.221E+03	1.894E+00
Ejima et al.	1977	CaCl <sub>2</sub>	1.739E+03	-2.386E+00
Dumas et al.	1973	CaCl <sub>2</sub>	-3.102E+03	2.926E+00
Zuca & Costin	1970	CaCl <sub>2</sub>	9.126E+02	-1.372E+00
Dumas et al.	1973	RbCl	-5.320E+02	9.064E-01
Dumas et al.	1973	CsCl	-1.536E+04	1.494E+01
Vignau	1968	Al	-1.921E+03	6.620E+00
Gebhardt and Detering	1959	Zn	2.959E+03	-3.450E+00